An investigation into the feasibility of combined diamond and diamond-like carbon coatings for effective dry turning of aluminium alloys

A thesis submitted for degree of Doctor of Philosophy

Nico Nelson

College for Engineering, Design and Physical Science

Brunel University

April 2016

Abstract

The efficacy of combined diamond and diamond like carbon coatings, to allow for effective and efficient dry turning of aluminium alloy Al 6082, has been investigated. Optimised diamond and diamond-like carbon (DLC) coatings were combined and deposited onto a WC-Co insert using chemical vapour deposition (CVD) methods. DLC coatings were developed by testing the effects of bias voltage, deposition time and gas pressure. During the development of the DLC layer, the effects of substrate geometry and positioning in the deposition chamber were investigated. It was discovered that coating characteristics could vary significantly across the samples as a result of geometrical effects. This contradicted claims that, as plasma enhanced CVD is a non-line of sight deposition method, any variation in the coating due to geometry would be negligible. SEM analysis revealed coating thickness to increase by over 50%. AFM measurements showed coating roughness to increase by up to 30 times, whilst Raman spectroscopy highlighted a significant decrease in sp^3 bonding. This variation in characteristics was seen, through the use of scratch testing, to translate into significantly reduced tribological performance. Friction was increased by 60% and critical load was only half of that of the coating applied to flat surface.

The combined coatings were characterised and machining performance was evaluated. Coating characteristics were examined using SEM, AFM and Raman spectroscopy. Cutting trials designed to simulate the expected tool life were conducted. Micro and nano-crystalline diamond coatings, with and without an additional DLC layer were trialled along with a single layer DLC coating. Commercially available uncoated and TiN coating inserts of identical geometry were also trialled as a reference. The results showed that the addition of the DLC layer effectively reduced the roughness of the diamond, however, this did not translate into reduced adhesion of the aluminium to the cutting tip. It has been shown that for this particular machining scenario, a smoother coating effectively increased friction and adhesion of the workpiece material. The investigation has highlighted that due to the complex dynamics of material transfer effects in sliding, it cannot be assumed that a smoother surface layer will lead to improved tribological performance.

Contents

Acknowledgements

First and foremost I would like to thank my supervisors Dr Richard Rakowski and Dr Ben Jones for their support and guidance throughout the course of the PhD. If it were not for their patience and understanding I would not have successfully reached this point. I would also like to thank Prof Tony Anson for his words of wisdom and assistance during the project.

I would like to thanks Dr Robert Bulpett, Prof Joe Franks, Tony Evans and Lumbini Tammita for their assistance with the production and analysis of the diamond-like carbon coatings, as well as Dr Chao Wang for his hard work and assistance with the material trialling process.

A big thank you must go to the project partners; Renishaw plc and the National Physical Laboratory, particularly Prof Paul May and Dr Judy Hart of University of Bristol, School of Chemistry for supplying the samples required for the study. I special thank you goes to all the staff at the Experimental Techniques Centre for their help with the material characterisation techniques.

Finally I would like to thank my parents Mike and Regina Nelson who made all of this possible for me and whose support and belief gave me the opportunity to complete my studies.

Declarations

I declare that the research contained within this thesis is the sole work of the author. The thesis has not been previously submitted to this or any other university for a degree and, unless otherwise indicated in the text, does not contain any material previously submitted for publication.

Signed:

Date:

April 2016

List of tables

List of figures

Equations

Symbols / Abbreviations

a-C	Amorphous carbon
a-C:H	Hydrogenated amorphous carbon
AFM	Atomic force microscopy
BUE	Built up edge
BUL	Built up layer
CVD	Chemical vapour deposition
COF	Coefficient of friction
DLC	Diamond-like carbon
HSS	High speed steel
HFCVD	Hot filament chemical vapour deposition
MCD	Micro-crystalline diamond
MQL	Minimum quantity lubrication
NCD	Nano-crystalline diamond
PECVD	Plasma enhanced chemical vapour deposition
Ra	Roughness average
Rq	Root mean square roughness
SEEM	Smart effective engineering manufacture
SEM	Scanning electron microscopy
ta-C	Tetrahedral amorphous carbon
TiN	Titanium nitride
TMS	Tetramethylsilane
UNCD	Ultra nano-crystalline diamond
WC-Co	Cobalt cemented tungsten carbide
WP	Workpiece

1. Introduction

This chapter introduces the investigations conducted in the course of the project. It begins by highlighting the scope of the project and the reasons why the study has been undertaken. Machining processes, with particular relevance to aluminium component production, as well as the application of diamond and diamond-like carbon (DLC) coatings are introduced.

1.1. Aluminium machining technology

Aluminium has become the material of choice for many engineering applications due to its high strength to weight ratio, its corrosion resistance and its ability to greatly vary its properties by the addition of other elemental species. For these reasons, the use of aluminium has become crucial to the aerospace industry. It has also become increasingly prominent in many other industries owing to its abundance and ability to be recycled. Lathe turning of aluminium forms the basis of this research project as turning tools account for a large portion of the overall cutting tool market. The market is estimated to be worth $5.98 billion; the machining of non-ferrous metals also accounts for 9.3% of this at $556 million. The market for these cutting tools has been growing steadily and predictions have suggested it will continue to grow in the coming year (British Economic Research Institute 2011).

This steady growth in the popularity of aluminium has led to the need to develop improved manufacturing methods for use in the production of aluminium components. The machining of aluminium and aluminium alloys is often problematic due to the physical, in some cases chemical, properties of the material. One of the main causes of tool failure during aluminium machining is not due directly to abrasive wear, but is as a result of adhesion of the aluminium to the tool tip. This failure mode is known as built-up edge (BUE) and built up layer (BUL) (Sánchez *et al.*, 2005; Carrilero *et al.*, 2002). In order to combat this, large amounts of lubricant or flood coolant are often required. These large amounts of coolant are not only costly, sometimes accounting for up to 17% of the total

machining costs (Kouam, 2012), but they are also potentially harmful to machine operators and damaging for the environment. These issues, exacerbated by increasingly strict environmental controls, are why it is becoming necessary for manufacturers to reduce the amounts of coolant being used, or to remove it completely and pursue alternative methods.

One of the more promising solutions to the problems associated with aluminium machining is the development of coated tool surfaces. The cutting tool materials currently being employed by manufacturers often show chemical affinity to workpiece materials at high temperatures, thus promoting friction and adhesion, they are also lacking in terms of their abrasive resistance when it comes to machining modern, tougher materials. Thin-film coatings consisting of carbides, nitrides and oxides, as well as the carbon coatings that include; poly crystalline diamond, micro and nano-diamond and diamond-like carbon, are already being utilised in order to increase tool life and improve machining efficiency. These coated tools, however, are yet to show the performance improvement required in order to make the switch from wet to dry cutting in intensive industrial machining applications.

Due to the added cost of coated cutting tools, as well reliability concerns resulting from the risk of coating failure, uncoated carbide inserts are still used extensively in aluminium machining applications and account for a large amount of turning inserts used for machining metals. This is despite the fact that in machining applications as a whole, coated tools now account for the majority of tools being used in industry.

Titanium nitride and aluminium oxide based coatings have become widely used as they have been shown to reliably improve the cutting performance in many applications. They are however, still not capable of allowing for effective dry cutting of aluminium and offer little improvement on plain carbide inserts. Carbon coatings on the other hand have become an increasingly popular field of study, as findings are beginning to suggest they are capable of efficient dry machining of common aluminium alloys in certain machining applications.

1.2. Main research challenges

The purpose of this project is to develop a combination of diamond and diamond like carbon coatings, and to test their effectiveness for the dry turning of aluminium alloys. To do this it will be necessary to consider two key points:

1. What are the current techniques being employed in order to machine aluminium efficiently with minimum costs and what issues are engineers facing when machining aluminium and aluminium alloys.
2. To test the efficacy of combined diamond and DLC coatings to change current trends by improving the performance of cutting tools sufficiently enough to eliminate the need for lubricants in the machining of aluminium alloys.

Point No.1 involves an investigation into the preferred cutting parameters and tool types, including geometries and coatings being used. It then considers the performance being achieved when turning aluminium and investigates what improvements are required and how they can be implemented.

Point No.2 will include an investigation into diamond and diamond like carbon coatings, their fabrication methods, material properties and tribological performance. Most importantly coatings will be developed, tested and evaluated to examine if these coatings can be used to improve machine tool performance and whether or not they can allow for effective dry turning of aluminium alloys.

The thesis presented here is based on an investigation which forms part of a UK government supported, collaborative project titled “Smart and Effective Engineering Manufacturing” (SEEM). The project was made possible with the aid of EPSRC and TSB, reference code: BD266E. The aim of the project is to develop technology and systems which will deliver a step change in tool performance and efficiency. This will be addressed by developing a tool coating arrangement designed to provide an improved cutting surface. Nano-crystalline diamond (NCD) will be deposited at the cutting tip to provide a hard wearing cutting edge. DLC will be deposited on the NCD to provide a durable lubricious surface preventing adherence of the cut material to the tool.

The aim of this coating combination is to reduce whole life-cycle costs of the cutting tools which will reduce manufacturing costs. This will be achieved by increasing tool life, which in turn provides the benefits of reduced machine downtime and reduced tool maintenance. The coatings should also reduce or even eliminate the need for coolants to be used in the machining process. Energy savings will also be a target of the improved cutting performance: DLC coatings being utilised have already been shown to offer a 36% energy saving in dry drilling applications (Zolgharni *et al.*, 2008).

1.3. Carbon coatings

Research into micro/nano-structured diamond and DLC coatings has increased greatly over the last few decades (Varnin *et al.,* 2006; Grill, 1999). Much of this investigation has been focused on the optimization of such coatings, as they can provide great benefits for numerous applications. This is made possible by varying the diamond, graphite and hydrogen ratios in DLC and optimising the extreme properties which can be found in diamond.

It is the combination of extreme hardness and thermodynamic properties that makes diamond an incredibly wear resistant material. For this reason, the unique properties of diamond are already being utilised for cutting, polishing, and grinding applications. Graphite, on the other hand, is a lubricious material whose properties can also be used to great effect.

1.4. Diamond like carbon

The emphasis of this project will be based on the fabrication and development of the diamond-like carbon layer. Diamond like carbon thin films are of great interest to engineers not only because of their unique properties such as high mechanical hardness, wear resistance, low friction, chemical inertness and biocompatibility, but also due to their ability to be tailored to meet specific requirements (Hainsworth *et al.*, 2007; Lifshitz, 1999). It is their unique tribological properties which have led them to be considered to offer improved performance for mechanisms subject to frictional wear. The aim of this project is to develop combined nano or micro-crystalline diamond and diamond like carbon coating, capable of further improving machining performance and efficiency. The role of the diamond is to provide a hard wearing cutting edge, which not only increases longevity, but also allows for improved workpiece surface finish. The DLC will be designed to offer a low friction surface to aid swarf removal and prevent the excessive adhesion of aluminium to the tooltip.

Diamond and DLC coatings have become the focus of many scientific studies not only due their unique characteristics, but also due to the flexibility they provide in terms of the ability to have properties tailored to suit specific requirements. Despite the numerous scientific advances in the past decades regarding diamond and DLC coatings, considerable research is still being conducted in order to further develop the technology and aim to overcome the limiting factors currently associated with diamond growth. Diamond and DLC coating have already been shown to provide improved characteristics for machining of aluminium. Diamond and DLC tools are in commercial production by several companies and are favoured by manufacturers for their improved performance in many applications. Even though diamond and DLC tools have already become a mainstream technology, research is still ongoing in an attempt to further improve the coatings for even greater efficiency in aluminium machining.

Diamond-like carbon is a metastable form of amorphous carbon whose unique material characteristics and mechanical properties are due to the surface structure and internal bonding. It consists of a combination of diamond-like sp^3 and graphite-like sp^2 bonds, and possibly a significant amount of hydrogen depending on the type of DLC (Robertson, 2002).

The first coatings coined as diamond-like carbon were created in 1971 by Aisenberg using a low energy ion beam deposition method (Aisenberg *et al.*, 1971). DLC has since been the term used to describe carbon coatings which contain an amount of sp^3 bonding, despite their properties often being very different from that of diamond.

There is currently very little research regarding the deposition of DLC onto a pre-coated diamond substrate, and as a result there are currently no reported issues on the topic. Initially there may be questions regarding how the NCD coating may be affected by the DLC deposition procedure. It is important to ensure that the diamond will maintain its integrity during the DLC deposition process. Due to the nature of DLC, in terms of its ability to mimic substrate topography, as well as the substrates ability to affect the characteristics of the coating, it becomes apparent any interlayer will have an effect on the growth of the final DLC layer.

Tailoring the DLC will be an important factor, as achieving the right balance of hardness and low friction may be the difference between success and failure. If the DLC is too soft, it will wear and delaminate from the tip. This may lead to increased surface roughness of the cutting tip, which will negatively affect the friction and cutting force. If the DLC is made harder the friction may be negatively affected. It will be important to systematically test a number of specifically tailored DLC coatings to ensure an optimal balance is achieved.

1.5. Project aims and objectives

The efficacy of combined diamond and DLC coatings will be explored by developing the multilayer coatings and build on the limited studies which have begun to examined the potential of diamond and DLC multilayer coatings. By combining the two coatings the study attempts to utilise both the low friction of DLC whilst maintaining the ultra-hardness of diamond. Each coating will provide unique benefits. The diamond will provide a hard wearing surface at the cutting edge as well as multiple cutting tips for improved workpiece finish. DLC will provide a smooth low friction surface aimed at improving swarf removal and reducing aluminium adhesion to the tool. It will also simultaneously decrease cutting forces and provide improved energy efficiency.

Aluminium machining currently requires lubricants in order to reduce cutting temperatures and prevent aluminium adhesion at the cutting tip of the tool. Although commercial diamond and DLC tools aim to reduce cutting temperatures and hence adhesion of the workpiece material, it is still recommended that lubricants are used for increased performance and tool life. This project will aim at creating a tool capable of dry machining aluminium to a good enough standard so that it will be able to compete with the most efficient tools currently on the market. Not only will this offer potential savings by removing the cost of lubricants, but will also remove the impact such lubricants have on the environment.

Diamond coatings will be deposited on selected WC-Co turning tools by hot filament chemical vapour deposition. These coatings will then be analysed using a number of surface characterisation techniques to ensure the coating is of comparable quality to already available commercial turning tools. Low force machining trials will be conducted to determine if the coating is adhering to the substrate in an effective manner. DLC will then be deposited onto the diamond coating. This combined coating will then undergo further analysis to examine the quality of the DLC coating as well as study how the DLC is affected by the diamond interlayer.

For the purpose of creating an optimal multi-layered coating, both the diamond and DLC will be developed individually. This is in part due to a limited amount of diamond coatings which can be produced in the time scale, however, it will also provide the opportunity to ensure coating performance can be associated directly to the relevant layer. This is important as the similarities in the diamond and DLC material will make distinguishing between the coatings difficult, particularly with the microscopy techniques being applied in this study. It will then be necessary to investigate how the coatings are interacting with each other to ensure the best possible combined performance is being achieved.

1.6. Scope of the dissertation

The following diagram shows the research elements being considered to investigate the efficacy of combined diamond and diamond like carbon coatings in order to improve machining performance when dry turning aluminium alloys (Fig 1.1).

The dissertation is divided into 8 chapters. Chapter 2 focuses on the current literature in regards to metal cutting, aluminium machining and tooling technology. Chapter 3 describes the methodology employed in order to develop and test the hypothesis.

Chapter 4 and 5 present the development of the individual diamond and diamond like carbon coatings respectively, whilst chapter 6 presents the development and characterisation of the combined coatings.

The full cutting trials are presented in chapter 7 in which the combined coatings are compared with single layer diamond and DLC coatings as well as commercially available turning inserts of nominally similar geometry. Conclusions and contributions to knowledge are then presented in chapter 8.

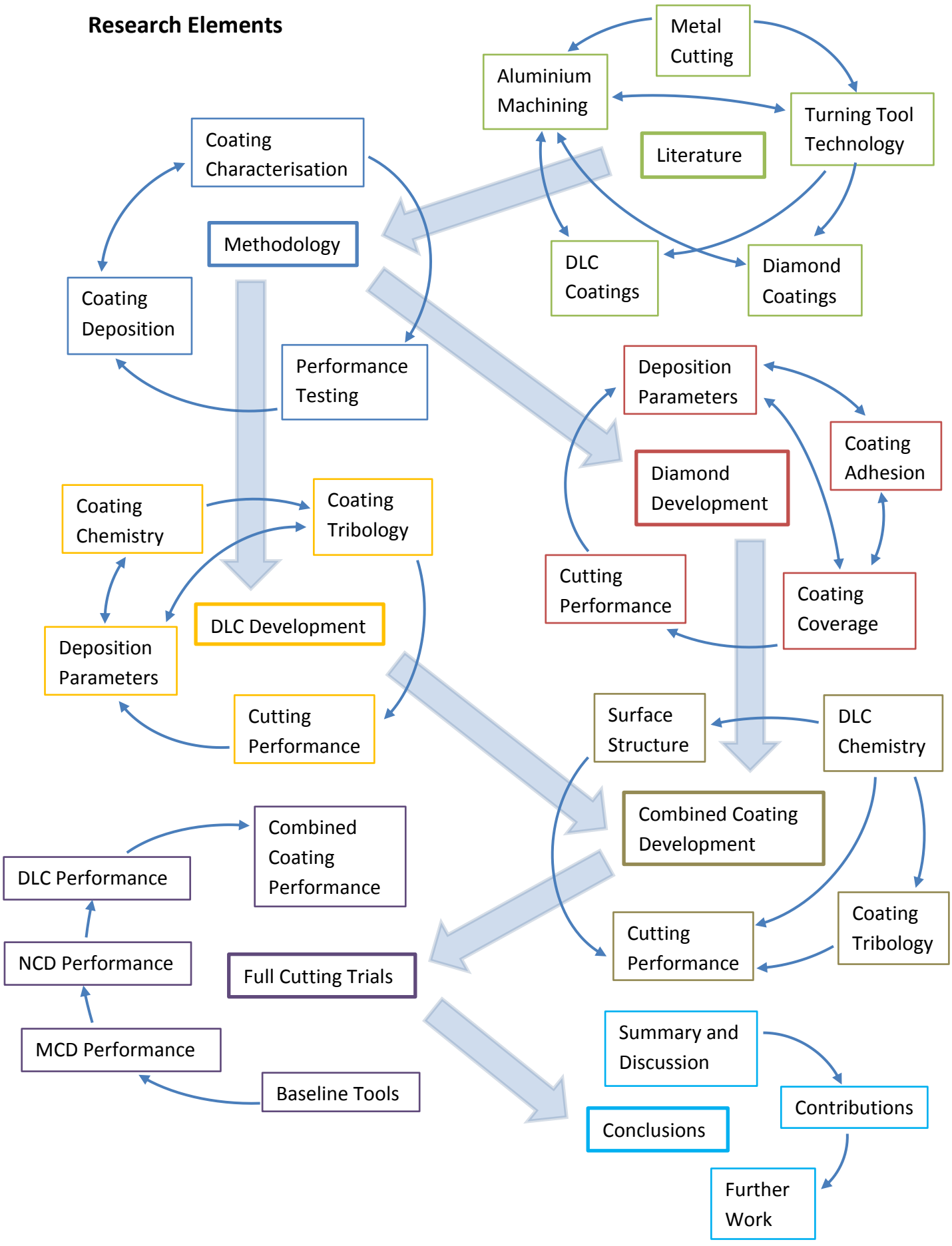

Figure 1.1. Map of research elements investigated within the scope of the project

2. Literature review

2.1 Introduction

This chapter discusses the relevant literature regarding tooling technology, in particular that which is associated with the dry turning of aluminium and the use of diamond and diamond like carbon coatings for machining applications. In terms of the scope of this project a number of key areas will therefore have to be examined to ensure the studies are valid and does not repeat work that has already been verified. The areas covered in this review will look at general machining processes, focused on the machining of aluminium alloys, in particular dry turning of aluminium. As well as this, the majority of the focus will be looking at diamond and DLC, the material characteristics, and tribological performance.

Due to the complex nature of synthetic diamond and DLC and their ability to be modified and manipulated to provide improved surface structures for numerous applications, it is no surprise that countless investigations into diamond and DLC have been conducted. These studies are based around improving coatings and deposition technology in order to increase performance in current applications as well as applying the technology to new engineering challenges. The nature of such films has also led to many studies aimed at simply gaining a better understanding of growth mechanisms involved, which will in turn allow for further developments in the field. For this reason it is important to have not only a detailed review of the literature, but also a focused review aimed at the most relevant articles. Initially it is important to understand the fundamentals of diamond and DLC technology, their tribology, deposition methods, effects of deposition parameters, how such coatings are characterized and also how the coatings are tested. It will specifically examine coatings on cobalt cemented tungsten carbide (WC-Co) substrates, however, it will also consider the use of interlayer materials which may aid deposition and adhesion. Due to DLC's ability to mimic the underlying substrates topography, as well as the fact that the substrate material will greatly affect the characteristics of the coating, it becomes necessary to focus on the substrates which are likely to

be used within the scope of this project. Silicon wafer, however, has become a favoured substrate material for research due to its smoothness and uniform surface texture, allowing for accurate comparisons of the effects of various DLC deposition parameters. Silicon will also be utilized for the purpose of this project and the findings will help develop the coatings for use with the WC-Co substrates.

With the main aim of the project being to examine the feasibility of combined coatings for dry machining purposes, particularly in regards to the machining of aluminium, it becomes important to investigate current trends in tooling technology. This includes determining performance of current tools, understanding how they are tested as well as examining how cutting parameters affect the tool, therefore, current international standards must be understood and implemented.

As well as looking at diamond and DLC coatings individually, any previous research into attempts to combine the coatings for any purpose will potentially be of great value to this investigation.

2.2. Machining process, cutting parameters and tooling

2.2.1. Cutting parameters

In order to develop coatings for improved machining performance, it will be first necessary to gain a good understanding of the main factors associated with metal cutting processes. There has already been significant development in machining technology, including an enhanced understanding of the intricate mechanisms involved in the removal of material by cutting. This understanding of tools and workpiece (WP) materials has led to significant improvements in cutting efficiency. These improvements have come from altering tool geometries along with machining parameters to suit different materials and environments. It will therefore be important to recognise these factors in order to ensure the correct cutting parameters are used, when conducting machining trials, to assess the developed coatings for this project.

The general process of machining materials is considered in terms of shear deformation in which the cutter deforms the material, essentially removing the unwanted material, in the form of chips, by overcoming its cohesive force.

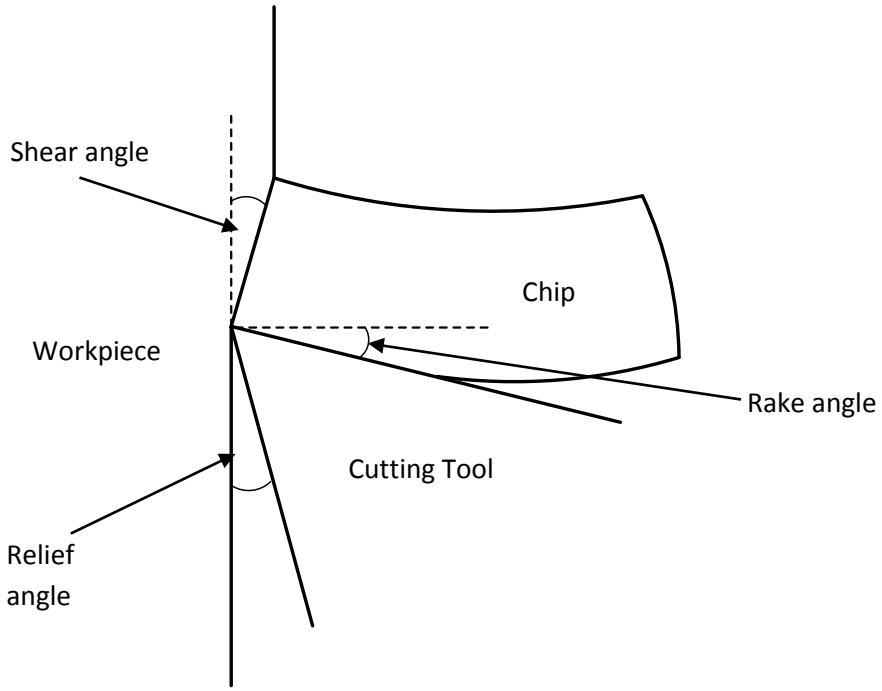

Figure 2.1. Orthogonal cutting Process

The shearing of the workpiece material, as defined by a two dimensional process (Fig 2.1) is known as orthogonal cutting. The cutting tool moves relative to the workpiece removing a surface layer in the form of chips. The diagram highlights a number of important factors regarding the tool geometry. First of all the rake angle of the cutting edge has a huge effect on the cutting process and is usually specifically designed for optimised cutting depending on the workpiece material. Bigger rake angles generally correspond to a sharper cutting edge, unless the relief angle is also altered, which reduces cutting forces but also tends to wear at a faster rate due to the reduced amount of cutting tool material and consequent shear forces applied to a smaller surface area. Sharper cutting edges can also reduce performance when certain tool coatings are applied, as the forces are concentrated leading to increased local pressure at the cutting edge causing chipping and delamination of the film.

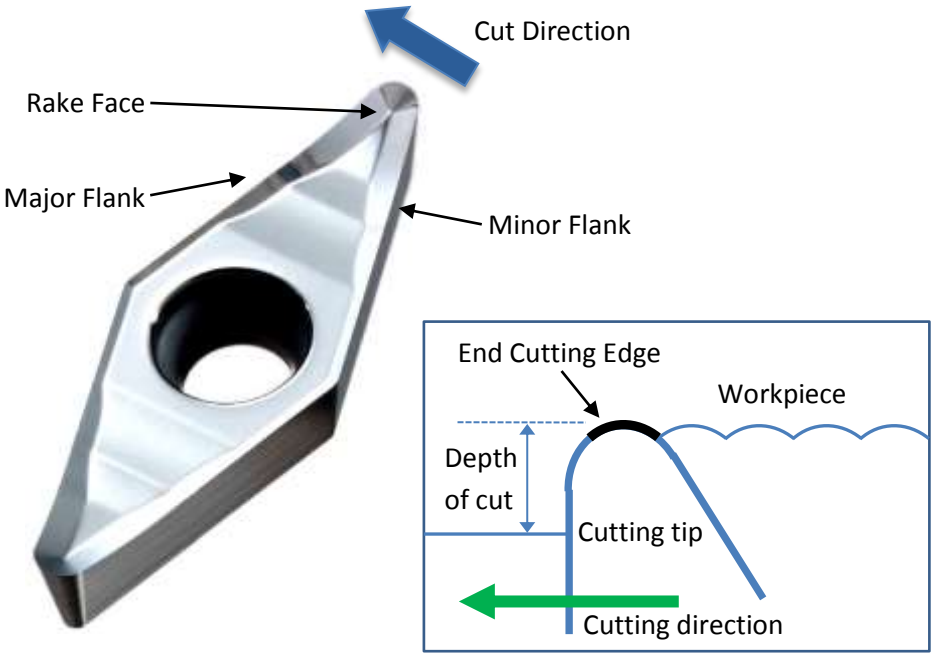

Figure 2.2. Typical turning cutting insert (directindustry.com, Jan 2016)

In the turning process the workpiece is rotated whilst the cutting tool moves along the X axis, removing the surface layer of the material as it travels. The top face of the tool is known as the rake face whilst the sides of the tool are the flanks (Fig 2.2). The major flank is the edge that does the cutting whilst the minor flank acts as a trailing edge. The end cutting edge refers to the part of the cutting edge in contact with the workpiece surface that is not subsequently removed in the next cut rotation. It is therefore responsible for the surface finish after cutting (Fig 2.2. insert).

The general factors and machine parameters that affect the metal cutting process have been listed in the table below, along with the influence they have (Fig 2.3). It is important to understand that there is a complex inter-relationship between the machining conditions which means the various aspects will constantly be influencing one another.

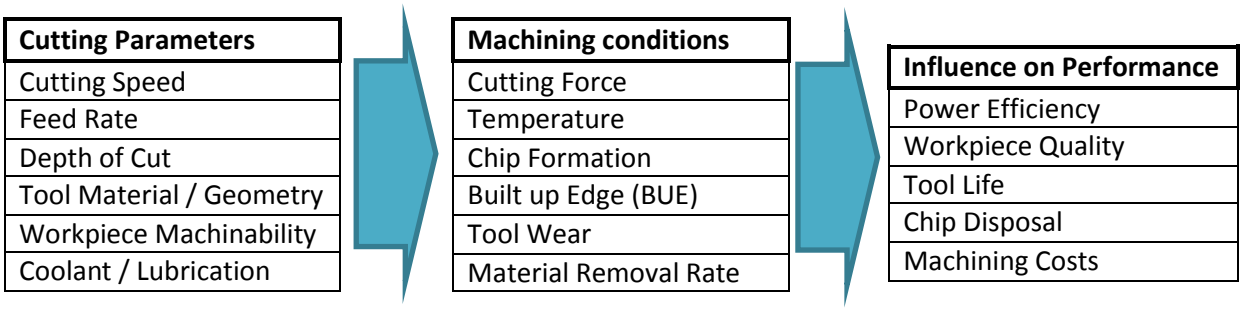

Figure 2.3. Inter-relationship of cutting parameters and influences on the cutting process

The parameters such as; cutting speed, feed rate, depth of cut and tool geometry, will be selected depending on the work piece material and its machinability, as well as the desired performance. The use, and type, of coolant will also depend on these factors. The machining processes will also be constantly interacting with one another. Cutting force and cutting temperature will affect the BUE, chip formation and tool wear, which will in turn influence the cutting force once again. It is this complex inter-relationship of factors which can mean slight variations in cutting conditions can compound to produce completely different performance (Ren, 2004; O'Sullivan, 2001; Grzesik, 1999). The cutting temperature is of significant importance as it will directly affect the material properties and hence the machinability of the workpiece. High temperatures will also compromise the tool by reducing the material durability (Konca, 2006; Helen, 2005). It is therefore important to try and ensure any potential variation in machining parameters is kept to a minimum to maintain consistency and allow for comparability in cutting trials.

It will be essential to understand the relationship between work piece machinability, tooling aspects and cutting performance in order to devise a valid test which will be comparable to industrial aluminium machining operations. Aluminium is a relatively soft metal which generally means higher cutting speeds can be effectively used without destroying the tool. In combination with this, larger rake angles are utilised to reduce forces and improve surface finish. Industrial aluminium machining processes will generally use carbide inserts along with large quantities of coolant to remove swarf

and reduce BUE. In contrast the parameters for dry machining will therefore be altered in order to compensate for the lack of cooling.

2.2.2. Tool materials and wear mechanisms

In industry today, high speed steel (HSS) and carbides account for the majority of standard tool materials used. Materials technology has been advancing rapidly, however, leading to a requirement for similar advances in the tooling technologies utilized in machining processes. Performance of these tooling materials is usually judged by three criteria: toughness, hardness and wear resistance (Byrne *et al.*, 2003). With the variety of materials being machined ever increasing, the cutting tool thermal and material properties are also of importance. Tool steels and high speed steels have been used as tooling material due to their high toughness, they are, however, not suitable for machining high strength materials, as their relatively low hardness causes them to wear quickly. Cast cobalt alloys, cemented carbides, cermets and ceramics, with up to three times the hardness of steel, have been developed to allow for efficient machining of high strength materials (Davim *et el,*, 2007; Jindal *et al.*, 1999; Jia *et al,*, 1997). Carbides, in particular cobalt cemented tungsten carbide, has become a popular tool material used in industry today, due to its high toughness and hardness (Polini *et al.*, 2003; Tiejun *et al.*, 2002).

Flank wear and crater wear, which refer to abrasion of the flank and rake faces respectively, are the two main forms of tool wear, for this reason they also act as the criteria for which performance standards are measured. It is the ability to be measured which makes them useful for judging tool performance and hence are used by international standards regarding tool-life testing for single point turning tools (ISO 3685). Although flank and crater wear are often measured and acceptable wear thresholds are given depending on tolerance requirements, there are a number of different forms of tool wear (Fig 2.4). Plastic deformation, notch wear, chipping and breaking of the cutting tip are more severe forms of wear (Astakhov, 2004). Current standards, however, are based around the

machining of iron and steels and are only designed to look at crater and flank wear of tools. A number of studies have concluded that current standards are no longer adequate and are in need of updating (Astakhov, 2004; Carrilero *et al.*, 2002). It is a common issue that manufacturers often have difficulty ensuring that a tool has been effectively used to its optimum. In many cases tools will be replaced between batches for convenience despite the tool not being fully worn out. In other cases machine parameters can be altered to compensate for a slightly worn tool, however this does then run the risk of having a tool catastrophically fail causing damage to the part being machined and leading to increased downtime (Kwon *et al.*, 2003).

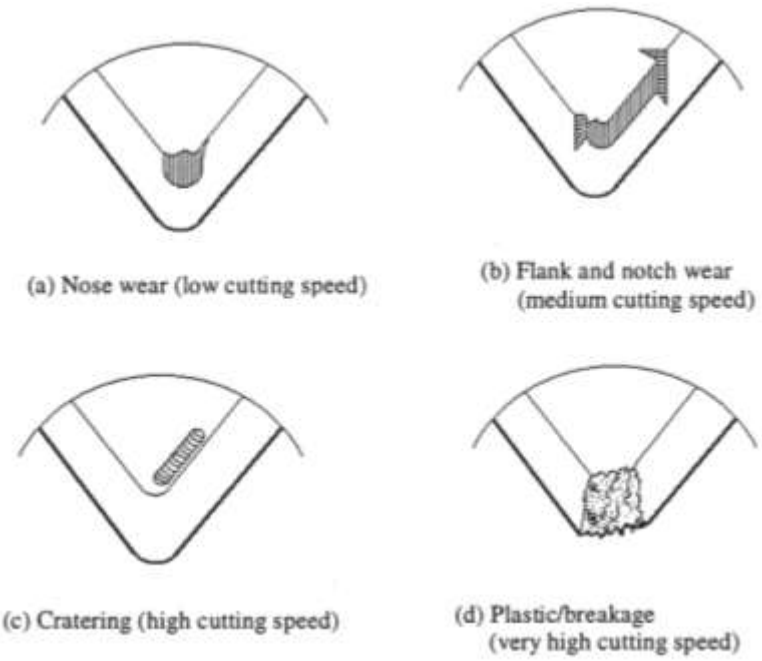

Figure 2.4. Common forms of cutting tool wear (Dimla Snr., 2000)

For aluminium machining, due to its relative softness, built up edge, despite not wearing the tool, becomes one of the main failure modes (Fig 2.5). BUE can be considered as a somewhat separate form of tool wear compared to crater, flank, notch, etc. as it tend to cause fluctuations in performance as the BUE gets deposited and removed progressively during machining. BUE has been shown to be unstable and unpredictable whilst having negative effects on many aspects of machining performance (Fang *et al.*, 2005). The phenomenon of the BUE associated with machining of softer materials has therefore been studied in great detail in itself so that techniques can be

employed to reduce its affect, although certain aluminium alloys, particularly ones with high silicon (Si) content, can cause additional problems when machining. This is because, as well as having the softness of the aluminium which adheres to the tool tip, the silicon rich particles are extremely hard and abrasive leading to the more traditional crater and flank wear mechanisms. This can be an issue as tools with high rake angles to reduce adhesion will have the cutting edge worn at a faster rate. Studies have found that high silicon aluminium alloys require harder tool materials to combat the abrasive wear of the silicon particles (Yanming *et al.*, 2000). They found that abrasive wear of the flank and as well as edge and corner breakage was common with hard tools. The size of the Si particles also made a significant difference with coarse particles increasing wear rates. Interestingly increased silicon content has also been shown to increase the amount of aluminium adhesion to the tool tip in both area and height (Yoshimura *et al.*, 2006).

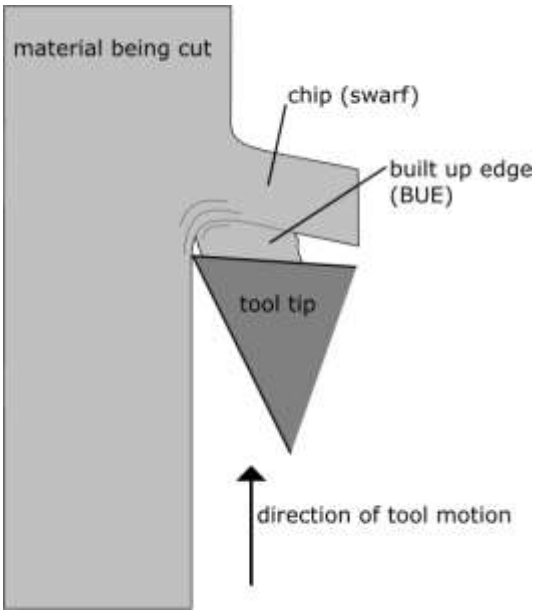

Figure 2.5. Built up edge on tool tip (wikipedia.org, 2015)

A number of studies have focused on the potential of effective dry and semi-dry machining of aluminium alloys in order to reduce costs and protect the environment. One study looked at the effects of different types of lubrication on the machining performance when turning Al 6061-T6 aluminium alloy (Kouam, 2012). Interestingly, as well as confirming that feed rate had the biggest influence on WP roughness, they found that dry machining consistently produced the best finish

compared to cutting with minimum quantity lubrication (MQL) and wet cutting. The investigation showed that the effect of lubrication on surface roughness increased with increasing feed rates. After cutting for 40 minutes at a depth of 1mm in dry, MQL and wet conditions, they found that WP roughness did not degrade in all conditions, implying that tool wear was negligible. Additionally they found that the tool wear was increased in wet cutting whilst aluminium adhesion was similar for all conditions. The majority of investigations into the dry machining of aluminium alloys have tended to focus on the adhesion of aluminium to the tool tip in the form of built up edge or built up layer (Kilic *et al.*, 2007; List *et al.*, 2005) as this still remains a major limiting factor when machining many aluminium alloys. They also confirmed that lower cutting speeds lead to increased Al adhesion which is why aluminium is generally machined at high speeds in order to combat BUE.

When considering tool failure due to adhesion of the WP material to the tool, it has also become important to understand that the adhesion mechanisms can vary. Distinguishing between the different types of adhesion then becomes necessary when trying to combat it. A number of studies have made a point of analysing the variations in aluminium adhesion, particularly the difference between built up edge (BUE) and built up layer (BUL). BUE is considered to be the formation of material on the cutting edge whilst BUL relates to adhesion on the rake face (Sánchez *et al.*, 2005; Gómez-Parra *et al.*, 2013). Investigations found that the BUL which initially forms at the cutting tip consisted of the metal matrix only, with the alloying particles mostly being removed with the chip. The BUE then forms on top of this, consisting of both matrix and alloy particles, along the cutting edge. This adhered layer can then grow beyond the edge of the tool affecting the geometry of the tool tip in turn potentially affecting WP quality (Carrilero *et al.*, 2002). They concluded that the Al BUL acts to reduce cutting temperatures due to it comparative softness which alloys the cooler harder material to maintain the strength to form BUE over the tool tip edge. Further studies showed that after just 10 seconds of cutting a BUE and BUL formation developed due to a combination of temperature and pressure at the tool-chip interface. Once the initial adhesion has occurred it becomes easier for further material to attach itself, however, after longer trials the BUE reached a

critical thickness and did not expand further (Sánchez *et al.*, 2005). The reduced temperature requirements for secondary adhesion wear were confirmed in a later study which also went on to show that WP surface roughness improved in the first few millimetres of cutting with the average roughness (Ra) value dropping by as much as half (Gómez-Parra *et al.*, 2013). Another study confirmed that diffusion can occur at higher temperatures, which leads to increased wear. This occurs as previously adhered WP material is removed in further machining, taking some of the tool material with it (List *et al.*, 2005). They concluded that the adhered material might even prolong tool life at higher cutting speeds providing the right conditions could be met.

Researchers went on to demonstrate that the tool-chip contact had three zones; an initial area of adhesion at the cutting edge, a sliding zone with no adhesion and then a final area of adhesion behind the sliding zone (Kilic *et al.*, 2007). It was deduced that the adhesion of the second sticking zone was due to the chip beginning to oxidize, this created an extra bonding mechanism between WP and tool through the more readily bonding oxygen. As well as the direct results BUE had on machining performance, one study also looked into how it affects the machining process in terms of its influence on machining vibrations. The investigation differentiated between different BUE regions which were dependant predominantly on cutting speed and slightly lesser on feed rate (Fang *et al.*, 2005). They found that at very low cutting speeds vibration amplitude was much less, yet it was also less predictable. As the cutting speed was raised past 20m/min the vibration amplitude peaked and any further increase in cutting speed had no further affect.

Although many studies have shown how cutting parameters can be altered to improve machining performance, tool materials have been shown to be a limiting factor when trying to effectively machine aluminium alloys in an efficient and environmental way. Thin film coatings applied to cutting tools have therefore been developed and used in order to improve cutting performance yet further.

2.2.3. Tool coating technology

Thin film coatings are already being utilized to increase the efficiency and performance of machining processes by improving the interaction between WP and tool, in fact the majority of carbide tools being used in industry are now coated, either by PVD or CVD methods (Astakhov, 2011). This is in part due to the fact that carbides provide an excellent substrate for many coating, particularly PVD deposited carbide and nitride coatings such as TiN, TiAlN and TiCN. For this reason carbide and nitride coatings are commonly used in industry. Cubic boron nitride coatings have more recently been developed to offer an improvement on the hardness of the ceramic coatings as well as reducing the chemical affinity when machining heat resistant super alloys, cast irons and hardened steels. Diamond and diamond like carbon coatings are currently being used to further improve the machining of modern materials (Byrne *et al.*, 2003). Diamond is considered to be one of the hardest known naturally occurring materials making it unparalleled in wear resistance, however, in addition to that the diamond is also chemically stable towards none-ferrous material, which has a positive effect on reducing potential adhesion of WP materials of this type (Chattopadhyay *et al.*, 2009; Beffort *et al.*, 2004). It is important to keep in mind that the benefits of the various tool materials are greatly influenced by the workpiece material. The hardest tool material is not necessarily the best for the job, it is also important to consider thermal stability, chemical inertness and of course cost, when choosing machine tools. Diamond coatings are expensive to produce meaning they are still not cost effective in many applications. DLC coatings can range from being relatively soft, to being almost as hard as diamond depending on the deposition method and parameters. Being carbon based they also benefit from chemical inertness whilst also being generally cheaper to produce than diamond. One drawback with some DLC coatings, however, is that the thermal stability can be too low to cope with high temperature machining operations (Pastewka *et al.*, 2010; Vandevelde *et al.*, 1999).

One of the biggest limitations to many tool coatings, particularly diamond and DLC coatings, is due to a build-up of residual compressive stresses in the material (Huang *et al.*, 2008; Wang *et al.*, 2007). These thermally induced stresses are as a result of the material cooling after the deposition process. For this reason the thickness of coatings becomes limited as an increase in coating thickness leads to an increase in residual stress (Wei *et al.*, 2007; Sheeja *et al.*, 2002). This is one of the main causes of delamination in coatings as the stresses overcome the adhesive force between the coating and the substrate. As well as coating thickness, the stresses will also be affected by substrate geometry, in particular sharp edges (Sheikh-Ahmad *et al.*, 2015; Erasmus *et al.*, 2011; Renaud *et al.*, 2009). Thermal processing through annealing, as well as doping with metals and silicon, have been shown to be effective in reducing residual stresses whilst minimising the reduction in film hardness, however, a balance needs to be achieved in order not to compromise the coating properties (McNamara *et al.*, 2015; Li *et al.*, 2006; Okpalugo *et al.*, 2004). Managing the residual stresses in the coatings will therefore be a significant issue when developing the coatings for this investigation.

2.3. Diamond coatings

2.3.1. Structure and properties

Extensive research into diamond coating has been conducted leading to constant improvements in coatings and coating deposition technology. Diamond as a material is of great interest to engineers due to its structural integrity, mechanical, electrical and optical properties. It is the strong covalent bonds between carbon atoms which create the extreme hardness and resistance to abrasion, for this reason the main wear mechanisms of diamond is usually chipping due to its brittle nature. The unique and extreme properties of diamond include an unmatched mechanical hardness of 100GPa, which allows for excellent wear resistance, as well as a thermal conductivity of 2,000W/mK at room temperature and high electrical resistivity of $10^{16}\Omega$cm. It is also well known for its corrosion and erosion resistance due to its chemical inertness (Varnin *et al.*, 2006).

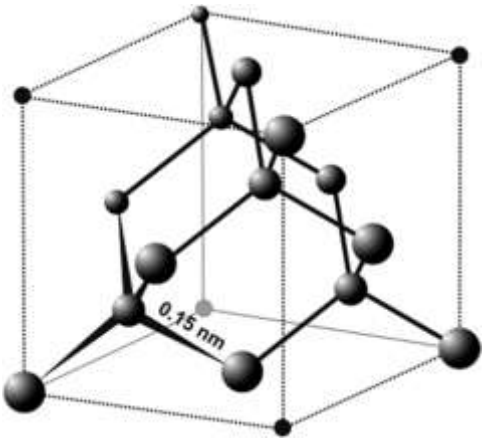

Figure 2.6. Diamond Structure (Gracio *et al.*, 2010)

The properties of diamond are due to its unique chemistry and bonding structure (Fig 2.6). Diamond is hard wearing and unreactive due to the strength of the covalent bonds (347kJmol^{-1}) which require large amounts of energy to break (Gracio *et al.*, 2010). It is the combination of light weight and strong bonding which gives diamond many of its unique properties. This structure allows for high vibration frequency which leads to high thermal conduction. In addition to the well-known properties of pure diamond it is also necessary to distinguish the variation between different forms of synthesised diamond structures. Synthesised diamond will usually be in the form of polycrystalline diamond (PCD) and CVD deposited diamond structures. Their individual properties will generally be affected by the crystal sizes of the diamond material whose grain size can range from the nano-scale to over 20µm in size. Any diamond layer containing crystals with average sizes over 1µm will be considered micro-crystalline diamond (MCD) whilst anything below is considered nano-crystalline diamond (NCD). In some cases diamond layers with crystal sizes of less than 10nm are produced and have been considered to be ultra nano-crystalline diamond (UNCD). The contact planes between the crystals create weak points and fracture planes which cause failures in the coatings. For this reason deposited coating with smaller crystal sizes will generally have an increased wear rate compared to larger crystal diamond structures. On the other hand internal stresses may be reduced, producing a tougher material, which may be preferable in conditions in which shock and vibration are predominant.

2.3.2. Deposition methods

Diamond synthesis was initially conducted using high pressure high temperature (HPHT) techniques and although initially reported from as early as 1880, reproducible results were not confirmed until 1955. Chemical vapour deposition (CVD) techniques were developed and confirmed around the same time. It wasn't until the 1960's, however, that efficient deposition techniques became a reality after it was discovered that hydrogen incorporation was key to increasing growth rates due to hydrogens preferential etching of graphite sites during deposition (Angus *et al.*, 1968). Improvements in deposition technology have meant that diamond can now be deposited using a number of different methods, each with their own strengths and weaknesses. The most common deposition methods are based around CVD technology, as it allows for much lower pressures and temperatures, which in turn permits a greater range of substrate materials. These methods include: thermal, DC plasma, RF plasma and microwave plasma (Bachmann *et al.*, 1992). The general mechanism for diamond growth involves the deposition of carbon atoms that come from the dissociation of a carbon containing gas onto a substrate (Gracio *et al.*, 2010). For the purposes of this project it will not be necessary to consider the potential of all methods, instead the main focus will be on thermal CVD, in particular the HFCVD method.

2.3.3. Hot filament chemical vapour deposition

Deposition of diamond using CVD techniques involves depositing carbon from the dissociation of gas containing carbon (Gracio *et al.*, 2010; Varnin *et al.*, 2006). The general conditions for the growth of HFCVD diamond include; substrate temperature 600°C – 1050°C, filament temperature 2000°C – 2400°C, chamber pressure 20mbar – 80mbar, and gas flow rates between 100sccm – 500sccm. The basic setup of a HFCVD system involves using a vacuum chamber, in which there is a filament positioned at a specific distance from a target substrate on which the diamond forms (Fig 2.7).

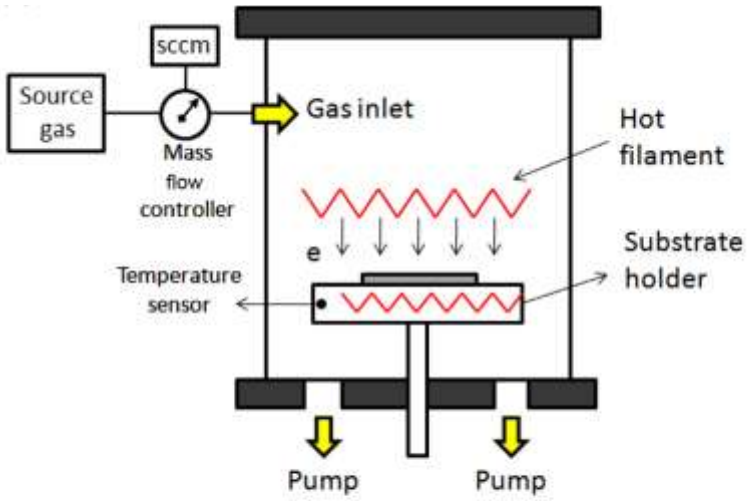

Figure 2.7. HFCVD apparatus diagram (Pessoa *et al.*, 2015)

A vacuum pump system is used to initially produce the very low pressures required. The gases, usually a hydrocarbon and hydrogen mixture, are let into the chamber at a ratio of around ≤2% hydrocarbon to hydrogen content. The gas phase is activated by the hot filament which provides the energy for the atoms to dissociate and deposit onto the target substrate. A bias voltage between the filament and substrate will also often be used to help attract the ionic species to the substrate surface. The substrate holder will often be heated, as a high substrate temperature is required in order for diamond growth to occur. Figure 2.8 shows the standard model describing the growth of diamond by way of a typical methane in hydrogen mix. Due to the concentration of hydrogen it is considered that for the majority of the substrate dangling bonds are passivated by hydrogen (H) atoms. These are then etched away by other H atoms until a carbon species attaches itself to the surface. Any H atoms attached will then be etched and replaced by further C-C bonds, which do not etch as readily, leading to a steady growth of tetrahedral bonded carbon.

Although this is a simplified model of diamond growth, it can be seen that in order for the carbon to deposit in a tetrahedral formation there needs to be a substrate which will promote the growth of the diamond layer.

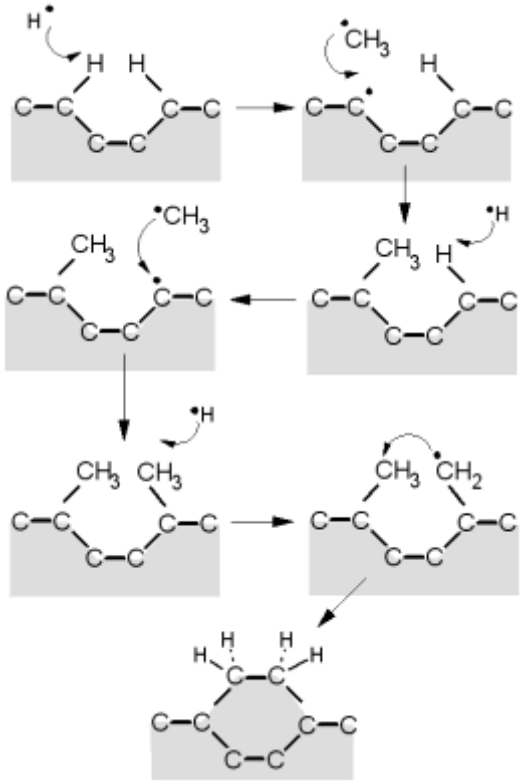

Figure 2.8. Standard growth model for CVD diamond (www.chm.bris.ac.uk, 2015)

Therefore when coating a non-diamond substrate there is usually a nucleation step required. This will often involve applying diamond seeds to the substrate surface from which the diamond films will nucleate and grow. HFCVD is a useful method for deposition diamond as it allows for easy manipulation of the properties by slightly altering deposition parameters, namely the amount of hydrogen (Gracio *et al.*, 2010).

2.3.4. Effect of deposition parameters

When setting up a HFCVD system for the deposition on diamond on a substrate, one of the initial parameters to consider will be the separation between the filament and the substrate. It is, however, worth appreciating that filament - substrate separation will be set in accordance with other deposition parameters. This is partly due to the affect it has on substrate temperature. One group conducted a comprehensive study of the effects of parameters on the growth rates of diamond coatings using HFCVD (Zhou *et al.*, 1994). It was discovered that growth rates increased as

distance decreased, however, if the distance was too small the substrate temperature became unstable, negatively affecting deposition.

Further studies highlighted that substrate temperature depended on the filament to substrate distance, smaller distances were shown to increased substrate temperature and produced larger crystals whilst lower temperatures produced a surface with a more nodular formation (Ali *et al.*, 2012). Similar observations were made in which Raman analysis was utilised to highlight an increase in graphitic structures at greater distances from the filament. This was coupled with confirmation of reduced deposition rates, as shown by thinner films, and visibly reduced crystal sizes as shown by SEM micrographs (Wei *et al.*, 2011).

Gas ratios have often been studied in conjunction with substrate to filament distances as well as temperatures of both substrate and filament. It has been shown that by altering the methane in hydrogen ratio and substrate temperature it is possible to create diamond films ranging from faceted crystalline, to fine ballas (nodular) morphologies (Bogus *et al.*, 2008). The different morphologies of the diamond coatings in turn have a significant effect on micro and nano-mechanical properties of the diamond films. Studies have shown that faceted (large crystal) diamond was found to have the highest hardness whilst the fine ballas diamond tended to have the lowest friction levels. Altering chamber pressure was also shown to affect the crystallinity, morphology and uniformity. Studies showed that pressures between 10 and 20Torr gave superior crystallinity to those with higher pressure, whilst lower pressures produced coatings with poorer uniformity (Chattopadhyay *et al.*, 2008; Sarangi *et al.*, 2008a).

As well as the traditional methane hydrogen mix employed in the majority of studies, the addition of argon (Ar) in the HFCVD process has also been investigated (Zhang *et al.*, 2001; Lin *et al.*, 2000). It was shown that by increasing the argon content it was possible to increase diamond growth rates, as well as alter the morphology of the coating. One study showed that when Ar concentration reached 90% the diamond film began to switch from an MCD to a NCD structure. Another study, however,

determined that as the argon content is raised above 50% the diamond quality begins to decrease due to increased amount of non-diamond carbon deposition (Benzhour *et al.*, 2010). Sun, et al. showed that the inclusion of acetone along with argon can potentially have a positive effect on diamond growth. The investigation confirmed that the reduced diamond formation which occurs with high Ar percentages, up to 90%, was shown to improve adhesive strength and surface roughness (Ma *et al.*, 2007). The study did not test the effect on hardness which would have likely been reduced as a result. As well as highlighting how the deposition parameters can alter the coating topography and mechanical properties, these studies have highlighted that the ideal coating won't necessarily be the hardest but will be a combination of hardness, friction, and adhesion to the substrate.

Despite CVD diamond being successfully grown on a number of substrates, there are still major issues concerning the growth of diamond on cemented carbides which must be overcome. The main issues include nucleation, internal stress and adhesion (Huang *et al.*, 2008; Sein *et al.*, 2004; Polini *et al.*, 2002; Endler *et al.*, 1996). It is widely known that the root of the problem regarding diamond adhesion to cobalt cemented tungsten carbide (WC-Co) is due to the cobalt binder (Lai *et al.*, 2011; Sarangi *et al.*, 2008b). This is because the cobalt increases formation of non-diamond carbon (graphitization) at the interface making it impossible to coat untreated substrates (Wei *et al.*, 2010; Sein *et al.*, 2004; Polini *et al.*, 2003; Sun *et al.*, 2003). The topography of the cobalt surface further reduces the potential mechanical adhesion between the diamond and WC-Co as it creates a flat surface which the diamond crystals are unable to lock into as they grow.

A number of different methods have been employed in an attempt to solve these problems of adhesion with some success. Acid etching has been considered as a viable method to remove the cobalt binder from the surface of the substrate (Sein *et al.*, 2004). It has become a common method due to its relative cheapness and availability. These methods, however, have had mixed results with some reporting that the reliability is low and can lead to poor uniformity (Chou *et al.*, 2010). One of

the reasons for this poor reliability is that often the substrates themselves will have inhomogeneous patches of cobalt rich or WC rich areas, making it difficult to ensure to etch the entire surface to a similar depth.

Attempts to improve acid etching techniques are on-going as they currently provide the simplest and cheapest way to promote reliable nucleation and adhesion. Acid etching treatments usually involve hydrochloric and nitric acid although many studies have considered the addition of potassium ferricyanide and potassium hydroxide (Murakima's reagent) (Wei *et al.*, 2010; Kamiya *et al.*, 2002; Polini *et al.*, 2002). Sulphuric acid and hydrogen peroxide are also used in conjunction for improved cobalt removal (Sarangi *et al.*, 2008a; Sarangi *et al.*, 2008b; Polini *et al.*, 2002). Although acid etching remains the most viable pre-treatment, investigations have been made into more reliable methods. Some groups have investigated the potential of plasma and laser etching compared to the well-known acid etching techniques (Tiejun *et al.*, 2002). This was with the aim of overcoming the reliability issues associated with acid pre-treatments. The advantage of this form of etching is that there is much more control over the level of cobalt removed. A study discovered that there was an optimal power which removed the cobalt without adversely affecting the WC structure. This form of pre-treatment had other benefits for the coating process. By decarburizing WC, the adhesion strength was greatly improved and residual stresses in the film were reduced (Barletta *et al.*, 2011; Sun *et al.*, 2003).

One of the issues involved in the acid etching process is that is can weaken the structure at the surface resulting in premature failure. For this reason other potential methods have been considered. Interlayers have been shown to help create a barrier to prevent the inhibiting effects of cobalt on nucleation and adhesion (Sarangi *et al.*, 2008b; Wei *et al.*, 2007; Endler *et al.*, 1996). Due to the high temperatures involved in HFCVD deposition, the interlayer materials are limited. Investigations have been made into the potential use of silicon, titanium, titanium nitride, titanium carbide and aluminium. Titanium coatings were found to offer little improvement due to high stress

differences between the layers and out of all titanium interlayers tested, pure titanium was shown to provide the greatest improvement to nucleation and adhesion (Sarangi *et al.*, 2008b). Silicon has been shown to provide a compatible surface with reduced stress for improved coatings capable of machining applications (Endler *et al.*, 1996). Aluminium has also been considered as an interlayer and was deposited onto WC as well as TiN coated WC. In both cases the aluminium was shown to greatly improve nucleation and adhesion of diamond (Li *et al.*, 2008). Tungsten particles have been used to enhance diamond growth. Various size particles were investigated and it was found that 2µm particles produced an optimum coating for abrasion resistance as it formed films with highest hardness (Lai *et al.*, 2011).

In order to further improve the coating – substrate interface, negative bias voltages have been utilized to enhance nucleation density and coating uniformity. Very high voltages were shown to reduce surface roughness leading to great improvements for tribological applications (Chattopadhyay *et al.*, 2008; Sein *et al.*, 2004). It was also discovered that different bias setting could also allow for further tailoring of the coating morphology (Whitfield *et al.*, 2000).

2.3.5. Diamond coatings for aluminium machining

In addition to investigations of the deposition parameters and the effects on coating characteristics and mechanical properties, further studies have been built on this to investigate the potential machining performance of various diamond coating morphologies. Many studies have tested diamond coatings for their potential in drilling, milling and turning applications. These studies considered the potential for improved machining performance in both dry and wet cutting scenarios, as well as semi-dry, which involves MQL.

Diamond coatings produced using the CVD method have been shown in a number of studies to offer improved performance, particularly in dry machining (Chou *et al.*, 2010; Hu *et al.*, 2007; Sun *et al.*, 2003). Results have shown that delamination is still a main cause of CVD tool failure and is

considered the limiting factor in tool life performance (Hu *et al.*, 2007; Polini, 2006; Polini *et al.*, 2003). Diamond coatings where found to offer improved cutting performance compared with other coatings such as TiN due to its reduced chemical affinity with aluminium (Chattopadhyay *et al.*, 2009; Roy *et al.*, 2009). When compared to a number of different titanium or aluminium oxide based coatings, MCD diamond was shown to suffer no BUE in short Al turning trials despite having a much rougher coating surface (Roy *et al.*, 2009). Recent studies have concluded that PCD coatings are often better performing than CVD diamond, due to the poor adhesion of MCD and NCD coatings. Delamination of the films leads to early failure, despite CVD initially creating improved workpiece finishes and improved efficiency. Others reported that with the right pre-treatment CVD could be as good as PCD (Polini, 2006). Delamination of MCD and NCD coatings was shown to be a catastrophic failure mode, even after just a few minutes of turning. It was also suggested that BUE may also be responsible for the onset of delamination of coatings (Hu *et al.*, 2007). The machining performance of coated tools, as well as being unreliable to predict, was greatly affected by hard non-metallic components of the WP and it was confirmed that the wear mechanisms of the tool is heavily dependent on the type of aluminium alloy being machined (Roy *et al.*, 2009). Studies of both drilling and turning applications found that for improved WP finish nano-crystalline diamond can be preferable, even ultra-nano crystalline diamond (UNCD) has been developed to further reduce coefficient of friction (COF) and improve WP quality (Hanyu *et al.*, 2003a; Hanyu *et al.*, 2003b; Sun *et al.*, 2003). The fine grained diamond coatings also improved tool life, particularly in drilling as they significantly reduced the development of BUE.

The key factors relating to the diamond deposition and coating properties for this project will relate to the adhesion between substrate and coating as well as the surface morphology of the films. The literature has shown that diamond coating, deposited onto cutting tools using the CVD method, have the potential to effectively dry machine aluminium alloys. It is imperative, however, to ensure that the pre-treatment of WC-Co substrates is sufficient to promote good adhesion of the coating. Delamination of the coating at the cutting tip is often considered catastrophic failure as it can lead to

unacceptable WP roughness as well as having deleterious effects on all aspects of machining performance.

2.4. Diamond like carbon coatings

2.4.1. Structure and properties

The properties of carbon have been utilized for many years, these properties however, are greatly dependent on the form the carbon has taken, be it the low friction of graphite, or the ultra-hardness of pure diamond (Fig 2.9). Since the initial synthesis of diamond it has been possible for engineers to create transition materials which contain both the diamond like sp^3 bonds for ultra-hardness and the graphite like sp^2 bonds associated with low friction surfaces. Synthetic amorphous carbon coatings such as DLC have been shown to have high hardness and wear resistance whilst simultaneously maintaining low friction coefficients (Robertson, 2002; Inkin *et al.*, 2000).

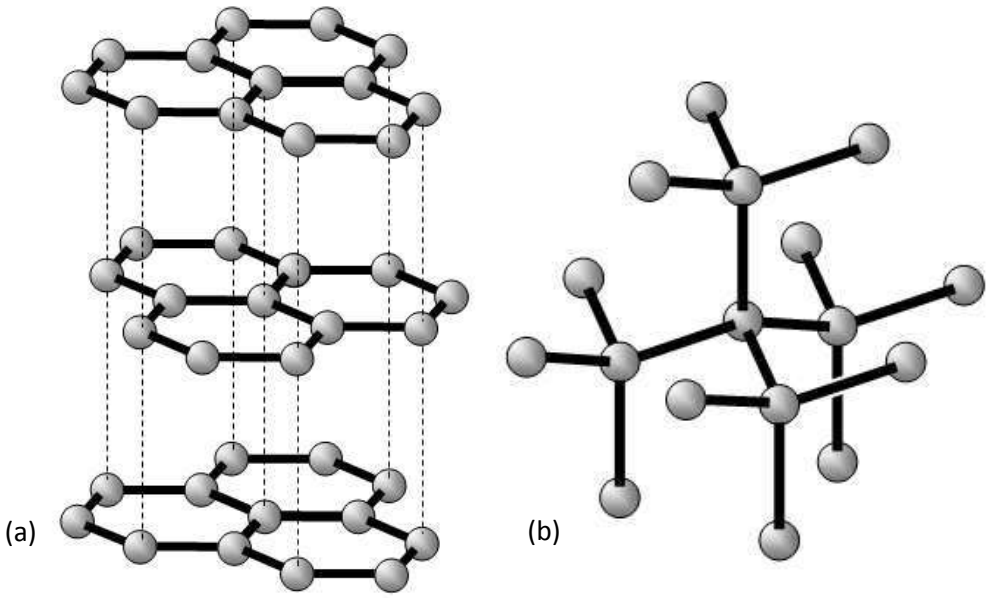

Figure 2.9. Structure (a) graphite (b) diamond (Hainsworth and Uhure, 2007)

Diamond-like carbon is a form of amorphous carbon which contains both diamond like tetrahedral sp^3, and graphitic sp^2 hybridised bonds. DLC can therefore simultaneously contain properties such as high hardness and corrosion resistance, as found in diamond, as well as the low friction, lubricating properties of graphite. They are generally not as hard as diamond coatings, however, they do have

many other advantages in comparison. On top of the significantly lower COF, DLC coatings can be deposited at much faster rates and significantly lower temperatures. This allows for lower production costs as well as providing the option for many more potential substrate materials, particularly ones with lower thermal stability.

Intense research of diamond like carbon coatings began in the mid-1980s (Erdemir *et al.*, 2006; Lifshitz, 1999), during which time several methods of been developed for the deposition of DLC thin films. The different deposition techniques, along with depositions variables, have allowed for a large range of DLC coatings to be created.DLC films have therefore been categorised further. They include hydrogenated DLC (a-C:H), non-hydrogenated DLC (a-C), tetrahedral amorphous carbon (ta-C) and hydrogenated tetrahedral amorphous carbon (ta-C:H). The bonding distribution of the DLC coatings can be broken down into three key areas, allowing for the different types of DLC coating to be compared using a ternary phase diagram (Fig 2.10).

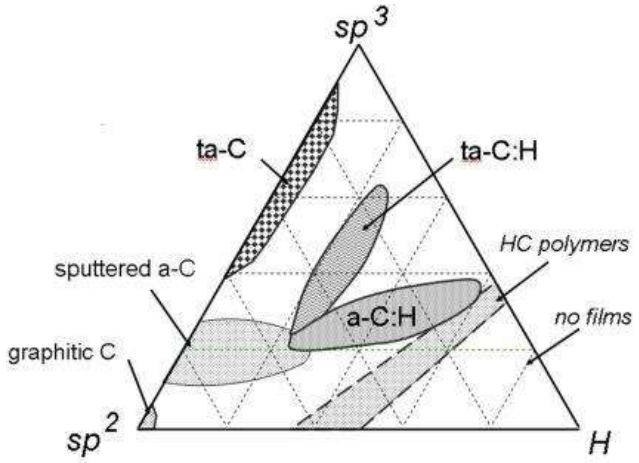

Figure 2.10. Ternary phase diagram of amorphous carbon (Robertson, 2002)

Dopant's such as silicon, nitrogen and metals are also being used to further enhance diamond like carbon coatings (Batory *et al.*, 2015; Wang *et al.*, 2007). The current methods used for depositing DLC can be split into two main categories, physical vapour deposition (PVD) and chemical vapour deposition (CVD). The common feature of all the deposition methods is that DLC films are grown using a beam of C^+ or C-H ions with energies around 100 eV. The PVD methods have a higher concentration of sp^3 bonds and are used to create ta-C and ta-C:H films. CVD methods are used to

produce ta-C:H and a-C:H films with stabilised sp^3 bonding. In order to engineer an optimal DLC coating, it will be important to understand the growth mechanisms involved in DLC deposition.

The hydrogen contents in DLC coating can range anywhere from 0 to 65% in concentration (Robertson, 2002). Generally the ta-C films have lower wear rates due to the higher percentage of sp^3 C-C bonding whilst the a-C:H films benefit from reduced friction. It has been shown that this is in part due to the graphitisation of the a-C:H films which leads to higher wear whilst simultaneously reducing friction (Ronkainen *et al.*, 2001). One of the main advantages of DLC compared to diamond is down to the deposition processes involved, much higher growth rates can be achieved at low temperatures due to the fact that DLC growth is not thermally activated, hence the sp^3 bonding can form at ambient temperature (Robertson, 2008). One article has created a visual depiction of the hydrogen containing amorphous structure of a-C:H coatings (Fig 2.11).

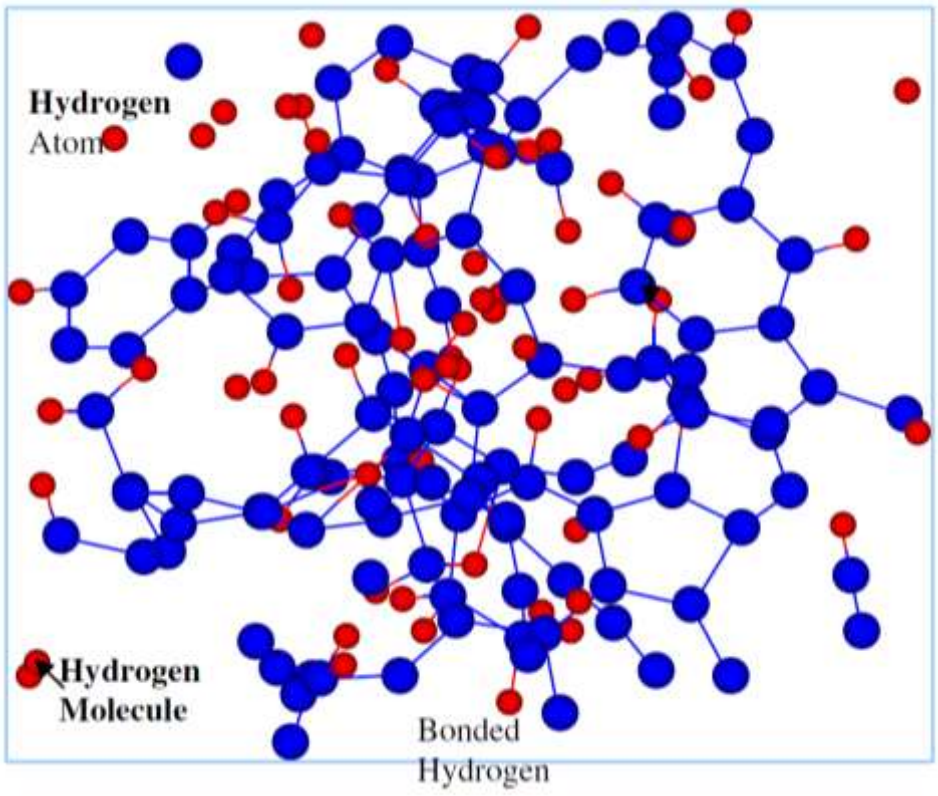

Figure 2.11. Hydrogenated DLC structure from (Erdemir and Donnet, 2006)

2.4.2. Deposition methods / mechanisms

Unlike diamond, the variability of DLC coatings means that a much broader range of deposition techniques can be employed. The two main deposition technologies, PVD and CVD, refer to processes which either generate the carbon species from a solid carbon source, or from hydrocarbon gases (Bull, 1995). Gas source processes include plasma enhanced chemical vapour deposition (PECVD), ion beam deposition and cathodic arc deposition. Solid source processes include sputtering, ion beam sputtering, laser ablation and vacuum arc (Hainsworth *et al.*, 2007; Grill, 1999). Each process has its own strengths and weakness which affect the growth rates, potential substrates and also the characteristics of the coating. Deposition methods have therefore often been divided into those useful for industrial applications and those more suitable for use in a laboratory environment (Robertson, 2002). The deposition methods can be split between hydrogenated and hydrogen free coating deposition methods with the PVD methods generally being responsible for the harder, hydrogen free coatings. These coatings will often have higher internal stresses which limit the potential thicknesses to no more than 1µm (Erdemir *et al.*, 2006). The hydrogen in the a-C:H coatings acts to reduce stresses, allowing for much thicker coatings, although they too will be limited to a few microns, as the internal stresses will become to great and coating failure due to delamination occurs. Due to the extensive range of deposition technologies and potential coating characteristics, it is necessary to draw the focus to the rf PECVD method that will be utilised for this project (Zolgharni *et al.*, 2008).

2.4.3. Plasma enhanced chemical vapour deposition

Radio frequency (rf) PECVD is widely considered to be the most common laboratory method as it allows for significant tailoring of the coating properties. The reactor contains two electrodes of unequal area with the rf power normally being coupled to the smaller electrode on which the substrate is attached. The other electrode is earthed. The rf power generates the plasma between

the electrodes which has a positive voltage in comparison. The negative voltage of the smaller electrode accelerates positive ions towards the substrate, facilitating the ion bombardment required to create the sp^3 bonds.

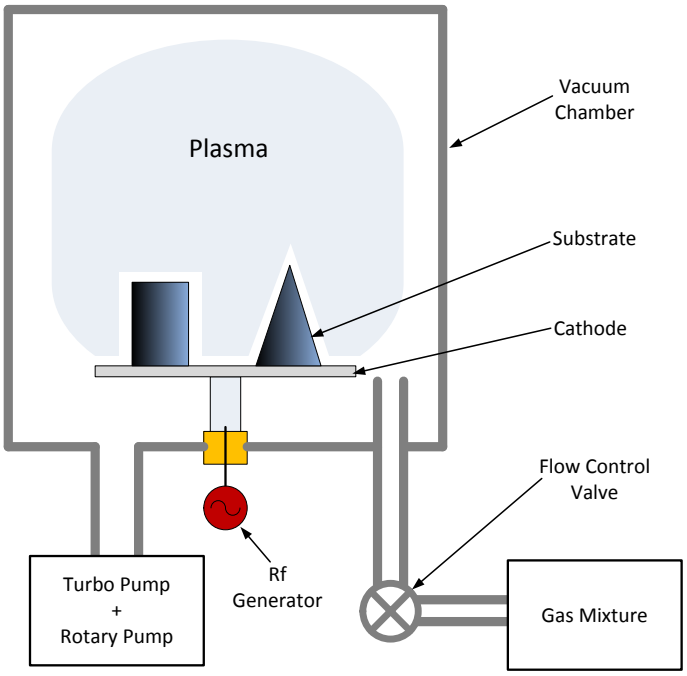

Figure 2.12. PECVD reactor diagram

Some PECVD systems will use two plates inside the reactor chamber to act as the anode and the cathode. The system used in this project, as shown in the diagram above (Fig 2.12), instead uses the metal shell of the chamber to act as the anode whilst a plate, or conductive object positioned in the centre becomes the cathode. The plasma therefore forms uniformly in the centre of the chamber. Low pressure is required in order to reduce molecular collisions which can cause the ions to lose energy, particularly as the ionised species are thought to only account for 5% - 10% of the gas particles in the chamber. It is important to minimise these collisions so that a narrow ion energy distribution can be maintained (Robertson, 2002).

The most significant aspect of the deposition is the sp^3 bonding which is known to be a physical process of ion bombardment. It is the C+ ions with energies around 100eV which form the highest sp^3 fractions (Lifshitz, 1999). The theories regarding mechanisms of DLC growth have been disputed, although a general consensus has been reached by the majority of researchers that subplantation is

responsible for the diamond like properties (Erdemir *et al.*, 2006; Robertson, 2002). According to this model a metastable increase in density, due to energised species penetrating the surface layer, causes bonding to change to sp^3. This theory is currently still being investigated and to a certain extent proved through analytical simulation (Kohary *et al.*, 2001). It has also been shown that at the initial stages of the deposition process the carbon begins to form on the substrate in small nucleation areas, or islands. These islands created from primary nucleation sites expand, and join nearby islands, whilst secondary nucleation sites begin to form more islands. These islands then coalesce to form a continuous film across the substrate surface (Maheswaran *et al.*, 2011).

2.4.4. Effect of deposition parameters

DLC coatings have been shown to exhibit many different properties depending on the deposition method and parameters. These properties range from ultra-hard ta:C coatings to softer, more lubricious, hydrogenated a-C:H coatings. The properties of the coatings are mostly attributed to the bonding structure, particularly the amounts of sp^2 and sp^3 bonding in the material. Although, where hydrogenated DLC coatings are concerned it must also be noted that H-C sp^3 bonding will also occur adding further variability to the properties. Researchers have investigated the effects of a range of parameters associated with DLC deposition in great detail. These parameters not only consider the settings of the reactor during deposition, but also the substrate preparation and post-deposition treatments that can be used to further enhance the thin film properties.

The investigations into effects of deposition parameters can be considered to be threefold, firstly there are the deposition parameters themselves to be considered, then there is the effect of the process parameters on the material characteristics and deposition rate, lastly how do the characteristics influence mechanical properties. Analysing the impact of parameters on the coating properties is complicated further due to the fact that they are not individually exclusive. For instance, the effect of bias voltage will be slightly different at a higher chamber pressure, than at a

lower pressure. In this section the general effects of the individual deposition variables will be explored, as well as giving consideration to how the variables can interact with one another, in order to be able to optimise the coating characteristics to their full potential.

Bias voltage is arguably the most important variable in the PECVD process. This is due to the fact that the coating characteristics are predominantly influenced by the energies of the impacting ionic carbon species which build up to form the coating (Theye *et al.*, 2001; Xu *et al.*, 1997). For this reason many investigations have focused on varying the bias voltage or RF power and measuring the effect on material characteristics and properties. Studies have found that increasing the bias voltage, as well as having an immediate effect on deposition rates (Capote *et al.*, 2006; Clay *et al.*, 1998), generally leads to an increase in the sp^3 C-C bonding as well as a reduction in the amount of hydrogen present in the films (Ravi *et al.*, 2007; Donnet *et al.*, 2000). This has been shown to create harder, smoother coatings with improved wear rates (Bao *et al.*, 2005; Choi *et al.*, 2005; Sun, 2000). Many studies did find, however, that there was often a peak voltage which gave the highest values for either deposition rate (Ravi *et al.*, 2007; Choi *et al.*, 2005), hardness (Bruno *et al.*, 2004; Sun, 2000; Xu *et al.*, 1997) or roughness values (Cho *et al.*, 2005; Sun, 2000). Despite increasing hardness of coatings, the majority of the studies reported a decrease in sp^3 bonding with increased voltage (Kim *et al.*, 2005). This is probably due to the fact that the measured sp^3 percentage is often conducted using Raman spectroscopy which doesn't differentiate between C-C and H-C sp^3 bonds. The sp^3 bonding only improves the hardness when it is between two carbon atoms otherwise it is simply passivated by hydrogen. There are also some contradicting results which show reduced hardness with increasing voltage (Choi *et al.*, 2004). Due to the great variation between the fixed parameters, as well as the different ranges being used in the variable parameters, studies have produced differing results (Maître *et al.*, 2005; Li *et al.*, 2004). Despite being classed as PECVD processes, there are also subtle differences in the equipment being used which can create further discrepancy (Wada *et al.*, 2011; Zhang *et al.*, 2002).

For this reason, as well as investigating the deposition parameters individually (Banerjee *et al.*, 2010; Choi *et al.*, 2005; Donnet *et al.*, 2000), the majority of studies looked at more than one parameter at a time to gain a better understanding of the interrelationships (Bao *et al.*, 2005). Many studies investigate the effect of chamber pressure in conjunction with bias voltage (Ravi *et al.*, 2007; Kim *et al.*, 2003; Sun, 2000). It has been shown that film roughness and deposition rate is greatly influenced by pressure. By increasing the pressure, the deposition rate could be increased and roughness reduced, however, there is a maximum pressure above which the deposition rate drops and roughness increases (Kim *et al.*, 2003). Higher pressures in the deposition chamber mean that there are more gas species, creating denser plasma, which initially increases growth rates. Increasing pressures, however, leads to a reduction in impinging ion energy due to an increase in collisions between the gas molecules. This reaches a point in which the average ion energy is too low to overcome activation barriers required for absorption (Cheng *et al.*, 2000). The variation in pressure is usually kept within a very small working range and has generally been shown to be useful for creating varying surface topographies which can affect friction and hydrophobicity properties (Banerjee *et al.*, 2010).

The effects of source gases mixtures and flow rates have been studied in great detail and have been shown to have a significant effect on growth rates and tribological performance (Hsu *et al.*, 2008; Erdemir *et al.*, 2000; Erdemir *et al.*, 1999). The most common carbon source gasses used in PECVD processes are methane and acetylene, usually in conjunction with argon or hydrogen. The C source along with Ar and H addition are generally considered as part of the standard coating regime. Addition source gases would be considered separately as doping agents designed to further modify coating characteristic to improve specific properties. For standard a-C:H coatings it was concluded that the effects of the source gases are due to the ratio of hydrogen to carbon atoms. Research has shown that by altering the C to H ratios the morphology of the coatings can be significantly altered. Increasing the H content in the source gas mix has led to smoother, harder coatings with improved wear rates (Hsu *et al.*, 2008), although studies with different systems have shown there to be peak

ratios for optimal deposition (Caschera *et al.*, 2011; Bruno *et al.*, 2004). It is also well known that the different gas sources work best at different bias voltages, this is due to the fact that for ideal deposition it is generally necessary to have 100V per carbon atom in the hydrocarbon molecule (Grill, 1999; Lifshitz, 1999). Due to this it was then found that acetylene produced coatings with improved mechanical properties whilst methane was preferred for electronic applications as it contained fewer impurities. Acetylene is a preferred carbon source, despite not having the highest deposition rate, due to it requiring low activation energy. Benzene has been shown to have a higher deposition rate, achieving this, however, requires much higher voltages, up to 3 times more, compared to acetylene (Robertson, 2002).

Argon dilution has also been studied in great detail as it has proven to be a useful etching agent for both, substrate pre-cleaning, and also for use during the film deposition stage to further enhance the conditions for improved coating properties. It was discovered that the percentage of Ar dilution not only alters the roughness of the coatings but also deposition rates. Roughness is reduced when Ar dilution is around 15% and greatly increases when Ar is above 30% (Jones *et al.*, 2011; Cheng *et al.*, 2000). It was also shown that deposition rates decreased with higher relative Ar gas percentages (Valentini *et al.*, 2001). As well as other common additional gas sources such as nitrogen (Tzeng, 2011), oxygen, helium (Clay *et al.*, 1998) and fluorine, vapour sources are also used to allow for alternative additives. Silane solutions are often used to create silicon (Si) species in the plasma either as an interlayer to improve adhesion (Zolgharni *et al.*, 2008; Capote *et al.*, 2006), or as an additive to the main DLC layer in order to alter mechanical, electrical and thermal properties (Schwarz *et al.*, 2008). Silicon incorporation has been shown to reduce friction (Kim *et al.*, 1999) and internal stresses with increasing Si content, although it also reduces hardness (Wu *et al.*, 1998). This is despite having an increase in sp^3 bonding (Zhao *et al.*, 2001; Buršíková *et al.*, 2002; Damasceno *et al.*, 2000). It was shown, however, that small amounts of Si, less than 2%, could also improve hardness and wear whilst still reducing compressive stress (Buršíková *et al.*, 2002; Damasceno *et al.*, 2000). Si incorporated coatings also showed improved thermal resistant with graphitisation occurring at

higher temperatures compared to standard a-C:H coatings (Wu *et al.*, 1999), as well as having a significant impact on electrical resistivity (Okpalugo *et al.*, 2004).

The requirement for a silicon interlayer for improved adhesion depends heavily on the substrate itself, not just the substrate material, but also the surface preparation prior to the coating deposition. Surface preparation can therefore take many different forms and can have an effect on the growth of the film, this in turn will potentially lead to large variation in characteristics between films which have been deposited with identical parameters. The potential pre-treatments will be as wide ranging as the potential substrate materials themselves, although there are a number of common treatments used in nearly all cases. A cleaning stage is nearly always used in which the substrate will be sonicated for roughly 10 minutes in pure water, followed by 10 minutes in a solvent, commonly acetone, isopropyl alcohol (IPA), ethanol or methanol. This is in order to remove any contamination from the surface. The samples will then be positioned in the deposition chamber and given an initial plasma etching cleaning stage in which an inert gas such as argon is used. This is to remove oxygen or other atomic scale impurities, which may impair adhesion, from the surface. Although, depending on the substrate material, it is sometimes necessary to ensure the correct etching time and power is used so that the substrate surface is not negatively affected (Jones *et al.*, 2011).

The substrate material is known to have an effect on the nucleation, growth, adhesion and morphology of the overlaying coating. Researchers discover which materials produced the best coatings and further studies strongly favoured silicon to base investigations on (Tzeng *et al.*, 2011; Ouchabane *et al.*, 2010; Ikenaga *et al.*, 2006; Kim *et al.*, 2003; Balachova *et al.*, 1999). This was partly due to good growth rates and adhesion properties between DLC and Si, as well as the fact that the smooth surface of silicon had less effect on the final coating topography than rougher substrates. When hardness and wear performance measurement were required, harder substrates such as tool steel were then used. Other substrate materials were therefore usually only used when researchers

were specifically interested in developing coatings for particular applications (Lin *et al.*, 2008). A number of researchers investigated the effect of the underlying substrate topography on the development of the DLC deposition and final coating structure. The effect of substrate roughness was often considered along with deposition time, as an increased deposition time meant thicker coatings which were able to deviate further from the original substrate topography. Generally rougher substrates led to rougher coatings (Singh *et al.*, 2008; Zhong *et al.*, 2008), although with increased deposition time the effects were reduced (Mousinho *et al.*, 2009). The rougher coatings associated with rougher substrates were also shown to have increased wear rates (Jiang *et al.*, 2000). Interestingly some studies highlighted an initial increase in roughness on rougher substrates with sharp peaks due to the DLC initially favouring deposition on the apices before filling in the lower valley areas (Zhong *et al.*, 2008; Vladimirov *et al.*, 2000).

One of the key limitations with DLC coatings is their dependence on the environment in which they operate. This could be considered to apply to: ambient gases, humidity as well as operating temperature and presence of contamination material or lubricating oils. Although the environmental conditions will generally not be controllable in this study, it will be important to understand how coatings have been modified to cater for specific environmental issues. Many studies have confirmed DLC coatings to be hard wearing whilst also maintaining low friction in controlled dry conditions, however, properties can degrade depending on the condition in which the DLC coating is being used (Bull, 1995). The effects that environment and atmosphere has on tribological performance of DLC coatings have been studied. It was discovered that highly hydrogenated DLC coatings had much less friction in a vacuum compared to non-hydrogenated coatings, whilst the presents of hydrogen and oxygen had adverse effects on the friction of all coatings (Andersson *et al.*, 2003). The effects of atmospheric composition on the tribology of DLC on aluminium have also been studied. Nitrogen was shown to create the highest friction coefficients whilst ambient air had significantly lower friction than dry air, hydrogen had the lowest friction of all atmospheres (Qi *et al.*,

2006). Wear rates of non-hydrogenated DLC coatings were also shown to decrease in air with humidity above 20% (Konca *et al.*, 2005).

Lubrication is still being used for machining with DLC coated tools despite previous research suggesting friction and wear properties are best in dry conditions. Mineral and biodegradable oils have been investigated for use with DLC tribological applications. It was found that biodegradable oils could improve the friction properties of DLC coatings. The use of additives further improved performance (Kalin *et al.*, 2006). The studies showed that DLC coatings will usually have to be optimised specifically for use with lubricant in order to attain the best possible tribological performance.

2.4.5. DLC for machining aluminium

The theoretical potential of carbon based coatings for the optimisation of aluminium machining has been well documented due to carbons lack of affinity towards aluminium. This means the tendency for aluminium to adhere to the cutting tip is reduced compared to other metallic based coatings, like titanium or aluminium oxides, or metallic tool materials such as steels, chromium and tungsten. Many studies have indicated that DLC coatings can significantly improve aluminium machining performance in a number of ways. The research conducted within this thesis will build on coatings, which have been previously developed for dry drilling of aluminium alloys, in which HSS drills were coated at various voltages and Ar dilutions. As described in the introduction, this trial showed that the DLC coating not only improved tool life, but also significantly improved machining efficiency by way of a reduction in the current required for the machine tool drive motor (Zolgharni *et al.*, 2008).

Some studies focused on the tribological interactions between DLC coatings and aluminium alloys at raised temperatures in order to test the efficacy of DLC coatings for machining. One study found that a-C:H coatings had increased friction and wear compared to a-C coatings at 25°C, though when tested at 240°C, the a-C performed significantly worse (Ni *et al.*, 2006). The DLC started to show poor

performance at just 150°C due to graphitisation of the coating, along with increased aluminium sticking as the material softened. Another study confirmed a significant decrease in friction and wear performance at a temperature of just 120°C. The investigation went on to show that it is the simultaneous increase in surface temperature during sliding contact that leads to greatly reduced performance. This was indicated as annealing prior to testing did not generate such a reduction in performance (Konca *et al.*, 2006). In dry drilling applications comparing a-C and a-C:H coatings it was found that both coatings significantly improved upon uncoated HSS, and the a-C:H coating had the best performance overall (Bhowmick *et al.*, 2008). In dry milling applications ta-C coatings were shown to improve WP roughness and tool life by preventing BUE forming, whilst reducing cutting forces by 50%. The coatings were shown to offer the same performance improvement in both wet and dry conditions (Fukui *et al.*, 2004). An investigation of optimal cutting parameters for turning aluminium with DLC coated tools found that WP roughness and heat generation followed similar patterns to uncoated tools in terms of feed rate, depth of cut and cutting speed (Mustafa *et al.*, 2011). Interestingly, a-C:H coatings applied to WC-Co turning tools were show to offer slight improvement to machining performance in a short dry cutting test. Feed force was slightly reduced whilst cutting force was not significantly affected (dos Santos *et al.*, 2007a). The lack of improvement was down to the fact that the DLC had completely worn away at the Al – tool contact area of the cutting tip. Due to the comparability of diamond and DLC coatings, the majority of investigations of machining performance examined both diamond and DLC in the same study.

2.5. Diamond and DLC coatings in aluminium machining applications

Although there are many similarities between diamond and DLC, certain distinctions must be made as each coating possesses its own individual characteristics. With similar production techniques and comparable properties, the distinctions between diamond and DLC coatings are becoming further reduced. For this reason researchers have already conducted direct comparisons of diamond and DLC coating for different applications (Robertson, 2008). The study looked at NCD and DLC, as NCD is

the most similar in structure to DLC coatings. ta-C coatings are also similar in structure to NCD as they contain the highest percentage of sp^3 bonding and no hydrogen. Friction and wear properties were also compared. Diamond films showed a relatively linear relationship between roughness and friction, with the friction reducing during sliding tests. DLC films generally had lower friction although there was some crossover with ta-C coatings (Erdemir, 2002).

In terms of machining applications different forms of diamond coatings have been shown to offer very different performance when compared to DLC coatings. In a milling trial it was recorded that sintered diamond produced a decrease in machining force due to significantly reduced BUE formation whilst the DLC coating increased forces compared to the uncoated cemented carbide tool (Yoshimura *et al.*, 2006). The study also confirmed greatly reduced BUE with increasing rake angle and stated that adhesion only occurs when COF is greater than 0.4.

It was confirmed that DLC generally has much better adhesion to the substrate as well as lower surface friction. Diamond wear rates are much better than DLC, however, diamond failure due to delamination occurs with much less wear than that of DLC (Zhang *et al.*, 2010; Dai *et al.*, 2000). Dry drilling of aluminium has already been shown to have improved efficiency with the use of diamond and DLC coatings. The performance of CVD diamond was shown to be highly dependent on tool geometry (Chou *et al.*, 2010).

2.6. Multi-layered diamond and DLC coatings

As of yet there have still only been a very small amount of groups examining the potential of combined diamond and DLC coatings. There have been studies into multi-layered coatings whilst only one group so far appears to have looked at the potential of a combined coating for improved machining performance (Hanyu *et al.*, 2005). There have, however, been no studies yet based on the turning of aluminium alloys using combined carbon coatings. Hanyu et al. conducted a number of studies on the use of fine grain diamond, particularly for dry and semi-dry machining applications. In

addition to this, one study looked at combined diamond and DLC coatings for the drilling of aluminium alloys using MQL. The study similarly utilised the HFCVD method to deposit the diamond followed by the PECVD method for the DLC deposition. They concluded that tool life could be improved with the double coating combination compared to any single coatings they tested. The investigation showed that friction coefficients and wear rates were greatly improved with a combined DLC on fine crystal diamond. Interestingly the fine crystal diamond single coating also performed better than the double layered DLC on coarse grain diamond (Fig 2.13). The combined coatings effectively halved the friction compared to the best single layer diamond coating and increased the tool life of drills by over 50%, however, the study did not examine the effect the coatings had on WP finish or measure the potential energy saving to be gained from the lower friction coatings.

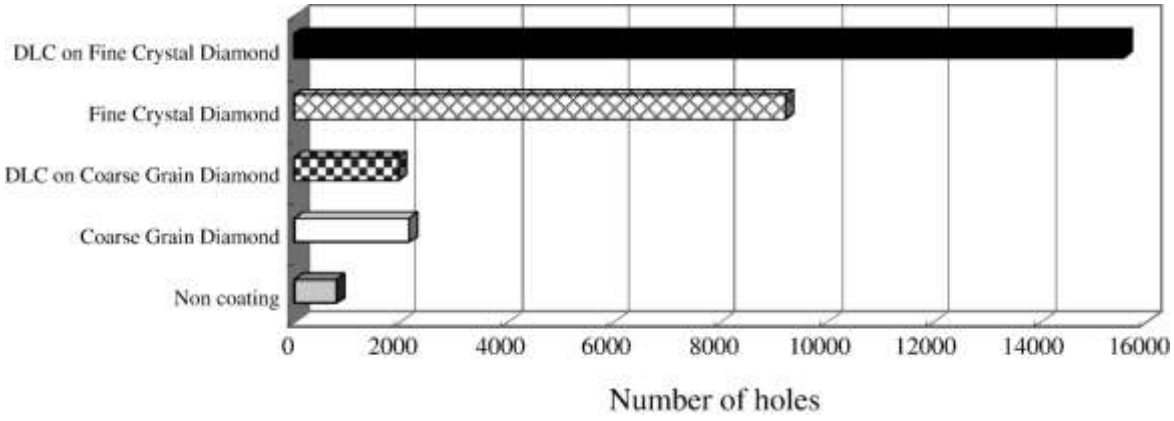

Figure 2.13. Drilling performance of combined DLC and diamond coatings (Hanyu, H. 2005)

The investigation by Hanyu et al. built upon previous work by Miyoshi 1997, which also looked at the friction and wear of DLC deposited on fine grain diamond (Miyoshi *et al.*, 1997). In this study, DLC coating produced using the ion beam method were deposited on CVD fine grain diamond. The friction and wear tests conducted involved testing the combined coatings in sliding contact with CVD diamond pins in, ultra-high vacuum, nitrogen and humid air. The results showed that combined DLC and fine grain diamond coatings significantly reduced friction and wear in all environmental conditions tested.

Another relevant study used a CVD diamond coating as a substrate material in order to test how the roughness varied with increasing thickness of DLC coatings (Salvadori *et al.*, 2006). In this instance the CVD diamond provided a specific homogeneous roughness which allowed the investigator to examine how the DLC formed and developed on a substrate with sharp peaks and valleys. Although the study was not concerned with the mechanical properties produced by the duel layer, it is of interest because it highlighted how the DLC develops on the MCD substrate in terms of the growth mechanisms. It is important as it showed that depending on deposition time, and hence coating thickness, DLC can increase the surface roughness.

A diamond DLC double layer was also investigated as a potential corrosive protective coating with the aim of creating a thin pinhole free layer for use in electrolyte solutions. A coating with significantly improved corrosive resistance was developed and optimum coating thicknesses were discovered (Csorbai *et al.*, 2007). Another comprehensive study investigated the friction of magnetron sputtered, thin layer, a-C and a-C:H DLC coatings on both NCD and MCD coatings. It was confirmed that despite the DLC coatings significantly reducing initial friction values in dry sliding, failure of the coatings meant that the DLC gave no long term benefit. The NCD coatings therefore gave the best overall performance as they maintained reduced roughness for longer. The diamond coatings were also shown to reduce in roughness during sliding as the protruding apices were worn flat over time (Amaral *et al.*, 2012).

Multi-layers deposited in a single coating run are common in diamond and DLC coatings as they have been shown to improve properties and allow for greater manipulation of such coatings. These multi layers usually involve adjusting deposition parameters in order to improve different aspects of the coating. A number of studies have considered alternate hard and soft DLC layers in order to allow for increased coating thickness and improved environmental stability (Zhang *et al.*, 2005; Meneve *et al.*, 1996). One group of researchers have created more distinct layers of diamond and DLC in just one coating run. The studies examined hybrid nano-crystalline and DLC coatings produced by alternately

depositing DLC and diamond films in the same chamber without breaking vacuum. The studies concluded that the coatings had the hardness of diamond whilst maintaining improved friction and roughness comparable with DLC. In sliding tests the individual NCD film was shown to have not only a greater COF but also a much more erratic and unpredictable one. The DLC had much lower friction but also suffered from fluctuations in performance. The hybrid coating on the other hand not only had the lowest friction but also showed markedly improved stability compared to the individual coatings (Sakudo *et al.*, 2008; Ikenaga *et al.*, 2006). Although there have only been limited studies concerning the potential of combined diamond and DLC coatings in different applications, research has highlighted some important variations in terms of tribological performance of these coatings. The benefits of combined coatings depend strongly on subtle variations between different diamond coating morphologies, as well as the variation in structure of DLC coatings, which are influenced by the deposition methods and parameters used.

2.7. Summary

The literature review has indicated a number of key factors which are prevalent regarding this project. The main point being that, although individual DLC or diamond coatings have been shown to improve machining applications and a combined coating has shown improvements in one particular drilling operation, the potential for combined coatings being used for other machining applications has yet to be proven. There have been limited studies on combined diamond + DLC coatings, with only one study looking at machining performance of drills (Hanyu *et al.*, 2005). Drilling applications are somewhat distinct to other forms of machining, such as turning and milling, as the overall contact area between tool and material is greatly increased. Turning and milling applications tend to use small replaceable inserts in which can have very small contact areas, sometimes less than $1mm^2$. For this reason it is necessary to investigate how combined coatings may benefit machining applications, in which small cutting tip - workpiece contact areas are involved, in applications where good quality surface finishes are paramount. The few friction tests conducted on diamond + DLC

coatings have had mixed results, with some studies showing reduced performance due to early wear of the DLC layer (Amaral *et al.*, 2012).

The important factors regarding the development of an optimised combined coating structure have been identified. For the diamond layer it has been shown that ensuring good adhesion between the coating and WC-Co substrate could be the most complex aspect. Although acid etching has been shown to be the cheapest and most available method for preparing the samples, it is also unreliable and has produced mixed results. The difficulty is due to the need to etch the correct amount of cobalt from the surface without negatively affecting the integrity of the cutting tool. The use of interlayers may be applicable, however, this would potentially increase production costs to unreasonable levels which would make them less viable for industry. By using the HFCVD method for the deposition of diamond, the material structure will be substantially tailorable, particularly in terms of crystal size, by adjusting the gas ratios of methane to hydrogen. Although it has been shown that the filament – substrate distance will have a significant influence over the coating morphology. It will therefore be important to ensure an optimal sample positioning in the reactor is achieved and maintained.

The research highlights that DLC coating properties will be mostly affected by bias voltages used in the deposition process. Higher voltage coatings will produce harder wearing coatings, however, it will also lead to increased residual stress which can cause early coating failure due to delamination. The bias voltage parameters may therefore need to be developed in conjunction with deposition time in order to achieve the best wear performance without suffering adhesion issues. The deposition time may also be important when coating rougher surfaces as there may be stages in the deposition process at which the DLC layer may increase surface roughness producing a detrimental effect on the coating friction.

Increased rake angles are used to reduce cutting forces and therefore cutting temperature, which leads to a decrease in BUE development. Chip breaker on the tools means that the effect of rake

angle will not be directly applicable, as the chip breaker acts to inhibit swarf flow by breaking the chips before they can form long swarf trails. This creates a secondary area for the aluminium to adhere other than solely on the cutting edge. In addition to this, sharp edges have been shown to concentrate stress in coatings (Sheikh-Ahmad *et al.*, 2015; Renaud *et al.*, 2009), meaning that failure due to delamination is likely to be more of an issue when sharp edged tools with large rake angles are used.

This project focuses on the use of diamond and DLC coated WC-Co tools for the dry machining of aluminium alloys. Diamond and DLC have already been shown to improve aluminium machining performance. The research has confirmed that further optimisation is still required in order for dry cutting of aluminium to be a viable option for industry and the potential for combined coatings in turning applications is in need of further investigation.

3. Experimental setup

3.1. Introduction

The following chapter presents the techniques used for the fabrication, characterisation and performance evaluation of the individual and combined carbon coatings. The developmental approach will be discussed in terms of the optimisation of the DLC coating design using an iterative process. The diamond and DLC deposition processes are discussed along with the system variables which will be investigated.

Due to the complex nature of the deposition mechanisms involved in the production of diamond and DLC coatings, a certain amount of material characterisation and mechanical testing will be required in order to find the optimal balance of deposition parameters. This is because, although the literature has highlighted how deposition variables are likely to influence coating properties, it is still not possible to predict exactly what the ideal deposition conditions will be. This is due to the variations in deposition reactor systems in terms of; chamber geometry, gas flows and plasma formation, as well as substrate variations such as material composition, morphology and surface preparation. DLC deposition will be emphasised, as it was the development of the DLC layer which formed the main focus of this study.

The techniques being used to characterise the materials are discussed along with the reasoning behind why they will be useful for quantifying and comparing carbon material structures. In order to get a good understanding of how the coating characteristics translate in machining performance, it will be necessary to acquire all the relevant information regarding coating morphology and bonding chemistry. The machining performance testing regime is then discussed in regards to the machine used, the chosen material, cutting parameters and measurements taken, both real time and pre and post-trial.

The basic iterative process being used to develop the coatings will be based around three main parts of work; firstly, the deposition variable themselves, then, an analysis of the coating characteristics produced by the different variables, and finally an examination into how these characteristic translate into machining performance (Fig 3.1). The below diagram illustrates the feedback approach being used to develop the combined coatings and then test the efficacy of the developed coatings for the dry turning of aluminium alloys.

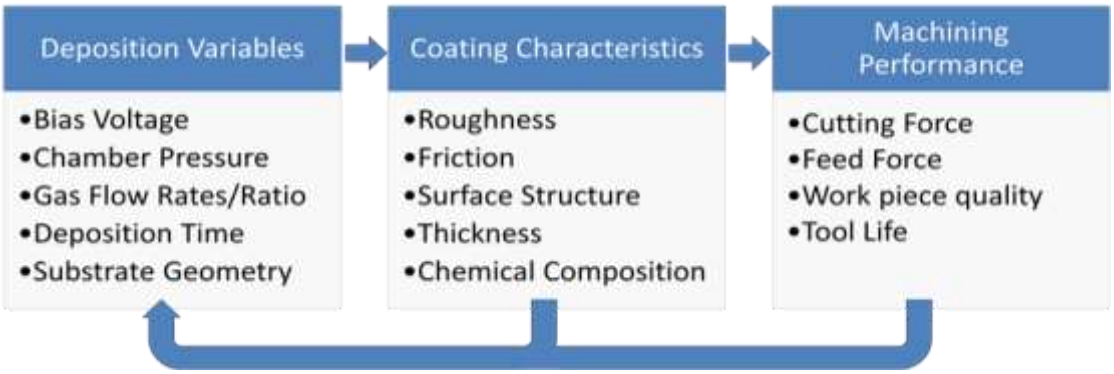

Figure 3.1. The iterative DLC development process

Investigations will be based around altering the deposition parameters such as bias voltage, deposition time and gas flow rates, along with examining the positioning of the substrates within the reactor chamber. The coatings produced will then be characterised using scanning electron microscopy, atomic force microscopy and Raman spectroscopy in order to quantify the material properties and surface conditions. The cutting trials will then be used to measure the parameters stated above which will provide sufficient detail to elucidate whether the combination of diamond and DLC will be effective for improving aluminium machining processes.

3.2. Coating deposition techniques

3.2.1 Diamond coating deposition

The diamond coatings were deposited at Bristol University School of Chemistry by means of a bespoke HFCVD deposition reactor (Fig 3.2). The coating conditions involved two phases, the first designed to encourage MCD growth and the second to promote NCD growth. In this particular system a tungsten filament was used to generate energised hydrocarbon species to form diamond coatings. Substrate temperatures would reach between 800°C and 1000°C, with a deposition time of up to 50 hours to achieve sufficient coating thickness. Due to process variables of the system, such as sample positioning, it was difficult to initially predict what the diamond growth rate would be. The high energy requirement coupled with lengthy deposition times meant that samples would be costly and hence only a limited amount of developmental iterations would be possible.

Figure 3.2. HFCVD reactor used for diamond coating deposition (P. May, 2012)

Due to the coating time constraints, a limited number of possible coatings were produced. This was exacerbated as the rig had to be set up specifically to accommodate variations of the substrate geometry, it was consequently only possible to coat specific cutting tool inserts chosen for the project. The rig was designed to ensure the inserts could be positioned effectively to optimize the coating at the tool tip as opposed to the complete cutting tool surface.

The system contained two filaments with space for 10 inserts to be placed around each filament, this allowed for a maximum of 20 inserts to be coated per deposition run. The filament runs from the top of the chamber to the base, as indicated by the red line. The inserts were fixed to the rig (Fig 3.3 a) which ran down the chamber alongside the filament, as indicated by the green circles (Fig 3.3 b). As previous research has suggested, positioning of the inserts will therefore be one of the first major aspects in the development of the coating as it has been shown in the literature, the deposition rates and coatings morphologies will be highly dependent on the position of the samples relative to the filament.

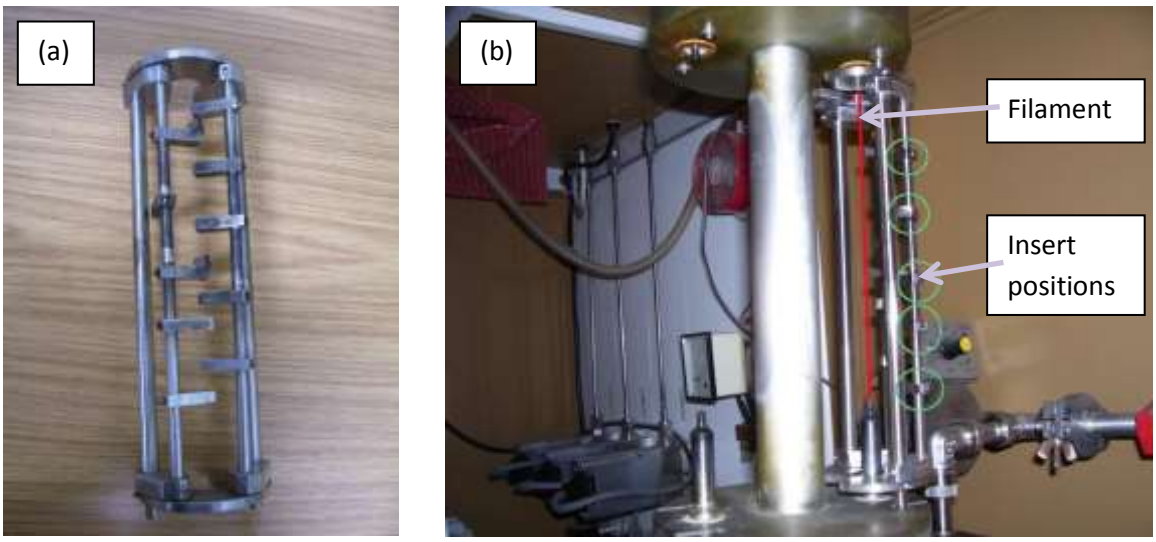

Figure 3.3. a) Insert positioning rig for diamond coating, b) Rig position in reactor (P. May, 2012)

The positioning of the samples in the rig and the angle relative to the filament will depend on the geometry of the insert. Factors such as rake angle, chip-breaker, flute design, nose radius and clearance angle influence how inserts need to be positioned in order to optimize coating the tool tip. Due the deposition being line of sight based, coupled with the need to coat the rake face and flanks of the tool tip, it was only possible to coat one tip on each tool. This is because, in order to attempt to coat both cutting tips, it would not have been geometrically possible to also coat the flanks. It was decided that the development would therefore focus on optimising one cutting tip.

The tool chosen as the baseline for the performance machining trials was the Sandvik coromant VBGT 331-UM H13A carbide indexable turning inserts (Fig 3.4). It can be seen that the complex geometry of the rake face and chip breaker feature, creates significant limitations for coating characterisation.

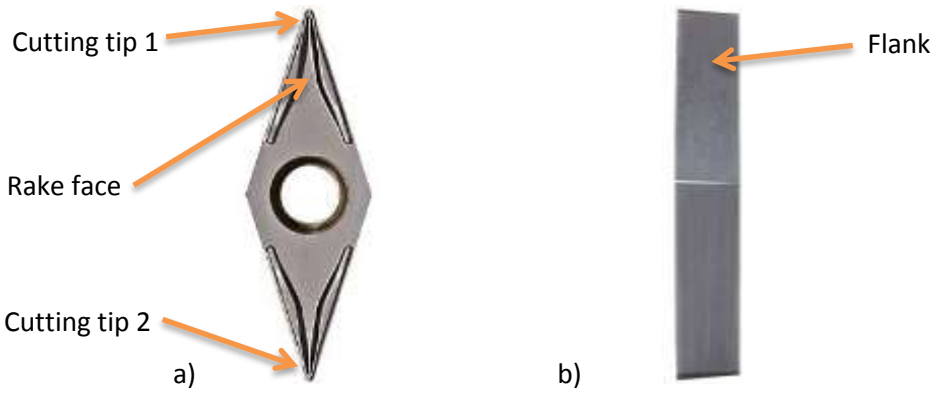

Figure 3.4. a) Top view of Sandvik insert b) Side view of Sandvik insert (amazon.com, 2012)

There are a number of important geometrical features regarding the insert being coated. These features will affect how the insert must be positioned in relation to the filament in order to optimise the coating at the cutting tip. The information provided by suppliers is displayed in table 3.1 below.

Relief Angle	5 Degrees
Insert Shape	35 Degrees Diamond
Chip-Breaker	UM
Insert Thickness	4.76mm
Nose Radius	0.4mm
Rake	Positive

Table 3.1. Insert Geometry (grainger.com, 2014)

The coating will not be homogeneous and will therefore be quantified relative to the cutting tip with the area of interest being dependent upon the contact area of the chip – tool interface during machining. This will only be confirmed with the first cutting trials and also depend predominantly on the cut depth used for the trials.

The HFCVD system incorporated methane and hydrogen as the precursors gases for the coating deposition. The variables to be considered for the sample preparation and coating deposition conditions are:

- Insert pre-treatment
  - Acid Etching
    - Acid composition
    - Etching time
  - Cleaning
    - Solvents
    - Ultrasonic
- Diamond Seeding
  - Effect on surface
- Substrate positioning
  - Distance from filament
  - Angle to filament
- Precursor gas ratios
- Deposition time
  - MCD phase
  - NCD phase

Pre-treatment of the turning inserts will form an integral part of the diamond coating process in order to ensure the WC-Co to MCD interface is optimised for maximum adhesion. It is known that the cobalt binder in the WC-Co inhibits adhesion of the diamond coatings to the substrate. It is therefore necessary to perform an etching stage in which an acid, commonly nitric or hydrochloric, is used to remove the surface layer of cobalt. This exposes the WC particles allowing for improved mechanical bonding at the MCD and WC interface. In order to ensure the desired amount of cobalt is removed to promote adhesion, the composition of the acid will need to be adjusted in terms of the type of acid, its concentration and the amount of time the insert is placed in the etching solution.

The insert must then be rinsed with solvents to prevent contamination which would otherwise compromise coating integrity. The use of inter-layers will be considered as an alternative or an addition to the acid etching process. An extra coated layer would inevitably add to the production costs and will only be considered if a significant advantage can be achieved. Due to the nature of the deposition process the substrates will need to be seeded with nano-crystalline diamond in order to initiate diamond growth. Ensuring an even seeding process for homogeneous growth is also an important factor. The development of these parameters is described further in chapter 4.

3.2.2 Diamond-like carbon coating deposition

DLC coatings were produced at Renishaw Advanced Materials ltd. using a bespoke rf-PECVD system. The setup involved using a 13.56MHz radio frequency to excite a gas or vapour source between two electrodes (Jones *et al.*, 2010). The coating chamber is of a cylindrical shape, 50cm in diameter and 50cm high. The vacuum system uses a turbo and rotary pump combination which brings the base pressure down to a fixed 10^{-5} torr. All fittings, inlets and outlets are positioned at the base of the chamber, however, an inner cage is used to direct the gas flow to the top of the chamber to ensure a more even plasma distribution (Fig 3.5). The system has three gaseous precursors which include; argon (Ar), tetramethylesilane (TMS) and acetylene (C_2H_2). The Ar is used as an etching agent for the plasma cleaning process prior to the deposition of the coating, as well as being used to promote growth during the deposition stage (Jones *et al.*, 2011; Jones *et al.*, 2008). The TMS forms a silane vapour which is used to create the adhesive silicon carbide interlayer, whilst the acetylene contains the hydrocarbon species for the deposition of the DLC top layer. The gases are all directed into the chamber through a single inlet which further guarantees that, when more than one precursor gas is being used, the different species will integrate prior to entering the chamber. This further improves the homogeneity of the plasma during the deposition stages.

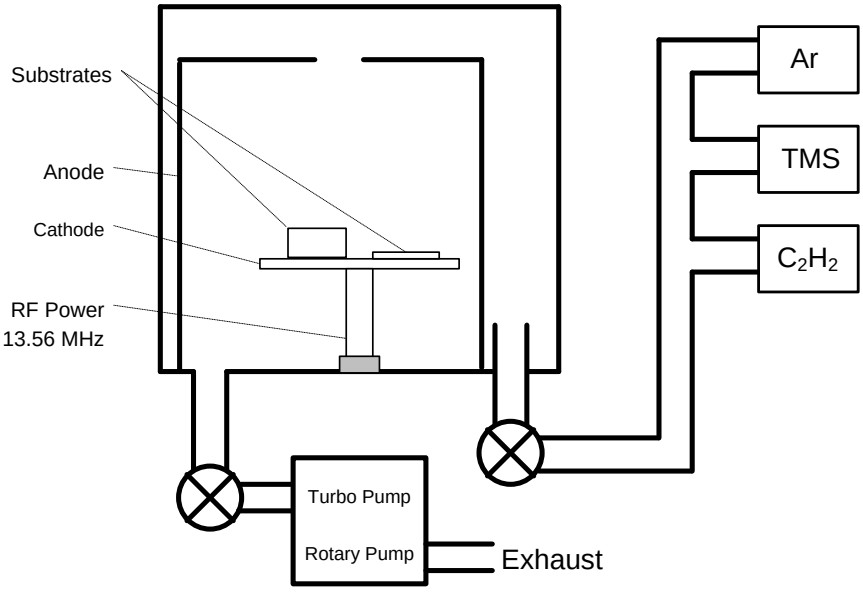

Figure 3.5. Diagram of PECVD deposition system

The adjustable deposition variables in this particular rf-PECVD system include:

- Bias Voltage (V_b)
  - V_b range 0 – 1100V
- Deposition Time
- Sample Positioning
- Gas Mixture and Flow (0 – 70sccm)
  - Argon
  - Acetylene
  - TMS vapour

The system uses an rf matching network to ensure energy is transferred to the plasma in the most efficient way. It achieves this by generating output impedance in the circuit that is purely resistive. This is done by way of manually adjusting the RF load and tuning relative to the conditions in the chamber. These conditions will depend on the geometry of the chamber in terms of anode and cathode size and position, as well as the gas species composition within the chamber. In this system, an Advanced Energy RF-10S power supply is used in which either the voltage or power can be set. The voltage, however, is the predominant variable, whilst the power will be directly, but not linearly, proportional depending on the given impedance of the system. It is necessary for the network balance to be set to 0W difference in order to prevent charging in the system which leads to power fluctuations that can affect the uniformity of the deposition (Fig 3.6).

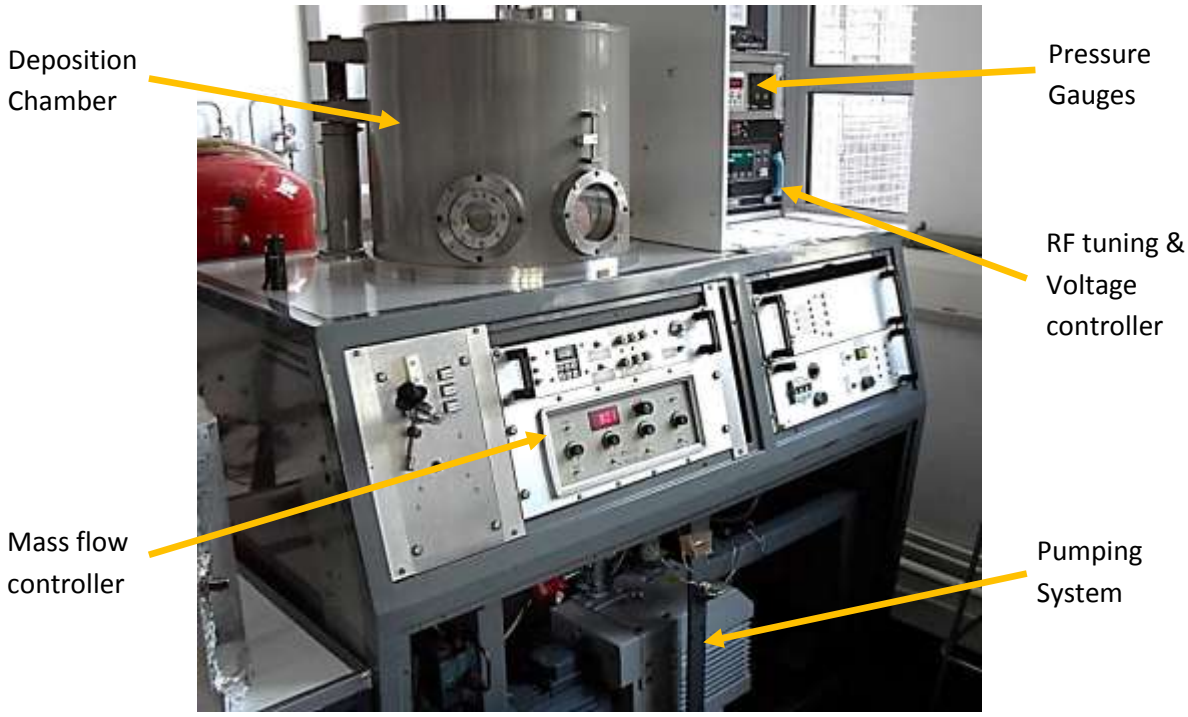

Figure 3.6. PECVD reactor in operation

For general coating deposition, the samples were placed flat on the cathode plate unless otherwise stated (Fig 3.7). The internal cage, which acted as the anode, was then fixed around the central cathode plate before the chamber lid was lowered into position.

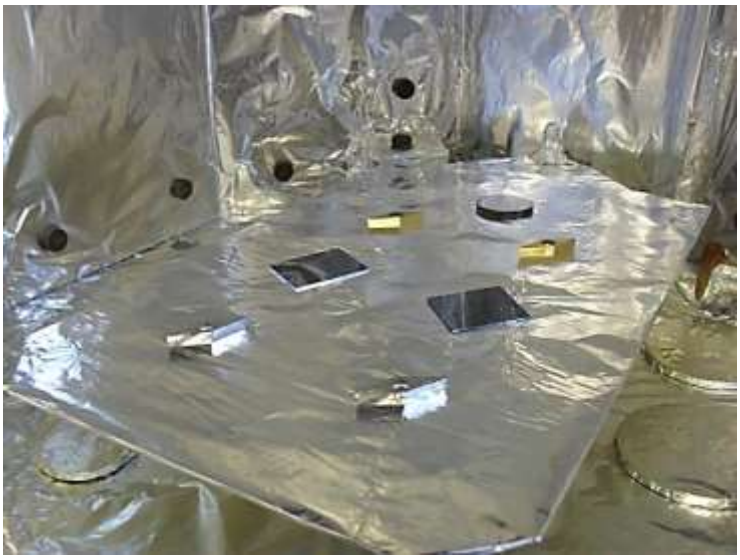

Figure 3.7. Samples positioned on cathode plate

Initial coatings were deposited using parameters developed in previous work for the optimization of high speed steel drills used in dry cutting aluminium (Zolgharni *et al.*, 2008). The samples were initially sonicated for 10 minutes in acetone before being laid flat on the cathode plate in the DLC reactor. The coating was applied in four stages. The first stage involves argon cleaning for 30 minutes with and argon flow of 30sccm with a bias voltage of 370V. The argon flow is then reduced to 10sccm, tetramethylsilane (TMS) is introduced and the bias is simultaneously set to 450V. The TMS flow is then set to 25sccm for 15 minutes. TMS is then reduced to 12.5sccm and acetylene is introduced at a rate of 60sccm for a further 15 minutes. Finally the TMS is completely removed and the acetylene flow of 60sccm is continues for a further 15 minutes to complete the cycle. This set of parameters was used as a standard DLC coating for tribological applications, in particular machine tools. These pre-developed parameters formed the basis of the DLC coating development for this project. Further details of the various parameters tested for the combined coating design are described in detail in the DLC results sections, chapter 5.

3.3. Coating characterisation

The coatings properties and characteristics will need to be analysed and quantified where possible in order to produce a clear picture of how the individual thin films are structured, as well as how they are interacting with each other, on a physical and chemical level. It will be important to use specific techniques to analyse surface structure and topography, as well as the internal bonding structure of the coatings to compare how these material characteristic influence the machining performance.

3.3.1. Scanning electron microscopy

The surface structure of the samples were analysed using a Zeiss Supra 35VP scanning electron microscope. The magnification range allowed entire tool tips to be viewed at the lowest magnification of X150, whilst nano-scale microstructures could be observed at higher magnifications, over X200k. SEM was an invaluable tool for analysing the turning inserts and coatings, be it coating uniformity, coating quality, presence of defects and coating / substrate interaction effects or simply substrate integrity. It is limited, however, in that it does not allow accurate analysis of the 3 dimensional surfaces, giving little indication of coating topography. There is also no way to quantify coating variations. In addition to providing a visual representation of the coatings through the generation of high resolution micrographs, the SEM system also incorporated an integrated electron dispersive X-ray (EDS) detector for analysing elemental composition. EDS analysis was used to measure coating quality and performance as it allowed for quantification of several factors. This includes measuring; tool tip coverage, coating uniformity, inhomogeneity, coating delamination, wear and aluminium adhesion.

As the electron beam interacts with the sample a number of particles are energetically ejected from the surface, as well as up to a few micro-meters in depth. This has been shown though monte-carlo simulations of beam – specimen interactions (Joy, 1991). The penetration depth will depend on beam energy and sample material, whilst the specific particles and emissions emanating from the sample will originate from different points in the interaction zone (Fig 3.8).

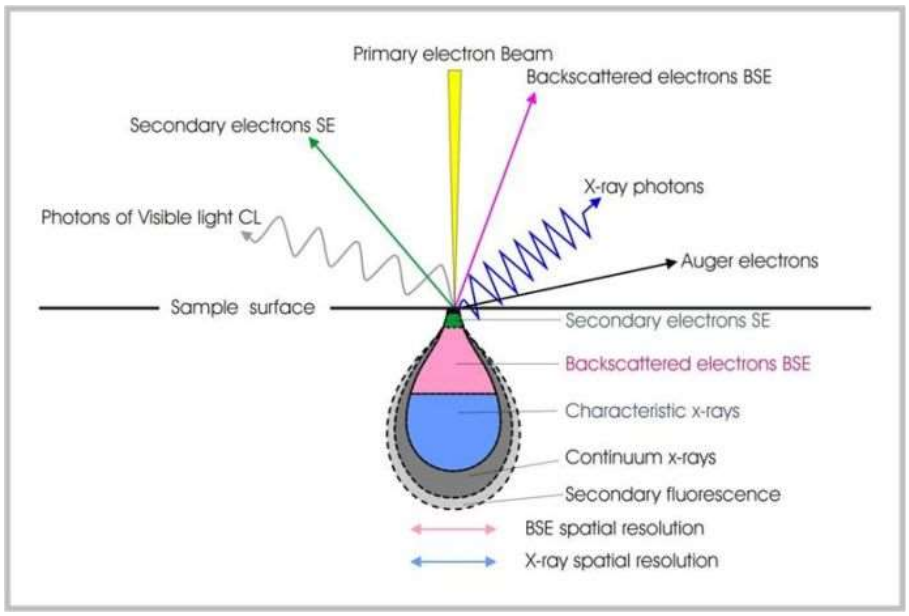

Figure 3.8. Electron interaction with sample surface (gla.ac.uk, 2014)

For high resolution images the secondary electron detection (SE2) was used at a relatively low gun voltage as this provided the best conditions for surface imaging. From figure 3.8 it can be seen that the secondary electron are emitted from a small area near the surface of the sample. The tear drop shape produced by the impinging electron beam highlights that the sharpest images will come from the particles emitted from the near surface interaction, in this case the secondary electrons. As the beam penetrates the surface further, the interaction zone widens, this means that resolution will be significantly reduced when analysing Back-scattered electron (BSE) or X-ray signals. BSE analysis will be utilised in order to visually highlight the elemental distribution in a given area. This is because in BSE mode the lighter elements appear darker whilst heavier elements appear lighter. This becomes very useful as the main elements being analysed all have very different elemental masses.

Importantly, the BSE analysis will be conducted at low magnification of the entire cutting tip, therefore the decreased resolution will not be a significant issue in this instance.

The EDS analysis was employed for the following reasons. It allows for the analysis and quantification of elemental composition of either a whole area or of specific chosen points. It will therefore prove useful in examining the effectiveness of the cobalt etching by quantifying surface cobalt content before and after etching. More importantly it will allow for accurate quantification of machining performance by measuring aluminium adhesion at the cutting tip, as well as delamination of the coating relative to the WC-Co substrate. Unfortunately it will not be useful for examining adhesion of the DLC layer to the diamond layer, as both consist of carbon and are indistinguishable from each other by this form of analysis.

The DLC coatings will not require any preparation for SEM analysis, other than ensuring a clean surface, as the standard coating is not electrically resistive. The diamond on the other hand may require an extra preparation step due to it being non-conductive. This is to ensure that imaging is not adversely affected by charging of the sample. Usually gold or platinum coatings would be applied to reduce charging effects, however, for pre-trial analysis this will not be viable as it will potentially affect the properties of the surface layer. Using variable pressure (VP) mode may therefore be necessary, although the drawback would be reduced resolution at higher magnification. As mentioned earlier, the SEM is limited to providing just a 2D representation of the surface. In order to gain a better picture of the topography of the coating surfaces further techniques such as atomic force microscopy will be applied.

3.3.2. Atomic force microscopy

To gain further insight into the substrate and coating topography, atomic force microscopy (AFM) was applied. The AFM used was a Digital Instruments Nanoscope Dimension 3100, this can be used to measure surface features from a scale of 100µm to less than 100nm, with a depth scale from below 1nm up to 4.8µm. This allows for coatings on flat surfaces to be measured easily and accurately, however, the geometry of the turning tools being investigated will make analysis of coatings on tools much more problematic. The use of test disks (chips / coupons) as well as Si wafers will be required to analyse coatings further, whilst keeping in mind, the coatings will be affected by the characteristics of the substrate being coated. The AFM measurements will be conducted using a long-lever tapping etched silicon probe (LTESP) produced by Bruker scientific. This tip was used for the analysis of the substrate and coating surfaces examined throughout this project. Tapping mode was considered the best option as it allowed for sufficient resolution without any potential detrimental effect on the sample.

It is important to differentiate between the values which can be obtained from AFM analysis for a number of reasons. The arithmetic average roughness (R_a) value is one of the more common measurements and is used widely when analysing surfaces. R_a is based on a calculation in which the surface profile is measured in terms of a summation of height measurements across a given evaluation length or area. The equation can be expressed by:

$$R_a = \sum_{n=1}^{N} \frac{|Z_n - \overline{Z}|}{N} \qquad \text{Equation 3.1.}$$

In this equation Z refers to the height measurement whilst N stands for the number of sample points in the area. Although this value is useful for basic comparisons this average can disregard significant information regarding the peaks and valleys. The root mean square (R_q) value offers some further information as the squaring of the measurements highlights if there is an increase in high peaks or deep valleys.

It is also important to understand that higher roughness does not imply higher friction and further values will offer a much improved quantitative picture of the coating topography. Values such as skewness and kurtosis are also of great benefit when considering how the tribological performance of a surface depends on the topographical values. A strong positive skew indicates the surface has sharp peaks protruding from a relatively level base, whilst a strong negative skew indicates that there are sharp valleys receding into a level base. The kurtosis value corresponds to the sharpness of the peaks and valleys. A kurtosis value greater than 3 suggests the surface has sharp peaks and valleys whilst a value less than 3 indicates a more gradual transition between peaks and valleys on the surface.

The peak counts may also be useful to judge the coatings as high peaks count may mean greater chance of adhesion developing depending on the bandwidth threshold, and hence size of the peaks in a given area. All of these factors will need to be considered in order to understand the potential adhesive qualities of each coating surface. Given the fact that adhesion is a chemical and physical phenomenon, as well as the AFM measurement of the topographical values, it is also necessary to consider the chemical aspect. With the DLC coatings it has been shown that graphitic sites can act as dry lubrication leading to reduced friction. It is therefore necessary to evaluate the chemistry of the coatings to determine the amounts of diamond like sp^3 and graphite like sp^2 bonding in the surface layer. Raman spectroscopy has been proven to be an incredibly useful tool for comparing these values in DLC, as well as characterising various types of diamond.

3.3.3. Raman spectroscopy

The Raman spectroscope used for the analysis of both the diamond and DLC coatings is a Renishaw Invia micro-Raman system fitted with a 514.5nm laser. The system was calibrated to the silicon peak 0f 520cm^{-1} prior to use. Raman spectroscopy is a non-destructive technique that operates by using a monochromatic light source to create inelastic scattering. This scattered light can then be quantifiably analysed to reveal chemical bonding within the sample. When analysing carbon materials, particularly diamond and graphite structured carbons, Raman spectroscopy provides an excellent tool for characterising the bonding arrangements of the bulk material. It is particularly useful in terms of allowing for a comparative assessment of the relative amounts of sp^2 and sp^3 bonds within the amorphous structure (Casiraghi *et al.*, 2005). One drawback is, however, that where hydrogenated coatings are concerned, the spectrum produced does not distinguish between C-C and C-H sp^3 bonding (Filik *et al.*, 2003). It is therefore necessary to have an understanding of the typical DLC curves produced using this technique, as well as a good comprehension of the deconvolution techniques used to generate a picture of the chemical bonding arrangement in the thin films. The standard Raman curve associated with DLC structures has been shown to generally contain two Gaussian peaks in the region of 1000cm^{-1} – 1800cm^{-1}, these are known as the disordered (D) and graphitic (G) peaks (Fig 3.9).

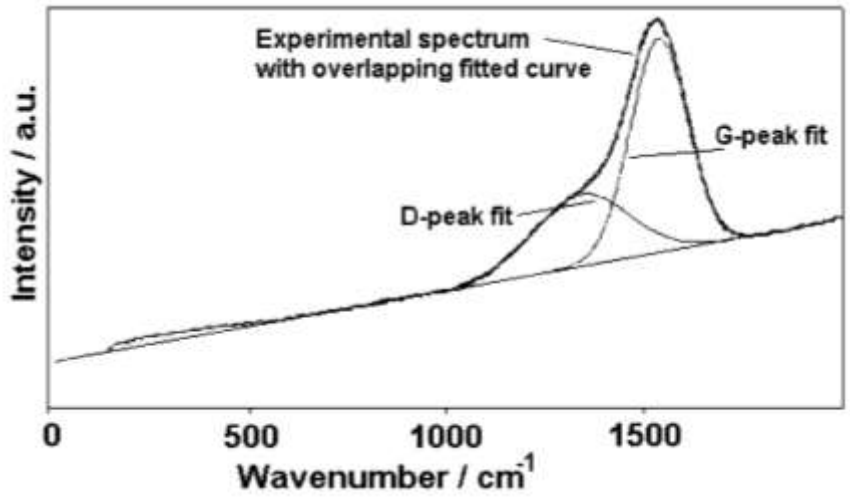

Figure 3.9. DLC Raman spectra showing D and G peaks (Filik *et al.*, 2003)

There are a number of factors which influence the peak pattern associated with the Raman signature of amorphous carbon. It has been shown that the D and G peaks in the Raman scattering of DLC is comparable to that of microcrystalline graphite (Nemanich *et al.*, 1988). It is the ratio of the D and G peak intensities that has been correlated to the sp^2 and sp^3 bonding (Ferrari *et al.*, 2004). The D and G intensities do not correlate proportionally to the bonding ratio as they do not directly measure the sp^3 bonding in the film, unless UV excitation is used, it instead looks at the vibration modes of the sp^2 phase, in terms of sp^2 clustering and presence of sp^2 rings and chains (Ferrari *et al.*, 2000). It is also important to bear in mind that the positions of the peaks will shift depending on the laser frequency used (Ferrari, 2002; Ferrari *et al.*, 2001).

Research has also highlighted that this system can be particularly useful for characterising the diamond structures expecting to be produced with the HFCVD system. Diamond has a characteristic peak at 1332cm^{-1} (Singha *et al.*, 2006; Schwan *et al.*, 1996). It has been shown that any shift in this diamond peak corresponds to an increase in residual stress of the film (Benzhour *et al.*, 2010). The stress is estimated by:

$$\sigma_D = \frac{E_D}{2}\left(1 - \frac{v_x}{v_{0D}}\right) \qquad \text{Equation 3.2.}$$

In this equation E_D refers to the Young's modulus of diamond (1050GPa), v_{0D} is the normal diamond line position (1332cm^{-1}) and v_x is the measured peak position (Fitzer *et al.*, 1988).

This section has shown how a combination of SEM, EDS, AFM and Raman spectroscopy can be used to characterise the deposited carbon films. The following section describes the machining trial parameters used, and performance criteria analysed, to evaluate how these material properties translate into machining performance.

3.4. Machining trials

Cutting trials were designed to assess the machining performance of the developed coatings in comparison to the uncoated baseline inserts. The lathe used for this project was a Gate G330-E CNC machine as it allowed for a full trial to be set up prior to cutting (Fig 3.10). This ensured there were no variations in the machining process between the first and last cut of the trials.

Figure 3.10. Instrumented lathe setup for cutting trials.

Cutting parameters for all tests were based on optimal machining guidelines for the Sandvik VBGT carbide insert being utilised for this project. These parameters are as follows:

- Cutting Speed 330mm/min
- Cut Depth 0.5mm
- Feed Rate 0.15mm

These parameters also corresponded to a number of studies focused on the turning of aluminium alloys, as mention in the previous chapter. The material used for all tests was Al 6082 T651, although the WP dimensions varied between tests, the details of which are specified in the relevant results chapters.

The orthogonal cutting force and feed force was measured using a Kistler dynamometer 9257ba, which has been shown to be effective for the measurement of cutting forces in a number of machining applications (Chen *et al.*, 2009; Almeida *et al.*, 2008; Martinho *et al.*, 2007; Xu *et al.*, 2001). The system has a range of 1kN with a sensitivity of 10mV/N.

The workpiece finish will be analysed using a Zygo 3000 white light interferometer. It was necessary to use this method, compared to the AFM for a number of reasons. White light interferometry allows for much larger scan sizes and roughness variations, as well as providing much quicker analysis, as detailed topography is not necessary. In terms of quantifying WP finish quality, basic R_a values are generally considered sufficient.

The general surface roughness of the finished workpiece can be predicted by the cutting parameters and tool geometry, providing that the cutting edge is unworn and maintains good tolerance. The equation used to predict WP roughness is as follows:

$$R_a = \frac{0.0321 f^2}{r} \qquad \text{Equation 3.3.}$$

In this equation 'f' denotes the feed rate and whilst 'r' refers the nose radius of the tool tip (Boothroyd *et al.*, 1989). When the numbers are entered into the equation, feed rate of 0.15mm and nose radius of 0.39mm, the predicted roughness will be 1.8µm. It can be taken from this calculation that the actual roughness will likely be more dependent on cutting parameters than cutting edge roughness. A filter will therefore be used in order to cancel out the overlying waviness produced due to feed rate and ensure better comparability of the effects of the tool coating.

SEM was used to analyse the sample insert cutting tips before and after the trials. During the coating development stages, SEM will be used to ensure the coatings have not failed prematurely. This is done by simple visual inspection of the cutting tip. For the full trials of the developed coatings a more detailed SEM analysis will be conducted to quantify failures for comparability.

3.5. Summary

This chapter has outlined the developmental process and techniques that will be used in order to test the efficacy of combined diamond and DLC coatings for dry turning aluminium. The deposition processes described will make it possible to produce a range of coatings each exhibiting slightly different morphologies and internal bonding structures. The characterisation techniques have been shown to provide an efficient and quantifiable method for the analysis of the coating material in terms of; coating uniformity, thickness, topography and chemistry, as well as the interaction between coating layers in terms of adhesion and delamination.

The cutting trials have been developed based on the recommendations from industrial partners, coupled with the finding from previous studies into the turning of aluminium alloys. The machining trials have been designed to ensure minimal variation between tests, which will allow for the best possible comparability of the thin films tested, whilst also simulating the demands associated with industrial manufacturing processes.

The remaining chapters present and discuss the development and testing of the combined diamond and DLC coatings. Chapter 4 discusses the development of the diamond layer, followed by the DLC optimisation and combining of coatings, before finishing with the full length cutting trials and concluding discussions.

4. Diamond coating development

4.1. Introduction

In this chapter we discuss the development of the diamond layer prior to its combination to the DLC layer which will be deposited on top. The diamond coatings were fabricated at the Bristol School of Chemistry and analysed at Brunel University using the surface characterisation techniques mentioned earlier. The Sandvik VBGT tool provided the substrate and coatings were deposited in batches of two to ten inserts. Only one tip of each insert was pre-treated and coated due to the nature of the deposition method, as mentioned in chapter 3. The batches were labelled alphabetically and each sample per batch was given a number relative to their position in the deposition chamber, a list of samples produced can be found in Table 4.1.

Diamond coatings were developed in an iterative process. In order to determine the quality of the coatings a set of targets were identified. These targets were devised based on the coating deposition method combined with the characterisation and testing techniques adopted for this project. These targets were designed to consider: coating coverage and thickness, hardness, adhesion and surface homogeneity. These various facets of the coating were optimised simultaneously from one batch to another, however, the following chapter looks at these factors separately whilst considering how they interact with one another in order to fully understand the characteristics of the coating.

This section begins with the underlying WC-Co insert analysis to show if they are forming a stable foundation for the overlaying coatings. A commercially available MCD insert of similar geometry was also analysed for comparison purposes. The stability of the baseline tool is considered, particularly after the pre-treatment regime, by analysing how it may be affecting the integrity of the material. The section then looks at the diamond coating development in terms of: coating coverage, coating adhesion and surface morphology and chemistry.

Diamond coating sample list

Sample set (samples)	Substrate	Deposition parameters		
		Pre-treatment	Deposition Time (Hr)	Gas Ratio (CH_4 in H)
AA (3)	WC	A	20M	2%
AB (4)	WC	A	72N	8%
AC (2)	WC	A	66.5M, 16N	2%, 8%
BA (5)	WC	B	23M, 66N	2%, 9%
BB (5)	MCD	C	24M, 69N	2%, 8.5%
C (5)	WC	B	24M, 48N	2%, 8%
DA (2)	MCD	C	6M, 72N	2%, 8%
DB (2)	MCD	C	20M, 72N	2%, 8%
EA (3)	WC	B	24M, 48N	2%, 8%
EB (3)	MCD	C	24M, 73N	2%, 8.5%
X (10)	WC	B	24M, 66N	1%, 4.5%
Z (10)	WC	B	24M, 66N	1%, 4.5%
M (4)	WC	B	98M	1%
R (5)	WC	B	42M, 76N	1%, 4%
PM (6)	WC	B	98M	1%
HB (4)	WC	B	98M, 24N	1%, 3%
I (7)	WC	B	100M	1%
Mol (4)	Mo	D	24M, 82N	1%, 3%
WC (3)	WC int	D	24M, 82N	1%, 3%
Si (3)	SiC	D	24M, 82N	1%, 3%

Table 4.1. List of diamond coated samples produced at the Bristol School of Chemistry

Substrate refers to either the uncoated WC-Co insert (WC) or the commercial MCD insert (MCD) except for the last 3 which utilised interlayers of molybdenum (Mo), tungsten carbide (WC int) or silicon carbide (SiC).

Pre-treatments refer to: A, 70% nitric acid treatment and diamond seeding, B, 70% nitric and 36% hydrochloric acid treatment and diamond seeding, C, 70% nitric acid treatment and no seeding and D, diamond seeding with no acid treatment.

Deposition time shows how many hours of deposition were completed using MCD conditions (M) and NCD conditions (N).

Gas ratio shows the percentage of methane in hydrogen being used relative to the deposition time.

4.2. Baseline cutting tools

4.2.1. Sandvik VBGT WC-Co insert

The diamond coatings were developed on a standard commercially available cobalt cemented tungsten carbide turning insert, as mentioned in chapter 3. It was therefore important to examine and test these tools in order to create a baseline from which to build on. Electron microscopy was used to investigate the integrity of the unused cutting tools to ensure the substrate had a reliable surface structure for the diamond coatings to be deposited on. The majority of the WC-Co inserts examined had a uniform surface with few defects, with the micrographs showing a relatively smooth cutting edge due to the surface layer of cobalt. The tops of WC crystals can be seen at the surface, however, they accounted for a small percentage of the surface near the cutting edge (Fig 4.1 a).

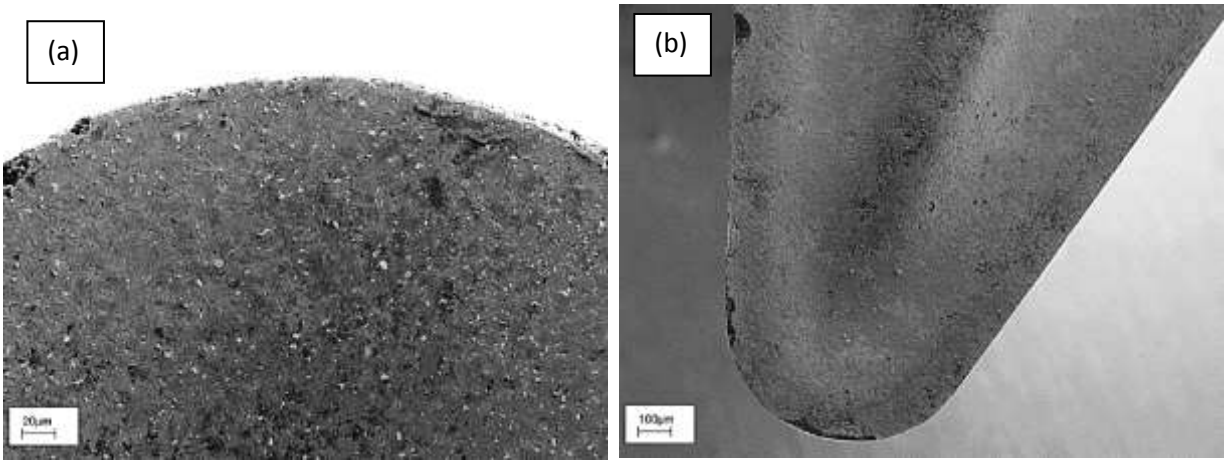

Figure 4.1. SEM micrographs of the cutting tips of WC-Co inserts at (a) X1k mag (b)150 mag

Small defects at the cutting edges of the tool were present on a number of inserts. It can be seen from figure 4.1 (b) that small sections of material have broken away from the insert. The darker areas at the cutting edge highlight small fractures in the material. These defects may have an adverse effect on any coating that is deposited on the surface.

In addition to many inserts showing small defects like this, in some extreme cases, more severe faults were present on a number of the tools. Micrographs showed some inserts to have significant damage prior to any use. It can be seen from figure 4.2, that the surface layer of cobalt has broken

away from the main body of the tool. This failure is likely due to defects caused by the sintering process employed in the manufacturing of the tool. As the WC crystals are compressed together in the cobalt binder, it forces the excess cobalt to the surface creating a cobalt rich layer. In some cases fractures can appear between this cobalt layer and the predominantly WC composition of the bulk material.

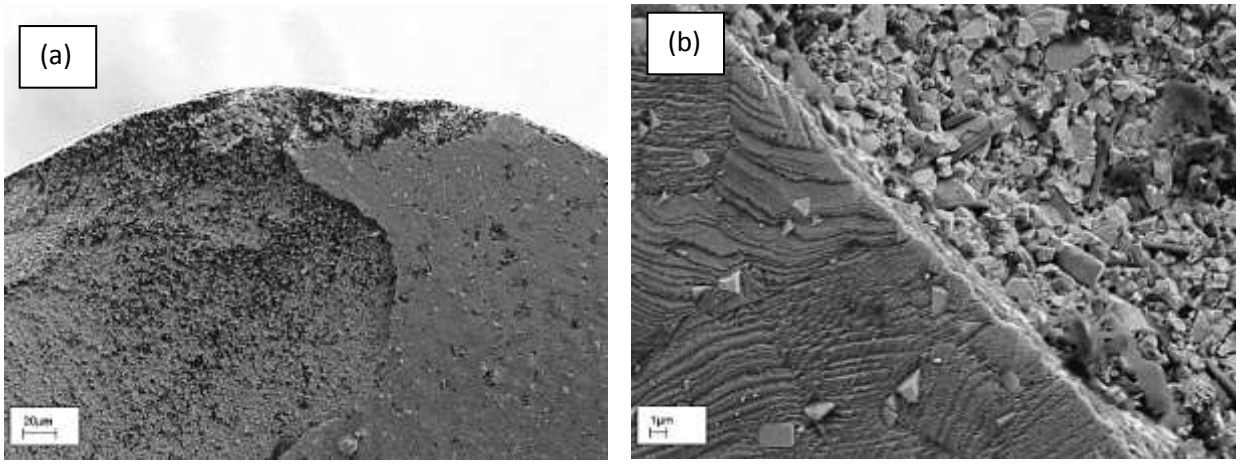

Figure 4.2. Uncoated WC-Co insert (a) cutting tip, (b) surface cobalt fracture edge

These defects in the underlying substrate can lead to problems when trying to deposit coatings. The etching process is designed to uniformly remove the surface layer of cobalt, exposing the WC crystals without compromising the integrity of the material. In areas where the surface layer of cobalt has broken away the etching process will begin to remove cobalt much deeper into the material creating inhomogeneity and weak areas in the tool and the coating which will further reduce the reliability of the tools.

In addition to the inhomogeneity caused by these clear failures in the tool material, there is also a certain amount variation in the surface composition of the defect free inserts. SEM micrographs highlight the variation in the surface at different points in the tool.

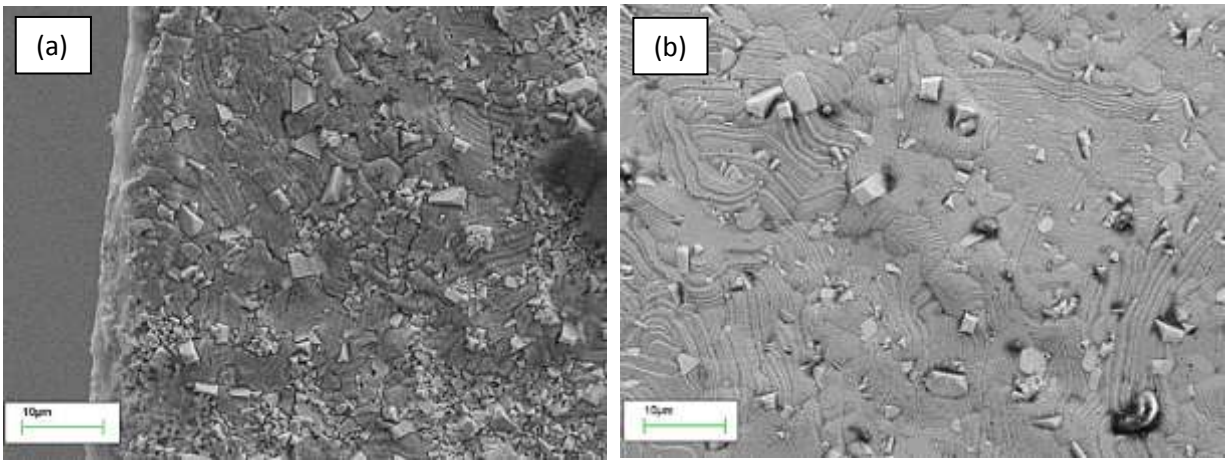

Figure 4.3. SEM micrographs of stock WC-Co tool showing cobalt binder covering Tungsten Carbide crystals at (a) cutting edge, (b) tool face

These variations are once again as a result of the manufacturing process. There are some patches at the tool tip in which larger areas of multiple WC crystals are visible at the surface (Fig 4.3 a), whilst other areas have relatively large distances between each visible WC crystal (Fig 4.3 b). These pictures reveal that the cobalt distribution at the surface is generally not homogeneous. This will be one of the contributing factors in regards to the difficulty of uniformly etching the cobalt from the surface.

It is clearly going to be necessary to monitor the inserts being used for the project to ensure they are of sufficient quality, as defect in the surface will likely have deleterious effects on the applied carbon coatings. This is because the substrate failures may alter the cutting edge geometry, thus creating weak points in the coatings due to areas of stress concentration, which may lead to delamination of the coatings. In addition to aiming to ensure the surface integrity of the inserts by SEM analysis, it will also be imperative to understand in which cases coating failure may have been as a result of defects in the underlying substrate material.

4.2.2. Sandvik VCGX micro-diamond insert

A nominally similar commercially available micro-crystalline diamond coated insert was utilised for the project in two ways. Firstly to test the performance of MCD tools as an added comparison to the NCD, MCD and DLC coatings being produced for the project, and secondly, to act as a foundation for the diamond coatings produced at Bristol School of Chemistry in order to test the performance of the coatings whilst the issues with adhesion were still being addressed. The insert used for this is the Sandvik coromant VCGX 160404 AL.

Figure 4.4. MCD insert from Sandvik (amazon.com 2011)

Analysis of the commercial MCD inserts revealed a uniform coating on the majority of inserts, with diamond crystal ranging from 2µm to 10µm in size at the surface. Analysis of multiple inserts, however, revealed a similar amount of reliability problems as seen with the uncoated WC inserts. Figure 4.5 (a) shows one tip of a new and undamaged MCD coated insert whilst (b) shows a new and unused insert which has suffered significant damage to the coating at the cutting edge.

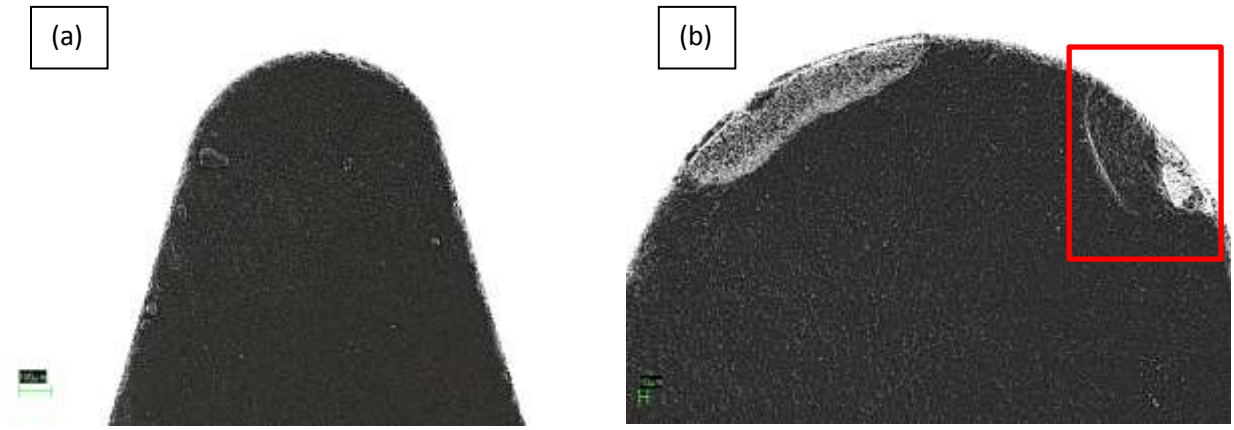

Figure 4.5. SEM micrographs of Sandvik MCD insert cutting tips (a) X150 mag (b) X1k mag

The highest incident of coating failure was delamination of the coating after the deposition, although interestingly, some of the delamination damage on the insert appears to have occurred during the deposition of the coating (Fig 4.5 b Red Box). This failure has created a step in the MCD coating near the cutting edge due to a variation in coating thickness. This has clearly created an area of weakness which may reduce tool performance considerably. Analysis of the areas of delamination of the commercial coating showed the coating to be between 7µm and 15µm thick with an average thickness of 10µm (Fig 4.6. a and b). The micrographs have also highlighted a clear issue in terms of the interface between the MCD and the WC-Co substrate. In the area highlighted by the red box in figure 4.6 a, it can be seen that the coating has come away from the substrate, likely as a result of compressive stress in the coating, and is only being held in place by the cohesive strength within the film.

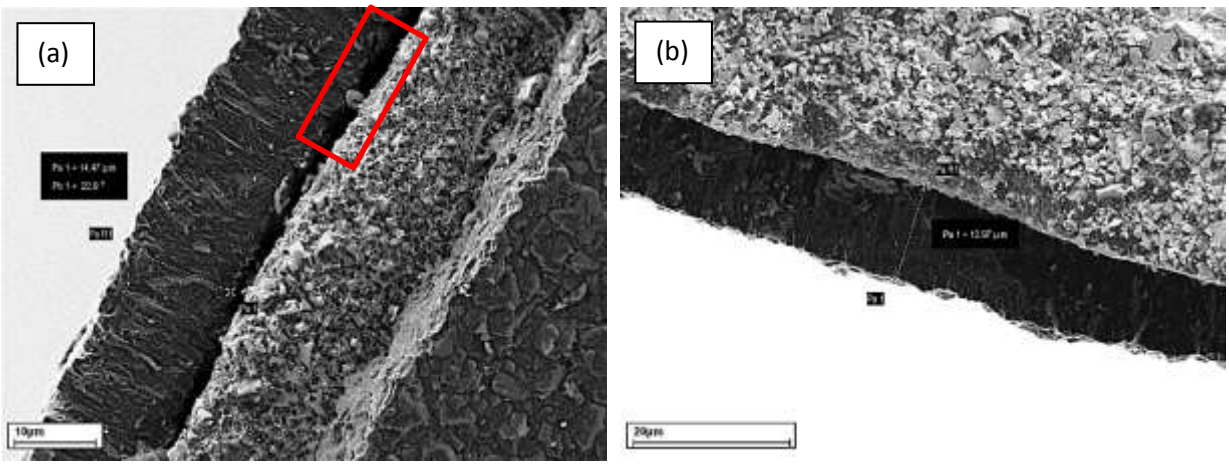

Figure 4.6. Micrographs showing delamination and coating thickness of Sandvik MCD inserts

Micrographs of the MCD tools revealed variations in the coating at different points on the tool surface. The majority of the coatings had deposited in such a way that the diamond crystals had grown and coalesced to form a continuous film covering the surface. In some areas (Fig 4.7. a) the crystals appear to have an increased growth rate, leading to raised clusters. At other points on the surface the crystals have not grown sufficiently to coalesce and the underlying tungsten carbide substrate material can clearly be seen through the gaps in the diamond coating (Fig 4.7. b).

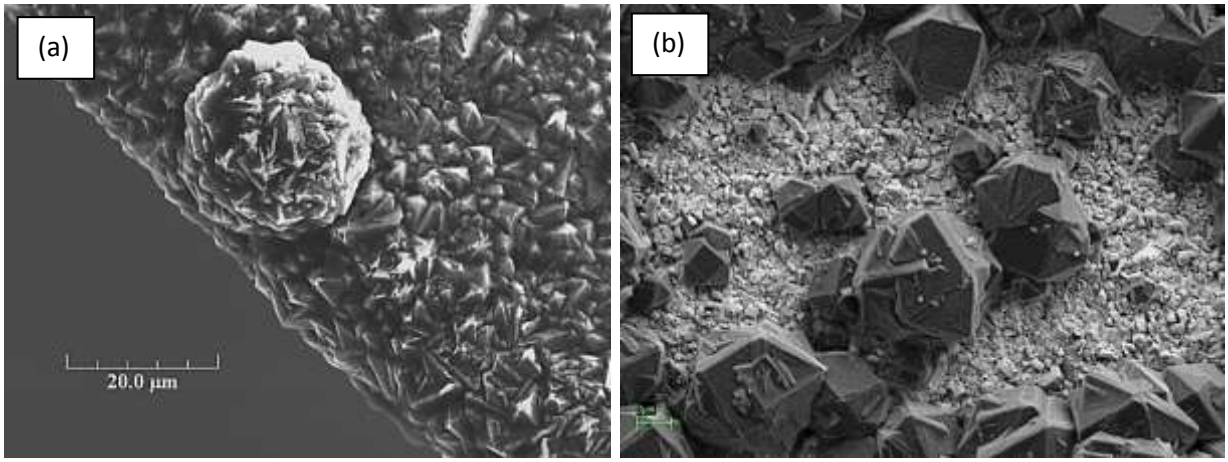

Figure 4.7.Micrographs of Sandvik MCD coating showing (a) raised cluster (b) gaps in coating

SEM analysis of the baseline WC-Co and commercially available MCD cutting inserts has highlighted a number of inconsistencies which are likely to effect the development of the coatings for this project. It has been discovered that the sample inserts will have to be monitored where possible to verify its integrity, and hence reduce any further variation which may occur due to disparity between sample substrates. The commercial MCD coatings have also been seen to have reliability issues, not only with the adhesion of the coating to the substrate, but also with variations in the surface morphology. These variations, in the form of raised clusters of gaps in the coating will potentially create weakness in the coating due to concentration of forces.

4.2.3. Initial baseline cutting trials

In order to be able to better judge the performance of the coatings being produced for the project some short trials were conducted. The sole purpose of this was to judge the potential tool life performance by examining BUE and BUL formation at the cutting tip. The Sandvik WC-Co insert and the MCD coated insert were both given a short dry cutting trial using the cutting parameters mentioned in chapter 3. The short trial consisted of 5 cuts, meaning the relative cutting distance was 2950m, as this was considered sufficient length to initially judge machining performance. The inserts

were examined using SEM before the trial to ensure there were no defects prior to machining. The insert was then re-analysed after the trial to check for sign of tool wear and aluminium adhesion.

Analysis of the WC-Co cutting tip revealed a significant amount of aluminium within the first 0.5mm of the cutting edge. The aluminium has adhered to a large percentage of the tool tip and can be seen over 1.5mm from the cutting edge (Fig 4.8). The green arrow indicates direction of cut.

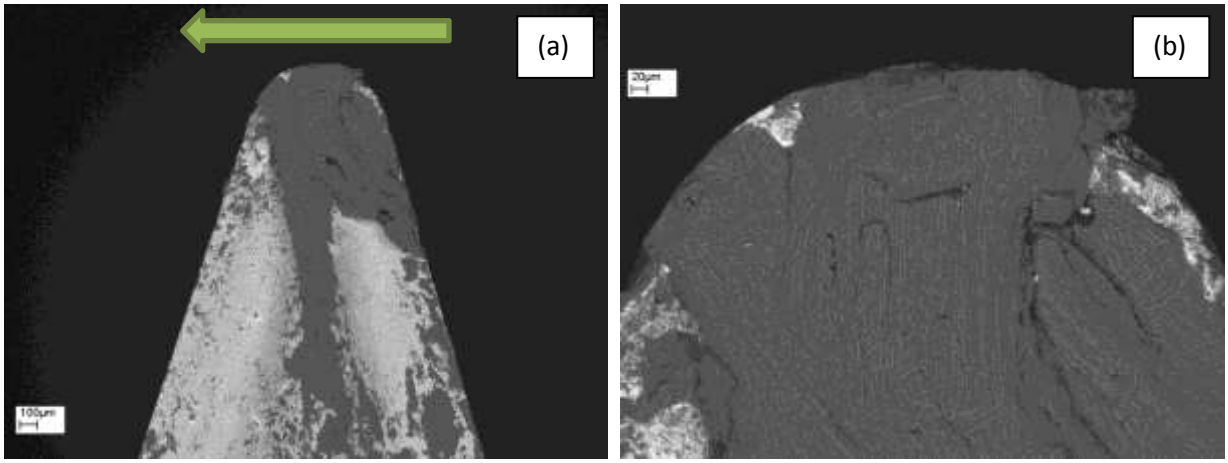

Figure 4.8. SEM micrographs of cutting tip of WC-Co after a short dry cutting trial

Tool wear has not become an issue at this stage of cutting as there is very little degradation of the cutting edge. The aluminium adhesion, the dark grey area at the cutting tip and chip-breaker, has clearly compromised the integrity of the tool. The entire cutting edge, particularly the end cutting edge, has suffered significant amounts of BUE which can blunt the cutting edge and alter the cutting tip geometry. This amount of aluminium adhesion can reduce cutting performance by increasing energy consumption, whilst also producing a poorer workpiece finish.

The commercial MCD, in comparison, suffered minimal aluminium adhesion which was confined to within 0.5mm of the tip, shown by the number 1 (Fig 4.9 a). There is also a very small patch of delamination to the left of the cutting tip centre (number 2). The aluminium adhesion was significantly reduced compared to the uncoated WC tool and can also be seen to have not affected the end cutting edge geometry.

There should therefore have been no effect on the machining performance of the cutting tool. High magnification micrographs show how the aluminium is adhering to the MCD (Fig 4.9 b).

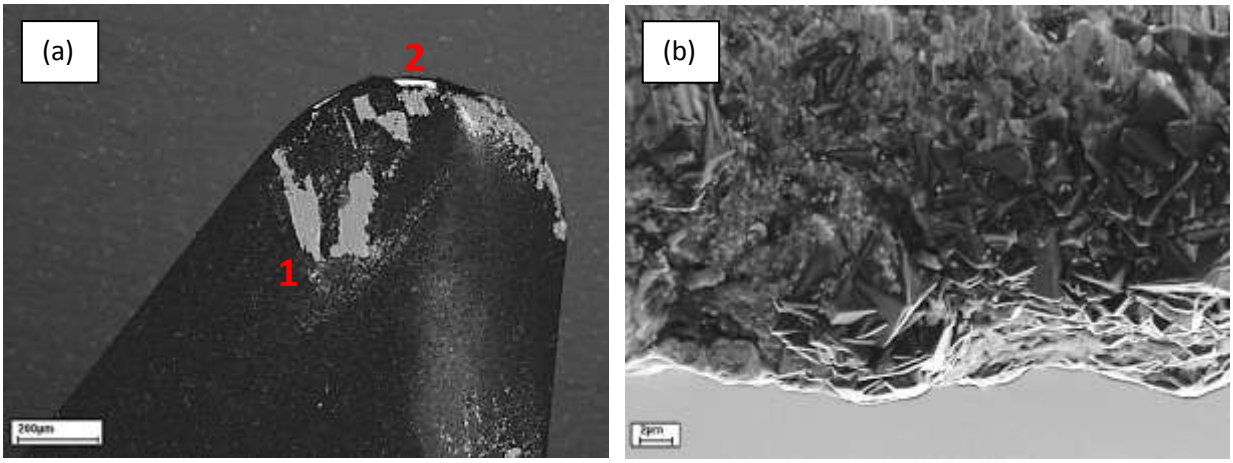

Figure 4.9. Commercial MCD tool after trial (a) cutting tip (b) cutting edge

Despite the MCD having a higher overall roughness the aluminium adhesion is significantly reduced due to the ultra-smooth sides of the MCD crystals. The aluminium has also adhered in a few small patches. This could suggest that small variations in the tool surface topography may have triggered the aluminium to initially adhere, which then encouraged further adhesion in those areas, whilst the majority of the tool surface remained aluminium free. The analysis of baseline tools has highlighted a number of issues which can influence the coating development for this project.

The integrity of the WC-Co material, particularly the Co rich surface layer, can vary immensely and will need to be monitored closely. This is to guarantee that only defect free inserts are coated, thus ensuring good comparability between samples. Short trials have also given an indication of what to expect in terms of tool life performance and development of BUE on the tool tip which will allow for more accurate judgement of the coatings produced.

4.3. Coating thickness and coverage

4.3.1. Coverage targets and development method

Due to the deposition being directional (line of sight) it means that the film growth will be optimised at the cutting tip and begin to diffuse as the distance from the tip increases. The diamond thin film will be required to uniformly cover the cutting edge of the tool, as well as a significant amount of the tool tip rake face and flank regions. Adhesion between the diamond and the WC substrate is often the weak point of the coatings as the bonding is mainly mechanical. The coating will therefore need to be thick enough at the cutting edge and chip-breaker to ensure it has the cohesive strength to withstand the machining forces which lead to crater and flank wear. Hence the coating will be deposited for optimum thickness at the top 1mm of the cutting tip (Fig 4.10).

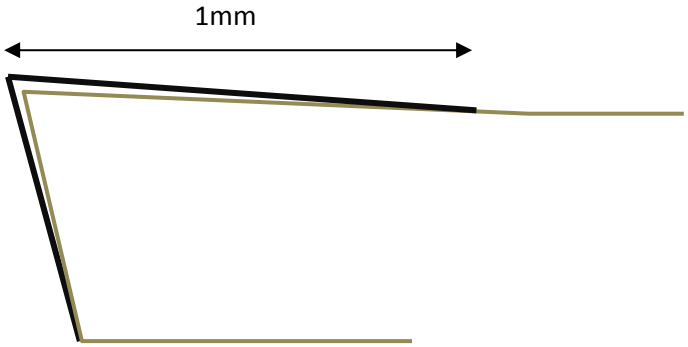

Figure 4.10. MCD/NCD coating thickness and coverage target

The HFCVD method employed for the deposition of the diamond coating was limited to a fixed rig for the positioning of the insert samples as well as a fixed filament for the sputtering source. The setup inside the reactor could then not be altered during the deposition process. This meant that the samples must be able to be positioned in such a way that the directional sputtering will coat the desired surfaces of the insert sufficiently. The complex geometry of the cutting edge of the tool makes this more difficult when attempting to coat the rake face and flutes, as well as the flanks.

Small variations in the positioning of the inserts in the reactor rig would have a significant impact on the coating. It is therefore important to ensure that not only the position of the insert in the reactor is optimal, but also that there is high tolerance in the rig so that the position remains the same relative to the filament for each coating.

Consideration of the dynamics of the cutting process would indicate that, at the cutting edge, it is important that the coating on the face of the tool is thicker than the coating on the flank. This is due to the forces the tool will be subjected to in the normal cutting process.

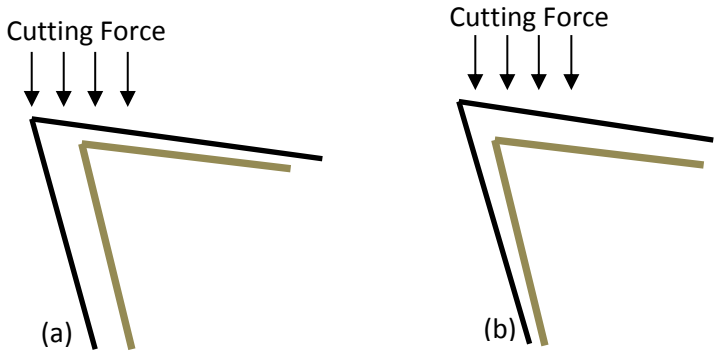

Figure 4.11. Coating target for cutting edge (a) Flank biased (b) Rake face biased

If the flank has a thick coating the cutting force will be more likely to break the coating away causing delamination at the cutting edge (Fig 4.11 a). This may make the tool unusable due to increased roughness of the cutting tip, which will lead to a poor or unacceptable work piece finish. A thicker coating on the face of the tool will be more likely to withstand the cutting forces. This is because the distribution of the force will be pushing the coating onto the substrate face, as appose to pushing it away from the substrate flank, as illustrated in figure 4.11 b. It is already understood that adhesion is likely to be a key issue with these coatings, therefore in order to reduce the chance of delamination it is important to ensure the cutting forces are directed through the coating into the insert. The coating on the flank must be thick enough, however, in order to anchor around the cutting edge to enhance its mechanical adhesion.

The main method for analysing the quality of the coating thickness and coverage will be by SEM. As well as providing visual verification of the coating quality through micrographs, it was also able to be used to quantify certain aspects of the film properties. At low magnification it is possible to look at the cutting tip as a whole, this allowed for reliable analysis of how uniformly the coating was being deposited, as well as the amount of coating being produced. In secondary electron detection mode the carbon coating is black, the tungsten shows up white and the cobalt appears light grey at a 6kV excitation energy.

The literature has shown that there will be a number of factors in the deposition process that will influence the coating thickness and coverage. Sample positioning will be one of the most important factors initially, followed by the deposition time. The positioning of the samples will be developed by analysing the distribution of the coating over the cutting tip, ensuring the flutes and flanks have a sufficient layer of diamond, as well as the cutting edge itself. The thickness will then be attributed to the deposition time of both the MCD and NCD layer.

4.3.2. Initial diamond coverage

The initial MCD growth parameters involved using 2% methane in hydrogen gas ratio for 20 hours, before switching to the NCD growth parameters of 8% methane in hydrogen for 72 hours. The aim was to create a 10μm MCD layer with a thin NCD layer at the surface.

Secondary electron (SE2) imaging of the first batch of ten inserts showed great variation in the quality of coatings in terms of thickness and deposition area (Fig 4.12). Micrographs of the top 1mm of the tool tips show some samples have failed to develop a homogeneous coating as the carbon can be seen to be patchy across the entire tool tip (sample AC3). The formation of the coating indicates that the diamond has begun to grow in small islands, although it has not grown sufficiently on the substrate to form a continuous film. The best sample had a continuous coating at the very tip of the

insert, yet within just 300µm from the cutting edge the coating has started to diffuse and the underlying WC-Co substrate can be seen (sample AC2).

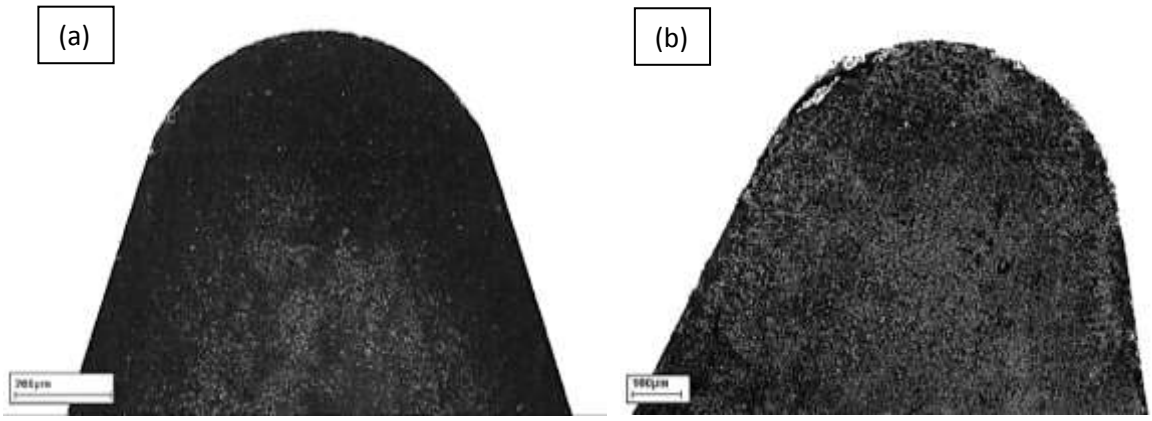

Figure 4.12. SEM micrograph of diamond coating samples, cutting tip of sample (a) AC2 (b) AC3

The SE2 images of the cutting tips show that the coatings appear to be relatively well distributed over the tip, which indicates the sample positioning in regards to the tip angle relative to the filament is adequate. It also suggests that the seeding process has been effective in creating a uniform distribution of diamond nucleation sites. The coatings are clearly not thick enough, however, suggesting that either the sample to filament distance, or the deposition time needs to be adjusted.

Higher magnification images of the cutting edge of the inserts revealed further weaknesses in the deposited coatings. Of the samples which had a continuous coating over the cutting edge of the tool tips, the majority of them had suffered some level of delamination. In this instance, the delamination was useful to highlight issues regarding the coating thickness.

It is evident that the visible patch of WC-Co is due to delamination and not poor growth of the coating (Fig 4.13.a). The fracture edge of the coating can be seen as a clear transition line between the coated and uncoated area. The coating thickness at the cutting edge appears to be less than 1µm thick, which is much less than the desired thickness required to ensure good cohesive strength in the coatings. It could be seen from the SEM images that coatings began to diffuse very close to

the tip, further indicating that the growth rate was not sufficient or the deposition time was too short.

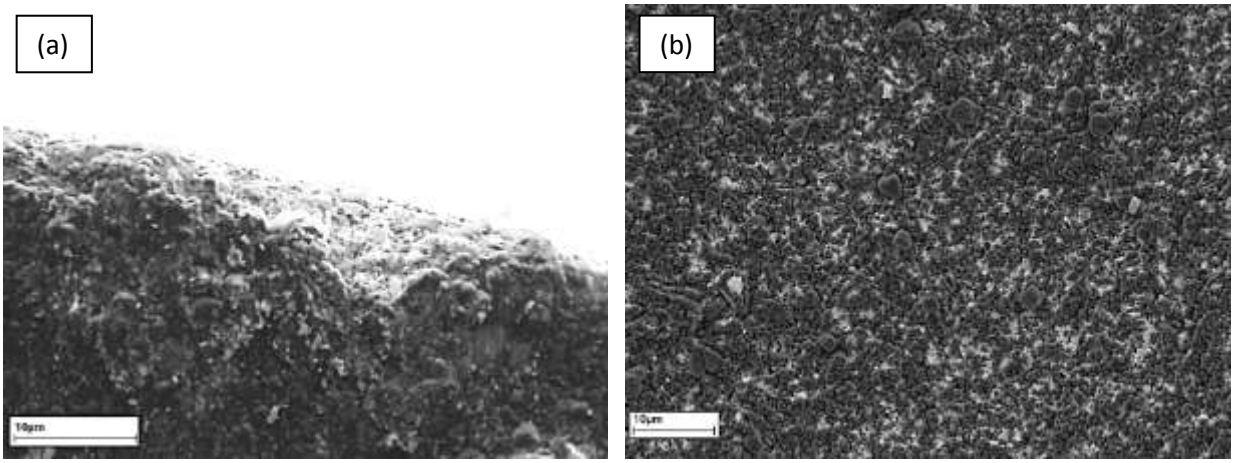

Figure 4.13. SEM micrographs of (a) cutting edge (b) coating diffusion boundary

As the coating reduces, the underlying substrate begins to become visible between the patches of diamond clusters (Fig 4.13 b). In order to develop the coating thickness and coverage, further coatings were produced with increased deposition times. Back-scattered electron analysis was used to quantify improvements in the coating coverage at the cutting tip and help determine the necessary deposition time and sample positioning required in order to achieve the desired coating characteristics.

4.3.3. Coverage development using backscattered electron analysis

SEM of the tool tip at 20kV in back-scattered mode penetrates the surface. Carbon, being a light element, shows up black, whilst the atomically heavy tungsten shows up white. It was therefore a useful tool for initially determining if the coatings are meeting the desired targets for thickness and distribution. Initial coating analysis revealed that a coating of 1mm was enough to ensure that a 20kV electron beam would not start to pick up the underlying substrate. This meant that for the coating to be of the required thickness, there should be no white areas visible in the top 1.5mm of the tool tip. This technique was limited, however, when trying to determine the ultimate thickness

of the coatings. In which case, analysis of delaminated areas, or sectioning of the insert was required to fully quantify coating thickness.

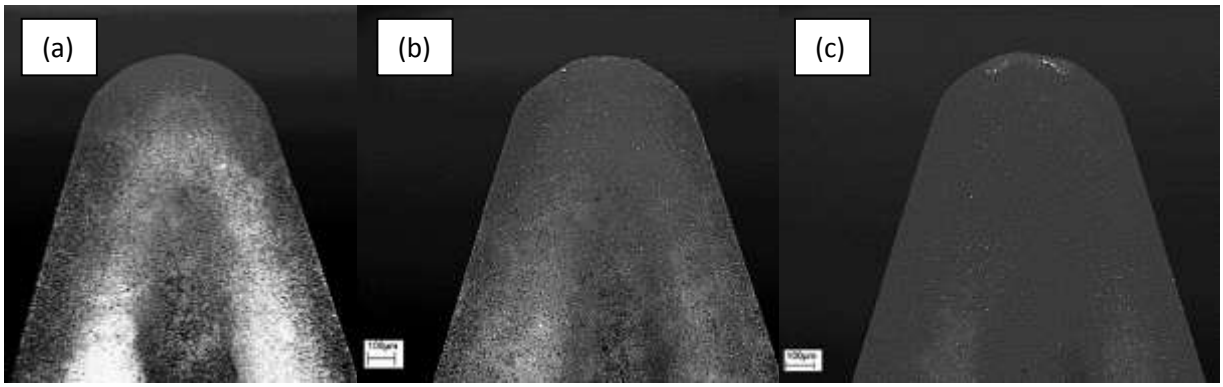

Figure 4.14. Backscattered micrographs of diamond coated tool tips at 20kV excitation energy

BSE imaging of the initial batches highlighted a number of discrepancies in the coatings in terms of quality and reliability. The range of quality of coatings varied greatly between inserts which were coated simultaneously in the HFCVD reactor. Some inserts had virtually no deposition whilst others had a relatively uniform coating across the entire tool tip. Figure 4.14 (a) shows a tool tip which has a thin coating at the cutting edge and at the chip-breaker of the tool, however, there is little or no coating in the flutes of the tool. Figure (b) shows a slightly improved coating with better tip coverage, although the flutes are still showing a reduced deposition compared to the rest of the tool tip. The same can be seen in figure (c) to a lesser extent indicating that the positioning of this sample may have been more optimised to compensate for the depression of the flute channels. It is worth noting that the flutes of the cutting tool will always show a reduced deposition rate due to the shielding effect of the raised cutting edge and chip-breaker surrounding it. Despite the significant variation in coatings, none of the initial samples had the desired coating thickness predicted for a deposition time of that length.

There are a number of reasons why the deposited coatings show such variation in quality. The manual processes involved in the preparation of the samples as well as the inherent variability of the samples themselves means that there will always be reliability issues even before deposition begins.

Although the coating thickness and distribution predominantly depends on sample position and deposition time, it will be influenced to a lesser degree by the other factors. Despite the acid etching technique being more attributable to coating adhesion issues, it will inevitably affect the diamond seeding distribution, and hence the coating uniformity. The diamond seeding process is a manual task in which nano-diamond crystals are ground into the substrate surface in order to seed the diamond deposition. For the diamond growth to be homogeneous the seeding crystals need to have a relatively uniform dispersion over the substrate surface. If the substrate surface is not homogeneous then the diamond seeding will be negatively affected as a result. Efforts were made to reduce variations in the seeding process, however, it was not possible to verify the diamond seeding of every sample. Other variations in the coatings were down to the deposition process. The rig that was used to hold the inserts required each sample to be positioned individually. The distance from the filament was nominally the same for each set of ten samples, although the direction of the tip towards the filament was set visually by hand. The slightest variations in position would lead to potentially large differences in the coating and was likely to be responsible for some of the differences. It then became apparent that despite the set of ten samples running parallel to the filament, there may be variation depending on which point along the filament the sample is positioned. The reactor was therefore mapped in order to test if there was a significant difference in deposition due to variation in energetic particles at different points across the filament.

4.3.4. Reactor mapping

An experiment was conducted in order to test how the vertical positioning of the inserts in the reactor may be affecting the quality of the diamond coating being produced. The inserts were labelled set X and Z, each set having 10 samples. The pre-treatment and deposition parameters used are shown in the sample list. Figure 4.15 shows the sample positioning in the reactor.

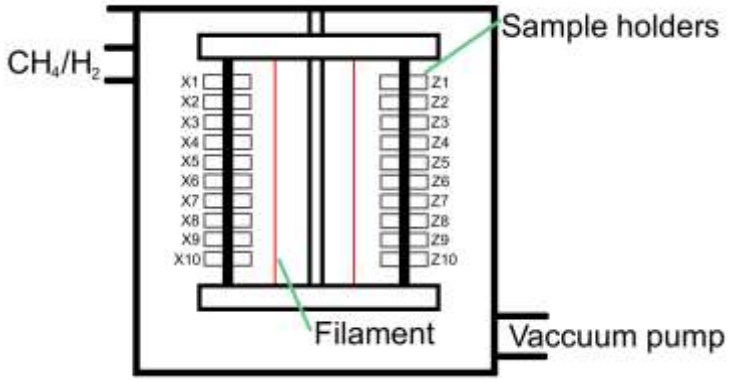

Figure 4.15. Diagram of the HFCVD reactor showing the positioning of each sample

BSE imaging was used to analyse the coating coverage of the tool tips in terms of coating coverage, uniformity and thickness. The images were then assembled together in order to visually compare the effect the position in the reactor has on the coating deposition (Fig 4.16).

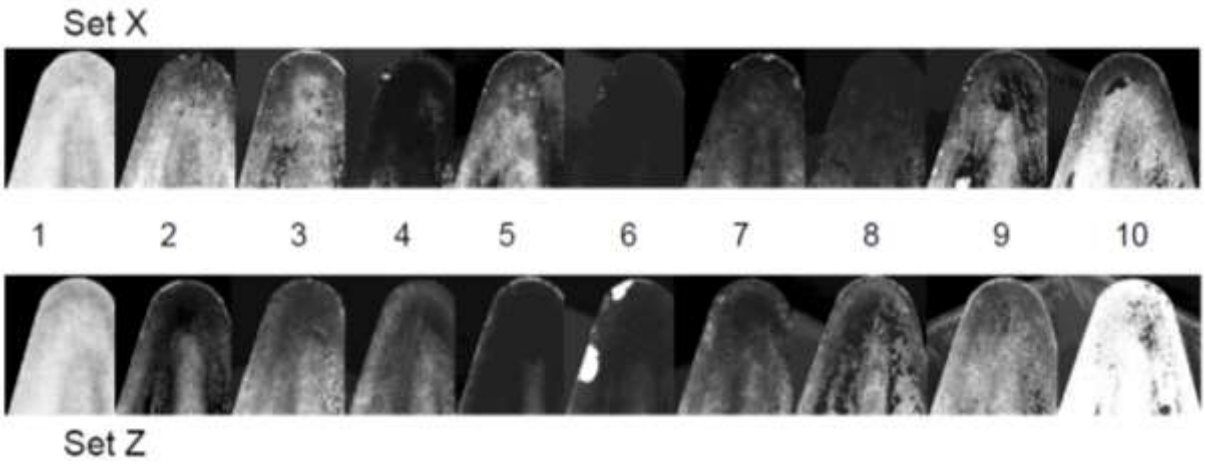

Figure 4.16. SEM micrographs of tool tips relative to their reactor position

It was clear from the BSE analysis that the samples at either end of the set of ten had not produced a coating, sample 1 of both X and Z sets shows no coatings at all. Samples 2, 3 and 9 of each set all had poor coatings whilst the thickest most uniform coatings appeared to be in the centre. The transition of coating quality between the edges and the centre of the filament is clear, however, it is not gradual, indicating that other factors in the pre-treatment or deposition have affected the coatings

significantly. This may be due to slight variations in the tip angle relative to the filament, as well as discrepancies in the pre-treatment. Several of the samples showed thick carbon deposits surrounded by little or no coating. These issues were likely to be related to seeding and adhesion issues.

With the preferred sample positioning confirmed it was just a case of increasing the deposition time until the coating thickness reached the desired targets. It was discovered that for the MCD layer to reach the required thickness, the deposition time had to be increased to over 90 hours.

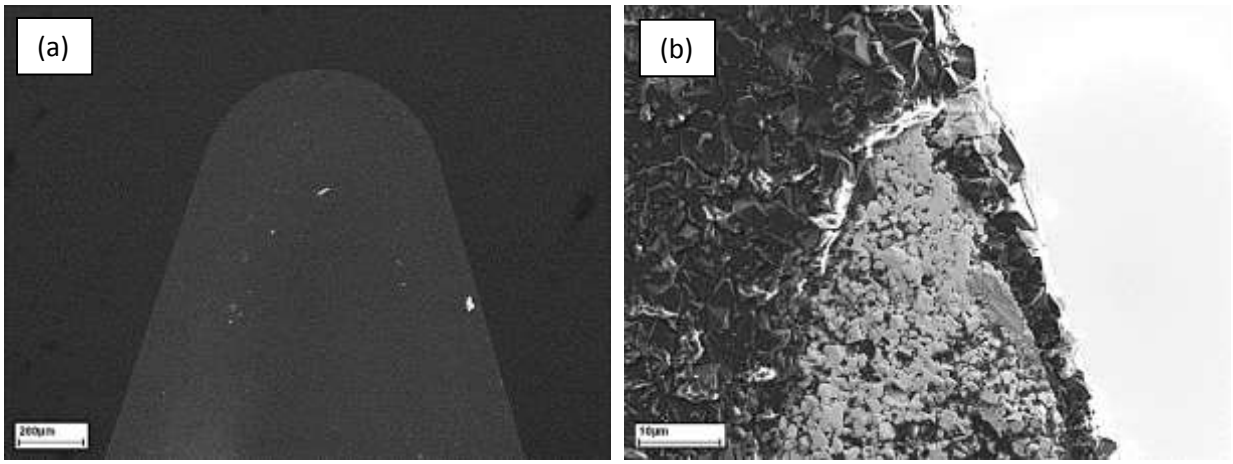

Figure 4.17. SEM micrographs showing (a) BSE image of well coated tip (b) SE2 image of thickness

With the aid of SEM analysis it was possible to develop the deposition parameters to ensure that the majority of tools coated had a sufficient coating. BSE micrographs were used to guarantee that the coating was fully covering the required area of the cutting tip (Fig 4.17 a). SE2 analysis of coating fractures and sectioned inserts confirmed that the coating at the cutting edge was at least 10µm in thickness, reducing to roughly 5µm in the first 0.5mm (Fig 4.17 b).

With the parameters regarding the thickness and distribution of the coating being established it became necessary to improve the interface between the coating and substrate as delamination was still affecting a large majority of coatings produced.

4.4. Diamond coating adhesion

4.4.1. Acid etching

Previous literature highlighted the currently ongoing issue regarding the deposition of adherent diamond coatings on WC-Co surfaces. The following section describes the development of the acid etching process used in this project, with the aim of producing a consistent method for depositing reliable diamond coatings on cemented carbide cutting inserts. SEM analysis was utilised along with energy dispersive X-ray spectroscopy (EDS) to evaluate the efficacy of the acid etching process for the removal of the cobalt surface layer. It was necessary to completely remove the cobalt from the surface of the insert in order to allow the WC crystals to create a surface in which the diamonds seeds can grow around the WC crystals. This will allow forming of the mechanical bonds necessary to create sufficient adhesion between the MCD and the WC, whilst simultaneously acting to prevent graphitisation of the interface.

The etching process initially used a 70% nitric acid in water solution in which the top 3mm of the tip was suspended in the solution for five minutes before being rinsed in methanol. SEM analysis of the insert after this etching procedure showed that the cobalt (darker grey colour) had not been sufficiently removed from the surface. Residue of the cobalt binder was evident in some sections, although other areas of the tool tip appeared to show no sign of the cobalt binder.

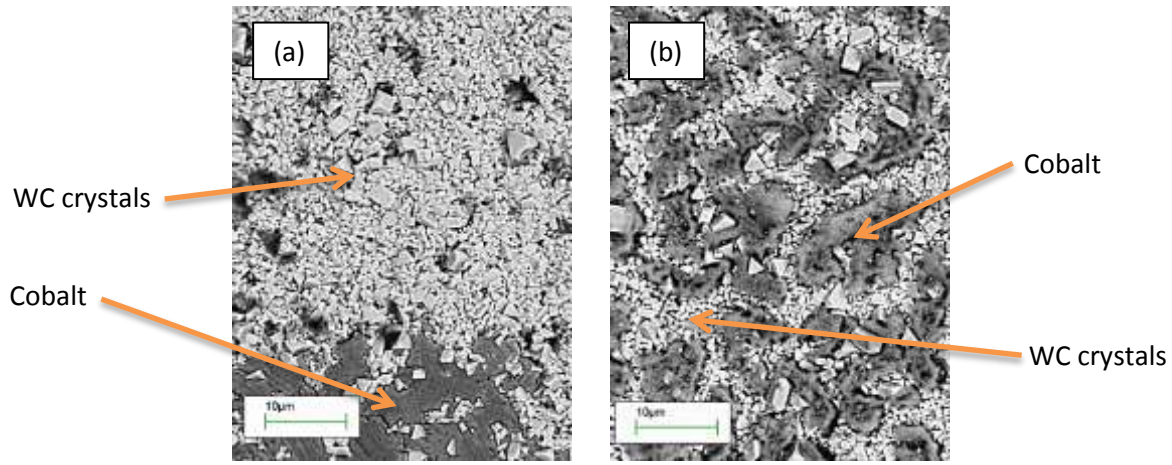

Figure 4.18. SEM micrographs of WC-Co surface after nitric acid etching

SEM analysis revealed patches of cobalt are visible at the central area of the cutting tip after etching in nitric acid. The results showed that in some cases larger areas appear to have been etched successfully whilst in other areas large deposits of cobalt remain at the surface (Fig 4.18 a). At other points on the insert the cobalt appeared to have been etched in such a way that irregular surface morphologies were being created (Fig 4.18 b).

The failure to remove the cobalt from the tool surface was apparent on many of the inserts and was also evident directly at the cutting edge itself (Fig 4.19). This highlighted that the current nitric acid treatment was not effectively etching the surface and an improved process was required.

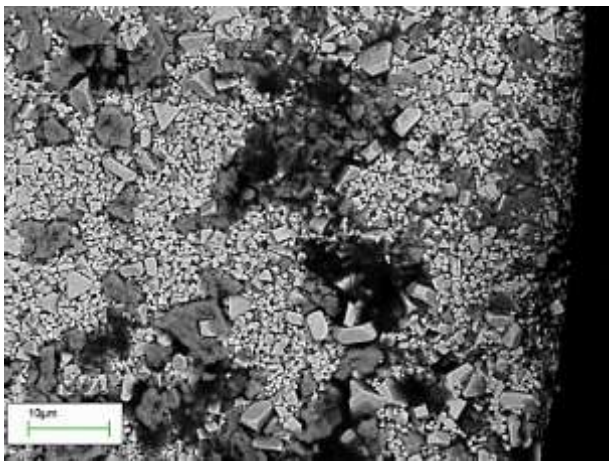

Figure 4.19. SEM micrograph of surface cobalt at insert cutting edge

It was clear that in many areas of the tool tip the cobalt had not been sufficiently removed, and in addition, the structure looked unaffected by the etching process. There were, however, also parts of the tool in which the structure and integrity of the cobalt had clearly been altered.

In some areas the cobalt has been affected, but not removed, by the etching. The cobalt layer has started to degrade yet remains at the surface, meaning there is loose layer contaminating the surface which can lead to a further impairment to the adhesion between the substrate and MCD, or often inhibit growth entirely (Fig 4.20).

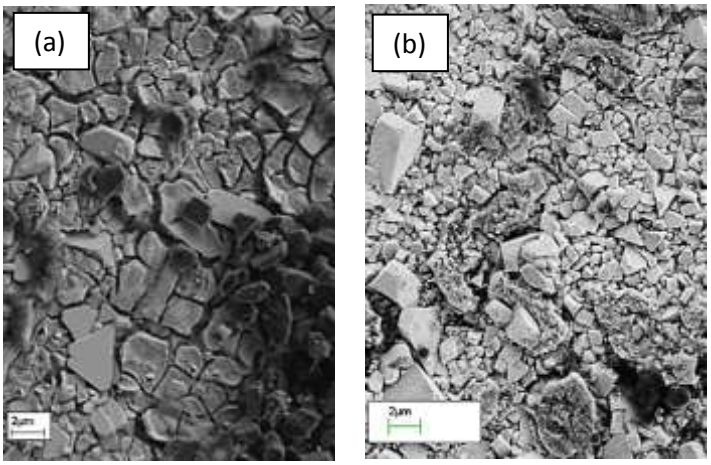

Figure 4.20. SEM micrographs of degraded cobalt (a) surface layer (b) irregular patches

It is important to try and ensure that the etching has removed the cobalt from the immediate surface but not any deeper as it would lead to degradation of the tool. SEM imaging can reveal if there is cobalt remaining on the surface but it does not show how much may be removed beneath. EDS was therefore used to quantify the cobalt removal and aid in the development of the etching process. With the use of EDS to quantify the cobalt concentration at the surface of the insert, it was possible to develop the etching process. This meant that the samples were suspended in the etching solution for the correct amount of time to remove the cobalt from the surface, whilst aiming to ensure the bulk cobalt matrix remained undamaged. It was discovered that the nitric acid solution in itself did not reliably remove the surface cobalt layer, even when suspended in the solution for a longer time, indicating that a revised etching solution was required.

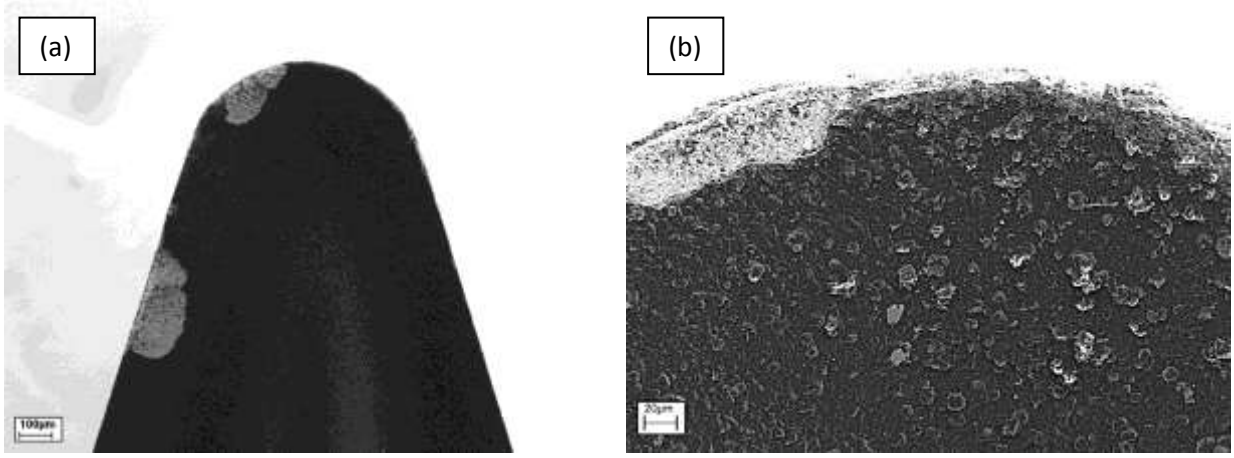

Figure 4.21. SEM micrographs showing delamination along the cutting edge

Delamination at the cutting edges remained one of the main issues regarding coating adhesion to the substrate (Fig 4.21). This is linked to an increase in residual stress concentration due to the geometry of the cutting edge (Renaud *et al.*, 2009), as well as the fact that the edges are more likely to suffer shock damage.

The initial aim was to etch the surface so that no cobalt residue or contamination could be seen at the surface of the tool. Figure 4.22 (a) shows an SEM micrograph of the insert surface that has been etched sufficiently that no cobalt is visible. It was found that this complete removal of cobalt was optimal for the deposition of adherent coatings (Fig 4.22 b). It can also be seen that the WC crystal size ranges greatly, from as small as 0.5µm up to over 5µm. The larger crystals on the surface create an inhomogeneous surface for the MCD nucleation and growth. In order for the seeding and deposition to be as uniform as possible the substrate also needs to be uniform. Protruding crystals can lead to an uneven distribution of seeding crystals, which can produce excessive and erratic growth in the form of raised diamond clusters. These clusters in turn lead to weaknesses in the structure of the thin film.

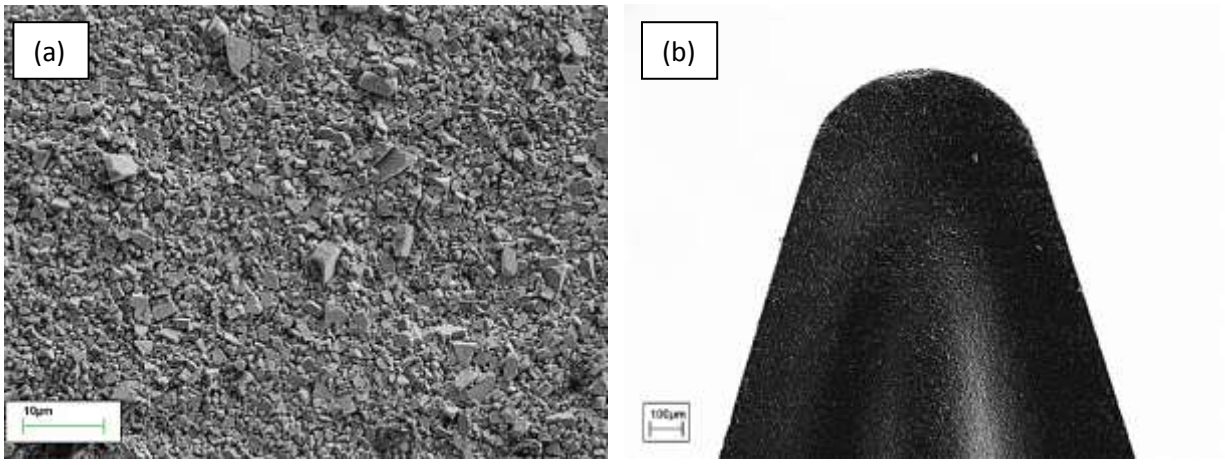

Figure 4.22. SEM micrograph of (a) cobalt free surface (b) adherent coating

The etching process was developed in order to achieve a more reliable removal of the cobalt surface layer. Acid treatment was altered to a mixture of 70% nitric acid in water and 36% hydrochloric acid in water, similar to literature (Wei *et al.*, 2010; Polini, 2006),as this had been shown to etch the surface more reliably.

Analysis of the diamond coatings showed that adhesion was improved significantly on the majority of inserts. Brief cutting trials were conducted to test the adherence of the coatings and ensure that the pre-treatment process was effectively preparing the surface for deposition.

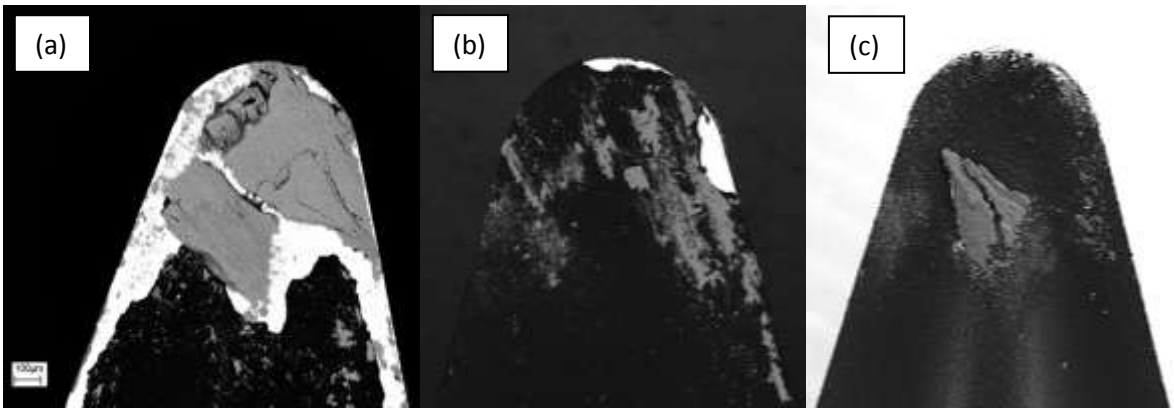

Figure 4.23. SEM micrographs showing the evolution of diamond coating performance

The drawback of using cutting trials to test the coatings is that it simultaneously tests the coating hardness, adherence and friction properties meaning that it becomes difficult to determine what aspect may be responsible for any failings in the coatings. SEM micrographs did, however, make it possible to determine delamination failure, as opposed to wear, due to the clear fracture plane in the coatings. Analysis revealed that initial coatings were virtually completely removed during a short cutting trial, due to the poor adhesion and low coating thicknesses. The development of the coating thickness, distribution and adhesion meant that the majority of diamond coatings deposited had sufficient performance to complete a short cutting trial without suffering delamination failure at the cutting tip (Fig 4.23). Reliability remained an issue, however, as there were still a significant number of failed coatings in each batch produced.

It then became necessary to develop the surface layer in order to ensure an optimal surface was prepared for the DLC layer to be deposited onto. It is worth bearing in mind at this point that the best individual diamond layer, in terms of machining performance, may not necessarily be the best for a combined DLC layer. The next section details the development of the surface structure, in terms of both morphology and chemistry.

4.5. Surface structure

4.5.1. Morphology targets

The following section discusses the development of the surface structure of the coatings. It looks at the deposition conditions required to produce the MCD and NCD structured diamond, which will then be compared and combined with DLC coatings to test the efficacy of the coatings for machining aluminium. There are already a number of expectations regarding the coating characteristics and performance. MCD surfaces are rough in comparison to the majority of surface finishes and coatings that are available for WC-Co cutting inserts. Uncoated inserts generally have a smooth cutting edge due to the cobalt binder which creates a continuous flat edge. Titanium and aluminium nitride based coatings are often rougher than the uncoated tools due to the PVD deposition process used in their fabrication, they are, however, still much smoother than MCD coatings. Diamond has been shown to be the hardest of these commonly used materials, with MCD being the most widely utilised. MCD allows for a very hard cutting edge with low friction due to the smooth crystal edges, however, the crystal size means that the work piece finish often suffers as a result. NCD and fine crystal diamond is being considered as a way of benefiting from the hardness of crystalline diamond whilst reducing the detrimental effects on work piece finish. MCD coatings were to be produced as an added comparison, as well as providing the base for the NCD coating. This is because an initial MCD layer is required to enhance coating thickness, strength and adhesion. The NCD layer then deposits over the MCD layer to produce the smoother surface for reduced friction and improved WP finish (Fig 4.24).

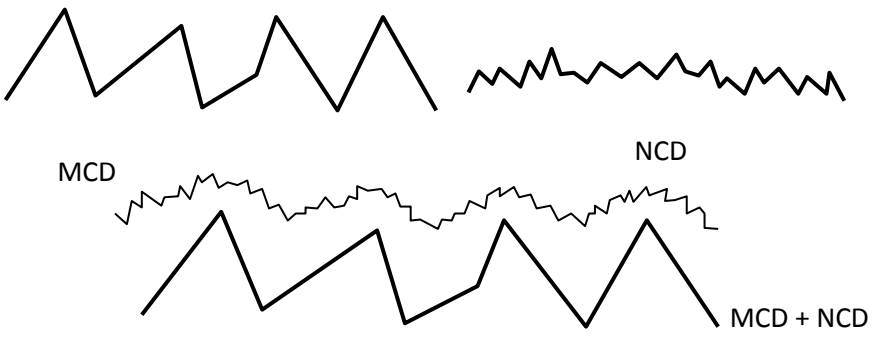

Figure 4.24. Illustration of MCD and NCD combination

4.5.2. Surface morphology development

The MCD layer of the coating was developed singularly to ensure that the deposition conditions being used were forming the desired structure. Several coatings were produced using the MCD deposition parameters, as shown in the sample list at the start of the chapter. Initial coating were deposited using 2% methane in hydrogen, however, SEM analysis revealed that the crystal sizes were below the expected 5µm in size, indicating that the methane content was too high. The ratio was then set to 1% methane in hydrogen which was found to produce the desired MCD morphology at the cutting edge (Fig 4.25 a).

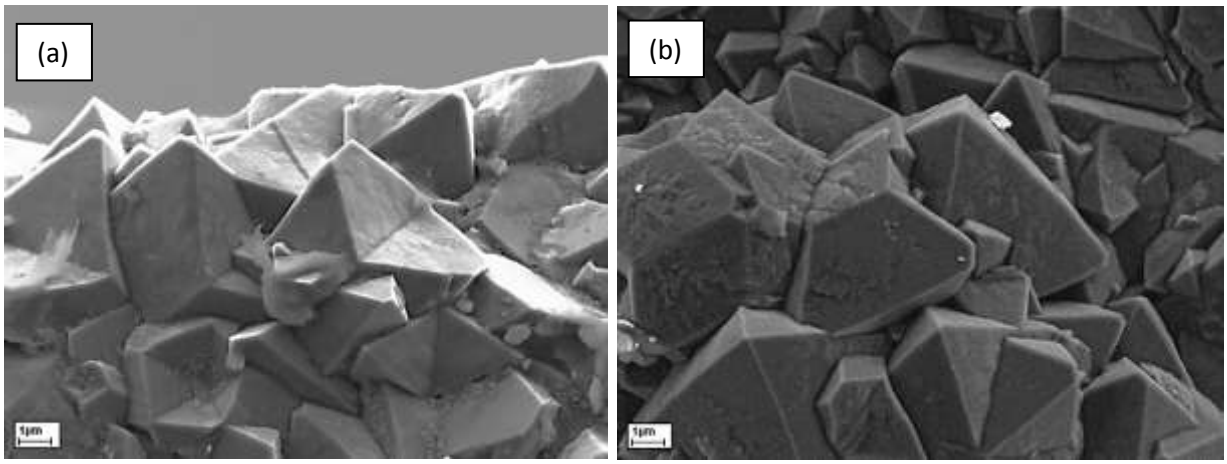

Figure 4.25. SEM micrographs of MCD coating showing (a) cutting edge (b) chip-breaker

SEM analysis of the MCD coatings showed a number of variations in the film surface. The majority of the coating contained diamond crystals ranging between 0.5µm and 5µm in size, with the largest reaching up to 10µm in size. The images show how the crystals have grown and coalesced to form a continuous film. It can be seen that despite the overall film roughness caused by the sharp protruding crystals, the faces of the crystals are very smooth. The faces are not atomically smooth, however, as nanoscale defects can be seen on the crystal planes in figure 4.25 (b). The largest crystals grew at the cutting edge of the insert where the deposition parameters had been set for the optimal diamond growth. Other areas of the insert showed variation, not only in the amount of coating deposited, but also the structure of the coating and crystal sizes. In other areas of the tool the coating varied significantly with the average crystal size being much smaller than at the tip of the

tool. The largest crystals, at a position 3mm back from the cutting tip edge, were less than 5µm and were imbedded in a matrix of much smaller crystals of sizes ranging from 300nm to 500nm. The smaller crystals can also be seen to have grown on the top surface of the MCD (Fig 4.26). It can also be seen that the crystals have not grown sufficiently in this area of the tool to completely cover the substrate surface. Although these gaps in the coating would usually be considered a source of weakness, they were far enough away from the cutting edge not to influence performance.

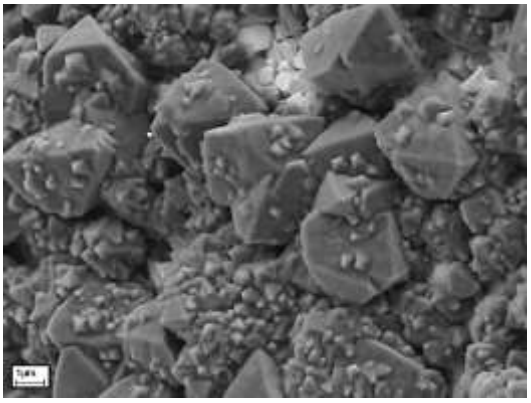

Figure 4.26. SEM micrograph of MCD crystal growth patterns

The MCD structured coating was unfortunately too rough to analyse using AFM and therefore white light interferometry was used to measure the surface roughness near the cutting edge. It was found that the MCD had an average roughness of 0.43µm in the top 0.5mm of the cutting tip. Raman analysis also confirmed strong diamond peak at 1333.7cm^{-1}, as well as a mix of disordered and graphitic peaks associated with CVD produced MCD coatings (Fig 4.27). The shift in the diamond peak from the 1332cm^{-1} position suggests that compressive stresses in the coating are relatively low.

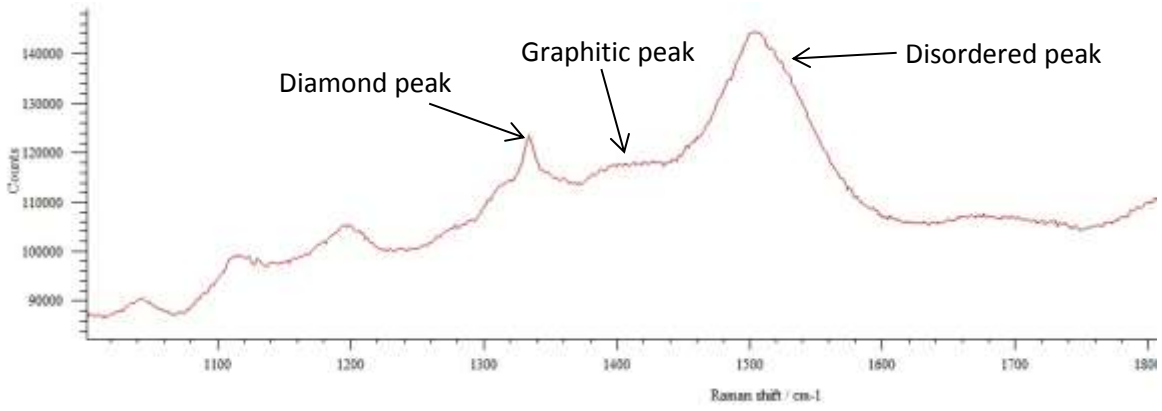

Figure 4.27. Raman spectrum of the MCD coating

The development of the NCD structure is more complex due to the greater range in morphologies that can be considered NCD or UNCD. Of the coating produced, SEM analysis has shown significant variation in the surface structure and topography, with some surfaces appearing to be more amorphous than crystalline in nature, whilst some areas contained a blend of crystalline and amorphous structures (Fig 4.28 a). It can be seen that MCD crystals appear to have grown at the surface, above an NCD layer, indicating that the NCD phase may be producing MCD under certain conditions.

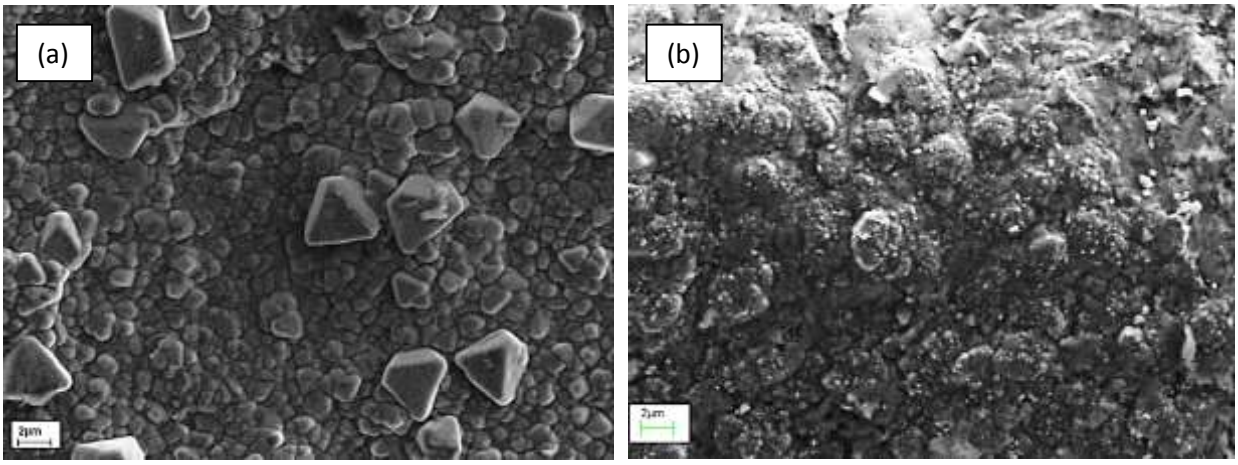

Figure 4.28. SEM micrographs of NCD surface with ratio of (a) 8% (b) 9%, methane in hydrogen

A gas ratio of 9% methane in hydrogen was found to create a nodular structure with regular nodules between 1 and 4 microns in size at the tool tip (Fig 4.28 b). The coating at this ratio is visibly very similar to that of amorphous carbon coatings. Although ultra nano-crystalline structures are present, the micrographs indicate that a significant amount of disordered and graphitic structures were also forming a large percentage of the surface structure. Raman analysis of the coatings showed great variation in the size and shape of the peaks, however, some key peaks were evident and it was possible to confirm the presents of non-diamond structures. Analysis of the coating deposited using 9% methane in hydrogen showed large characteristic graphitic peaks at 1,380cm^{-1} and 1,510cm^{-1}. Interestingly, the diamond peak, although reduced in intensity, had not shifted from the peak position measured on the MCD sample (Fig 4.29).

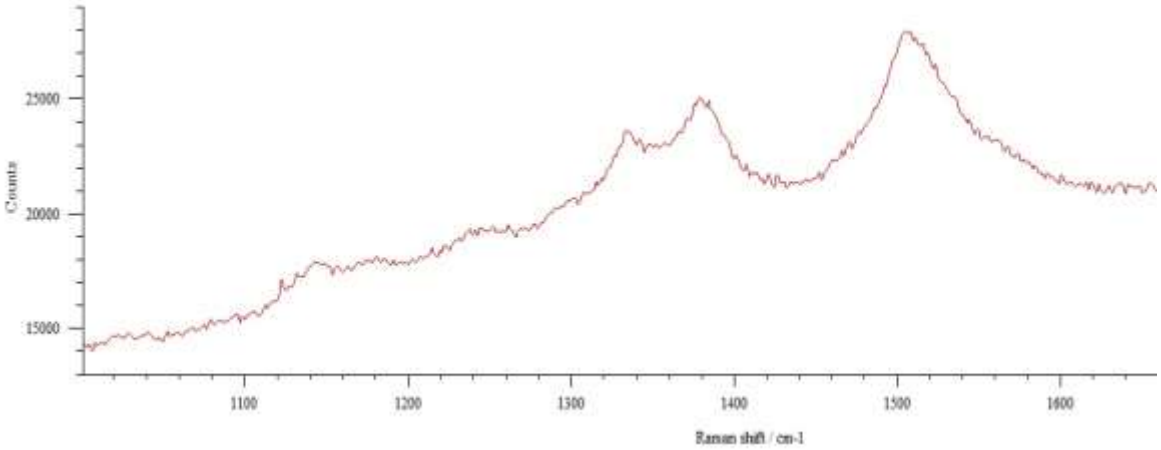

Figure 4.29. Raman spectrum of graphitic NCD layer

The gas ratio was the key variable used for altering the diamond structure, however, micrographs show that distance from the cutting edge, hence distance from the filament, also produced variation in the coating. SEM analysis indicated that crystal size generally reduced as the distance from the tip increased, although in some instances inhomogeneous diamond structures had grown at various points on the cutting tips. Clustering of diamond crystals could also be seen in a number of samples and can be seen to vary greatly in size and structure (Fig 4.30). These irregularities in the coating may be a result of slight imperfections or protrusions in the substrate or diamond seeding layer. These protrusions may act to facilitate increased diamond growth as they capture a larger portion of the sputtered particles leading to exponential growth in these areas.

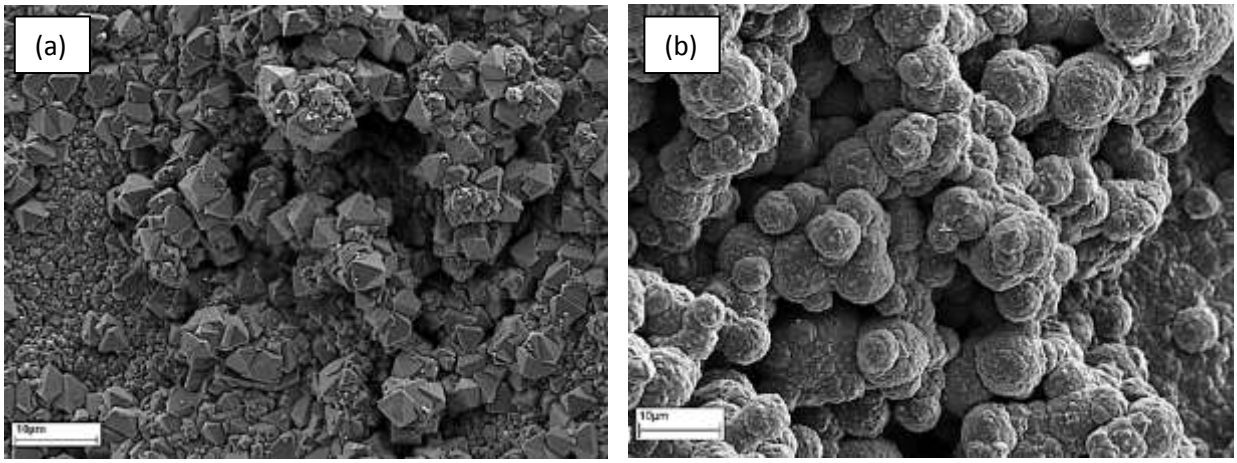

Figure 4.30. Diamond crystal clustering (a) MCD clusters (b) NCD clusters

Figure 4.31 (a) shows large micro-crystals with regular tetrahedral shapes of similar size with smaller crystals surrounding them. The larger clusters of MCD crystals are up to 15µm wide and have grown in such a way that large cavities have formed between the raised peak clusters. NCD crystalline clusters have grown in spherical clusters protruding from the surface creating a structure in which the nano-crystals appear to be blended with amorphous carbon in spheres ranging between 3µm and 10µm in diameter (Fig 4.30 b).

Several methane in hydrogen ratios were examined, with the surface morphologies and bonding chemistry being analysed for each one. SEM analysis initially revealed the variation in coating structure due to not only the gas ratio, but also the deposition time of the NCD layer. Figure 4.31 shows the variation in coating morphologies produced at the cutting edges of the inserts. The coatings ranged from a bed of micro-crystal type structures to nano-diamond formations imbedded in a matrix of disordered and graphitic structures (Fig 4.31).

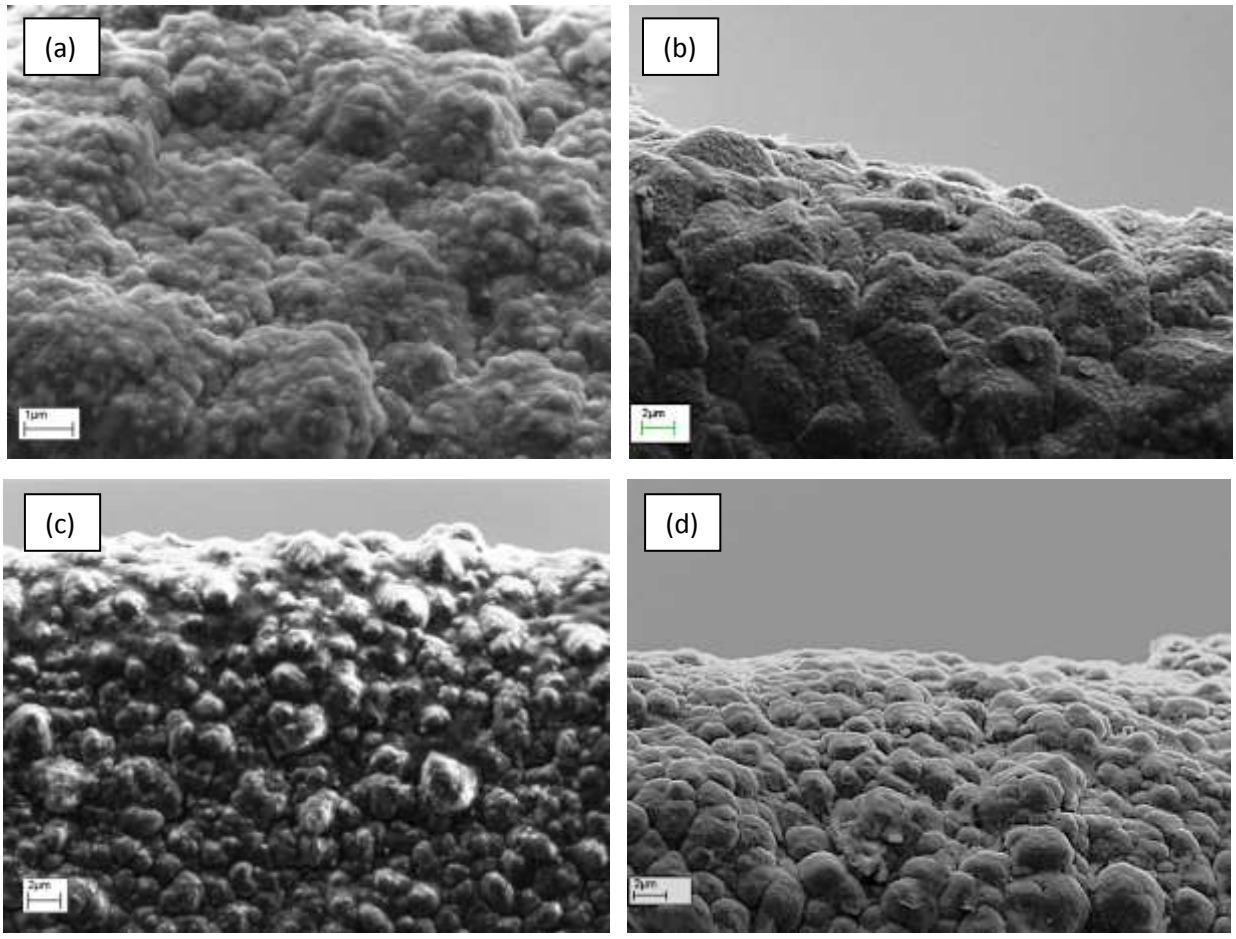

Figure 4.31. SEM micrographs of NCD coating morphologies from batch (a) Z (b) HB (c) G (d) BA

The NCD was seen to transform the sharp peaks, as seen in the MCD sample, into a nodular or "cauliflower" structure. The pictures show how the surface structure can vary depending on the gas ratios and deposition times used for the NCD layer. The micrographs indicate the NCD phase of the coatings to be predominantly amorphous, with ultra nano crystals imbedded in the surface structure. Figure 4.31 (a) shows a uniform covering of crystals over the surface of the MCD at the tip of the tool, however, the size of the crystals has remained similar at roughly 100nm – 200nm. This is generally considered to be in the MCD range as NCD refers to crystal sizes less than 100nm. In some instances the underlying MCD was still evident in the surface structure (Fig 4.31 b). Although the NCD phase has produced a continuous coating, it is thin enough that the topography of the MCD is still coming through. The micrographs in figures 4.31 (c) and (d) show examples of NCD structures, which exhibit a smoother surface, with a nodular texture similar to that of DLC. The NCD deposition time was long enough to remove the topographical effects of the MCD coating, whilst the gas ratio produced nodular NCD structures with much lower roughness, as confirmed by AFM. Raman analysis also confirmed the bonding chemistry to be similar to the NCD coatings described in the literature. The MCD and NCD coatings showed a similar position for the diamond peak of around 1333.5cm^{-1} with the range shifting by just ± 0.3cm^{-1}. All coatings showed a significant amount of the disordered and graphitic peaks associated with NCD structures (Fig 4.32).

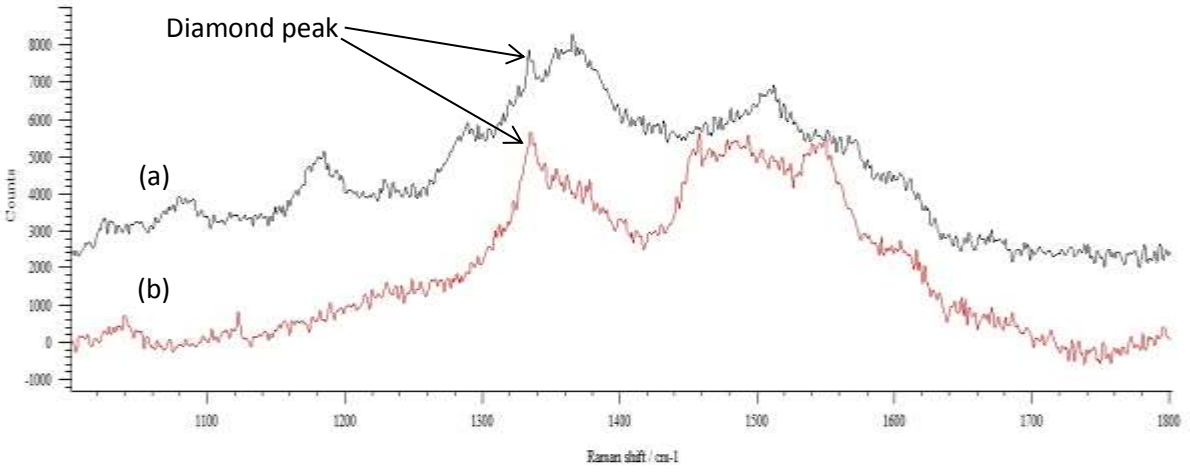

Figure 4.32. Raman spectrum of samples from batches (a) BA (b) G

The topography of the surfaces was analysed further and quantified using AFM. The NCD layer was shown to effectively reduce the roughness of the MCD layer beneath. The average roughness of the thicker NCD coatings was below 200nm with the lowest being just 105nm. Cross sections of the AFM scans further highlighted variations in the topography which are likely to further influence friction and adhesion. Large peak to valley distances could be seen with samples with reduced NCD deposition time due to the underlying MCD structure (Fig 4.33). The NCD was seen to increase nanoscale roughness but decrease overall roughness which is highlighted in the 3D images of the surface (Fig 4.34).

Gas ratios for the NCD layer were varied between 1% and 9% methane in hydrogen, often with a slight variations in the mixture ratio having a significant effect on the diamond structure. It was found that the most stable coatings were produced by using 1% methane in hydrogen for the MCD phase, whilst 4% methane in hydrogen produced the best NCD structures at the cutting tip. A deposition time of at least 60 hours was also necessary to overcome the underlying MCD roughness.

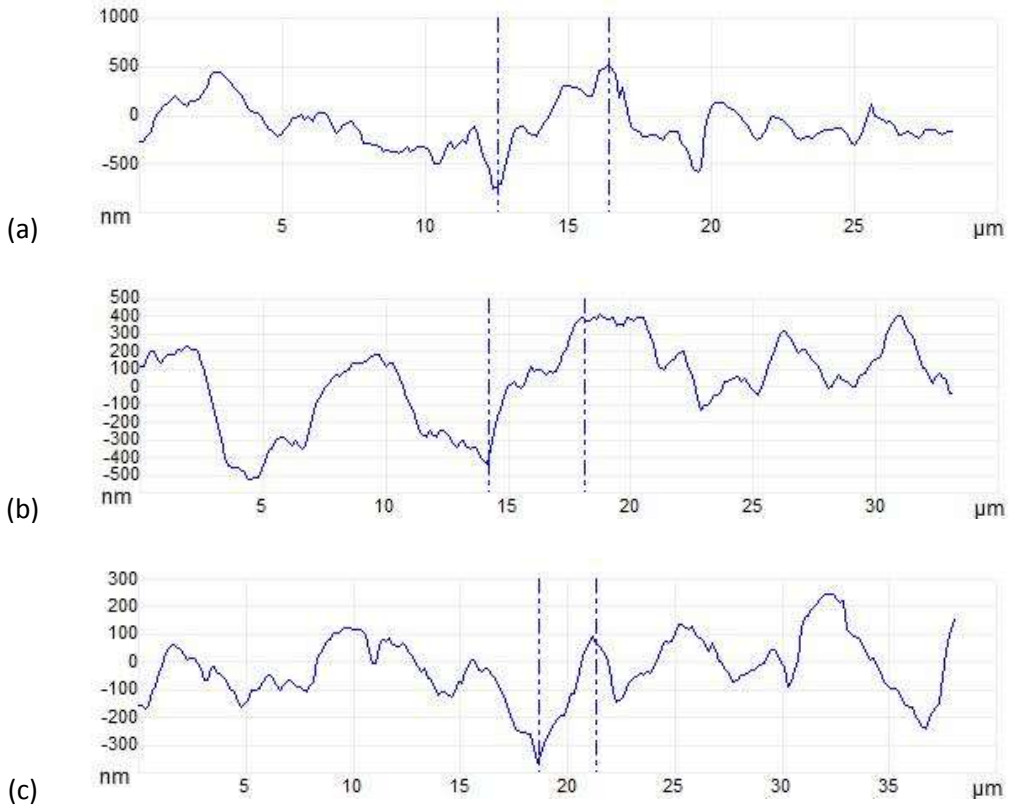

Figure 4.33. AFM cross section of samples from batch (a) HB (b) Z (c) G

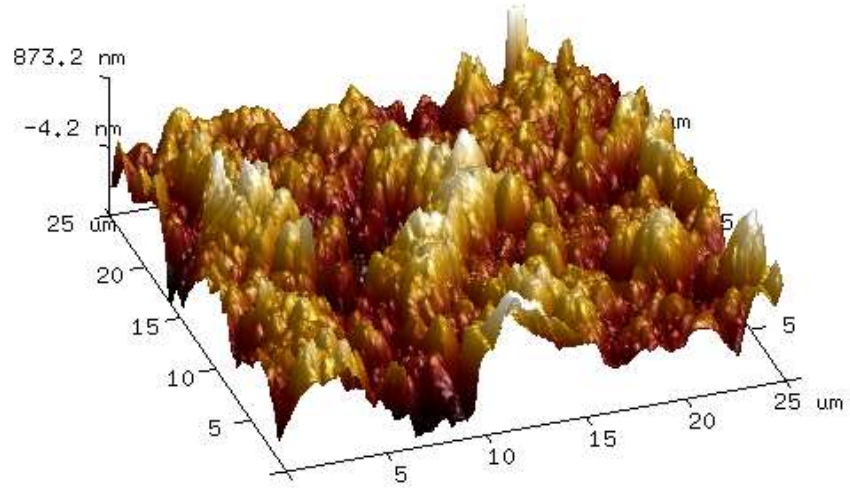

(a)

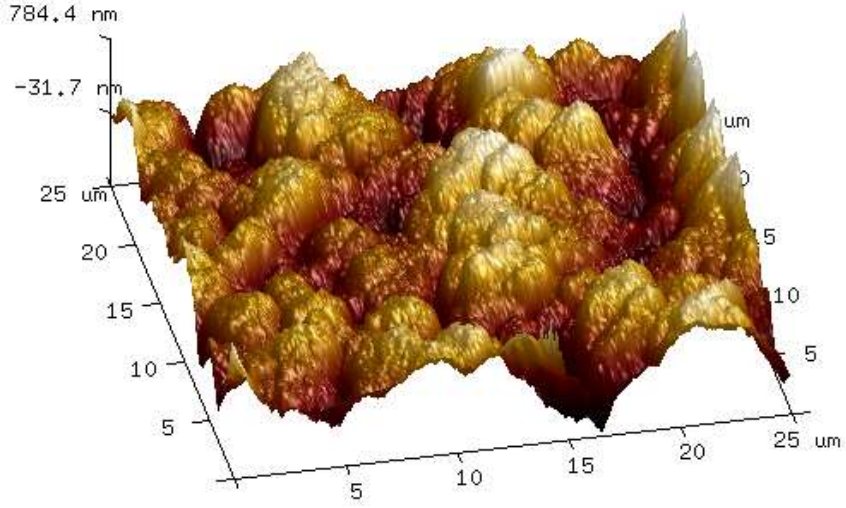

(b)

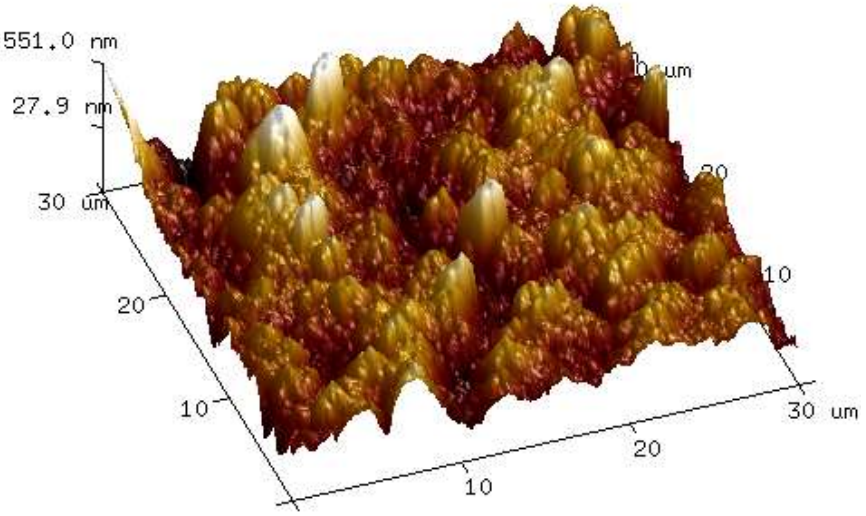

(c)

Figure 4.34. 3D AFM micrographs of NCD surfaces of sample batch (a) HB (b) Z (c) G

4.6. Conclusion

Diamond coatings, produced using the HFCVD method, have been developed by altering pre-treatment processes as well as the deposition conditions. The aim was to create a stable coating of sufficient quality on the WC-Co cutting insert designated for the project.

The first issue to be addressed was concerning the coating coverage and ensuring the insert cutting tip was sufficiently coated across the required area with the desired coating thickness. Sample positioning in the reactor, as well as coating deposition times, have been developed to ensure that the coating has sufficient cohesive strength to maintain its integrity at the cutting tip under the machining loads experienced in the cutting of aluminium. It was discovered that the predicted deposition times were producing coatings which were only 2µm thin and needed to be increased by a factor of 3 in order to achieve the desired thickness.

Adhesion between the WC-Co substrate and the diamond coatings was found to be the biggest issue regarding coating integrity. It was responsible for the majority of tool failures due to delamination of the MCD layer. It was already known that the cobalt binder inhibits adhesion and required removal from the surface through etching to allow for the diamond to mechanically adhere to the WC. It was discovered that a mix of nitric and hydrochloric acid gave the best results for the tools utilised in this project. It was possible to produce well adhering coatings although reliability remained an issue.

To achieve the desired coating morphology the gas ratio of methane to hydrogen was altered. The varying ratios produced diamond coatings ranging from MCD, using 1% methane in hydrogen, to ultra nano-crystalline diamond. The NCD phase showed more significant variation in coating structure. A ratio of 3% to 4% methane in hydrogen was found to most reliably produce an NCD layer with the desired surface morphology.

5. Diamond-like carbon coating development

5.1. Introduction

This chapter discusses the development of the DLC coating prior to being applied to the diamond layer. It was necessary to initially develop the coating independently due to the limited amount of diamond coating samples available. In this chapter the influence of substrate material and surface morphology are considered, as well as the effects of deposition variables associated with the PECVD technique, including the position of the samples in the reactor chamber. The iterative process, described in chapter 3, is used to compare how adjustments in the deposition process affect the coating characteristics and in turn, how this affects the machining performance of the inserts.

The development of the DLC coating will start by looking at a standard coating which was developed for drilling aluminium alloys. The coating was developed for HSS drills and has already been shown to significantly improve machining performance (Zolgharni *et al.*, 2008). The standard coating deposition parameters have been described in the experimental section, chapter 3. Due to the different requirements of this project it is expected that the deposition variables will have to be altered for the coating to perform optimally. This is due to the different substrate material and geometry, as well as the different dynamics associated with turning aluminium, compared to drilling.

This chapter presents a number of investigations into the effects of: bias voltage, deposition time and gas flow rates, as well as examining the variations caused by the positioning of the sample in the chamber. The influence that the substrate material and surface preparation have on the DLC coating also needs to be considered. The DLC coatings will therefore be deposited on a number of different samples so that the results can be extrapolated in order to minimise the need to use the diamond coatings in the development stage. The preferred coating parameters will then be selected for the DLC coating to be applied to the diamond layer for further combined coating development in chapter 6.

5.2. Standard DLC coating on WC-Co insert

5.2.1. DLC coating characterisation

The previously developed standard coating was deposited onto WC-Co inserts to initially evaluate how the coating performs on this substrate material and geometry, as well as examine performance in a brief cutting trial. The initial coating involved the deposition of the DLC film at a 450V bias, as described in the experimental section. The inserts were positioned on the cathode plate with a spacing of at least 50mm between samples. This was to minimise any potential distortions in the plasma formation caused by neighbouring objects.

Initial inspection of the DLC coatings showed that the standard coating, which had been developed for HSS, appeared to produce a uniform coating across all the tool surfaces. The flanks and cutting face were coated, however, it appeared that the flank faces may not have coated as effectively as the rake face due to a slight shielding effect.

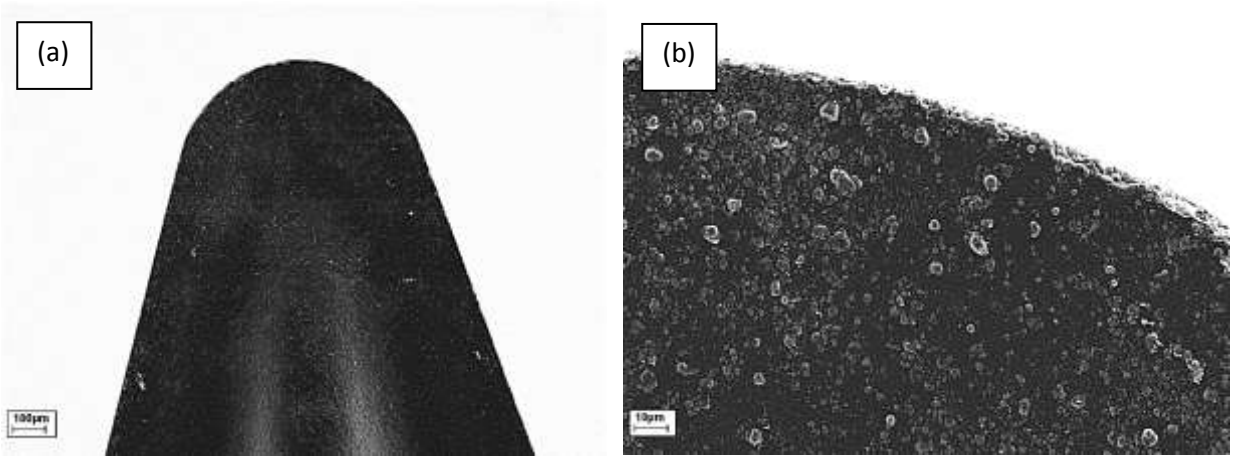

Figure 5.1. SEM micrographs of standard DLC on WC-Co tool (a) cutting tip (b) cutting edge

SEM images of the insert tips and cutting edge show the coating to be uniformly covering the substrate with no signs of delamination (Fig 5.1 a). Higher magnification micrographs (Fig 5.1 b) show that the surface of the coating consists of relatively smooth areas with intermittent raised nodule clusters protruding from the surface.

On closer inspection it can be seen that the DLC coating maintains a similar topography to the cobalt binder, as seen in figure 5.2, and appears to mimic the surface structure. Both pictures show two different areas roughly 1mm from the cutting tip edge. The micrographs show that where the DLC does not resemble the cobalt surface, it has grown in a nodule structure unlike any of the substrate surface structures.

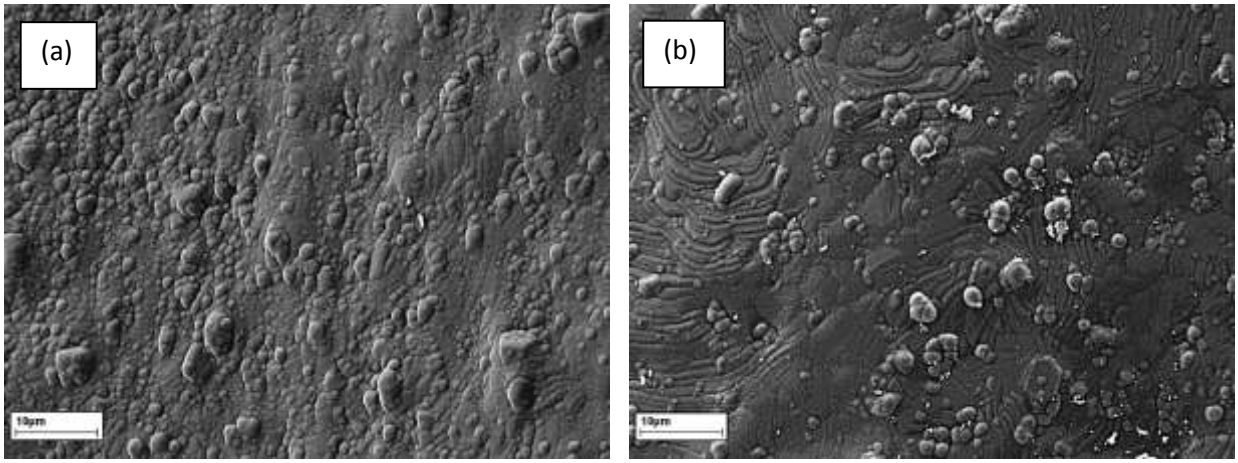

Figure 5.2. SEM micrographs of standard DLC coating on WC-Co insert at X5k

The left side of figure 5.2 (a) shows a large area of nodular growth whilst (b) shows a more sporadic nodular deposition, with the majority of the surface area showing the pattern indicative of the presence of the cobalt binder. When compared to images of the uncoated substrate it becomes apparent that the nodular growth occurs due to WC crystals at the surface of the substrate. The inconsistent distribution of the different types of growth, are very similar to the distribution of the WC crystals at the surface.

Due to the amorphous nature of DLC it is clear that it cannot maintain a similar morphology to a crystalline substrate, however, when deposited on material with small grain sizes, such as the cobalt, the film will often maintain similar topographic features. When a large grain crystal structure is coated with DLC, the resulting coating is often of a nodular structure due to the preferential nucleation and growth from crystal edges (Salvadori *et al.*, 2006). When many crystals are present this creates nodular patches as seen in figure 5.2 (a), whilst solitary crystals create intermittent clusters consisting of roughly 1 to 5 nodules as seen if figure 5.2 (b).

5.2.2. Standard coating machining performance

An initial test was conducted to evaluate the machining performance of the standard coating applied to the WC-Co substrate. As the DLC coating is deposited evenly on both cutting tips, it was possible to conduct two trials in order to check the reliability and repeatability of the trials. The test involved short cutting trials as described in chapter 3. The trials were conducted in order to test DLC coating performance such as coating adhesion, friction and wear properties. The samples were analysed using SEM to ensure there were no defects in the substrate or the coating. SEM analysis of the insert after the trial showed that the coating had suffered wear at the cutting tip, as well as incurring aluminium adhesion at the cutting edge and chip breaker.

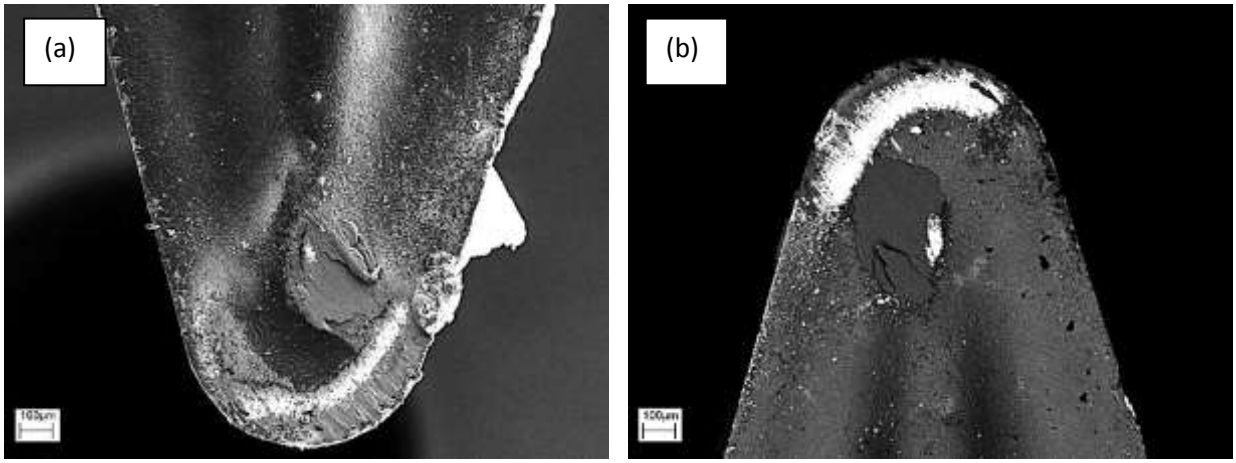

Figure 5.3. SEM micrographs of DLC coated insert after trial (a) SE2 image T2 (b) BSE image T1

SEM analysis revealed that the tool life performance of the coating was very similar, with both cutting tips showing a comparable amount of wear and aluminium adhesion. The SE2 image shows the amount of aluminium adhesion at cutting tip 2 (Fig 5.3 a). The largest amount of build-up has occurred at the rake face on the major flank side of the chip breaker. It can also be seen that the majority of build up is 0.5mm from the tip of the tool which corresponds to the 0.5mm cut depth used in the trial. BSE images (Fig 5.3 b) highlight the wear that has occurred just off the cutting edge of the tool tip. This shows that the majority of the force is acting just behind the cutting edge, as well as at the chip-breaker, leading to increased wear in this area. Also, despite the DLC wearing through to the substrate, it has not lead to further delamination of the film, which suggests good adhesion at

the interface between the DLC and WC-Co substrate. Throughout the machining process aluminium is expected to build up on the tool and then be removed by the workpiece material, before building up again. This process slowly increases the amount of aluminium that remains permanently on the cutting tip (BUE) (Gómez-Parra *et al.*, 2013; Sánchez *et al.*, 2005). The large piece of aluminium that has adhered at the major flank in figure 5.5 would be unlikely to remain in its entirety with further machining, unlike the build up at the cutting edge and chip breaker. It is this build up that is most likely to cause the tool to fail as it will interfere with the cutting edge profile and inhibit the chip-breaker from functioning correctly.

Higher magnification images reveal further details of the cutting performance of the standard DLC coating when turning aluminium. It becomes clear that the DLC coating, similar to micro and nano-diamond coatings, may also have a negative effect on cutting performance if it begins to wear or delaminate (Fig 5.4). It can be seen that the wearing of the DLC coating appears to have led to increased aluminium adhesion along the transition line from the substrate to the coating. It also appears that the aluminium is adhering to the DLC coated surface, indicating that the friction and adhesion properties of the DLC surface needs to be improved if it is to aid swarf flow and reduce built up edge on the insert.

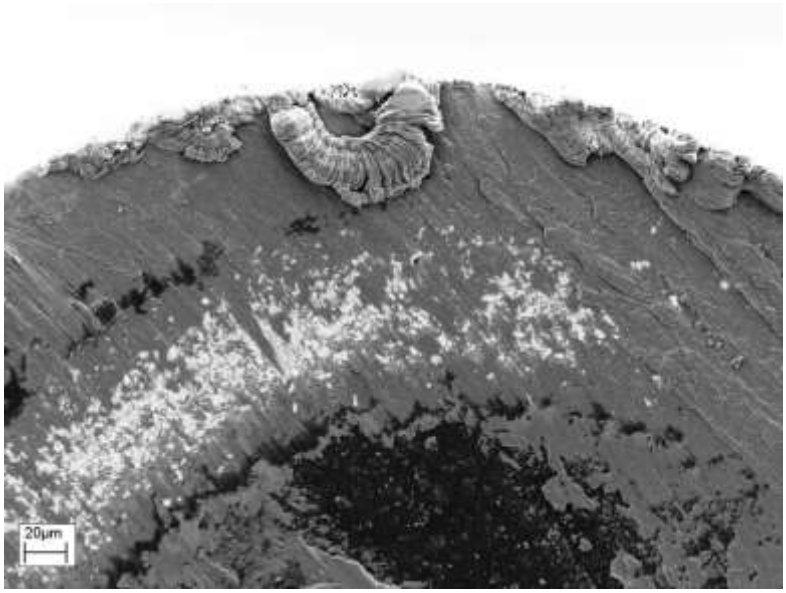

Figure 5.4. SEM micrograph of cutting tip of DLC coated insert after trial

Analysis of the initial cutting trial of the DLC coating highlighted a number of performance issues that needed to be addressed. It is evident from the post-trial analysis of the coated inserts, that DLC is wearing much faster than anticipated for this type of cutting regime. After just a short machining trial a significant amount of the coating is completely worn through to the substrate. This indicates that the standard coating designed for drilling applications does not have sufficient hardness and wear resistance for this application and further development will be required.

Although the DLC coating has already shown an improvement in aluminium adhesion compared to the uncoated insert discussed in chapter 4, there is still aluminium adhering directly to the DLC. The friction properties may therefore also require improvement in order to allow for efficient dry cutting. There are a number of aspects of the coating that need to be considered if it is going to be possible to improve the performance in these areas.

One aspect to test will be the silicon interlayer used to improve the adhesion of the coating to the substrate. As this interlayer was developed for steel substrates it may not be necessary for adhesion to WC-Co, as well as for the diamond coating it will eventually be combined with. The bias voltage will also require investigation as it has been shown to have the greatest impact on sp^2 and sp^3 bonding ratio's in the coating, and hence the hardness and wear rates (Batory *et al.*, 2015; Ouchabane *et al.*, 2010; Li *et al.*, 2004). Chamber pressure and deposition time will also be considered as they have been shown to affect the surface structure of the coating and may allow for improvements in the friction coefficients against aluminium alloys (Salvadori *et al.*, 2006; Kim *et al.*, 2005). The effects of the substrate morphology will be considered in greater depth when looking at combined coatings as the diamond will likely alter the overlying DLC coating to some extent, particularly the coating topography (Singh *et al.*, 2008; Zhong, Zhang *et al.*, 2008).

5.3. Effect of silicon interlayer

The silicon interlayer was developed in order to allow for the DLC coating to adhere to HSS. This was required to overcome a lattice mismatch which otherwise lead to delamination of the coatings due to stress concentrations at the coating – substrate interface. As these tools consisted of cobalt cemented tungsten carbide, it was necessary to test if the silicon interlayer was still required. The need for a silicon interlayer was investigated, with the uncoated WC-Co, in order to gain a further understanding of the adhesive properties of the DLC layer.

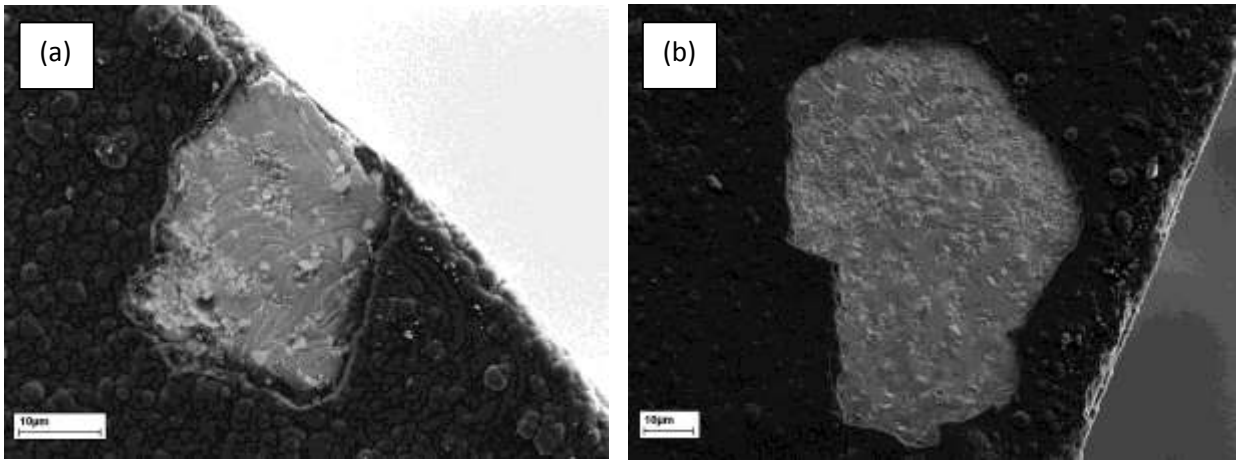

Figure 5.5. SEM micrographs of delamination of DLC at (a) cutting edge tip (b) flank edge

Micrographs of the insert reveal patches of delamination at the cutting edge and cutting tip which were not present on any of the sample coatings which incorporated the interlayer. This confirms that adhesion between the DLC coating and the WC-Co substrate is reduced when the Si interlayer is removed (Fig 5.5 a and b). Although the silicon interlayer was developed for improved adhesion with steel substrates, literature has shown that interlayers are necessary for many substrates, as the DLC itself will delaminate from most metallic surfaces (Wada *et al.*, 2011; Wei and Yen, 2007). This is partly due to the silicon acting as a stress reliever by producing a softer interface between the DLC and the substrate (Silva *et al.*, 2015; Schwarz *et al.*, 2008).

In some cases the coating begins to delaminate during the deposition process. It can be seen that the delamination occurred during and not after the film deposition as further film growth has continued on some of the patches of delamination (Fig 5.6 a). This adhesion failure also increases the risk of loose particles landing on the substrate surface and interfering with deposition.

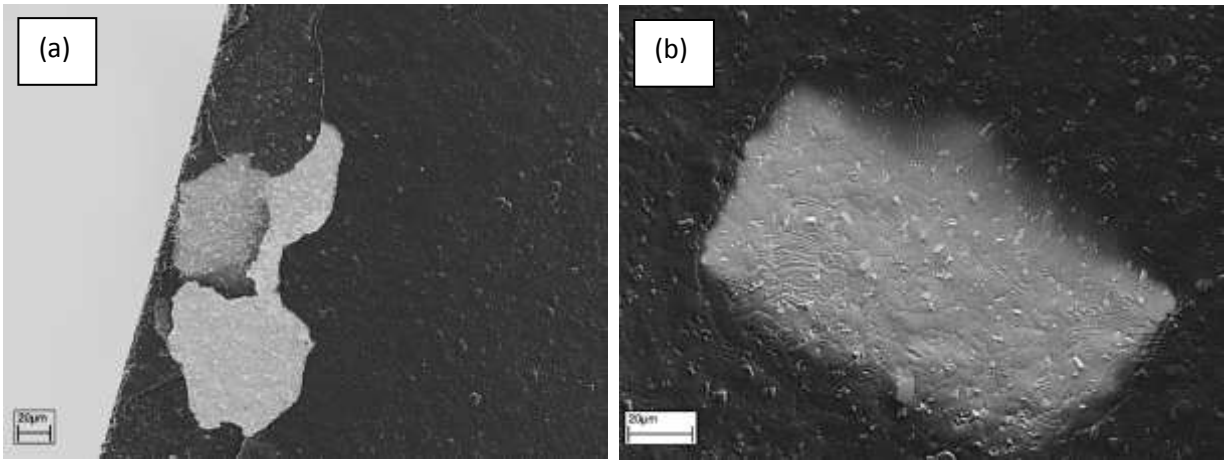

Figure 5.6. SEM micrographs of delamination during deposition (a) delamination and partial re-growth (b) Uncoated patch from loose particle

Figure 5.6 (b) shows an SEM micrograph of an uncoated patch, which is likely to be a result of a delaminated section resting on the surface of the substrate during the film deposition. This can be seen due to the fact there is a transition between the coated and uncoated area. The formation of the transition is indicative of shielding of the surface due to a loose particle. This is evident due to the gradual transition from coated to uncoated surfaces.

Having deposited coatings, both with and without the silicon interlayer, it became clear that it would be necessary to maintain the Si interlayer. When considering the DLC coating on diamond, the test will be repeated again. This is because adhesion between DLC and NCD /MCD coatings will theoretically be much better due to the potential C-C bonding at the interface.

5.4. Investigation of bias voltage

Previous research has shown that bias voltage has the greatest effect on the properties and characteristics of the DLC coating (Ouchabane *et al.*, 2010; Zhang *et al.*, 2002; Xu *et al.*, 1997). This is due to the fact that the coatings are heavily influenced by the ion impingement energies, which are in turn directly related to the bias between the cathode and anode in the reactor (Ogwu, 1999). It was therefore necessary to investigate the effects of bias voltage on the morphology, and bonding chemistry of the coatings deposited on the WC-Co insert, before being subject to short cutting trials to test machining performance.

Effects of bias voltage have been discussed in the literature review in chapter two. The effects of bias voltage have been investigated in many studies regarding a number of different deposition methods, both CVD and PVD based. Studies have shown that higher bias voltages generally lead to harder coatings due to an increase in diamond like tetrahedral C-C bonds (sp^3), and hence a reduction in weaker lattice bonding (sp^2) associated with graphitic structures. This is due to an increase in the energy of impinging ions subplanting into the coating as it is being deposited. This increase in energy densifies the coating forcing an increase in the C-C sp^3 bonding within the film.

Investigations involving the use of DLC coatings for the machining of aluminium highlighted that it will not necessarily be the hardest coating that produces the best cutting performance. A harder coating will be likely to endure higher internal compressive stresses, which may lead to delamination of the coating. It is also the graphitic structure which in many applications provides low friction properties of DLC coatings. These factors are both important when looking to improve the efficiency of machining processes. On one hand, the hardness will be required to ensure the coating does not wear away prematurely, whilst the low friction is required to improve energy and cutting efficiency by aiding swarf flow and reducing aluminium adhesion at the cutting tip.

5.4.1. Methodology

Coating deposition

For this test, DLC coatings were deposited on the standard baseline turning tools Sandvik VBGT, as well as a single sided silicon wafer. All samples were placed flat on a horizontal cathode plate, with an even separation ensuring samples would not be effected by each other during deposition of the coatings. All variables other than the bias voltage remained the same throughout the experiment. The cathode plate, and number of samples, remained unchanged in order to minimise other potential variables in the deposition such as power. The experiment involved producing 6 coatings at bias voltages between 100V and 600V with 100V increments. The coatings characteristics were then analysed and the inserts were used in short cutting trials in order to compare coatings.

Characterisation

SEM analysis was conducted, using SE2 mode, in order to visually inspect the quality of coatings on the WC-Co substrates. AFM was then used to examine DLC coatings on silicon wafer samples and quantify any variation in topography. Raman spectroscopy was also conducted on the silicon samples and WC-Co insert. This was to quantify the effects of the bias voltage on the bonding structure within the DLC coatings, whilst additionally examining any potential variation which may have occurred due to substrate material. The details of the experimental techniques are described in more detail in the experimental section, chapter 3.

Machining performance

The coated inserts were then subject to a short cutting trial in which the cutting forces, WP finish and tool wear have been analysed to test how the coating characteristics influence machining performance.

5.4.2. Results / Discussion

SEM analysis of the samples revealed that all voltages produced similar surface coating structures. Coatings deposited with bias voltages between 300V to 500V all had homogeneous coatings with few signs of defects, whilst the 600V coating had suffered delamination during the deposition process. The 100V deposition run did not produce any coating viable for testing as the substrate was clearly visible after deposition, whilst 200V produced a coating in which visual disparities, compared to the standard coating, were clearly visible.

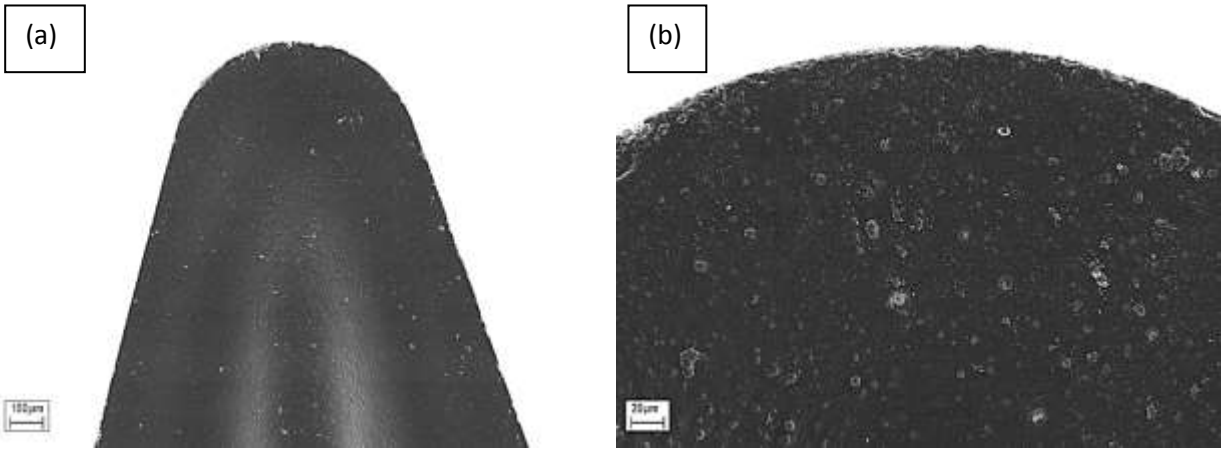

Figure 5.7. SEM micrographs of coated tool tips (a) 300V coating X200 (b) 500V coating X1000

It can be seen from the images (Fig 5.7) that the coatings between 300V and 500V are virtually indistinguishable and all exhibit the same features as the standard DLC coating. The micrographs show that the surface of the film contains a blend of nodular structures as well as the areas which mimic the underlying cobalt substrate.

Below 300V the deposition energy becomes too low to form a significant amount of the C-C sp^3 bonds required to create diamond-like material and instead, deposits a more polymeric structure. This has an effect on all aspects of the coating, as well as altering the bonding chemistry of the material, the topography also shows significant differences compared to the higher voltage depositions (Fig 5.8 a).

SEM analysis of the coatings at 200V revealed a very different surface structure compared to the coatings deposited at a bias of 300V and above. Visual inspection of the insert tip shows what appear to be pinholes throughout the entire surface of the insert. It is likely due to the impinging ions settling on the surface of the coating, as opposed to penetrating the surface and subplanting, which is widely considered to be the mechanism that leads to the smoother harder DLC coatings.

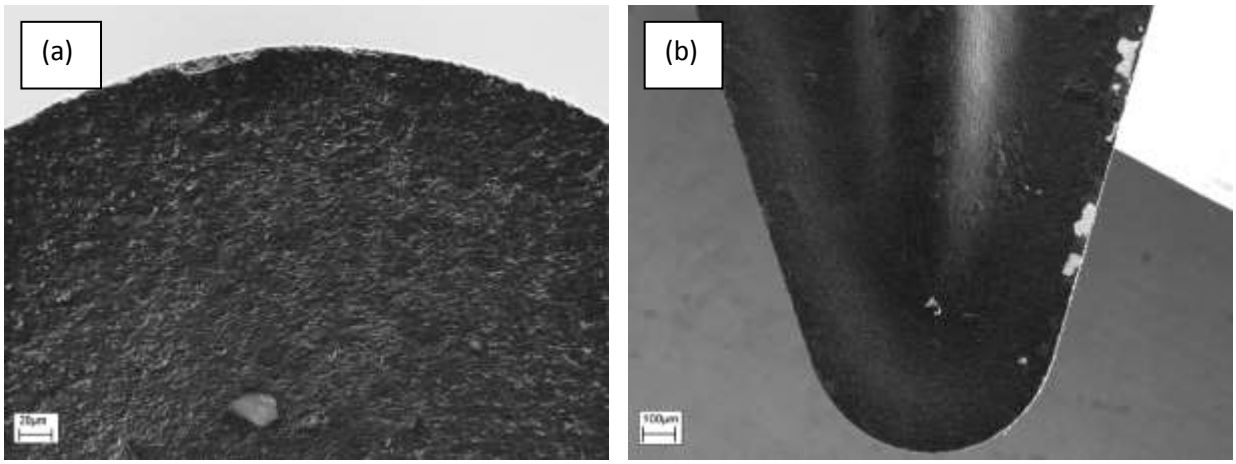

Figure 5.8. SEM micrographs of coated tool tips (a) 200V coating X1000 (b) 600V coating X200

It was predicted that coatings above 500V would build up enough internal stress that the force would overcome the adhesion between coating and substrate and lead to delamination. The insert coated at 600V had already suffered from delamination which was localized at the edges of the rake face near the flanks (Fig 5.8 b). This may be simply due to increased stresses due to the geometry of the sharp cutting edge, or may be due to inconsistencies in the underlying substrate.

Due to the variations in the substrate, it is difficult to predict what may have initiated delamination of the coating in a particular area. In some instances the same component may have patches of well adhering DLC whilst other areas have suffered severe delamination. A coating which initially appears to be of good quality may have areas of increased internal stress and poor adhesion which lead to failure as soon as a load is applied.

DLC bonding chemistry

Raman spectroscopy generates a curve containing two peaks, (D) disordered and (G) graphitic. It is from these peaks that an estimation of the sp^2 and sp^3 bonding ratios can be derived, however, there is a significant margin of error, meaning the technique is more useful as a comparison of samples, compared to a direct quantifiable measurement.

Raman analysis of the DLC coatings revealed a linear increase in the Id / Ig peak ratios. This result confirms that, as the deposition power is increased, the amount of sp^3 bonding in the coating decreases (Fig 5.9). This is due to a reduced amount of hydrogen in the film, as hydrogen in the coating readily bonds to the carbon in the form of sp^3 bonds. These C-H sp^3 bonds are picked up in the Raman analysis and are not distinguishable with the sp^3 C-C bonds that produce the diamond-like structure of the film. It is therefore difficult to correlate the bonding ratios calculated via Raman spectroscopy, to the actual properties of hydrogenated DLC without knowing the amount of hydrogen in the coating.

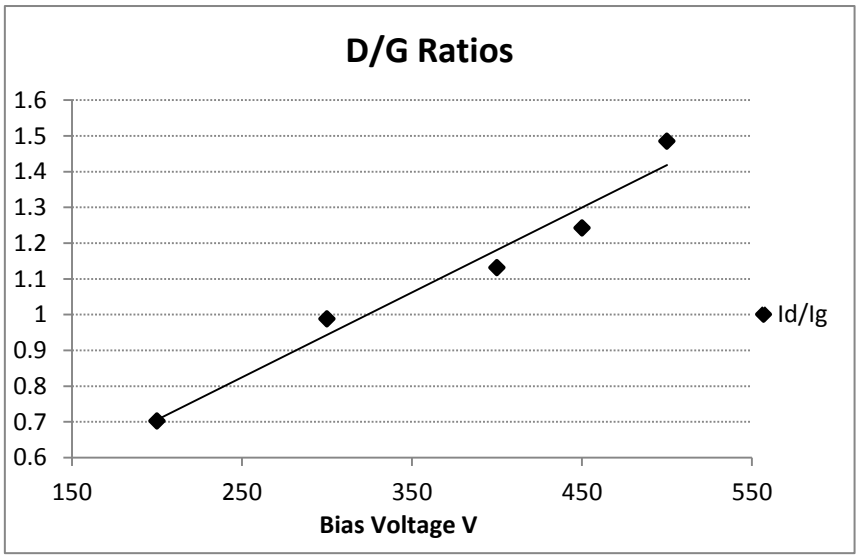

Figure 5.9. Id /Ig ratios of DLC coatings between 100V and 500V bias voltage

The results clearly show a decrease in the sp^3 bonding as the bias voltage is increased from 100V to 600V. This will be as a result of the reduced hydrogen content in the film and should therefore correspond to an increase in coating hardness and reduced wear rate.

Surface topography

AFM analysis was conducted on coatings, in the range of 200V to 500V. The analysis was conducted on the silicon wafer samples, as a reference, in order to negate any potential variation which may have occurred with the coatings on the WC-Co samples. AFM measurements revealed that within the range of viable coatings, 300V to 500V, the surface topography was not significantly affected by the different voltages. The 200V coating had some variation in topography. Although the roughness average remained similar to the other coatings, at around 0.43nm ±0.03nm, slight variations in the skewness, kurtosis and peak counts, indicated that the 200V coating had a higher abundance of peaks, however, the peaks were no sharper than those on the other coatings (Fig 5.10).

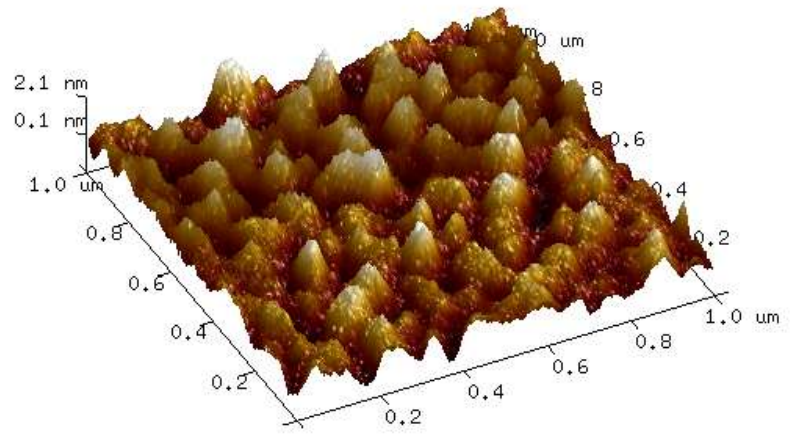

(a)

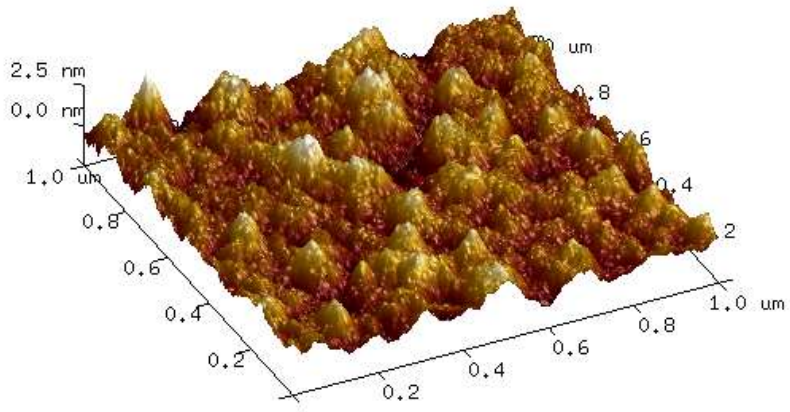

(b)

Figure 5.10. 3D AFM images of coating topography (a) 200V coating (b) 400V coating

Machining performance

In order to test the effectiveness of the coatings in terms of efficiency and tool life performance the inserts were subject to a short cutting trial. These trials were designed to test how variations in coating characteristics translated into performance for these particular inserts. Both tips of each insert were given the same short trial as described in chapter 3.

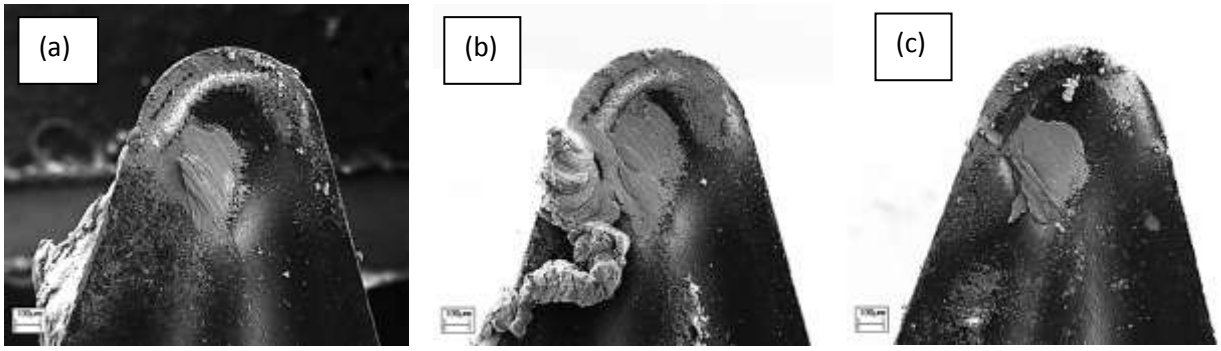

Figure 5.11. SEM micrographs of cutting inserts after short trial (a) 300V (b) 400V (c) 500V

Figure 5.11 shows SEM micrographs of the cutting tips of the trialled inserts. As the trial consisted of a short dry cutting run, the inserts could be taken straight from the machine trial to the SEM for analysis without any cleaning required, hence the aluminium adhesion on the tool surface is as it would have been at the end of the trial.

From figure 5.11 it can be seen that aluminium has adhered to the surfaces of the cutting tips in a number of different ways. Similarities between the aluminium adhesion in certain areas of the cutting tips are evident in all micrographs. Every sample shows adhesion just left of the chip breaker, roughly 0.5mm from the cutting edge, as well as adhesion directly on the cutting edge.

Figure 5.11 (a) shows that the cutting tip of the insert coated at 300V has a relatively large amount of aluminium adhered to the major flank, the 400V coating (Fig 5.11 b) has aluminium on the leading edge of the rake face. The 500V coating does not have a similar large piece of aluminium and has only the aluminium build up at the cutting edge and chip-breaker, which is evident on all trialled samples. It is this built up layer that will likely lead to tool failure as it will interfere with the cutting process by masking the cutting edge, as well as hinder the swarf flow at the chip-breaker. The larger

pieces of aluminium, as seen on the 300V and 400V samples, are unlikely to remain with continued cutting, however, their repeated adhesion and removal will lead to an increase in overall BUE, whilst causing fluctuations in performance.

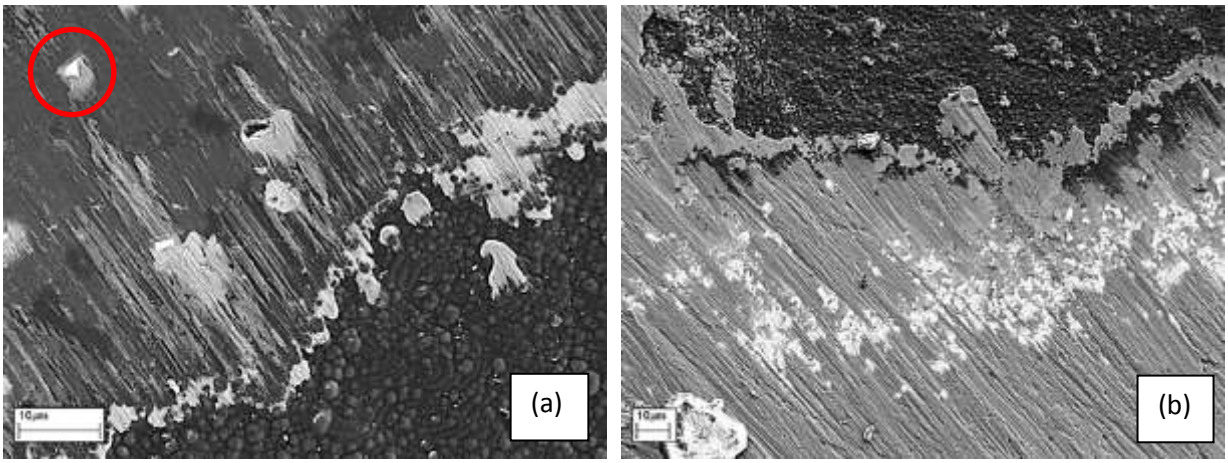

Figure 5.12. SEM micrograph of wear at the cutting tip (a) 500V (b) 400V

The biggest difference between the 500V sample and samples at lower voltages, is the fact that despite suffering similar wear in the same areas, the DLC layer has not completely worn through to the underlying WC-Co substrate. Figure 5.12 shows SEM micrographs of the wear track just off the cutting edge of the 500V and 300V, both images are taken near the centre of the cutting tip. It is clear from these images, as well as figure 5.11, that the 500V DLC coating has worn at a reduced rate, compared to the lower voltage coatings. This is indicative of an increase in hardness and wear resistance of the coating. Figure 5.12 (a) shows that in some areas the substrate material is visible (highlighted by the red circle). It is likely that the first point of breaching of the underlying material through the DLC coating will be from WC crystals protruding from the substrate. The straight edges of the visible area of the substrate highlighted indicate that this is the case.

The images also show that, although aluminium adhesion is found on all surfaces, the transition area at the edge of the wear track appears to have increased adhesion which leads to an increase in the built up layer formation. It is clear from figure 5.12 that aluminium adhesion is significantly increased in area where the DLC has worn through to the substrate. The transition layer between the WC-Co and the DLC in figure 5.12 (b) has incurred far greater aluminium adhesion than the similar area in

figure 5.12 (a). This is a further indication that once the DLC coating has worn through to the substrate, aluminium adhesion may build up at a faster rate than on an uncoated insert due to the added roughness of the transition area.

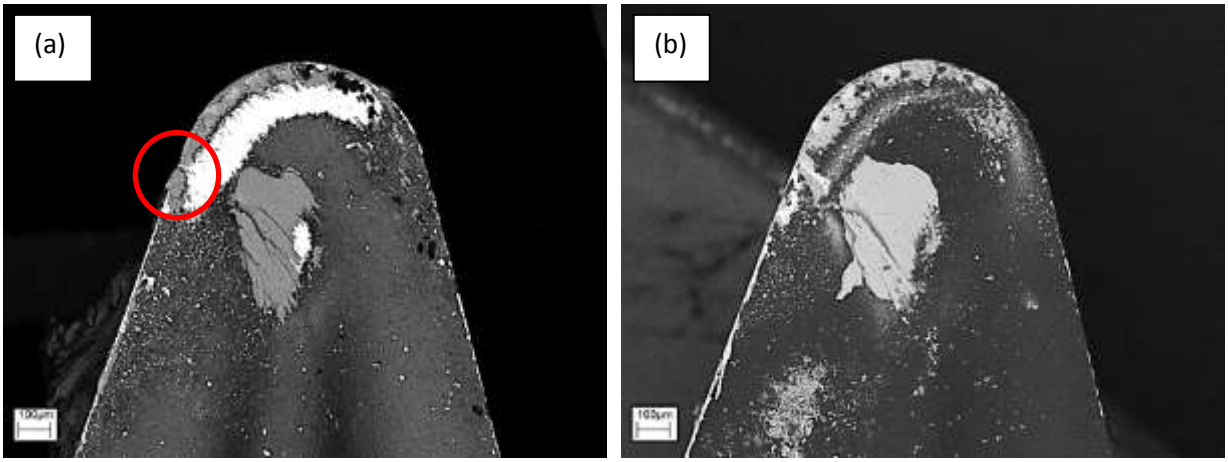

Figure 5.13. Back-scattered images of cutting tips after trial (a) 300V sample (b) 500V sample

SEM backscattered imaging of the 300V sample further highlights areas of wear caused by the machining process (Fig 5.13). Both micrographs highlight, as seen by the coating wear, that one of the first areas at which the coating wears excessively is on the leading edge of the rake face 0.5mm off the cutting edge (highlighted by the red circle in figure 5.13 a). This is as expected due to the depth of cut being 0.5mm which means this is the part of the tool doing most of the cutting and enduring the majority of the cutting forces. The coating at the cutting edge has worn away as expected, however, as well as wearing on the leading edge, it can be seen that delamination has occurred further down the leading edge and on the trailing edge. This further indicates that the coating integrity at the cutting edges may be compromised and be of different quality than the coating on the flat surfaces. The typical wear patches can be seen on the samples coated with a 400V bias or less. The crater wear and chip breaker wear patch could be clearly seen as bright white areas using BSE analysis. The 500V sample showed an improvement with no substrate material showing through. The experiment has also highlighted variations in the cutting process which has lead one sample to have excessive aluminium adhesion on the major flank, whilst another has large deposits on the rake face.

Machining forces

Cutting force and feed force were measured using a Kistler dynamometer in order to test for cutting loads in the machining process. Reduced forces means a reduction in the energy required to operate the system. Each sample completed 5 cutting passes, with the cutting forces of each pass being averaged (Fig 5.14).

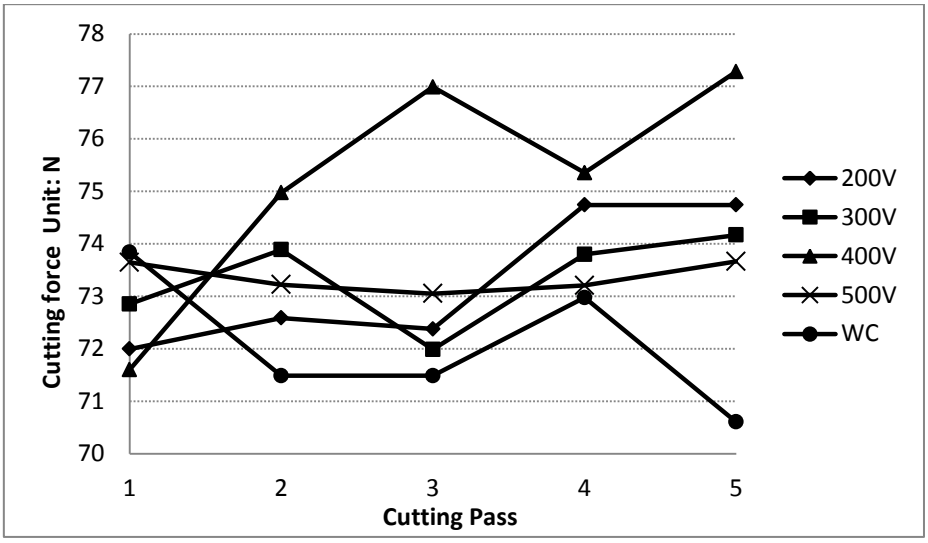

Figure 5.14. Graph of cutting forces of bias voltage samples

The results show that the cutting forces between the samples remained relatively similar throughout the test with cutting force ranging up to a maximum of 7N. There is also no clear pattern that has emerged, indicating that fluctuations in force are largely due to the normal inconsistencies expected in an intermittent cutting process involving a chip-breaker. This noise in the system makes it difficult to derive any finer details from the force measurements, however there are still a number of points that can be noted. The results show that there is not only little difference between the cutting forces for all DLC coatings (200V – 500V) in the early stages of cutting, but also that there is no initial improvement when compared to the uncoated WC insert.

It can also be seen that the 500V DLC coated sample appears to have maintained a much steadier force and does not fluctuate in the same way as the other samples have. This may be due to the fact

that the coating has maintained its integrity throughout the test, which in turn has reduced the rate of aluminium build up and allowed for a more consistent machining process.

There are also a number of factors affecting the initial cutting of a new tool. It is clear that the surface of the tool at the chip-breaker is altered significantly in the first stages of cutting as crater wear begins to form. Initially, abrasive effects due to cut material, act to smooth the surface of the tool tip at the chip-breaker on both the coated and uncoated samples. This process is occurring simultaneously to the initial aluminium build up. It is therefore unsurprising that in the initial stage of machining it is not possible to accurately judge how the tool might fair when subject to the length of cutting expected in industrial machining processes.

The test has further highlighted that the DLC coating, when worn through to the substrate can lead to an increase in built up edge as the aluminium adheres to the transition boundary between coating and substrate. The workpiece roughness was also measured using white light interferometry, however, there was no discernible variation due to the coatings.

The test revealed a number of issues regarding the DLC coating when applied to this specific tool geometry. The coating wear rate at the chip-breaker is far greater than expected. Initial predictions estimated that the DLC should wear at the cutting edge and remain at the cutting tip in order to improve swarf flow and reduce BUE. Due to the nature of the chip-breaker design, however, the DLC coating is wearing at the point at which the aluminium adheres. The wearing of the DLC layer creates a transition layer, which can increase the rate of aluminium adhesion to the tool. It has been shown though, that increasing the bias voltage has led to reduced wear and improved machining performance from the DLC coating.

5.5. Investigation of deposition time

The deposition time of the coating is directly linked to the coating thickness which in turn affects the residual stress levels within the coating. Along with poor adhesion, the internal stress is also a large contributor to failures in the coatings due to delamination (Wang *et al.*, 2007; Zhang *et al.*, 2006). The investigation into bias voltage highlighted that the DLC was already near the limit with the 500V coating. This is evident as the 600V coating clearly failed to adhere sufficiently to the WC-Co substrate. The bias voltage experiment highlighted that the lower voltage coatings, despite having reduced internal stresses, were too soft for this application. This further test was therefore conducted to test if any further benefit could be gained from thinner coatings, which would have a reduced residual stress (Sheeja *et al.*, 2002). It is also worth noting that the substrate material and roughness will also have an effect on the ideal thickness of the coating (Wei *et al.*, 2007).

5.5.1. Methodology

The deposition process involved parameters as described in chapter 3, however, the bias voltage was now fixed at 500V. The deposition time for each coating stage was reduced, apart from the Ar cleaning stage which remained at 30min. Three coating runs were completed with the deposition time of each stage being set to 5, 8 and 11 minutes, meaning that total deposition times were 15, 24 and 33 minutes. This is compared to the total 45 minutes for the standard coating.

The coatings on the WC-Co inserts were analysed using SEM in SE2 mode to verify the quality, whilst Raman spectroscopy was used to compare the bonding structure. AFM analysis of the Si samples was completed to check for any variation in topography.

The coated inserts were then given a short trial and re-analysed using BSE micrographs to test for any improvements in machining performance. During the trial cutting forces were again measured and the WP finish was then examined after the test.

5.5.2. Results / Discussion

SEM analysis in SE2 mode showed no variation in the coatings as they all appeared to be of good quality with no defects. Raman spectroscopy also confirmed that there was no discernible change in the bonding chemistry due to the reduced deposition times. AFM analysis revealed a slight change in topography due to coating thickness. The thinner coatings had a reduced average roughness of 0.356nm with an equally reduced peak to valley distance of 1.368nm (Fig 5.15). Other aspects such as skewness and kurtosis remained similar, suggesting that the features remained the same but were just enlarged by increased deposition. This is due to the fact the Si substrate is already very smooth meaning that there was no initial roughness to overcome. The effects will vary when the coatings are applied to the rougher surface of the MCD and NCD coatings, however, this experiment provides an initial indication of the potential benefits of a thinner coating.

(a)

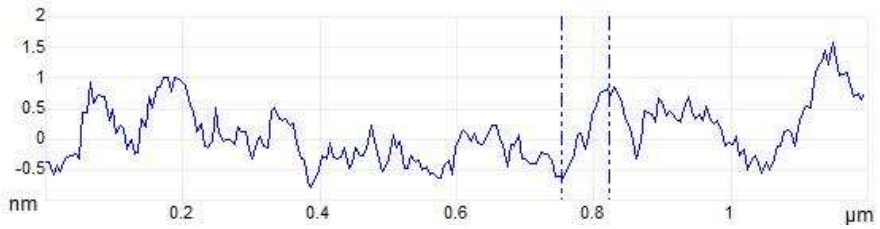

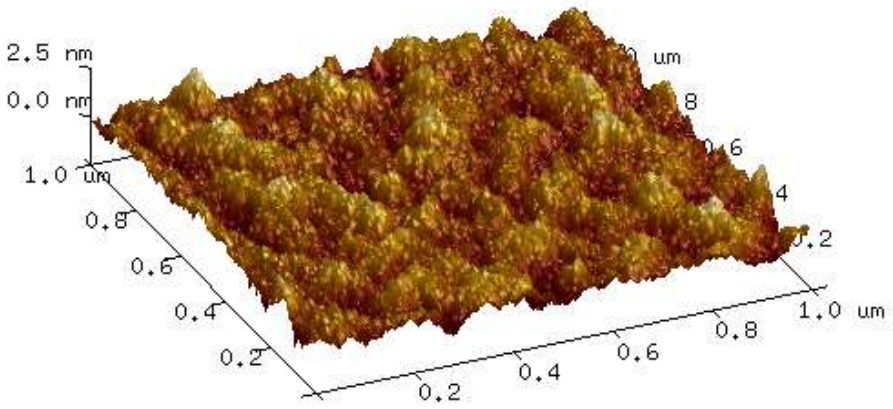

(b)

Figure 5.15. Topography of 24min deposition time coating on Si wafer (a) 2D section (b) 3D image

Short cutting trials showed that there was no significant improvement to be made from reducing the deposition time. The performance remained similar for all samples with there being no difference in the cutting forces or WP finish. BSE analysis of the inserts after the trial did highlight that the thicker coating had suffered less BUE, particularly further down the major flank. It appears that the thinner coatings are likely to have worn away or delaminated due to less DLC mass, as well as due to a reduced cohesive strength in the thinner coatings. This has led to an increase in BUE at the cutting edge of the major flank as well as a general increase in aluminium adhesion on all coatings compared to the standard 45 minute deposition time (Fig 5.16).

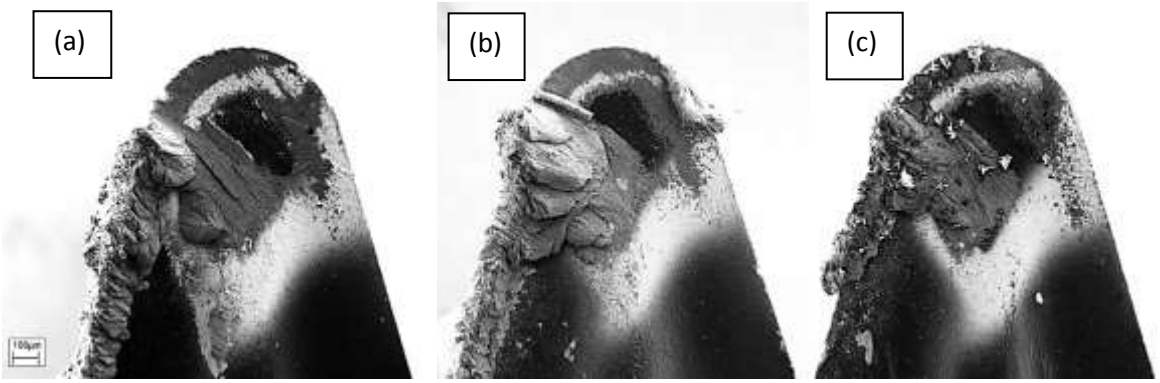

Figure 5.16. SEM micrographs of cutting tips after trial (a) 15min (b) 24min (c) 33min

The coatings with reduced deposition time had decreased performance compared to the standard time at 500V. It is necessary to balance a number of factors when determining the ideal thickness for the deposited coatings. These factors include; surface roughness, internal stress, adhesive and cohesive strength of the coating and friction and wear rates. The thinner coatings likely suffered from reduced cohesive strength and quicker wearing through of the film. As the coating wears and the substrate is revealed, the adhesion of aluminium increases and a larger BUE is formed.

5.6. Investigation of gas flow rate / pressure

The literature suggested that slight alterations in the deposition process gas pressure can have a significant influence on the morphology and chemistry of the coating produced (Zhong *et al.*, 2007; Kim *et al.*, 2005). Although the PECVD system used for the deposition of the DLC coatings did not have a variable pressure adjustment, it was possible to alter the deposition pressure by reducing or increasing the rate of flow of the precursor gases into the chamber. Chamber pressure has been shown to affect coating deposition in a number of ways. As described in the literature section, PECVD of DLC coatings require low pressure in order for the impinging ionic species to maintain a free path to the substrate surface. If the pressure is too high, the impinging species will undergo too many collisions with non-ionic particles, which will reduce the impinging energy and inhibit the formation of the C-C sp^3 bonding. If the pressure is too low then there will not be enough precursor gas present in the chamber to form the plasma and deposition will not occur.

5.6.1. Methodology

For this experiment all parameters were kept the same except for the gas flow rates. The voltage was once again kept at 500V. Gas flow rates were altered to 1/3, 1/2, and 2/3's of the standard coating flow rates used on all stages, except for the Ar cleaning stage which remained the same throughout. This meant that for the final deposition stage of the three different coatings, the acetylene was set to; 20sccm, 30sccm and 40sccm, compared to the usual 60sccm.

The coatings were analysed using SEM, Raman spectroscopy and AFM similarly to the previous experiment. The inserts were given a short cutting trial and re-analysed using BSE imaging.

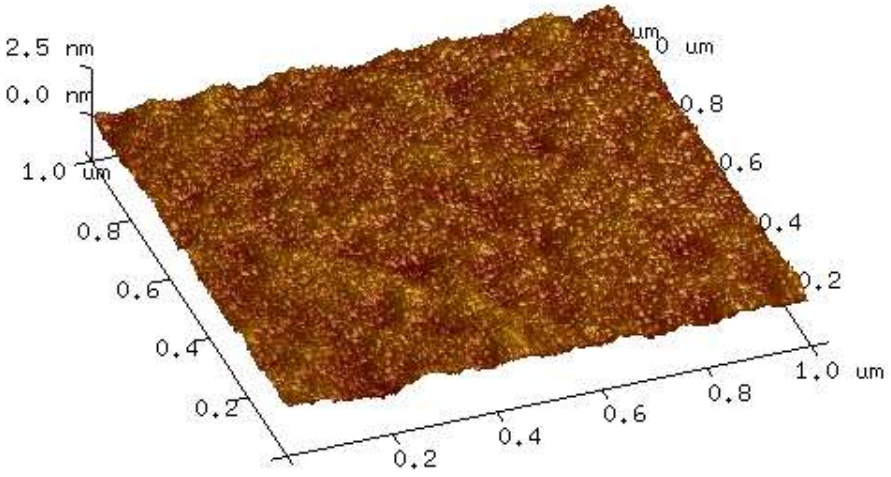

(a)

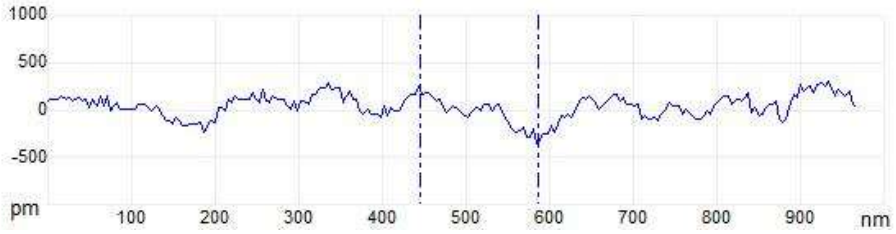

(b)

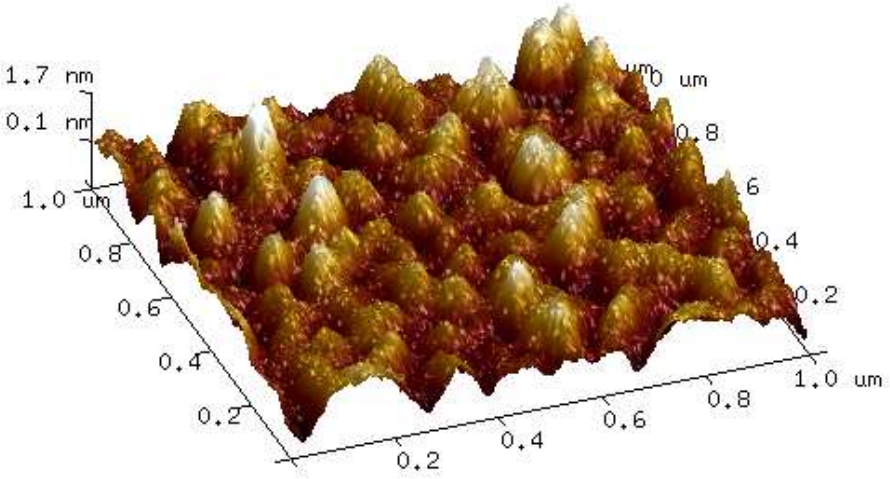

(c)

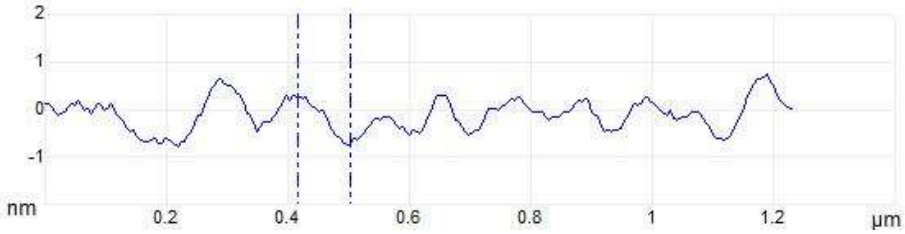

(d)

Figure 5.17. AFM images of 20sccm coating (a) 3D image (b) 2D section, and 40sccm coating (c) 3D image (d) 2D section

5.6.2. Results / Discussion

Initial SE2 analysis of the deposited coatings on the WC-Co inserts showed no visible difference between the DLC surface and no defects were present. All samples showed a good uniform coating across the entire top surface. Raman spectroscopy showed little difference between the samples with the sp^2 / sp^3 ratios being comparably similar. AFM analysis, however revealed significant variation in the roughness of the coatings. The coating with the final flow rate of 20sccm showed the lowest average roughness of just 0.127nm with a peak valley distance of 0.609nm (Fig 5.17). Once again, the coating morphology remained otherwise similar with no variation in skewness or kurtosis.

BSE analysis of the inserts post-trial revealed a number of things about the coatings as well as their machining performance. It is clear from the micrographs that the coatings deposited at lower flow rates are much thinner than those at higher flow rates. This is evident due to the lighter colour of the coating which is a result of the electron beam penetrating through the DLC layer and revealing the WC-Co underneath. Despite this difference there was no improvement in performance compared to the standard coating gas flow rates.

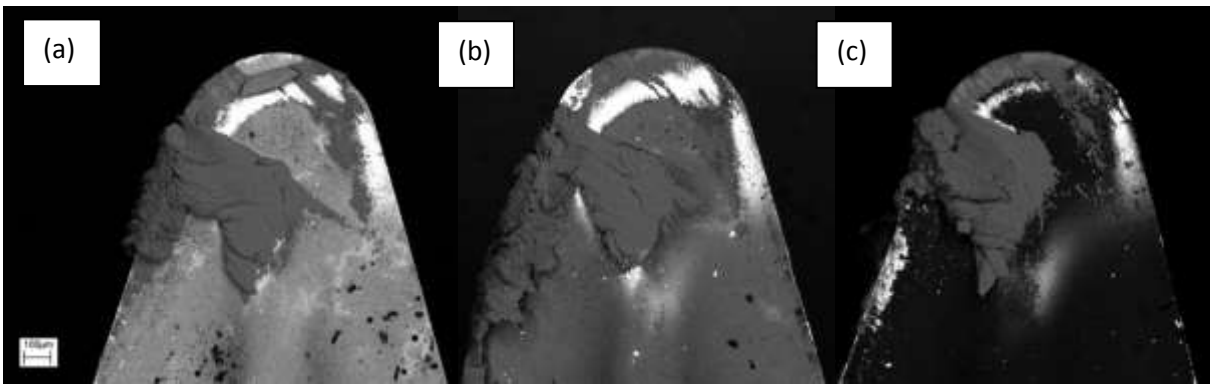

Figure 5.18. BSE micrographs of inserts after trial, with final flow (a) 20sccm (b) 30sccm (c) 40sccm

Reducing the flow rates and hence the deposition pressure led to reduced deposition rate and significantly thinner coatings, which also meant smoother coatings on the Si substrates. Machining performance was not improved and BUE seemed to have increased compared to the coatings deposited with a final flow rate of 60sccm (Fig 5.18).

5.7. Influence of deposition surface orientation

From the initial experiments conducted regarding the DLC coatings it became clear that the geometry of the substrates was having a significant effect on the quality of the coatings. Researchers have investigated the effect of substrate material and how the micro topographical features can alter film growth (Zhong *et al.*, 2008; Salvadori *et al.*, 2006), however, investigations of how larger geometrical variations of the substrate may affect the film properties were yet to be investigated. This is due to the fact that in a non-line of sight (NLOS) process such as PECVD the effects have been considered negligible (Grill, 1999). It was therefore necessary to devise a number of experiments to confirm how substrate positioning and surface orientation may influence coating properties. The following section describes the investigations which looked to evaluate the potential variation in material characteristics and how this might alter tribological performance.

5.7.1. Methodology

An experiment was devised to test of the effects of simple variations in cathode geometry by altering the position of the cutting inserts being coated. For this exploratory test, triangular titanium coated inserts were DLC coated using the standard three stage coating process. Two similar TiN coated inserts were DLC coated simultaneously, with one positioned flat on the cathode plate and one positioned vertically on its side (flank face) (Fig 5.19).

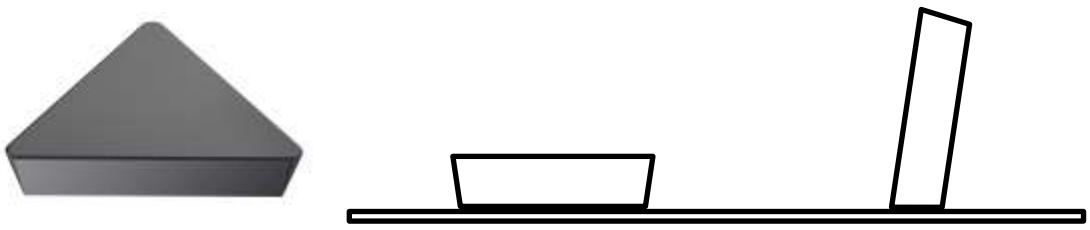

Figure 5.19. (a) Insert used (b) Positioning of inserts in DLC reactor

This was done in order to test the effects of the plasma field forming around the samples and analyse how it affects the coating characteristics. It was expected that variation in the properties of the DLC would occur due to shielding and the edge effect. The positioning of samples was therefore designed to maximise these effects in order to analyse how they affect the coating. It is already well documented that the edges of thin sheets being coated using the PECVD method will suffer from variations in the coating characteristics, however, little research had been conducted to test how the thickness or edge radius may interact with this effect. Attempting to quantify the effects of complex substrate geometry would require extensive testing, even more so when variation due to process parameters such as bias voltage and deposition time are incorporated. It was therefore important to initially test the extremes of what may occur with the geometries of the tools being utilised in this project. It will then be possible to quantify the maximum potential effect it may have on the coating characteristics and mechanical properties.

It could be seen in the reaction chamber that the plasma sheath was forming roughly 20mm from the substrate surface, thus giving an indication of how close two substrate surfaces may be before they begin to have an effect on the deposition of the DLC. When substrates of more complex geometries, such as 90 degree angles, sharp edges, concave spaces, etc. are coated, it creates areas where the sheath thickness varies slightly compared to the average which is seen when a flat surface is coated. This undoubtedly produces slight variation in the coating as a result because the impinging ion energies will be more variable.

The following section shows the results of the experiment in which two nominally similar triangular TiN coated inserts were coated simultaneously with one position vertically and one horizontally on the cathode plate. The samples were positioned 100mm apart to ensure there was no interaction between the samples in terms of their effect on the surrounding plasma.

5.7.2. Results

The samples were analysed using SEM in order to initially determine if there was any significant variation in the coating surface. High magnification micrographs of the horizontal sample showed that the majority of the coating was smooth and uniform. The general structure and surface morphology resembled that of the majority of DLC coatings produced (Fig 5.20 a and b). SEM analysis of the vertically positioned sample, in comparison, revealed significant variation to the usual topography, particularly at the top cutting tip. The nodular structure has been replaced by a seemingly rougher surface which exhibits a completely different surface morphology to the normal coatings. The top tip of the vertical sample showed a surface full of pits and valleys, as opposed to the usual nodular structure (Fig 5.20 c and d).

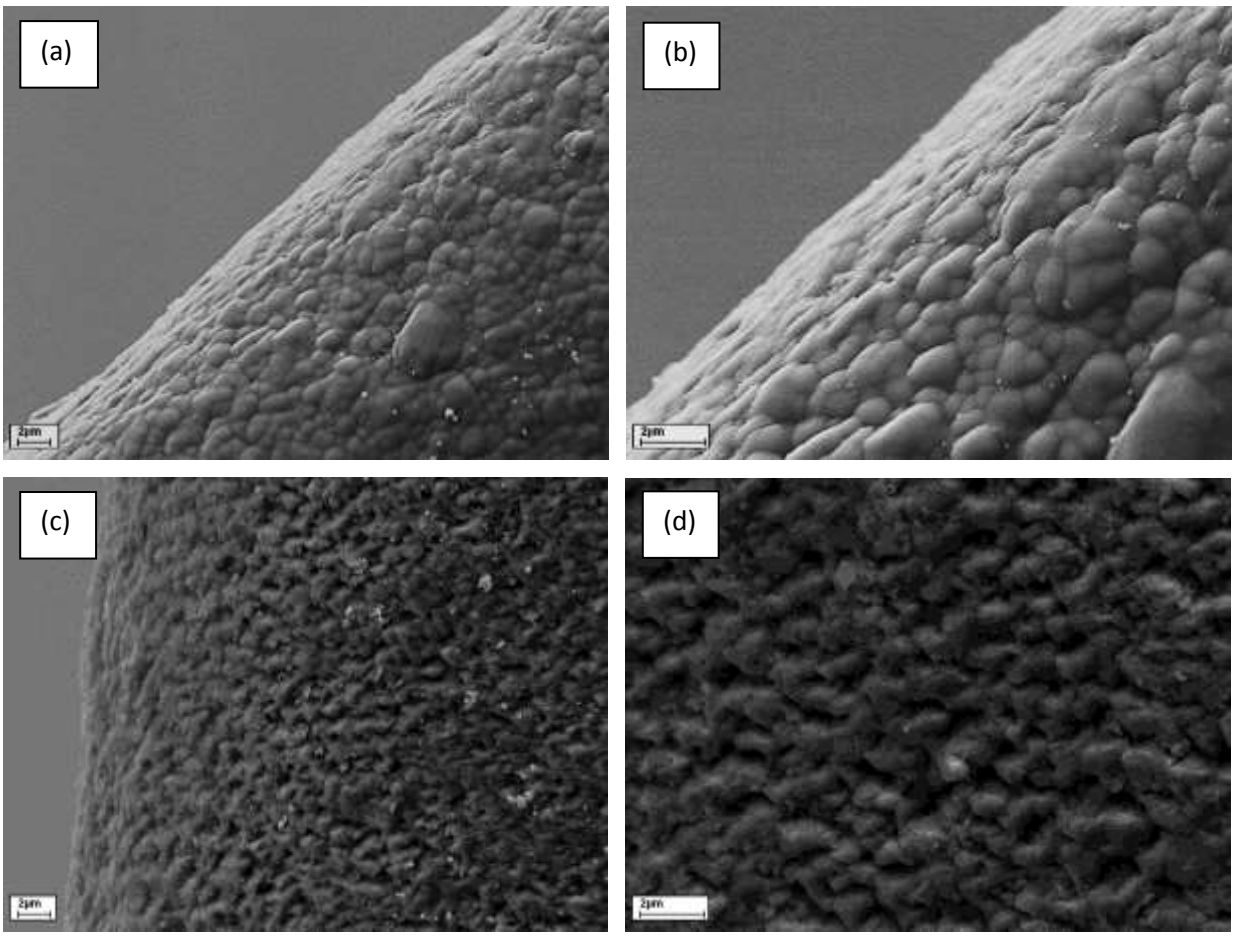

Figure 5.20. SEM micrographs of horizontal insert (a) X10k magnification (b) X20k magnification, and vertically positioned insert (c) X10k magnification (d) X20k magnification

The entire surface structure has been altered by creating a slight variation in the plasma field through sample positioning. Due to the lack of current research into the effects of substrate geometry or positioning, it became necessary to devise an experiment in order to examine the maximum potential variation that may occur due to either sample positioning or geometry. As well as examining the surface structure and topography, it was important to analyse the film chemistry and then determine the extent of these effects on the tribological properties.

Variations in DLC coatings due to substrate geometry have been examined for other DLC deposition methods. Bobzin et al (Bobzin *et al.*, 2009) investigated substrate geometry effects in magnetron sputter ion plating by altering substrate orientation and effectively varying the ion impingement angle. Ding (Ding *et al.*, 2004) completed a detailed study regarding the effects of substrate geometry of chromium doped DLC deposited using unbalanced magnetron sputtering. The investigation revealed how coating thickness, microhardness and bonding ratios were affected by the shielding of surfaces in close proximity.

Very little has been done in terms of investigations specifically focusing on substrate geometry in a PECVD system. A previous study highlighted how small differences in substrate thickness can affect the deposition rate of DLC in a parallel plate PECVD process (Balachova *et al.*, 1999). Simulations conducted by Waddell used a dome shape to examine how slight variations in substrate geometry can affect coating thicknesses and deposition rates (Waddell *et al.*, 2011).

5.8. Investigation of edge effect on DLC structure

Researchers are aware that certain substrate geometries will be more difficult to coat as adjacent surfaces will be shielded from impinging ions whilst sharp edges and points will lead to a concentration of ions impacting the surface (Daudt *et al.*, 2012; Neto *et al.*, 2008; Chabert, 2007; Zhang *et al.*, 2006), however, the extent of the effects are currently unknown. This following study, based on a publication (Nelson *et al.*, 2014), focuses on how variations in the orientation of substrates within the PECVD reactor can affect the coating characteristics and mechanical properties, which in many applications, will lead to reduced performance of the DLC thin film.

5.8.1. Experimental details

Film deposition

DLC coatings were deposited on 10mm^2 single sided (100) silicon wafer, of thickness 0.66mm. Silicon was chosen as it provides a smooth uniform surface and promoted good adhesion. The uniformity removes further potential fluctuations in the coating, which may be due to slight topographical variations, ensuring that the heterogeneity measured in the samples can be attributed solely to the sample positioning in the reactor. All samples were ultrasonically cleaned in acetone for 10 minutes before being placed in the deposition chamber. The samples were placed horizontally and vertically on the cathode plate. The horizontal samples were simply placed flat on the plate whilst the vertical samples were clamped at the base (Fig 5.21).

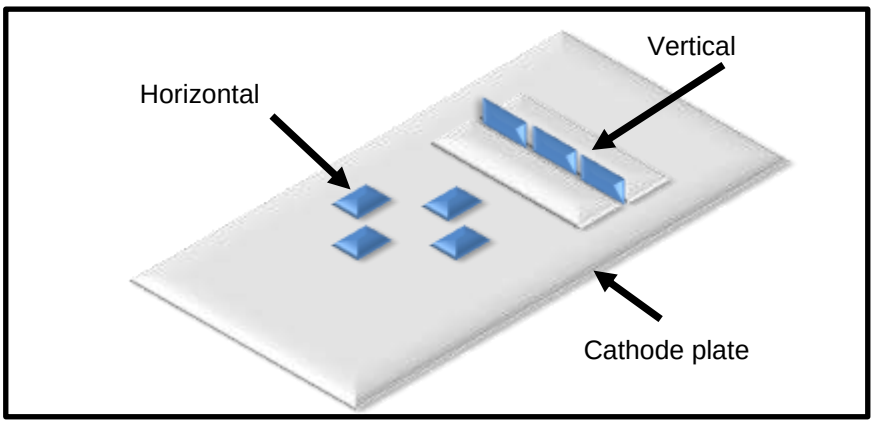

Figure 5.21. Diagram of the substrate positioning on cathode plate

Surface characterisation

Surface structure was analysed using SEM and AFM. SEM has been used to create micrographs of the sample surface, the voltage was set at 6kV for improved surface resolution. AFM was used in tapping mode to measure the roughness (Ra), skewness and kurtosis of films at specific points on the samples. Scans of 10µm × 10µm were conducted using a 190kHz silicon cantilever with a force constant of approximately 48N/m and nominal tip radius of 8nm. The horizontal and vertical sample was measured in 1mm increments from edge to edge and top to base respectively. Each area was measured four times, an average roughness was taken and deviations were calculated.

Film thickness

The horizontal and vertical samples were sectioned edge to edge and top to bottom respectively, the sections were then analysed using SEM and coating thicknesses were measured at specific points.

Bonding structure

Raman spectroscopy was conducted to compare the areas of the disordered (D)and graphitic (G) peaks. The horizontal sample was measured at 1mm increments from edge to edge whilst the vertical sample was measure in 1mm increments from the top to the bottom of the sample. The peaks were fitted using two 100% Gaussian curves.

Microtribology tests

Scratch tests were conducted by the National Physical Laboratory. The friction and hardness of the films was measured at specific points on the samples. Measurements were conducted using a 250µm radius diamond indenter. All tests involved a 5mm long scratch, a load ramp from 0.5N to 20N was used, in 30steps, at a speed of 0.1mm/sec. In all these tests the substrate was blown clean before and after every scratch to remove debris that might affect the subsequent scratches. Similarly the indenter tip was wiped with alcohol to remove debris between tests. Due to the weakness of the substrate it was not possible to conduct scratches at the very edge of the samples. Horizontal and vertical samples were scratched at 2.3mm, 4.6mm and 6.9mm from the edge / top respectively. The scratches in the vertical sample were parallel to the top edge.

5.8.2. Results

Topography

The SE2 micrographs of the film surface show variation in the topography at the very top of the vertical samples, whilst the horizontal samples and lower areas of the vertical samples appeared relatively featureless in comparison (Fig 5.22).

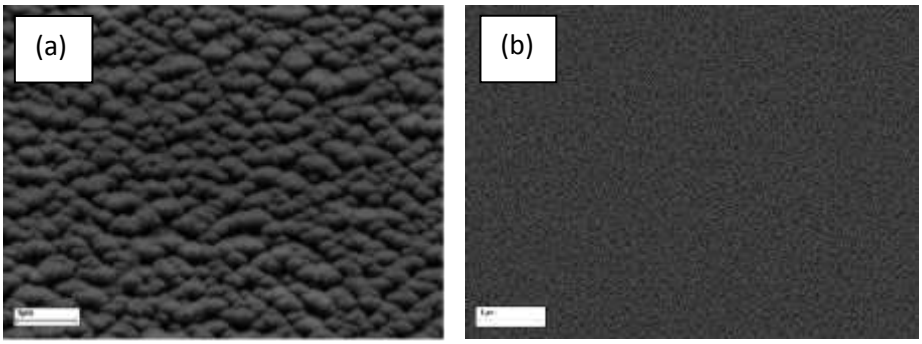

Figure 5.22. SEM image of DLC at (a) top of the vertical sample (b) horizontal sample

AFM images also highlighted the variations in the topography of the coating as well as directionality in the surface structure (Fig 5.23). The DLC near the top of the vertical sample has formed a ridged

structure parallel to the top edge, whilst the vertical mid sections and horizontal sample coatings show no immediate indication of how they were positioned during deposition.

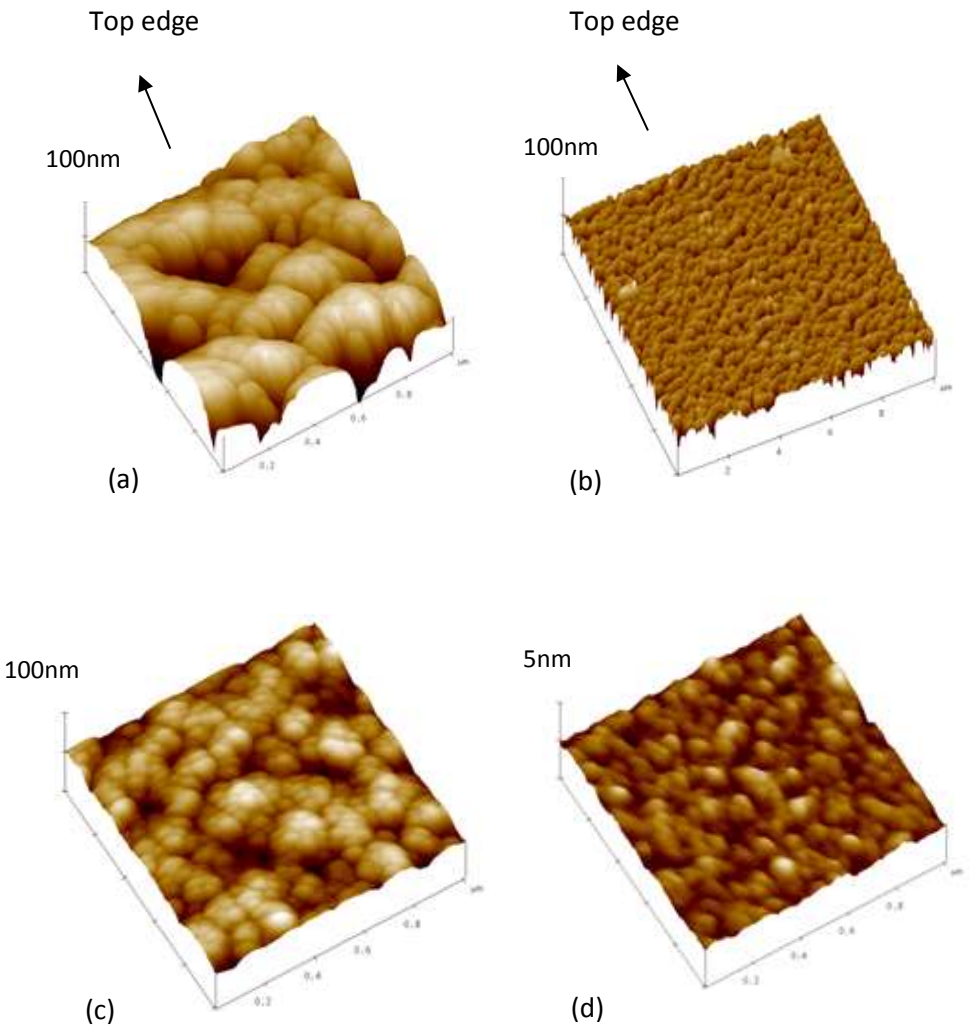

Figure 5.23. AFM images of surface topography at (a) top of vertical sample 1micron scan size (b) top of vertical sample 10micron scan size (c) middle of vertical sample 1micron scan size (d) middle of horizontal sample 1micron scan size

AFM measurements confirmed that roughness values varied significantly between the samples. The horizontal samples had the lowest roughness of 0.37nm ± 0.03nm whilst the vertical samples had a roughness of 15.4nm ± 2.4nm and 1.29nm ± 0.09nm at the top and middle respectively. Skewness

and kurtosis measurements also highlight the variation in the surface structure in the top 1mm of the vertical sample (Fig 5.24).

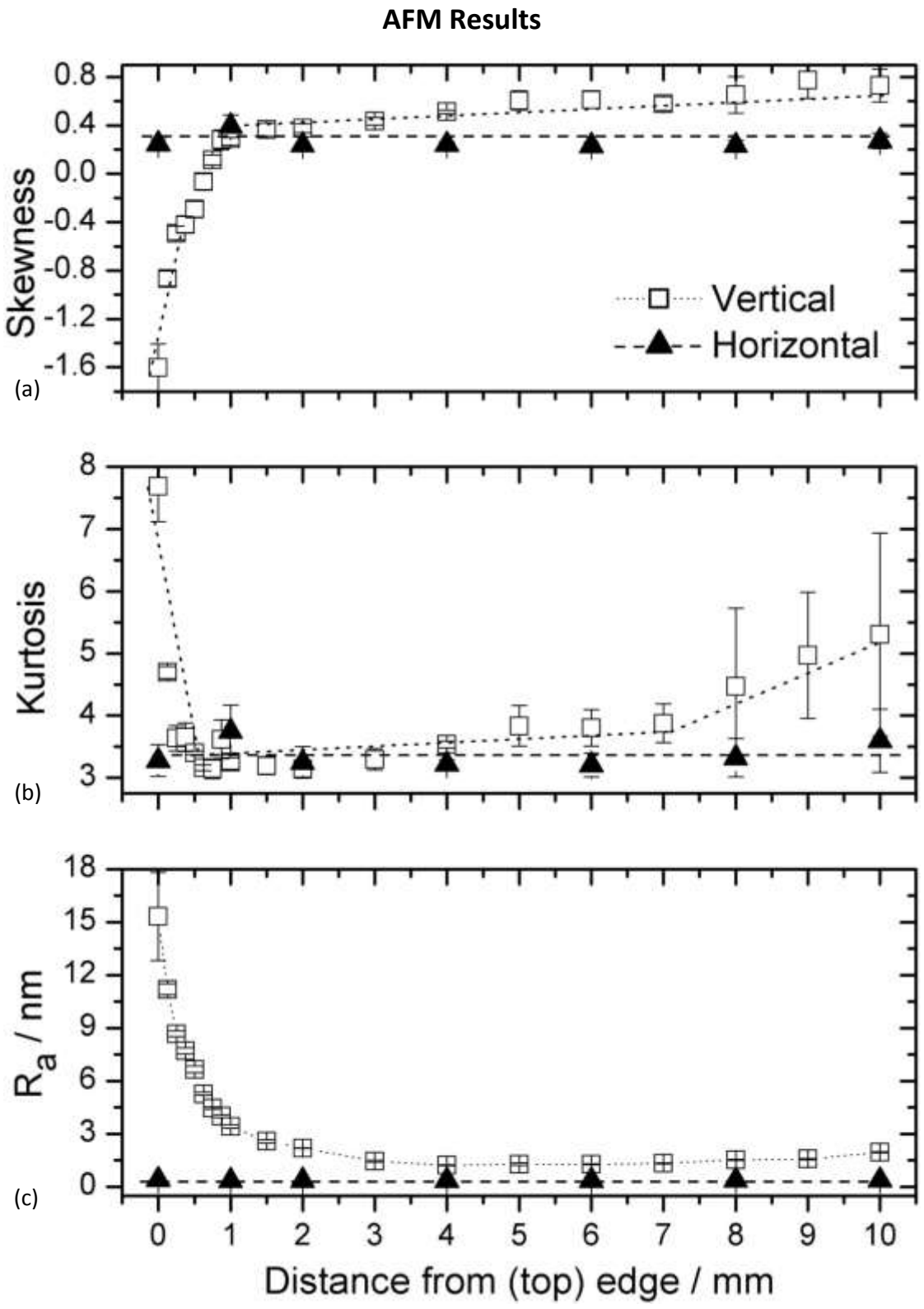

Figure 5.24. Graphs showing (a) roughness, (b) skewness and (c) kurtosis, against distance from top/edge of horizontal and vertical samples

Coating thickness

SEM analysis of the sectioned samples showed the top of the vertical sample had a nodular growth pattern throughout the silicon and carbon layers, compared to the horizontal sample which had a much more uniform coating with clear transition lines between layers (Fig 5.25). Measurements of the coatings show that the thickness of the horizontal sample remained constant at 1.69µm ± 0.04 µm, the vertical sample in contrast showed large variation of the film thickness. The thickness at the bottom of the sample was 1.2µm, rising smoothly to 1.8µm at the top (Fig 5.26).

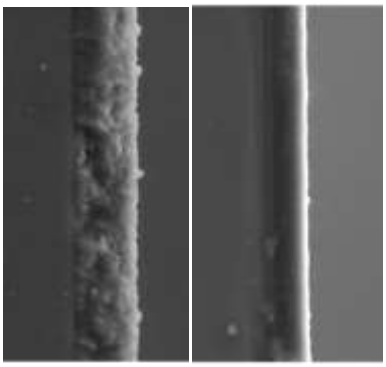

(a) (b)

Figure 5.25. SEM micrographs of sectioned samples (a) top of vertical sample (b) horizontal sample

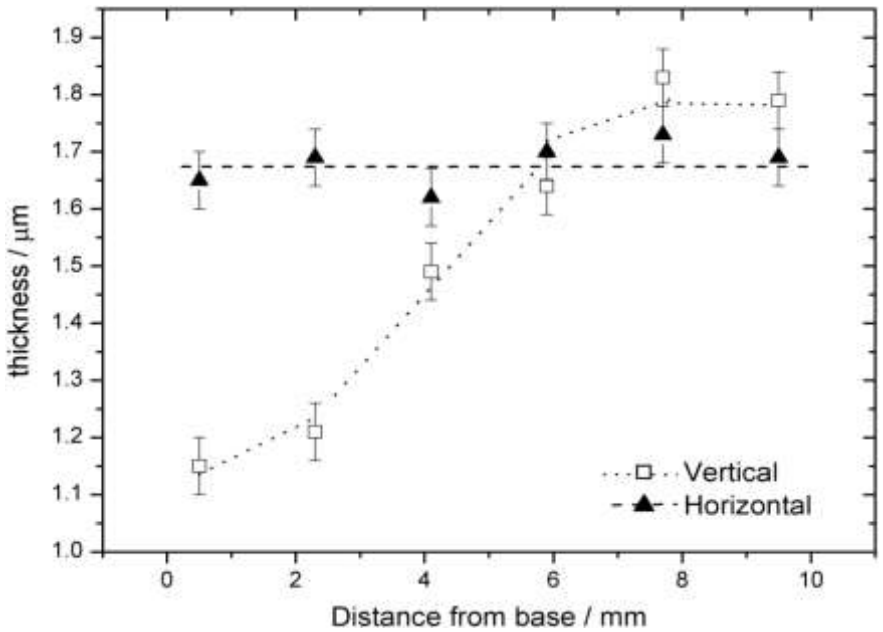

Figure 5.26. Graph of coating thickness relative to edge/base of the horizontal and vertical samples

Bonding chemistry

Analysis of the I(D)/I(G) ratios of the samples indicated that the horizontal sample had a higher average sp^3 content compared to the vertical sample, I(D)/I(G) area ratios were 1.07 ± 0.02 for the horizontal sample compared the 1.67 ± 0.08 in the middle of the vertical sample. In the top 2mm of the vertical sample the ratio increased up to 2.63 ± 0.09 (Fig 5.27). It was also noticed that accurate measurements were not possible within the top 1mm of the vertical sample due to significant amounts of background noise caused by the photoluminescence effect of the rougher surface. It has been shown that such variation corresponds to an sp^3 concentration of 40% in the horizontal sample and between 25% and 30% in the vertical sample (Ferrari *et al.*, 2000).

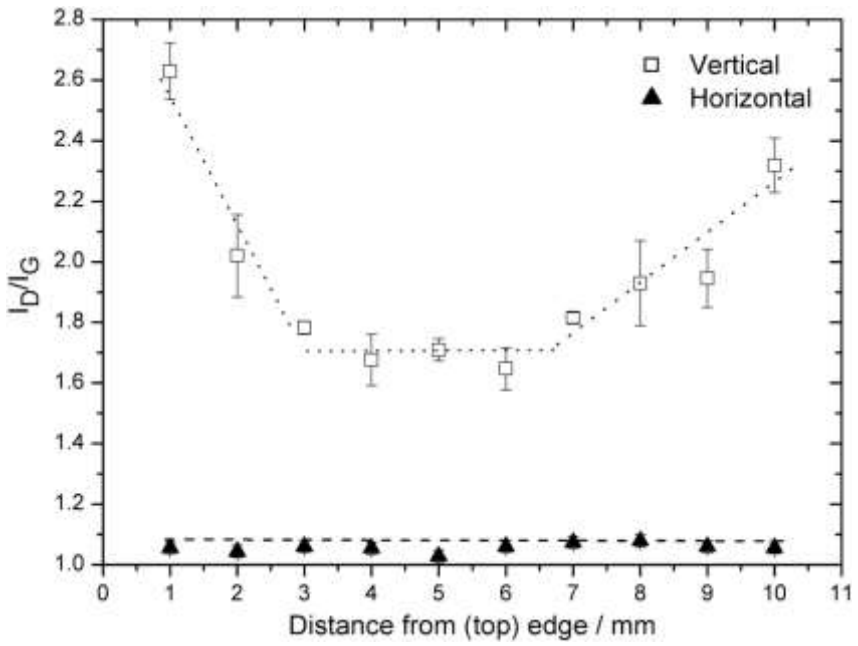

Figure 5.27. D/G area ratios of vertical and horizontal sample

Tribology

Scratch testing determined the failure load of the film for the horizontal sample to be on average 8.0N. The failure load of the vertical sample was found to be roughly half that value at 4.0N. Friction measurements before failure showed the horizontal sample to have the lowest friction coefficient at just under 0.08. The vertical sample was marginally better than the bare silicon at 0.13 compared to

0.16 (Table 5.1). Measurements of friction and failure load between the top, middle and bottom of the vertical sample showed little variation.

Sample	Friction	Damage Load (N)
Silicon 1	0.16	6.6
Silicon 2	0.17	6.4
Silicon 3	0.16	7.1
Horizontal 1	0.075	8.8
Horizontal 2	0.08	7.4
Horizontal 3	0.08	7.8
Vertical 1 (upper)	0.12	4.1
Vertical 2	0.13	3.9
Vertical 3	0.14	4.0

Table 5.1. Friction and critical load measurements from scratch testing

5.8.3. Discussion

Growth mechanisms will vary slightly depending on the substrate, this can be seen as the macrostructure of a PECVD deposited DLC film is often able to mimic the topography of the substrate being coated. The growth of DLC, however, will usually lead to a microstructure which has a nodular formation (Jones *et al.*, 2011; Mansano *et al.*, 2009; Peng *et al.*, 2001; Sun, 2000). The smooth Si minimises the effects of substrate roughness allowing DLC to be deposited uniformly across the sample, providing other variables are also minimised. One study used AFM to show that in this case, the DLC deposited on Si wafer nucleates in individual islands, these islands grow before combining to form a continuous coating (Maheswaran *et al.*, 2011).

The observed variations in film roughness between the horizontal and vertical samples, as well as the deviations within the vertical sample, can be explained by considering the physical deposition mechanisms associated with the PECVD process. The variations are likely to be as a result of a number of geometrical differences in the sample. Firstly, the orientation of the substrate surface relative to the cathode plate, and hence direction of the ions varies between the horizontal and vertical sample. Secondly, the distance from the cathode plate will have an effect on the vertical sample, and finally the protruding top edge of the vertical sample will lead to a concentration of

impinging ions whilst the lower half will be shielded. It also has to be considered that the electrical and thermal conductivity of the substrate will have an effect, however, further investigations of these effects were beyond the scope of this investigation.

At the top / edge of the substrate more carbon ions are impacting a smaller surface area with a much greater impact angle range. The subplantation model of DLC growth describes how the ions impact the surface displacing other atoms before coming to rest (Robertson, 2002). Ions of energies below the penetration threshold have been shown to bond at the surface of the film forming a more uneven and less dense coating containing higher amounts of sp^2 bonding. Ions with energies exceeding the penetration threshold will travel deeper into the deposited layer before relaxing, dissipating energy to surrounding atoms, maintaining a much smoother surface and an increase in sp^3 bonds. For efficient subplantation the ions should also be travelling normal to the substrate surface, this ensures the majority of their energy is used to penetrate the surface (Ma, 2007). On the vertical sample and particularly at the top edge, as the direction of the impinging ion deviates from the normal line, more energy will be required for the ion to reach the same depth. The irregular growth at the top of the vertical sample may therefore be attributed to lower effective energies of ions impacting the surface. These reduced ion energies will be partly due to angle of attack, i.e. a higher percentage of ions will be hitting the substrate at angles further from the perpendicular. The larger impact angles reduce the overall effective energy meaning that fewer ions can penetrate the material creating more disruption in the coating surface and increased in roughness and sp^2 bonds.

The top of the sample will also be subjected to a concentration of impinging ions which will in turn reduce the mean free path. This will lead to increased collisions between the ions which reduces the ion energies before they contact the substrate (Peng *et al.*, 2001; Sun, 2000). This means that the concentration at the tip will not only lead to an increased number of impinging ions per mm^2, but also reduce the overall energy of the ions so that a reduced percentage will subplant whilst more will settle at the surface.

The shielding of the surface on the vertical sample has a much more significant effect on the coating thickness, this suggests a severely reduced deposition rate. The reduced deposition rate can be attributed to fewer impinging ions impacting the surface. The roughness would also suggest that the impacting energies are higher than that of the top of the vertical sample but lower than that of the horizontal sample.

Raman analysis indicates the sp^3 concentration in the vertical sample was reduced in comparison to the horizontal sample, it also shows the sp^3 content to be lowest at the top of the vertical sample where the roughness is at a maximum. These results are in keeping with current theories regarding the deposition mechanisms involved in the PECVD process (Robertson, 2002; Peng *et al.*, 2001; Lifshitz, 1999). The variations between coatings are indicative of differences in the energy of impinging ions, with higher energies promoting suplantation, smoother surfaces and sp^3 bonding, whilst lower energies cause an increase in surface bonding, leading to rougher surfaces and reduced sp^3 concentrations.

Being a hydrocarbon process the effects of hydrogen etching must also be considered, it is likely that a plasma concentration at the tip would have increased the amount of impinging hydrogen ions. This would in turn increasing the etching effect, which has been shown to lead to surface roughening (Robertson, 2002; Peng *et al.*, 2001; Grill, 1999), however, the increased concentration would also reduce the nominal energy due to increased collisions. The effects may therefore only account for a small part of the increase in roughness on the vertical sample. Sputtering from carbon containing species will also influence the surface roughness, however, without further investigation it is not possible to know exactly how sputtering and etching will be affected, particularly when considering the likely deviations in the ion impingement angle at the top of the vertical samples.

These variations in the coating topography and structure have in turn had a great effect on the mechanical properties. Lower sp^3 concentrations generally lead to softer coatings, however, the large difference in the critical load values between the horizontal and vertical samples will, in most

part, be due to the differences in the surface structure of the coatings. The increased roughness of the vertical sample has led to increased friction coefficients and, along with the reduced sp^3 content, has lowered the critical load values compared to the horizontal sample.

5.8.4. Conclusion

The investigation has highlighted that substrate geometries have the potential to significantly alter coating characteristics of DLC deposited using the PECVD method. SEM initially highlighted variations in the surface structure of the vertical sample. Surface roughness varied greatly between the vertical and horizontal samples as well as between different areas on the vertical sample. Roughness peaked at the top of the vertical sample at 15.4nm whilst to horizontal maintained a constant 0.37nm.

Analysis of the bonding structure showed the vertical sample to have lower sp^3 content than the horizontal, with the top of the vertical sample having the least sp^3 content, 10% less than the horizontal. Teer scratch tests revealed that these variations can increase the friction coefficient from 0.078 to 0,13 whilst reducing the critical load of the film from 8.0N to 4.0N.

Sharp edges on the substrate act to concentrate the impinging ions, which lead to an increase in deposition rate, whilst the shielded region has a reduced amount of impinging ions which decreases the deposition rate and final film thickness. Plasma concentrations and reduced ion energy efficiency mean that fewer impinging ions can penetrate the surface. This in turn leads to rougher coatings with reduced tribological performance. It has been shown that in a PECVD system, small variations in substrate geometry can lead to very large differences in the characteristics and mechanical properties of the DLC coating.

5.9. Cutting insert positioning

It was apparent that the positioning of the inserts during deposition would also need to be investigated in further detail to ensure that the coating was optimised at the cutting tips. This means ensuring the major flank has a good coating as well as the rake face. Further test were therefore conducted to test if the use of sample jigs could be utilised to improve the coatings quality and coverage in the desired areas.

5.9.1. Methodology

Inserts were positioned to optimise the coating on the major flank as well as the rake face. For this test two inserts were positioned on the cathode plate with the major flank facing upwards, whilst two were suspended from the centre hole by a conductive wire. The inserts were coated at 500V, other deposition parameters were as per the standard coating parameters.

SEM imaging was then used to analyse the samples and examine the effect that it may have on the coating morphology at the cutting tip, rake face, major flank and cutting edge. Raman was then used to compare any variation that may have occurred in the surface chemistry of the DLC thin film.

5.9.2. Results

SEM analysis highlights the variation in the surface morphology of the DLC coating on the WC-Co cutting inserts. Micrograph analysis revealed that the DLC topography of the samples positioned flank upward, as well as those suspended from the centre had a significantly transformed surface pattern. It can be seen from the images that the morphology of the DLC coating on the rake face of both of the alternately positioned samples is quite distinctive to that of the samples coated with the rake face pointing upwards (Fig 5.28). For the samples positioned on the cathode plate, both rake face up and major flank up, the coating on the cutting edge showed similar morphology. They both

displayed the previously documented clustered nodular structure that is expected from many DLC films. Just off the cutting edge, however, the pattern begins to change greatly between the samples.

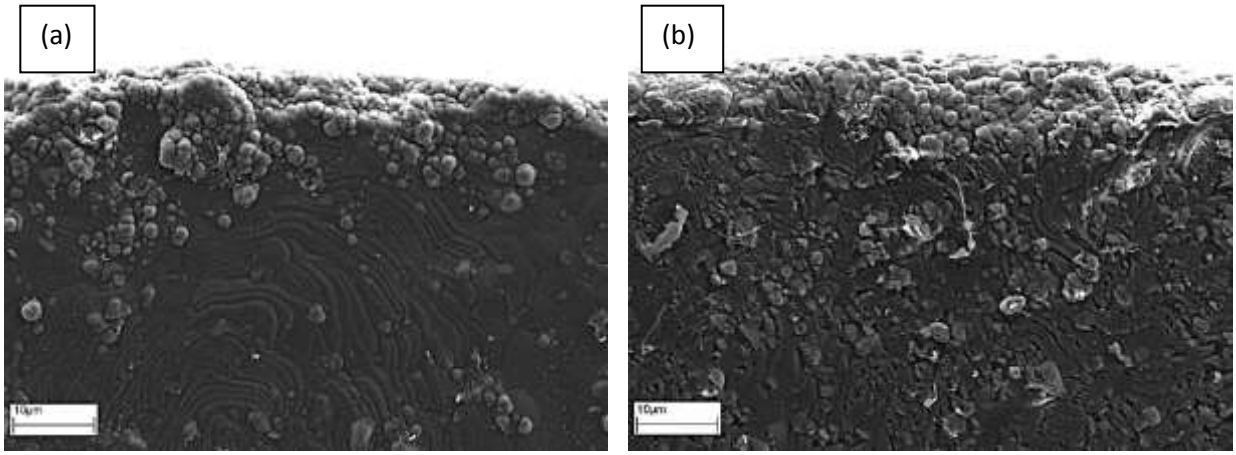

Figure 5.28. SEM micrographs of cutting edge of insert with (a) base on cathode (b) flank on cathode

The insert which was positioned on its base, rake face up, clearly showed the distinctive pattern of the cobalt substrate, whilst the insert that was positioned major flank up has produced a much more erratic surface. The features of the underlying cobalt are still visible, to a lesser extent, however, the effect of the positioning has produced a less homogeneous surface with many defects which have compromised the integrity of the coating at the cutting tip.

Micrographs of the flanks showed little variation between the samples. The DLC coating maintained a similar topography to the underlying polished pattern that runs along the insert flanks (Fig 5.29).

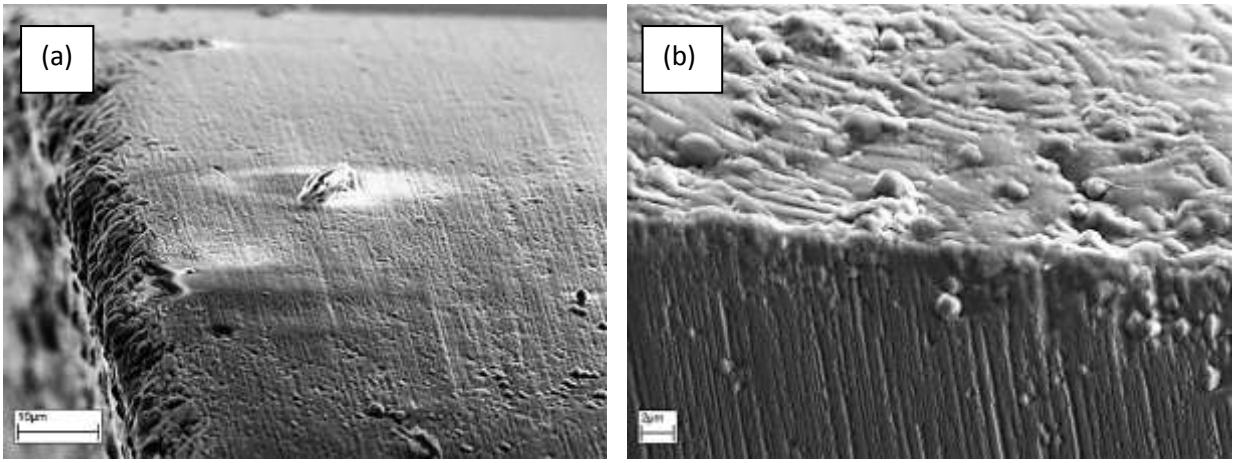

Figure 5.29. Flank/tip of insert coated rake face up (a) Flank and cutting edge at X5000 magnification (b) Flank and leading edge at X10K magnification

The analysis highlighted the importance of ensuring the coating was of sufficient quality on the rake face at the cutting tip as this area seemed to be affected to the greatest extent. There are a number of reasons this may be the case. Due to the processes involved in the production of the inserts the rake face and major flank surfaces have very different topography. The sintering process compresses tungsten crystals within the cobalt matrix which creates an uneven surface morphology in which some areas contain a larger percentage of tungsten crystals at the surface, whilst other areas are predominantly cobalt. The flanks on the other hand have been polished which has created a much more homogeneous surface for the DLC to bond too. The contours of the rake face also add to the potential inhomogeneity of the coating compared to the flat sides of the flanks as it will have a slight effect on the surrounding plasma. This in turn will have an impact on the effective energies of the impinging ions producing further variation in the coating characteristics and material properties.

The samples suspended from the centre hole where of significantly poorer quality in comparison to those on the cathode plate and did not produce a viable coating. The wire through the centre clearly had an impact on the plasma formation around the tool and coupled with the increased geometric effects of the suspended insert meant that all areas suffered from a defective coating. The following images show the extent of the coating failure (Fig 5.30). Near the centre of the insert it can be seen that significant delamination has occurred during the deposition process. It is clear from figure (a) that delamination occurred intermittently producing slightly different degrees (shades) of coating. The delamination continued to within 0.5mm of the cutting edge whilst the coating at the cutting edge itself had delaminated completely. It was also evident that the DLC coating deposited had a very different surface structure and had not mimicked the underlying substrate in any way unlike the samples on the cathode plate.

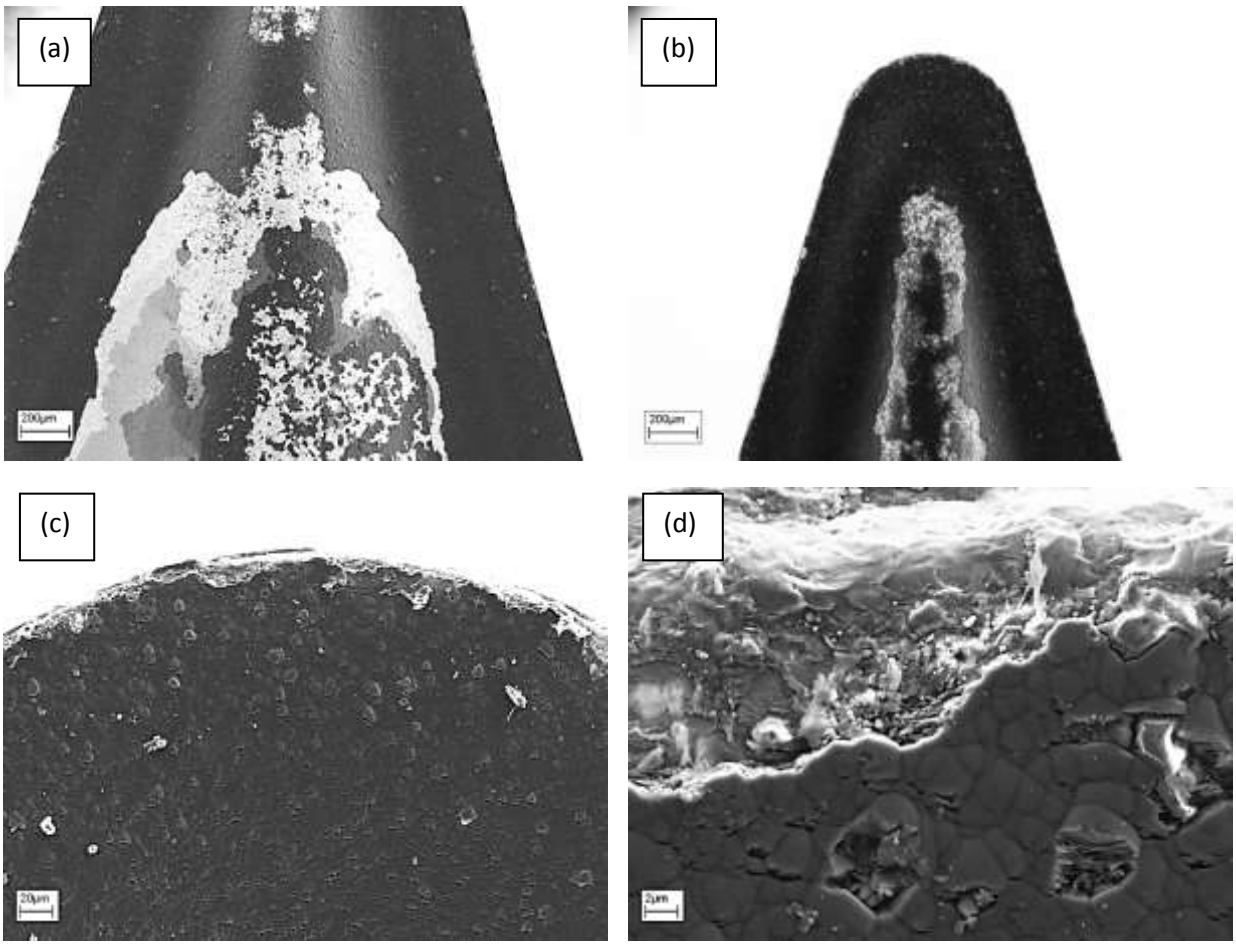

Figure 5.30. SEM micrographs of suspended insert (a) centre (b) tip (c) cutting tip (d) cutting edge

5.10. Conclusion

The DLC coatings produced on various substrate materials and geometries, using a number of different deposition parameters, have been evaluated in order to ensure that the development required when the DLC is applied to diamond coatings will be minimal. A number of parameters were examined including bias voltage, deposition time, gas flow and sample positioning. It was confirmed that the main factor affecting the coating characteristics was bias voltage, whilst other factors had little impact on the ultimate machining performance. It became evident that the wear rate of the coating was an issue and higher voltage coatings performed best. This is shown by the reduced wear rates, as described in section 5.4.2. The deposition energy, however, was limited due

to the residual stresses present in the coating which lead to delamination when voltage was increased further.

Investigations into the effects of the sample geometry (section 5.8) also showed that the coatings may not have been performing as well as expected in certain areas of the tool. When flat surfaces are coated using the PECVD method, the characteristics of the DLC coating exhibit the desired properties of low roughness and high hardness. When surfaces which are not flat are coated they have been shown to have an increased average roughness of up to 30 times. This variation, coupled with reduced sp^3 bonding, produces a DLC coating with increased friction and reduced hardness. This was evident as Teer scratch tests revealed the critical load values to vary by 50% between samples. These results contradict a common consensus that substrate geometry has little effect on coating quality in non-line of sight deposition processes such as PECVD. Experimentation has revealed how the tool geometry and positioning during coating can produce variations in coating characteristics and tribological performance. When applying DLC coating to the diamond surfaces, it will be expected that the crystalline substrate will produce a slightly different effect on the deposited thin film, particularly at the cutting edge. The diamond coating should, however, produce a homogeneous surface across the entire tip which should lead to a more homogeneous DLC layer.

6. Combined coating development

6.1. Introduction

The following chapter discusses the development of the combined diamond and DLC coatings. The surface DLC layer of the combined coatings are characterised in terms of the quality of uniformity, surface topography and bonding chemistry. The DLC is examined in order to assess the influence of the underlying substrate and to quantitatively evaluate any variation caused. The analysis will also examine how the varying substrate material may affect to the DLC layer.

The combined coatings were analysed using SEM to ensure the coatings produced were of good quality and well adherent to the substrate. Raman spectroscopy was used to test for any variation in the bonding chemistry of the coatings, whilst AFM was used to measure the change in roughness and other topographical effects brought about by the coating combination. Raman spectroscopy and AFM analysis will be conducted in a similar position on the rake face of the inserts to allow for an accurate comparative assessment of the variation. Measurements were also taken at other points on the insert surface in order to examine the potential variation across the tool as a result of the geometry of the cutting tip, as well as any disparity caused by the gradually diffusing diamond layer.

The analysis of the combined coatings allows for an improved evaluation of the efficacy of combined coatings for machining aluminium alloys. This is done by enabling the cutting performance to be directly attributable to coating characteristics. DLC coatings deposited on TiN, MCD and NCD are therefore characterised and contrasted against one another, as well as being compared against the cutting performance of the individual coatings.

6.2. Diamond like carbon on TiN

The DLC coating was applied to nominally similar commercially available TiN coated inserts. This was in order to provide additional information and comparison on the performance of the combined coatings. The TiN coated insert was identical in geometry to the WC-Co tool and hence could be used as part of a direct comparison of the coatings. The 500V DLC coating was deposited on the inserts using the parameters described in chapter 5, section 5.4. SEM analysis of the coatings showed that the DLC had adhered well to the TiN surface and there were no visible signs of defects or failure in the coatings.

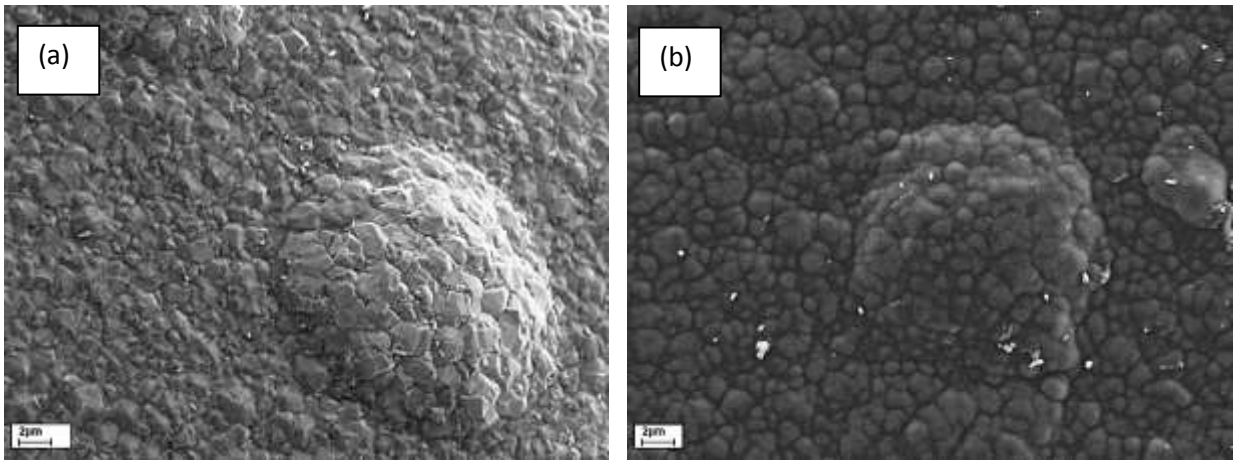

Figure 6.1. SEM micrographs of protrusion on (a) TiN coating (b) DLC on TiN coating

SEM analysis highlighted a number of small imperfections in the surface homogeneity of the TiN coatings, which have been carried through to the DLC surface (Fig 6.1). The micrographs show that both the TiN and DLC coating surface contains raised areas which are likely to have been initiated by the TiN coating process, as uncoated WC-Co inserts did not show similar discrepancies.

It can also be seen that the growth of the DLC nodular structure corresponds to the TiN crystal structure. This is due to the DLC nodules preferentially nucleating at the edges / fissures in the TiN surface, which is similar to what has been shown in the literature (Salvadori *et al.*, 2006).

AFM measurements were taken in an area which did not contain the raised patches, as mentioned above, in order to get a more accurate measurement of the coatings nano-scale features. Analysis of the topography of the combined coating showed that the DLC layer has reduced the surface roughness marginally (Fig 6.2). The TiN coating had an average roughness of 91.7nm whilst the addition of DLC reduced it to 79.1nm. The RMS roughness and Z range followed a similar pattern with a reduction from 116nm to 100nm and 1036nm to 808nm respectively. The skewness varied slightly from 0.247 to – 0.039 with the addition of the DLC layer, indicating that the topography varied from a slight peak bias to a trough based surface. Kurtosis on the other hand did not show any significant variation.

Raman spectroscopy of the coatings showed that the variation of the TiN and WC-Co substrate material did not significantly affect the chemistry of the surface layer. The Id/Ig ratio of the DLC on WC-Co was 0.47 ± 0.06 whilst the DLC on TiN measurement was 0.49 ± 0.05.

6.3. Diamond like carbon on micro-crystalline diamond

6.3.1. 500V coating with silicon interlayer

The DLC coating was applied to an MCD coating using the parameters described in chapter 5 for the 500V coating. The properties of the coating were then characterised in order to evaluate the potential effect that may be caused by the diamond layer. SEM analysis of the coatings showed that the DLC uniformly covered the surface of the sample insert with no signs of failures or defects in the coating. Micrographs revealed that the DLC layer deposited in a nodular structure as expected due to the nature of the substrate morphology. It can be seen that the insert cutting edge has been transformed from sharp crystalline peaks (Fig 6.3 a) to a more rounded cutting edge (Fig 6.3 b). The micrographs did also highligh slight variations in the coatings at different points on the sample. At 5mm from the cutting tip edge the morphology was notably different (Fig 6.3 c).

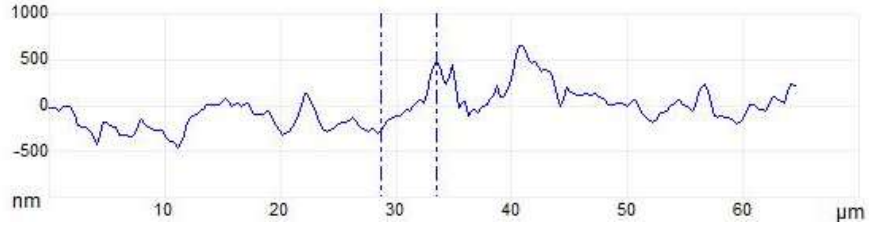

(a)

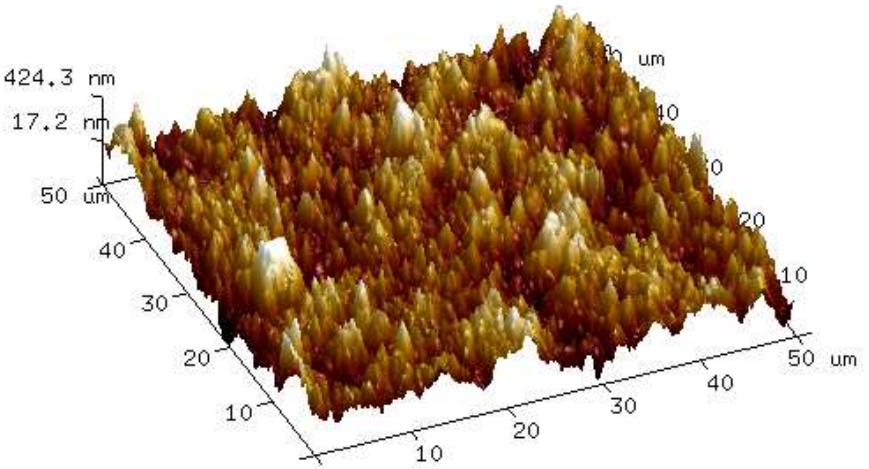

(b)

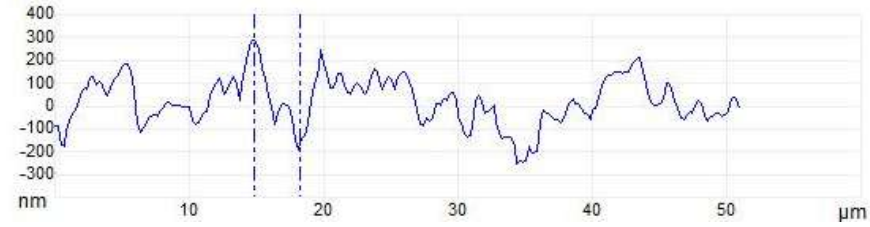

(c)

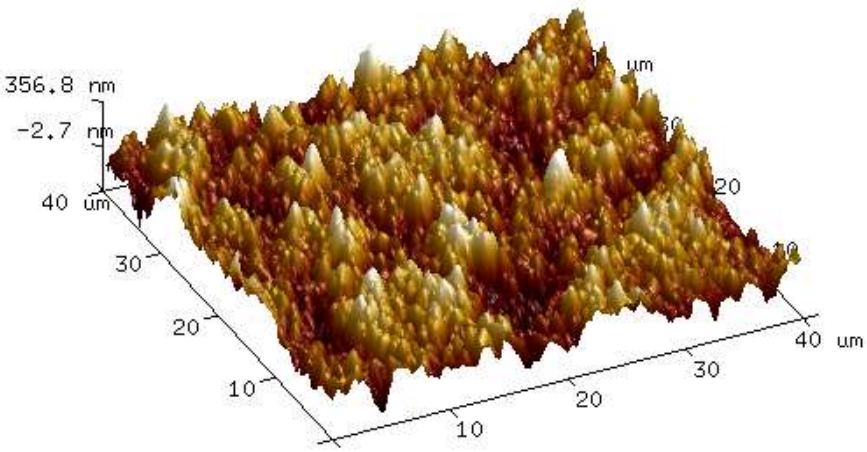

(d)

Figure 6.2. AFM images of (a) 2D section (b) 3D image, of TiN coating and (c) 2D section (d) 3D image of DLC on TiN coating

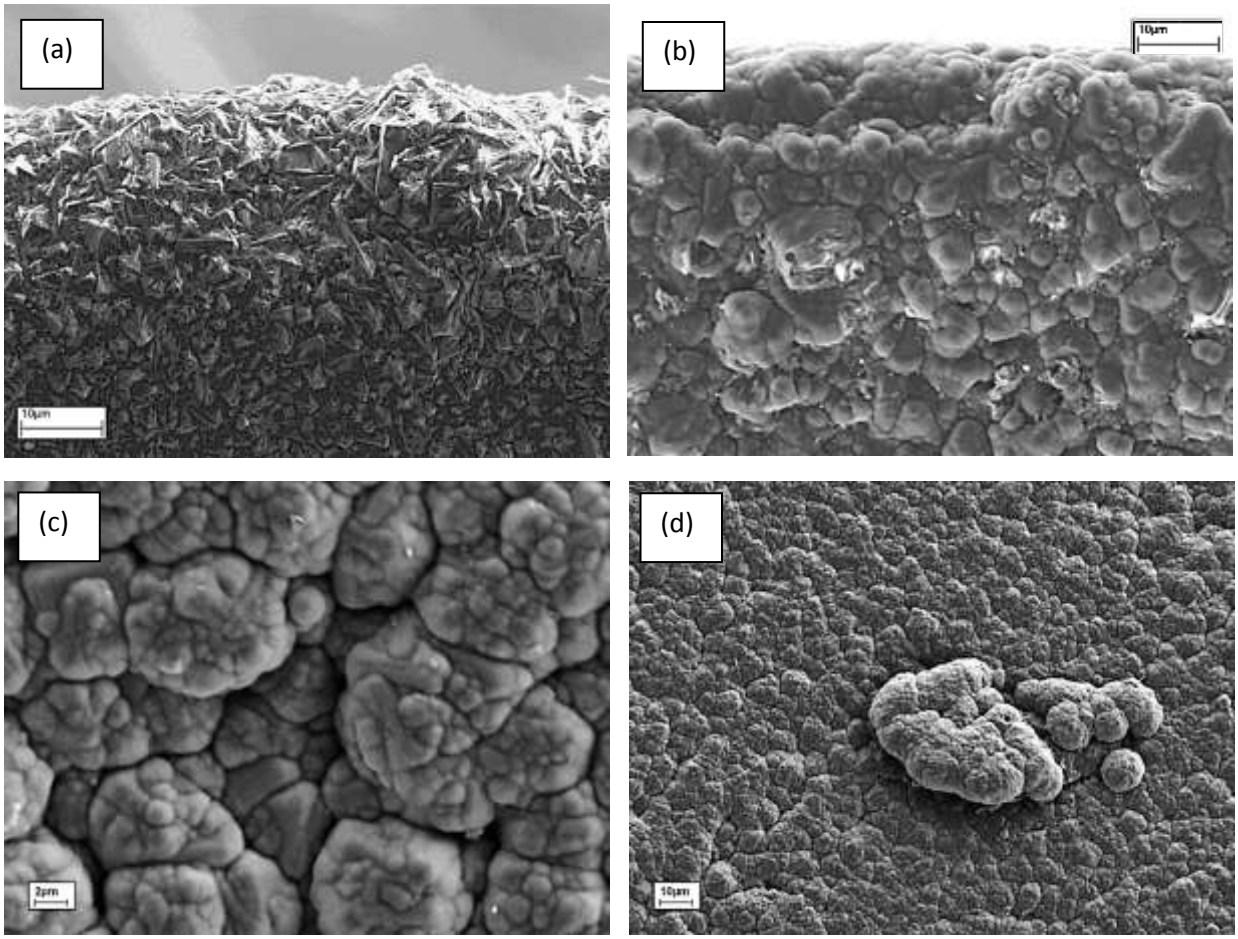

Figure 6.3. SEM micrographs of (a) MCD cutting tip edge (b) DLC on MCD cutting tip edge (c) 5mm of cutting tip edge (d) raised cluster

It can be seen that the DLC coating, in areas in which the MCD layer has started to diffuse into the substrate, has created a surface with large fissures between the nodular clusters. This is likely due to the fact that in the diffusion zone, gaps begin to form between the MCD crystals. As the DLC layer deposits, it preferentially grows out of the crystal peaks. Due to the increased spacing of the crystals in the diffusion zone, it means that the clusters grow larger before coalescing. This then leads to larger gaps and fissures in the surface. Raised MCD clusters also appeared to be exacerbated by the DLC coating which had the potential to increase roughness when such areas were present (Fig 6.3 d).

Raman spectroscopy showed that the bonding chemistry was also not largely affected by the underlying substrate, as the Id/Ig ratio remained similar at 0.50 ± 0.03. AFM measurements showed the average roughness to be 182nm, significantly less than the 430nm of the MCD surface. The DLC layer has clearly reduced the general roughness as well as altered other aspects of the topography.

(a)

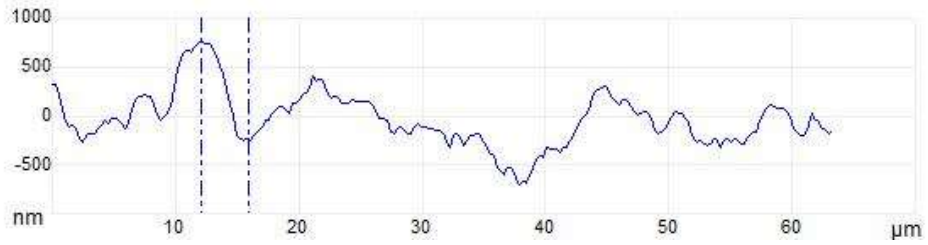

(b)

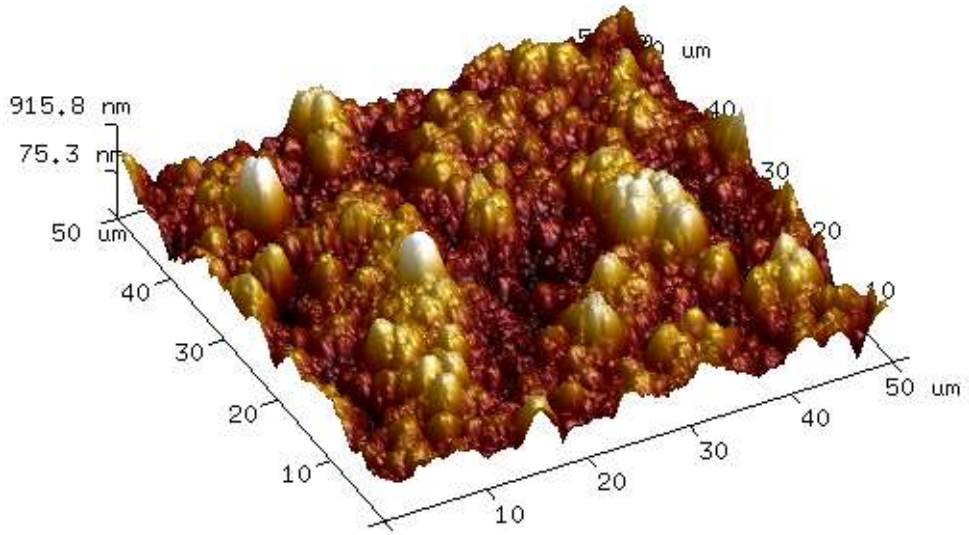

Figure 6.4. AFM images of DLC on MCD (a) 2D section (b) 3D image

The Z range was measured as 1720nm with peak to valley distances of around 1030nm. The skewness was increased compared with the values for the DLC on WC-Co and TiN. This indicates that the coating on MCD has more of a peak bias compared to the other substrates tested. On the other hand, kurtosis showed little discernible variation to other coatings. It is clear from the results that the DLC coating has significantly reduced the roughness of the MCD coating, however, due to the underlying substrate roughness, the final roughness is still much greater than the coating on inserts with smoother surfaces, such as the WC-Co or TiN.

6.3.2. 500V coating without silicon interlayer

The DLC coating was deposited on the commercial MCD insert, described in chapter 4, in order To test the necessity of the Si interlayer when depositing DLC onto a diamond surface. The earlier test, in which DLC was deposited on WC-Co without the interlayer, indicated that an interlayer was

required for the majority of substrates. Although, as the diamond layer comprised of carbon, it was consider that the DLC layer may adhere without the need for the silicon interlayer. SEM analysis of the deposited coating soon revealed that adhesion had suffered as a result of the omission of the Si interlayer (Fig 6.5).

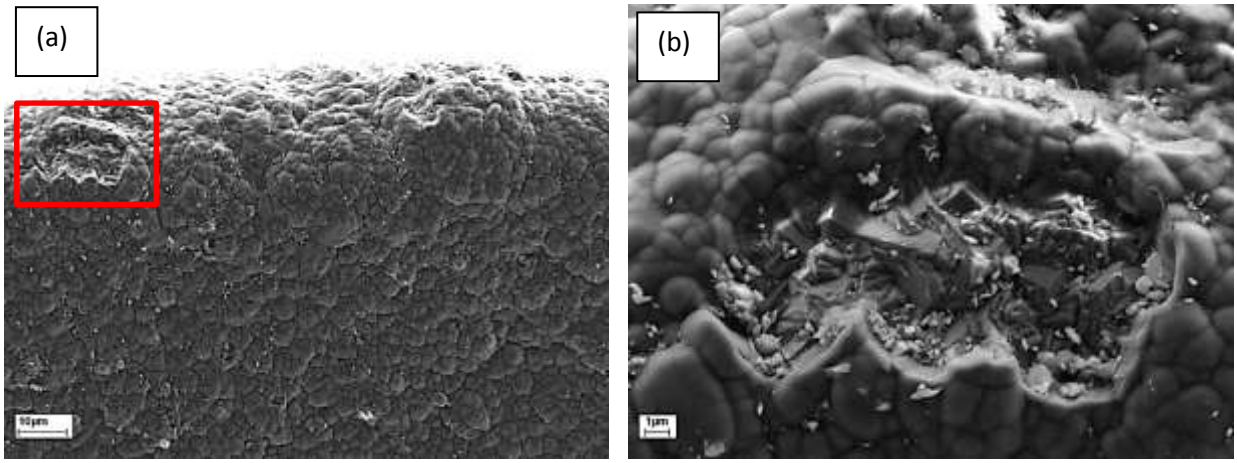

Figure 6.5. SEM micrograph of DLC on MCD with no interlayer at (a) X3k and (b) X15k magnification

Small patches of DLC had clearly delaminated from several areas of the sample, however, it was seen that the adhesion properties were still improved compared to the DLC on WC-Co test. It wasn't possible to see if this was due to the substrate chemistry or topography.

High resolution micrographs also highlighted that the DLC has delaminated cleanly at the coating interface (Fig 6.5 b). This could be indicative of a lattice mismatch between the diamond and DLC. It therefore became clear from the test that the Si interlayer would still be necessary to ensure good adhesion between the diamond and DLC layers.

6.3.3. Short cutting trial

A short cutting trial of was completed in order to ensure the DLC layer was adhering sufficiently to the MCD. The insert sample consisted of a 500V DLC coating on the commercial MCD tool. The trial parameters used were as described in chapter 3. Post-trial SEM analysis revealed that the addition of the DLC layer has led to a marked increase in aluminium adhesion (Fig 6.6 a), although the results

are not directly comparable due to the slight variation in insert geometry. It can also be seen that the DLC peaks have begun to be worn down in the areas of increased wear, however, it appears that the aluminium is adhering readily in the areas around the worn peaks (Fig 6.6 b).

The picture shows that the aluminium initially adheres to the nodule peaks before expanding and merging into larger masses of aluminium. Figure 6.6 (d) shows how the aluminium adheres to the rounded peaks of the DLC coating. These patches of aluminium expand with further machining and can then begin to combine to form large areas of adhered aluminium. Despite having a much smoother surface, the broader peaks of the DLC compared to the sharp peaks of the MCD appear, in this instance, to cause an increase in BUL (Fig 6.6 c). It can be seen that small islands of aluminium deposit on the DLC peaks before coalescing to form a BUL.

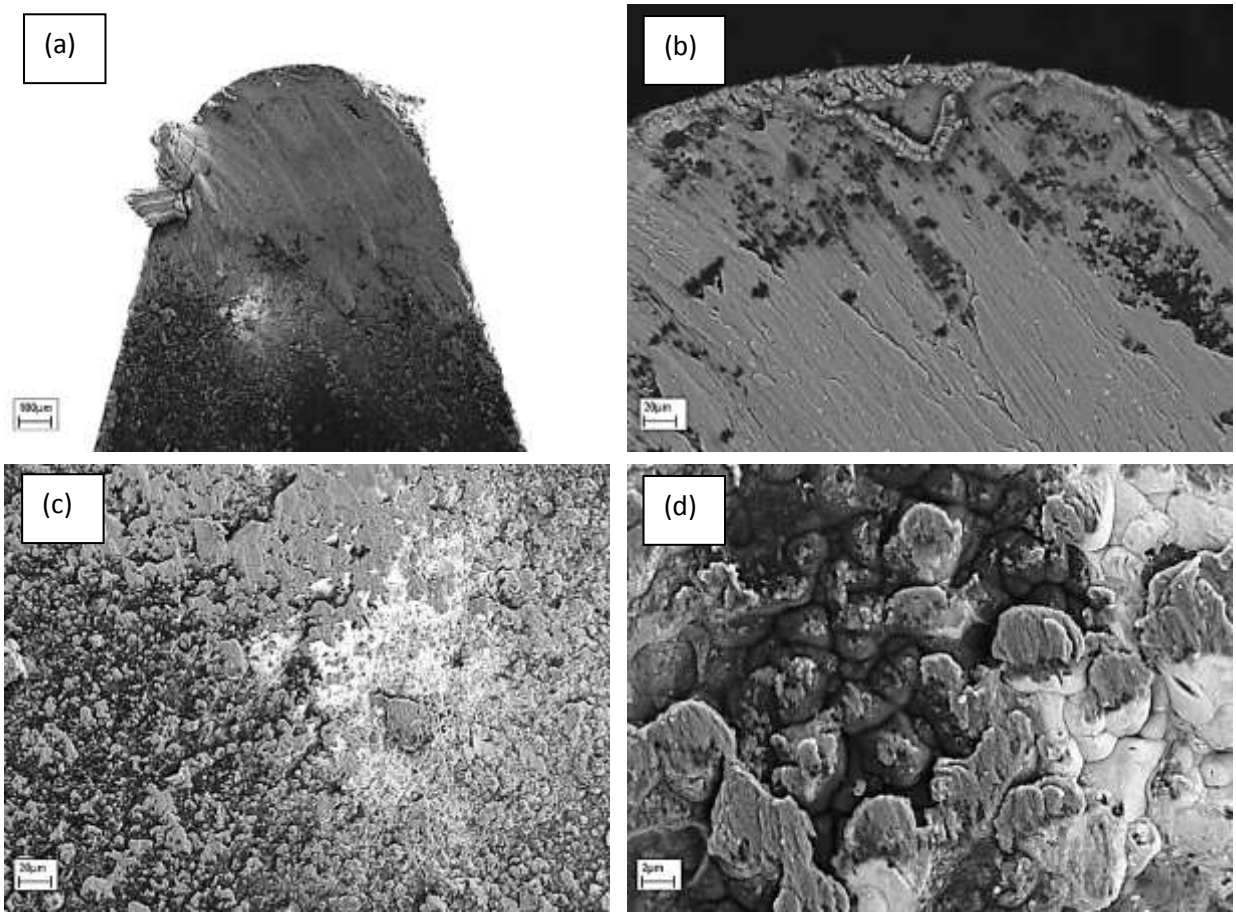

Figure 6.6. SEM micrographs of DLC coated MCD insert after short trial (a) cutting tip (b) cutting tip edge (c) aluminium adhesion (d) adhesion origin

6.4. Diamond like carbon on nano-crystalline diamond

Due to the large variation in surface structure of the MCD and NCD coatings, it was important to characterise the potential effect the different substrate surface morphologies may have on the DLC layer. The DLC coating was therefore deposited onto an NCD coated sample using the 500V coating parameters. The chemistry and morphology of the resulting surface was then analysed. SEM analysis showed the DLC coating to be uniform with no defects (Fig 6.7 b). The surface morphology was that of the nodular structure as seen in the previous coatings, however, there were subtle variations compared to the DLC on TiN and MCD. It can be seen that the NCD coating creating a relatively smooth cutting edge. This is due to the fact that the deposited layers effectively blunt the cutting edge slightly, by creating a more rounded tip. This has meant that the DLC layer appears to have deposited more uniformly around the cutting edge due to the reduced edge sharpness.

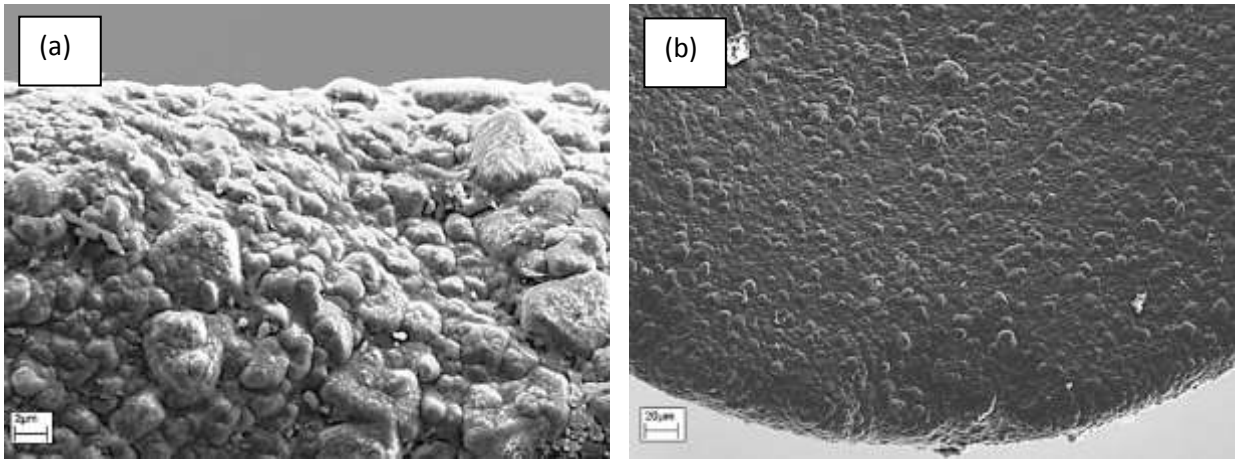

Figure 6.7. SEM micrographs of cutting tip (a) NCD coating (b) DLC on NCD coating

Raman spectroscopy produced a similar curve to the DLC on MCD, with an Id/Ig ratio of 0.49 ± 0.03. This result confirmed that there was no significant variation in the bonding chemistry as a result of the different substrate characteristics. AFM analysis of the combined coating shows that the average roughness has been reduced to 140nm, with a Z range of 1522nm (Fig 6.8). This is still relatively rough compared to the DLC on TiN coating, although it is smoother than the DLC on MCD. The peak to valley distance was almost halved compared to the DLC on MCD, at 584nm, whilst both the skewness and kurtosis remained similar to that of the DLC on MCD coating.

The NCD + DLC combination has therefore allowed for the surface roughness to be reduced to levels slightly greater than that of the uncoated WC-Co surface, yet significantly less than the DLC on MCD coating. The combination of coatings has also meant that the DLC formation on the cutting edge appears to more homogeneous with the coating across the rake face, possibly due to a reduced edge effect.

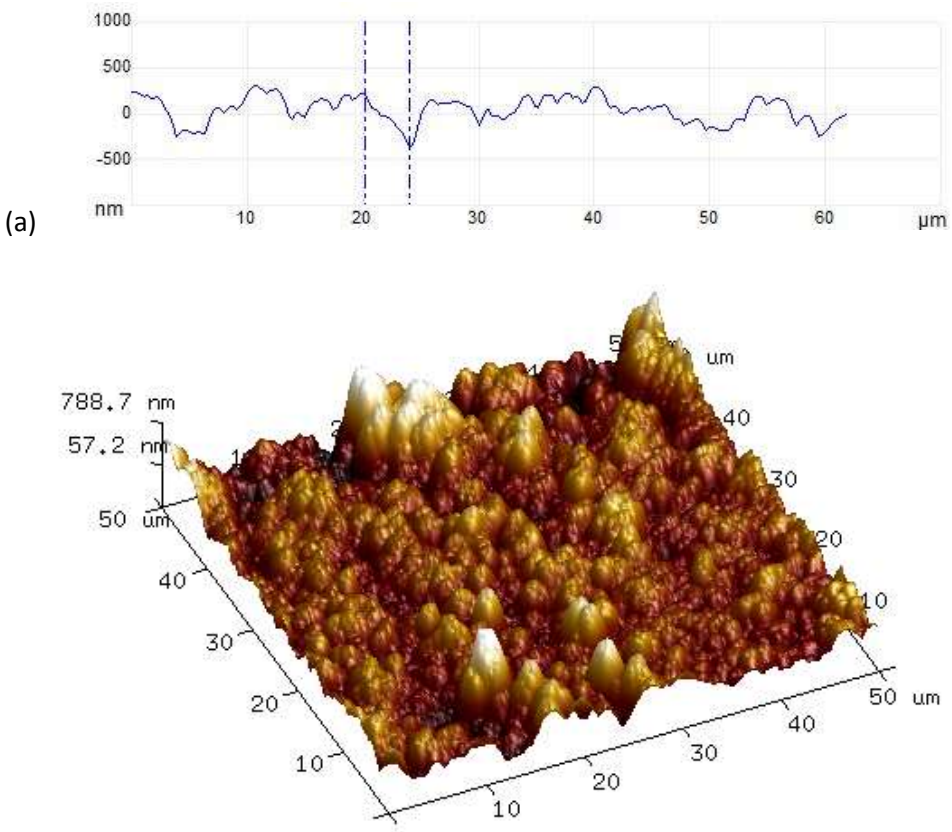

Figure 6.8. AFM images of DLC on NCD coating (a) 2D section (b) 3D image

6.5. Conclusion

DLC coatings have been applied to a commercially available TiN and MCD coated inserts, as well as to the nano and micro-crystalline diamond coatings developed at Bristol School of Chemistry. The coatings have then been characterised using SEM, AFM and Raman spectroscopy. Further coating performance assessments were completed through the use of short cutting trials. SEM analysis showed that the DLC coatings adhered well to all substrates, although the silicon interlayer was

shown to be necessary to prevent delamination. All substrates tested can be seen to allow for uniform, high quality coatings to be produced. The results of the AFM analysis showed variation between the topography of the combined coatings, whilst also highlighting the effects of substrate surface roughness. The DLC coating effectively reduced the average roughness on all substrates except for the uncoated WC-Co. The roughest substrate, the MCD coating, had the biggest reduction in roughness, whilst the smoothest coating, TiN, benefitted the least from the DLC coating.

In addition to confirming previous finding in regard to the relationship between substrate roughness and coating roughness (Zhong *et al.*, 2008; Ma *et al.*, 2007a; Salvadori *et al.*, 2006), the results highlighted that relatively thick, 2µm DLC coatings, will still be much rougher when deposited on a rough substrate. Subtle variations on surface morphology can be seen between the DLC coatings as a result of the different substrate characteristics. All coatings could be seen to have the typical nodule cluster formation, however, the size and distribution of the clusters depended heavily on the underlying substrate. The increase in roughness of the WC-Co sample is attributed to the significant variation in surface structure due to cobalt rich and tungsten rich areas. The different areas appeared to produce raised clusters due to the WC crystals whilst the cobalt areas remained much smoother. Raman spectroscopy revealed that the bonding chemistry was unaffected by the substrate material as the graphitic to diamond bonding concentrations remained similar. Cutting trials highlighted the fact that the reduced roughness created by the addition of a DLC layer to the diamond will not necessarily lead to a reduction in aluminium adhesion. It can in fact lead to a significant increase in adhesion due to the larger contact area between the cutting tip and evacuating chip. This finding was in contradiction to previous reports of combined coating performance which showed either, a reduction in aluminium adhesion in drilling applications (Hanyu *et al.*, 2005), or a decrease in long term performance directly attributed to the delamination of the DLC layer (Amaral *et al.*, 2012). The benefits of a combined diamond and DLC layer are therefore much more application sensitive than previously considered.

7. Full cutting trials

7.1 Introduction

In this chapter the results of the full machining trials are presented. The previous chapters have discussed the development of the individual and combined coatings in preparation for an extended comparative evaluation of cutting performance. Short cutting trials were used earlier as a development tool to assess the initial coating performance in terms of the wear rate, wear pattern and adhesion to the substrate. These short trials were used to aid in the development of the coatings and ensure a sufficient quality of coating was achieved. The final cutting trials discussed in this chapter were used to provide a comparison of performance of the developed coatings in order to assess the efficacy of combined carbon coatings for dry machining aluminium alloys.

The aim of the extended cutting trial was to create repeatable cutting conditions which represent the expected life cycle for industrial scale manufacturing. From the results of the trial it should therefore be possible to determine if this particular type of combination coating would be suitable for dry turning applications. The test parameters are described, followed by the results and final discussion of the findings.

Figure 7.1. Instrumented lathe with Dynomometer

7.2. Test parameters

The specific parameters of the final cutting trial are as follows:

The lathe and work-piece material are the same as that used for the shorter developmental trials, they are described in further detail in the experimental section, chapter 3.

The aluminium billet (Al 6082) was initially cut to a length of 470mm before being placed on the lathe and machined to a diameter of 100mm. The bottom 120mm was machined down to a diameter of 40mm as shown in figure 7.2a.

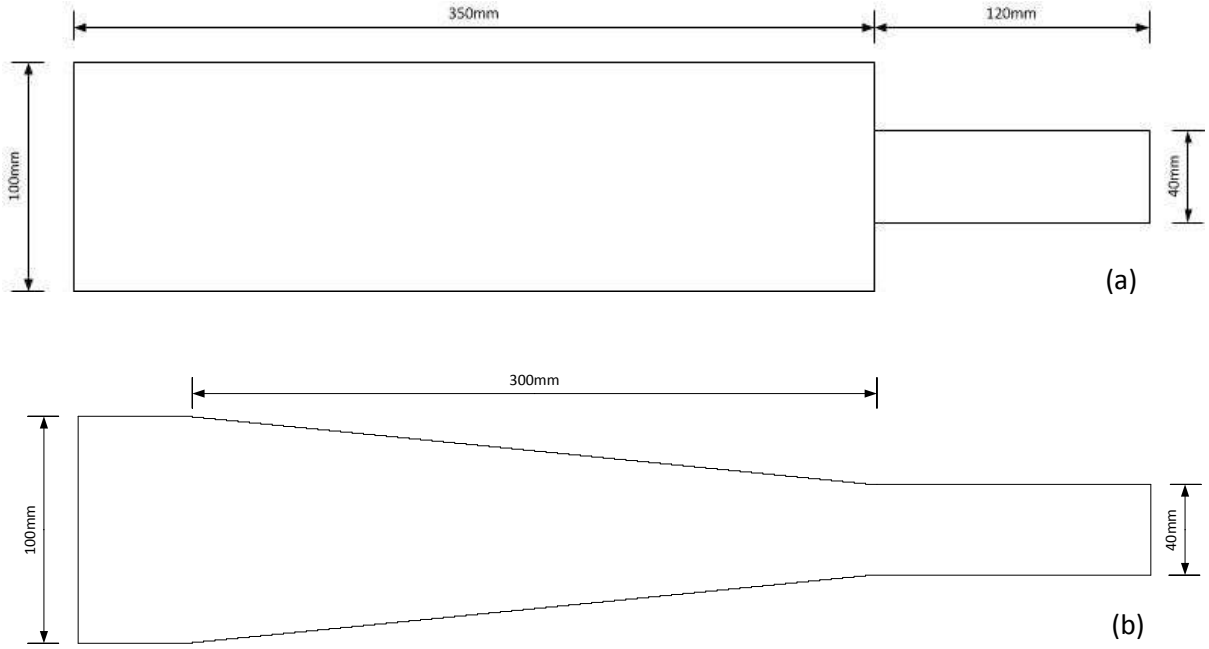

Figure 7.2. Diagram of work-piece (a) before trial (b) after trial

The trial involved using the sample inserts to cut along the length of the work-piece. The first cut was 300mm and each successive cut was 5mm shorter. This created a stepped work-piece so that the roughness of the WP finish, throughout the entire trial, could be measured at the end of the test (Fig 7.2 b). The cutting parameters such as cut depth, cutting speed and feed rate were kept the same as in the short trials described in the experimental chapter.

From these parameters it is then possible to calculate important factors such as: cutting distance, cutting time and volume of material removed.

The **length of cut** was calculated by adding the lengths of each consecutive cut, i.e.

Distance of cut 1 = Circumference x number of revolutions

Initial diameter = 0.1m

Initial WP length = 0.3m

If feed rate is 0.15mm per revolution

300mm / 0.15mm = 2000 revolutions

$2\pi r \times 2000 = \pi 0.1 \times 2000 = 628.3m$

For cut 2

Diameter = 0.099m

Length = 0.295m

295mm / 0.15mm = 1966.7 revolutions

$2\pi r \times 1966.7 = \pi 0.099 = 611.7m$

Adding all 60 cuts gives a total of **15.4km**

The **volume of material cut** was calculated by:

Volume of cut 1 in $cm^3 = (30 \times \pi 5^2) - (30 \times 4.95^2) = 46.86cm^3$

Volume of cut 2 in $cm^3 = (29.5 \times 4.95^2) - (29.5 \times 4.9^2) = 45.62cm^3$

The results were extrapolated to get a total volume of **$1147cm^3$**

Cutting Time for each cut was calculated by dividing cutting distance by cutting speed

Cut 1 = 628 / 330 = 1.9min

Extrapolating this for all 60 cuts gives a total time of **46.6mins**

The cutting speed was fixed, as appose to the rpm, as it ensured better continuity throughout the trial. Otherwise as the diameter reduced the speed would have otherwise reduced. The rpm of the workpiece therefore increased incrementally throughout the trial in order to compensate.

The final cutting trials were conducted to test the effects of the insert coatings on cutting force, feed force, work-piece roughness, coating degradation, tool wear and Al adhesion. The machining forces were measured using a Kistler dynamometer during the trial. All other measurements were conducted post-trial.

Post-trial analysis

Work piece roughness (R_a) was measured using the Zygo white light interferometer as described in the experimental section chapter 3. The picture (Fig 7.3) shows an example of how the workpiece appeared at the end of the trial.

Figure 7.3. Work piece after testing

The WP roughness was measured 5 times for each cutting step to ensure a reliable average could be calculated. The roughness measurements focused on a filtered result which had been designed to remove the effect of cutting tip geometry. This was completed so that the emphasis would be on the effect the coating surface morphology has on the workpiece quality.

Cutting insert analysis

Prior to the trial, all samples tested were analysed using SEM SE2 imaging to ensure the quality of the insert and coating. As well as using SE2 imaging to examine the coatings after the trial, BSE and EDAX was used to quantify the performance of the sample coating in terms of amount of aluminium adhesion at the cutting tip. The aluminium was then removed by placing the insert in a 5% sodium hydroxide solution, designed to remove the Al without causing further damage to the coating.

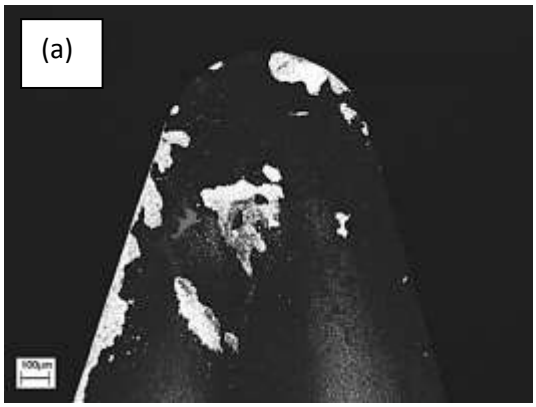

(b)

Element	Weight%
C	63.66
O	9.94
Mg	0.74
Al	0.18
Si	4.32
W	21.15
Totals	**100.00**

Figure 7.4. (a) Back-scattered image X200 (b) EDAX measurement of material at cutting tip

The cutting tip was then re-examined and the elemental composition was measured. Figure 7.4 (b) shows an example of the results of EDAX measurements. The coatings would show up as just carbon (C), as hydrogen is too light to be measured, whilst the insert substrate mostly showed a strong tungsten (W) signal with small amounts of carbon and cobalt. The aluminium, being an alloy, also contained significant amounts of silicon and also trace amounts of other metals. All EDAX analysis was conducted using X200 magnification as this included the top 1.5mm of the cutting tip. Each sample was positioned at the same distance from the detector to ensure high count rates, although slight variation in the count rates would not have affected the compositional accuracy, as only the signal intensity would be altered and not the percentage distribution. The cutting tips were also positioned in such a way that the sample platform was not being read and hence did not affect the results. Using this method it was possible to effectively quantify the performance of the tool coatings in regards to their most important properties, friction, wear and adhesion to substrate.

7.3. Results

7.3.1. Complete performance comparison

The cutting trials have shown how the coatings performed throughout the duration of an extended dry turning process. The various coatings each showed different levels of performance for each of the measured criteria. As well as considering how the coatings directly compared to each other, in terms of cutting efficiency and workpiece quality, it became important to consider the variations between the nominally similar coatings. This is also due to the fact that reliability remained an issue and coating failure / delamination will potentially alter the results significantly.

Initial analysis shows that the MCD coated inserts had a greatly reduced amount of Al adhesion compared to all other coatings, as well as generating the least amount of forces during the machining process. The NCD coatings show a similar pattern in terms of Al adhesion and cutting forces, all be it slightly increased compared to the MCD samples. The WC and TiN inserts on the other hand had a much greater amount of Al adhesion along with increased cutting forces. The DLC coatings showed similar performance to the baseline WC and TiN inserts in terms of machining efficiency. The work-piece finish depended more heavily on the reliability of the coatings at the cutting edge, although the diamond coatings generally led to increased roughness of the aluminium workpiece (Table 7.1).

Sample	Cutting Force (N)	Al Adhesion %	Film Delamination %	WP Roughness (µm)
WC 1	80 – 100	33	N/A	.25
WC + DLC	78 – 96	40	51	.24
TiN 1	85 – 104	35	9	.22
TiN +DLC	82 – 90	42	35	.23
MCD 1 (M3)	69 – 68	12	5	.69
MCD 2 (PM19)	75 - 69	15	16	.24
MCD 3 (PM14)	72 – 73	21	21	.43
MCD + DLC	83 – 91	38	46	.28
NCD 1 (R6)	75 – 74	14	11	.27
NCD 2 (R3)	77 – 70	18	14	.41
NCD 3 (R4)	76 – 83	27	26	.42
NCD + DLC	81 - 87	38	29	.46

Table 7.1. Performance comparison of the sample coatings

The cutting force was measured in real time which made it possible to track the variation throughout the trial and determine if and when significant changes occurred.

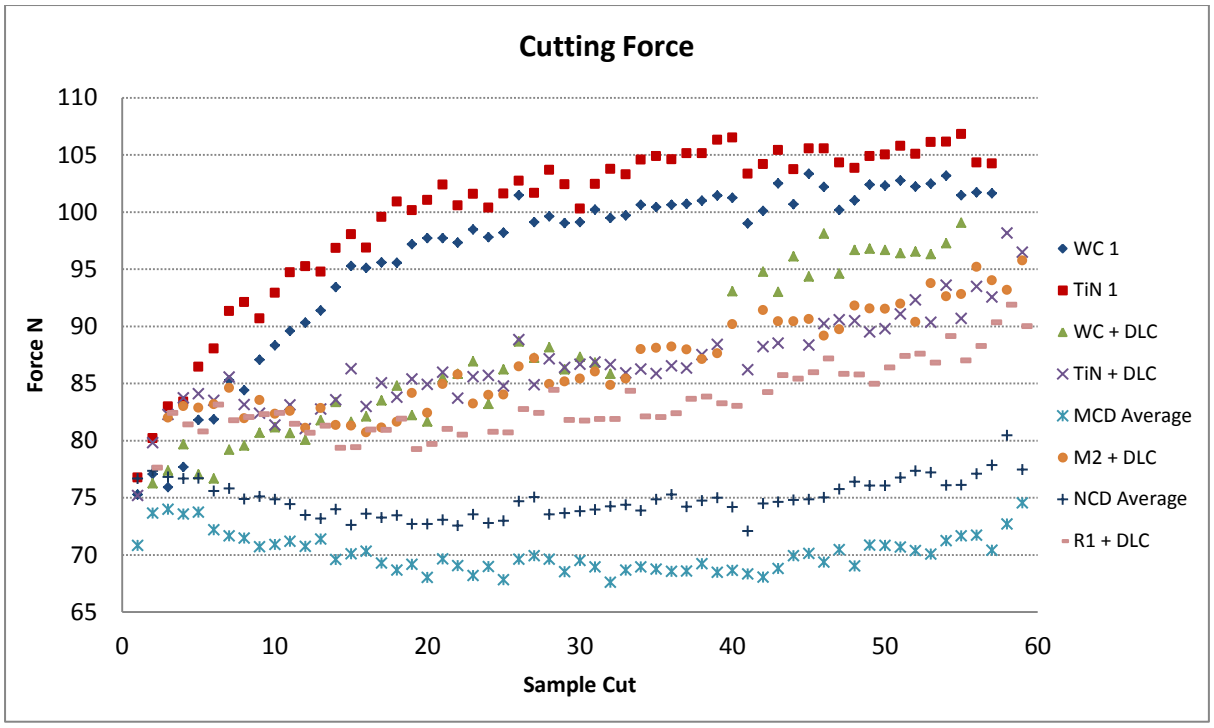

Figure 7.5. Graph of cutting forces of all sample coatings

Analysis of the cutting forces highlighted key variations in the performance of the tools throughout their expected cutting life. Clear pattern could be seen between the performance of the various coatings and coating combinations (Fig 7.5). This is despite them all beginning the trial with very similar cutting forces, between 75N and 85N. The baseline WC-Co and TiN tools show a rapid rise in the cutting force for the first 20 cuts, from 75N to 100N before levelling out and eventually plateauing after 40 cuts at around 105N. The DLC coated inserts all followed a similar path to one another by having a more gradual rise in cutting force throughout the duration of the trial. This trend is evident on all DLC coated inserts despite them having very different substrates morphology and chemistry due to the interlayer coatings.

The diamond coated inserts gave the best performance in terms of machining efficiency as they showed no overall rise in cutting force throughout the trial. The cutting forces even reduce in the

first 20 cuts and only begin to rise again after 40 cuts. By 60 cuts the forces begin to rise beyond the initial starting force. The feed force generally showed a similar pattern to the cutting force although some slight deviations are mentioned in the discussion.

The actual surface roughness of the WP after the trial tended to range from 1.6µm to 1.9µm which corresponds to the predicted roughness of 1.8µm as described in the experimental section. The following graph shows the filtered WP finish, removing the effect of tool nose geometry (Fig 7.6).

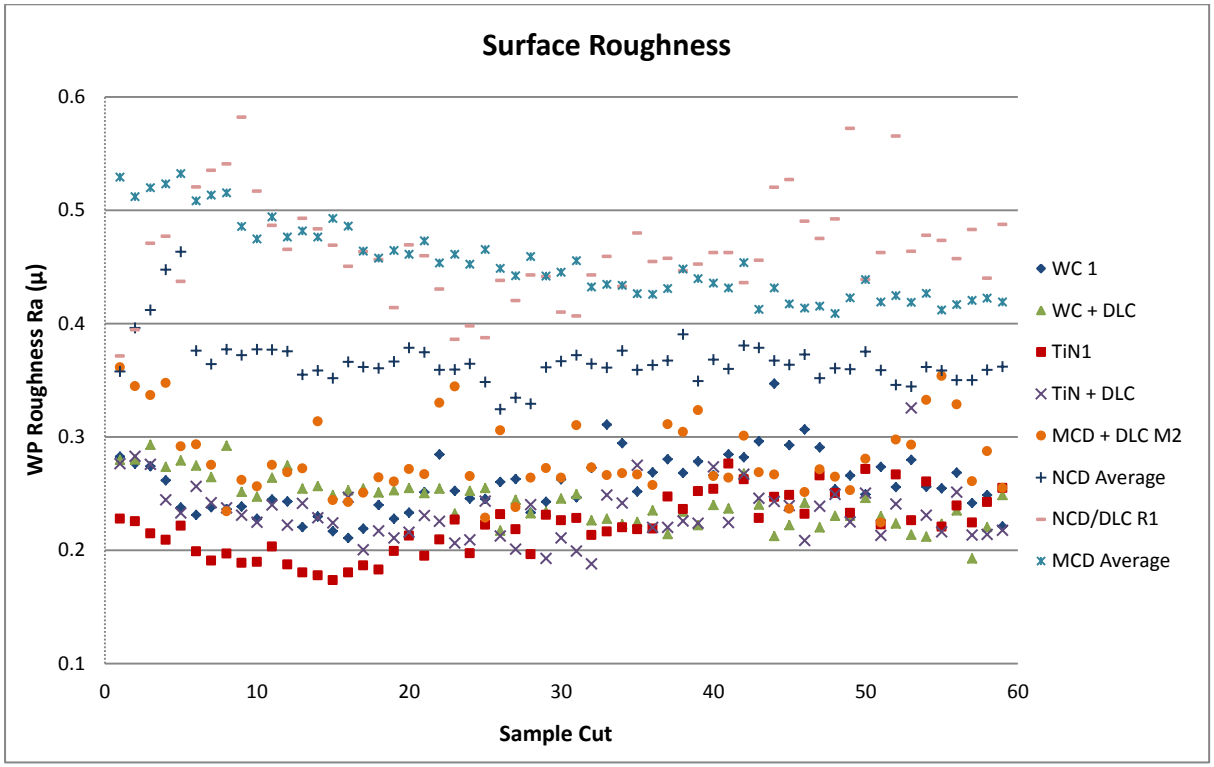

Figure 7.6. Graph showing average workpiece roughness for all coatings

The workpiece roughness highlights a clear differentiation between the qualities of the surface finishes at various points during the cutting trial. The majority of the inserts produced a filtered surface roughness between 0.2 and 0.3 microns. As can be seen from the graph showing the workpiece roughness produced by each type of coating (Fig 7.6), the diamond coated inserts have produced a significantly higher roughness than all other coatings, with the MCD producing the roughest finish (between 0.4 and 0.5 microns), followed by the NCD at 0.35 microns.

Analysis of the cutting trials highlighted a number of factors relating to the performance of the coatings as both single and combined layers. Due to the variation in cutting performance between nominally similar coatings, it became apparent that as well as comparing the different coating types, it will also be necessary to look at how some of the insert samples performed individually. This is in part due to the limited number of samples as well as the inconsistency in performance. The results look at how the different factors have affected each other, for instance, how coating delamination corresponds to the aluminium BUE, as well as how this relates to the machining forces and work-piece finish.

Detailed SEM micrograph analysis was used in order to not only determine how the coatings had performed during the trial, but discover the potential contributing factors. SEM analysis was only performed at the start and end of the trial, so it is difficult to determine when failures may have occurred unless it is indicated in the force or WP finish measurements. By correlating the post-trial analysis of the tool condition to the cutting force and work piece finish measurements, it was possible to understand not only how the tool degraded but also at what point in the trial failures may have occurred.

The sample have therefore been categorised into three sections. These include baseline, MCD and NCD tools, with the DLC coatings being compared within these categories. This has been done so that an emphasis can be placed on considering how the addition of the DLC layer has influenced the performance of the various samples.

7.3.2 Baseline and single layer DLC samples

Two geometrically similar commercially available inserts were used to form a baseline for the cutting trials and so help determine the change in performance due to the applied coatings. The commercially available WC-Co and the TiN coated insert formed the basis for the trial. This section

looks at the individual baseline tool performance and compares it to the performance when a DLC coating is applied to them.

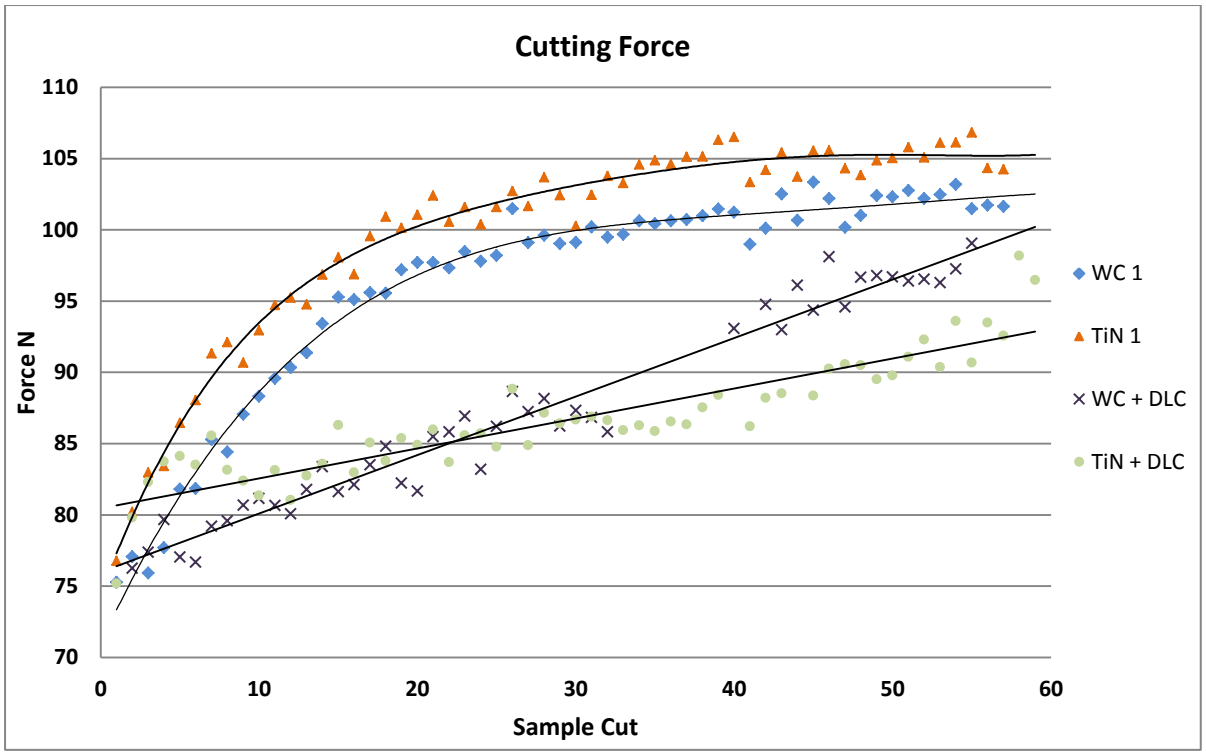

Figure 7.7. Graph of cutting force for baseline and DLC coated inserts

A direct comparison between the uncoated and TiN coated inserts reveals that they have shown very similar performance in all measured criteria. The similar pattern in the progression of the cutting forces indicated that the TiN coating not only offered no advantage in machining efficiency, it actually has an increase in forces compared to the uncoated insert (Fig 7.7). The TiN coating offered no improvement to the uncoated WC-Co insert in terms of cutting force and BUE. The baseline inserts both suffered similar amounts of Al adhesion at roughly 40% of the cutting tip.

The application of the DLC coating has clearly had a large effect on the cutting forces throughout the duration of the trial. It is clear from the cutting force measurements that, despite all samples having a similar force at the start of the trial, the DLC coating has significantly reduced the rate at which the forces increase. The DLC also led to a much more consistent increase and by the end of the test clearly remained below the level of the baseline tools.

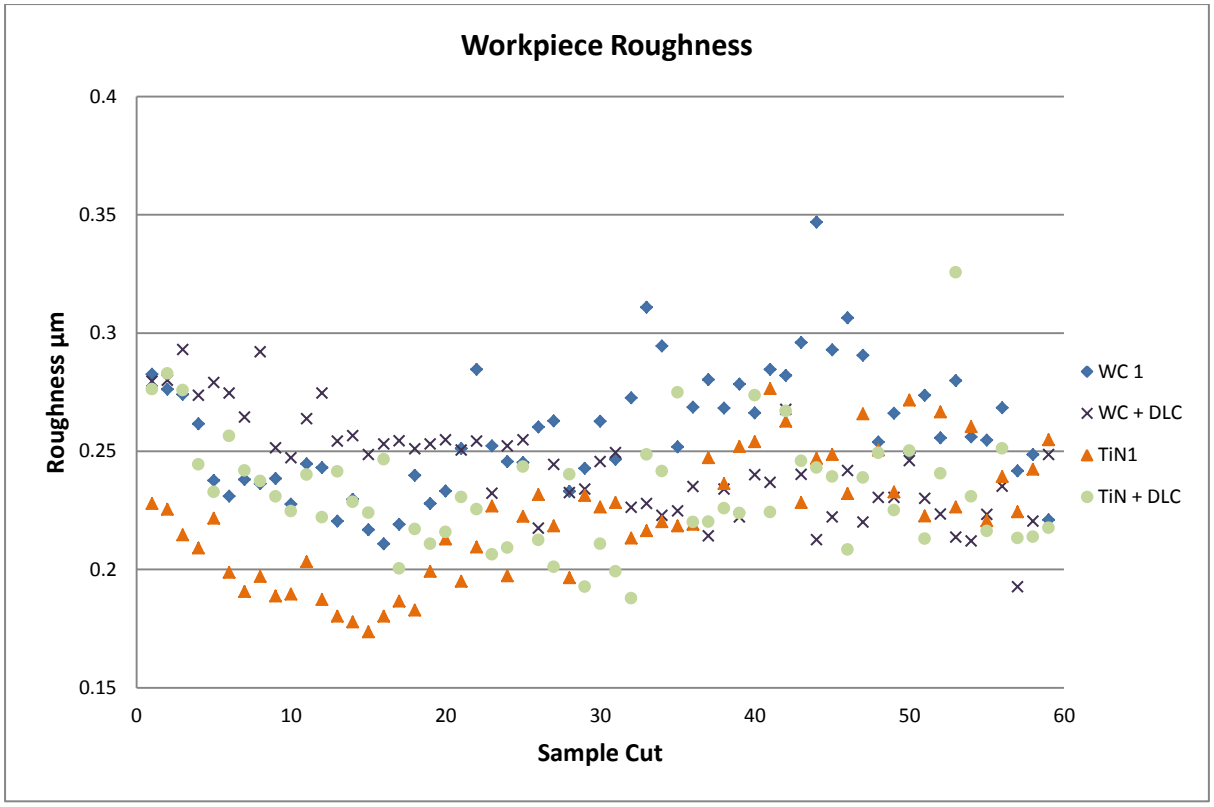

Figure 7.8. Graph of workpiece roughness for baseline and DLC coated samples

The overall work-piece finish remained relatively similar for all the baseline samples, even when coated with DLC (Fig 7.8). It can be seen from the graph, however, that the DLC also appears to have slightly improved the stability of the WP finish compared to the uncoated samples. All samples showed an initial decrease in roughness over the first 15 cuts, however, the DLC coated samples then maintained a relatively steady performance through the remainder of the trial. The baseline samples on the other hand showed a steady increase after cut 15, although due to the fluctuations in performance, it did not significantly affect the total roughness measurements in table 7.1.

The baseline WC-Co and TiN inserts showed similar BUE profiles as well as having a similar total amount of Al adhesion. When analysing how the BUE has deposited it is important to consider the cutting parameters to understand how the wear and Al adhesion has developed at the cutting tip. With a cutting depth of 0.5mm and a feed rate of 0.15mm/rev it can be seen that only a small area of the cutting tip would be in constant contact with the work-piece during cutting. The red area highlighted indicates the actual cutting area at the tool tip (Fig 7.9). The small double ended red

arrow shows how small the end cutting edge is compared to the entire tip. As mentioned in the literature, this is the only part of the cutting edge which has direct contact with the final WP. The rest of the cutting edge only removes material which will be subsequently removed in the next cut revolution and hence will not directly affect the finish quality. The outer cut edge refers to the point furthest down the cutting edge which actively cuts the WP. The direction of swarf flow is shown as the large red arrow and is roughly predicted from the Al adhesion pattern.

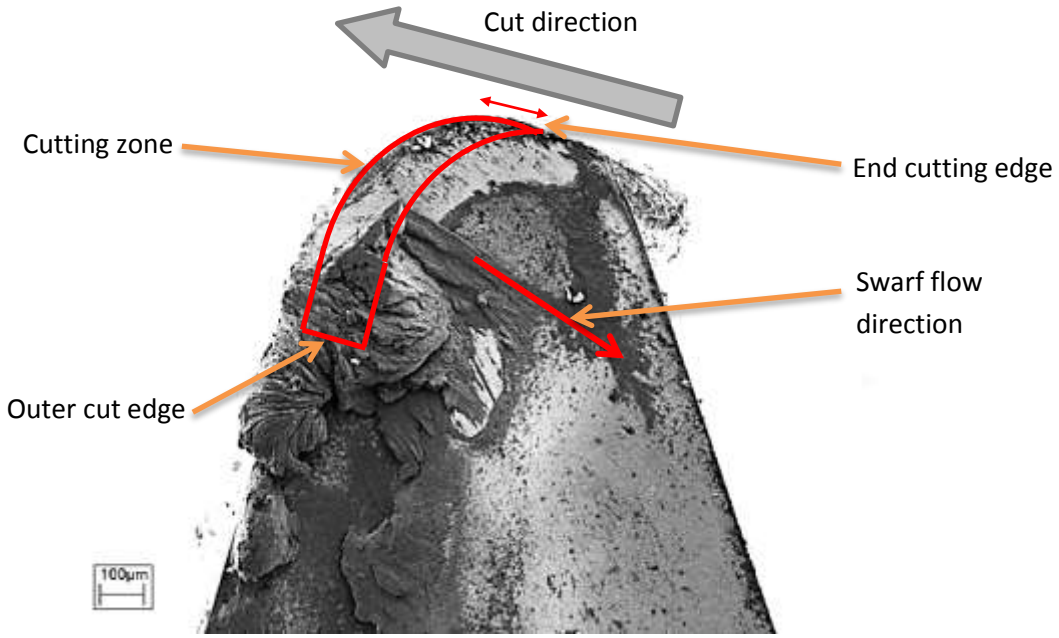

Figure 7.9. SEM images of baseline WC-Co insert after trial

The SEM micrographs of the baseline WC-Co and TiN samples show that the main area of the Al adhesion is centred on the outer edge of the cutting zone (Fig 7.10). This BUE extends along the flank in both directions in a segmented, or layered formation, as well as being spread across the cutting tip in the direction of the swarf flow. The micrographs also show that the aluminium has adhered to the major and minor flanks on both of the baseline tools. The adhesion on the major flank will have the effect of interfering with the swarf flow which may be a contributing factor to the increase in cutting forces throughout the trial. The smaller patch of adhesion on the minor flank is positioned just behind the end cutting edge. This means that there is a possibility that when segments of this BUE breakaway, they may be deposited onto the workpiece. This will potentially

have a negative impact on the final WP finish. It is also evident that the aluminium has adhered to the rake face along the first 0.5mm of the minor flank edge (Fig 7.10 a and b).

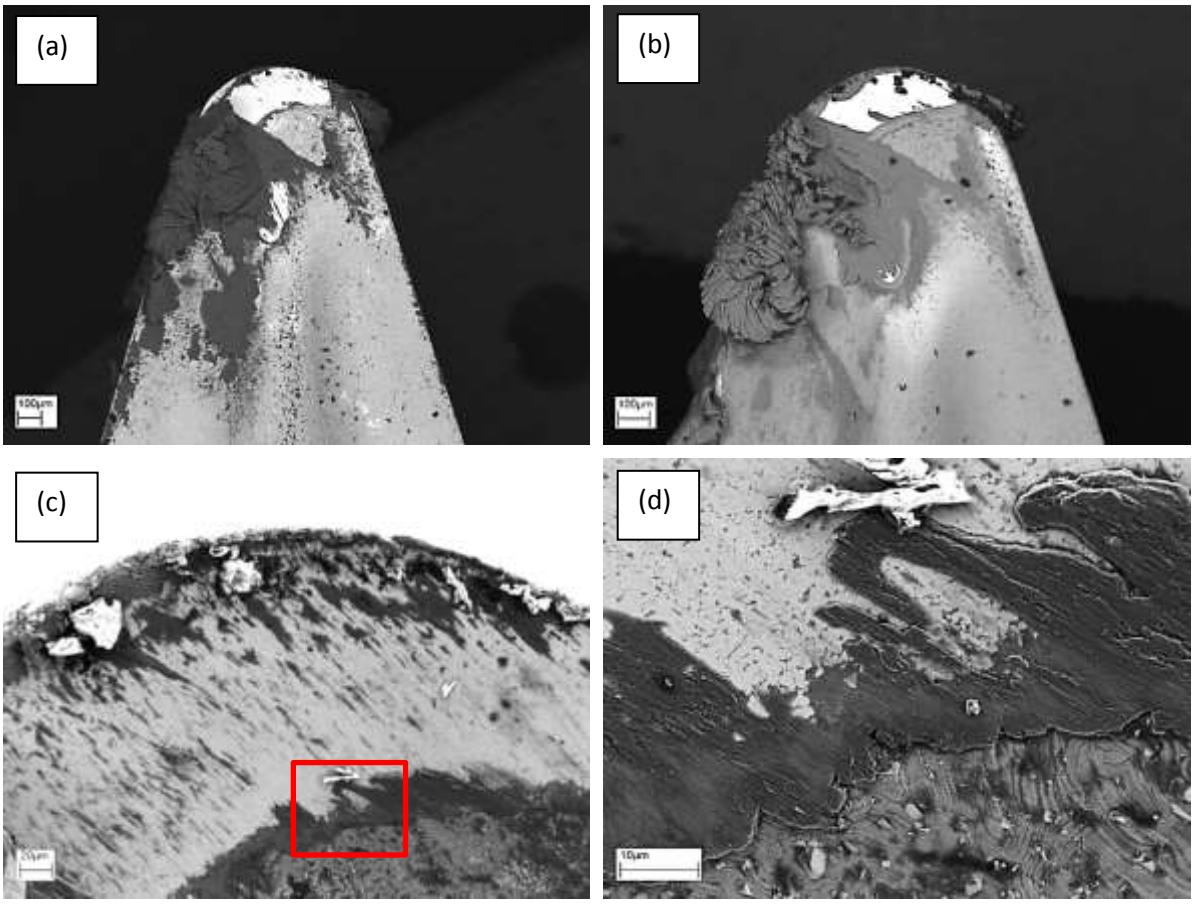

Figure 7.10. SEM micrograph of cutting tips after trial (a) WC-Co (b) TiN coating, and (a) crater wear of WC-Co insert (b) High magnification image of wear transition line

Similar to the adhesion pattern seen in the earlier short cutting trials, the aluminium has adhered at the edges of the crater wear track, particularly the trailing edge (Fig 7.10 c and d). There is a clear transition line between the smoother wear patch and the rougher unworn cobalt surface. This has created a lip that can be seen to promote aluminium adhesion. Although there are small amounts of aluminium adhering to the crater wear patch, it is unable to develop into a significant BUE as the cutting process constantly removes the deposited material in this area.

SEM analysis of the TiN tool, after the aluminium was removed, highlights the evolution of the wear pattern that has occurred on both the crater and the chip-breaker. The micrographs show that the crater wear expands, predominantly towards the cutting edge (Fig 7.11). It shows that the wear area

first contacts the insert edge near the point of the end cutting edge. As the crater and flank wear coincide it will compound the degradation of the cutting edge, which, in this area, will have a negative impact on the WP finish. The micrographs also reveal the extent that the flank wear has on the insert geometry. The active cutting edge has clearly been worn away by a few micrometres, particularly at the point near the outer cutting edge, as can be seen by the groove in the cutting edge profile (Fig 7.11 a).

The TiN insert has also developed a small failure in the form of a fracture near the mid-section of the active cutting edge. This would have likely contributed to an increase in cutting forces, although the aluminium BUE would have reduced the effect it may have.

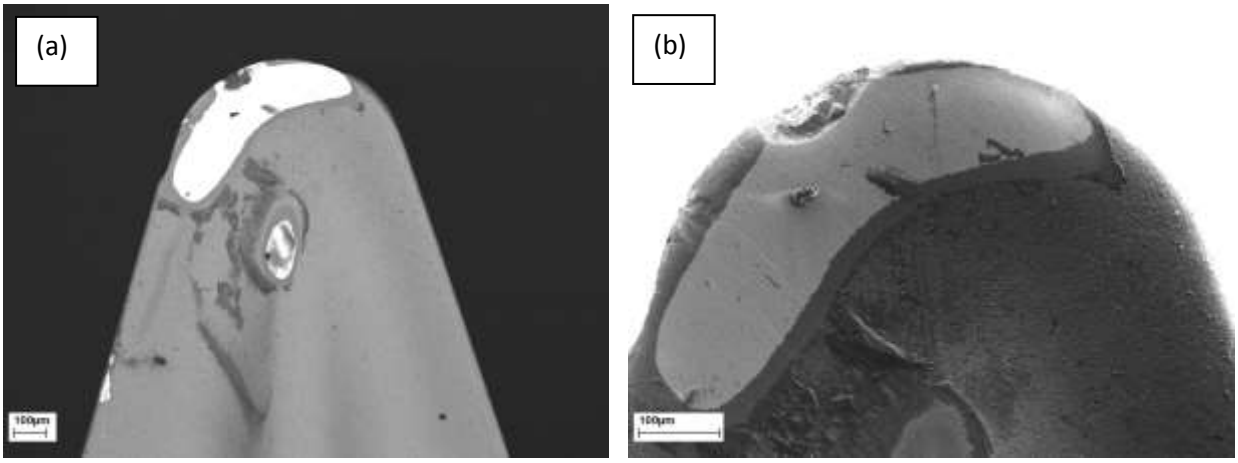

Figure 7.11. SEM micrograph of TiN insert with Al removed (a) X150, (b) X500 magnification

There is a clear variation in the formation of the BUE compared to the uncoated WC-Co tool, the DLC coating has led to an increase in BUE in some areas of the cutting tip (Fig 7.12 a). The main body of aluminium has built up in the same point at the outer edge of the cut, however, the aluminium has also adhered along the entire cutting tip edge. It can be seen though, that the BUE has not changed the profile of the cutting tip and hence would not have affected the workpiece finish (Fig 7.12 b).

Backscattered SEM images reveal the extent of the additional delamination which has occurred with the DLC coating (Fig 7.12 c). The delamination appears to be an extension of the wear patches, albeit more complex and less predictable in nature. From the micrographs of the cutting tip after Al removal, it is evident that the majority of the Al adhesion occurred on the areas in which the DLC has delaminated. The progressive delamination of DLC appears to have led to aluminium adhering to a greater extent in some areas. The DLC has also acted to reduce the progression of the crater wear patch as well as flank wear (Fig 7.12 c and d).

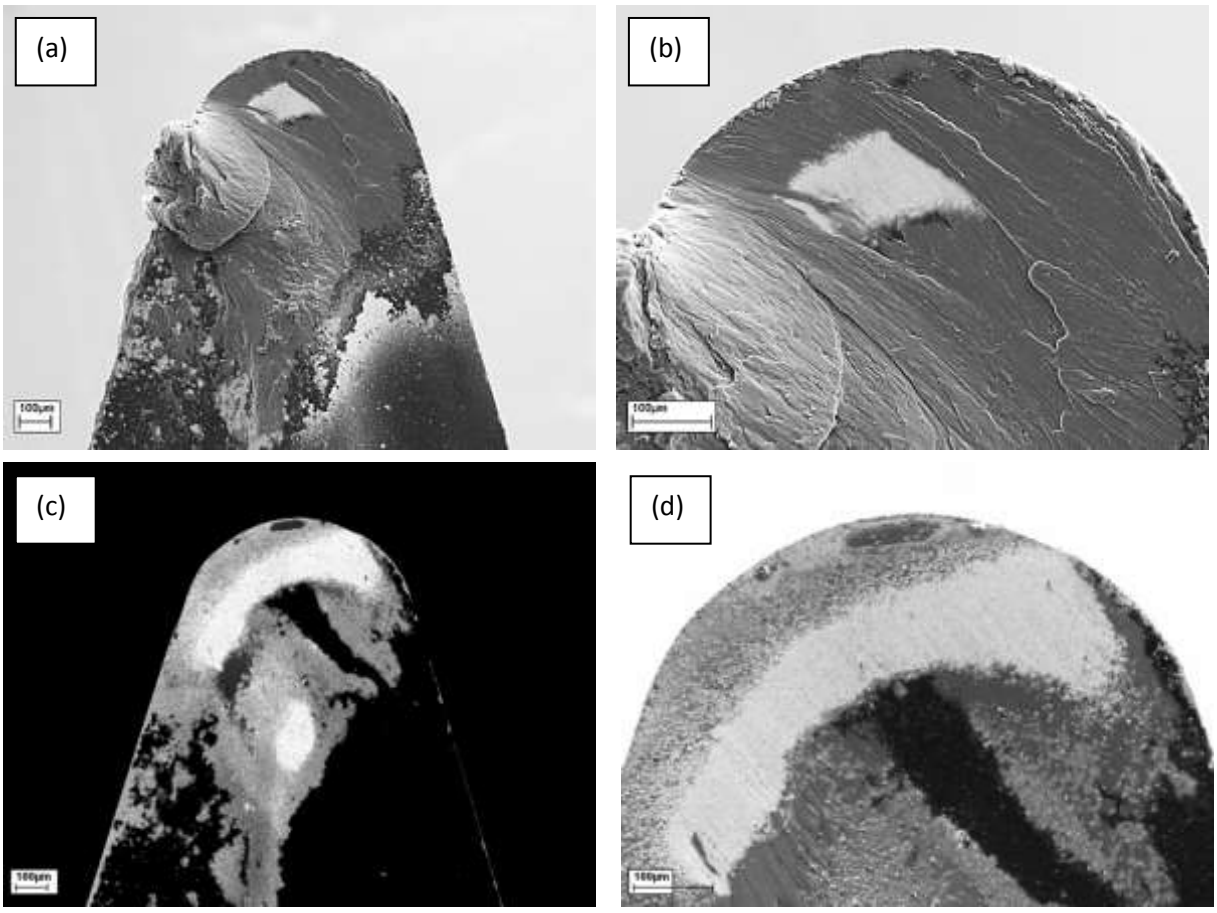

Figure 7.12. SEM micrographs of DLC coated WC-Co insert cutting tip after trial (a) X200 (b) X500, and after Al removal (c) X200 (d) X500

The aluminium has adhered over the wear patches suggesting that the wear occurs at an earlier stage in the cutting process. It is possible that adhesion of aluminium to the DLC has contributed to the excessive delamination. This may be due to the potential for the aluminium to bond to the DLC surface with sufficient strength so that instead of simply being removed with subsequent machining,

it acts to pull the DLC away from the surface. This is also clearly a result of extended machining due to the fact that this delamination was not occurring during short cutting trials.

The failure of the DLC coating appears to be predominantly due to delamination, as opposed to the abrasive wear mechanisms. This indicates that the adhesion of the coating to the WC-Co substrate, particularly the cobalt rich surface layer, has not been sufficient. SEM analysis highlighted the variation between the areas of wear and areas of delamination, as the wear patches are show up in white due to the tungsten. The areas of delamination show up light grey in comparison. The delamination pattern does, however, correspond to the geometry of the tool tip and the areas which are likely to endure increased load have suffered delamination. Although it is clear that the load is insufficient to cause any significant wear in the substrate material.

The patchy areas at the major flank side of the rake face are further proof of the inconsistent bonding between the DLC coating and the WC-Co substrate. It shows that some areas have bonded much better than others, either chemically or mechanically. This could be due to the inhomogeneity in the surface layer of the cutting insert which will potentially affect both the chemical and mechanical bonding of the DLC.

The performance of the DLC coating on the TiN sample produced some notably different results compared to the DLC on the WC-Co. The aluminium adhesion pattern has some key differences compared to the other baseline samples. Most notable is the fact that the main body of adhesion is not centred on the outer cutting edge, but instead is predominantly at the chip-breaker. It is also clear that, although the aluminium has adhered to the cutting edge on the major flank, it has not developed into an overhanging BUE (Fig 7.13 a).

The adhesive interface between the DLC coating and the TiN was significantly better than that of the DLC on WC-Co, as shown by the reduced delamination (Fig 7.13 b). The combined coatings have also clearly slowed the progression of the crater wear. The elemental analysis of the cutting tip after the trial also showed no tungsten or cobalt signal, thus confirming that the crater wear and chip-breaker wear patch did not break through to the WC-Co substrate.

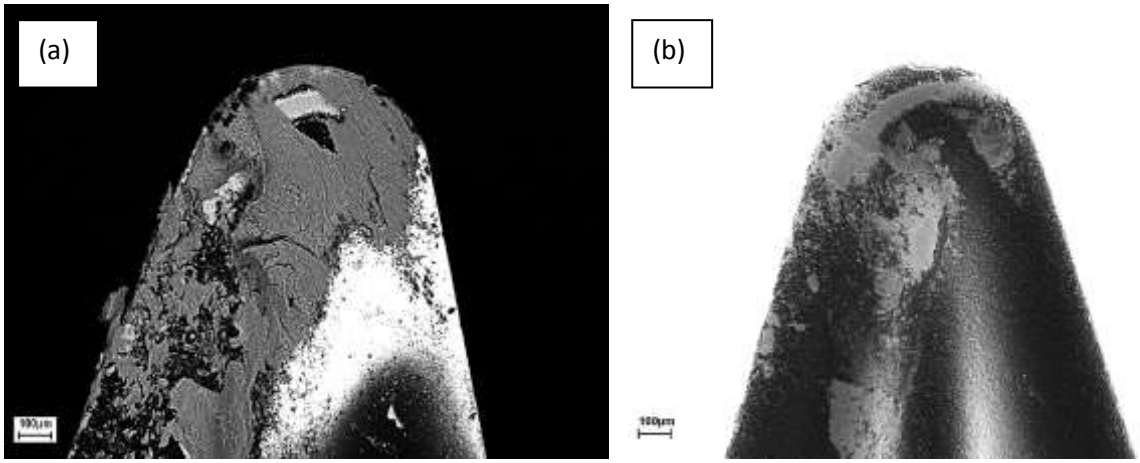

Figure 7.13. SEM micrographs of the DLC on TiN sample (a) after trial (b) after Al removal

There are a number of reasons why the DLC may have adhered to the TiN better than the uncoated WC-Co substrate. The surface homogeneity produced by the TiN coating will have reduced the reliability issues caused by the varying material and morphology of the WC-Co. It may also be the case that the cobalt was creating similar interface issues as with the diamond, albeit to a lesser extent. Due to the fact that the silicon interlayer contains a certain concentration of carbon, there is also the potential for graphitisation at the interface, although this could not be confirmed.

7.3.3. Micro-crystalline diamond samples

Three MCD samples were selected from two batches which each produced slightly varying surface morphologies at the cutting tips. SEM analysis showed that sample M3 exhibited a clear micro-crystalline structure with many of the crystal sizes ranging between 5µm and 10µm. Samples PM14 and PM19, despite using the same deposition parameters produced morphologies with generally smaller crystal sizes of less than 5µm. They also appeared to contain an increased amount of graphitic structures as confirmed by Raman spectroscopy.

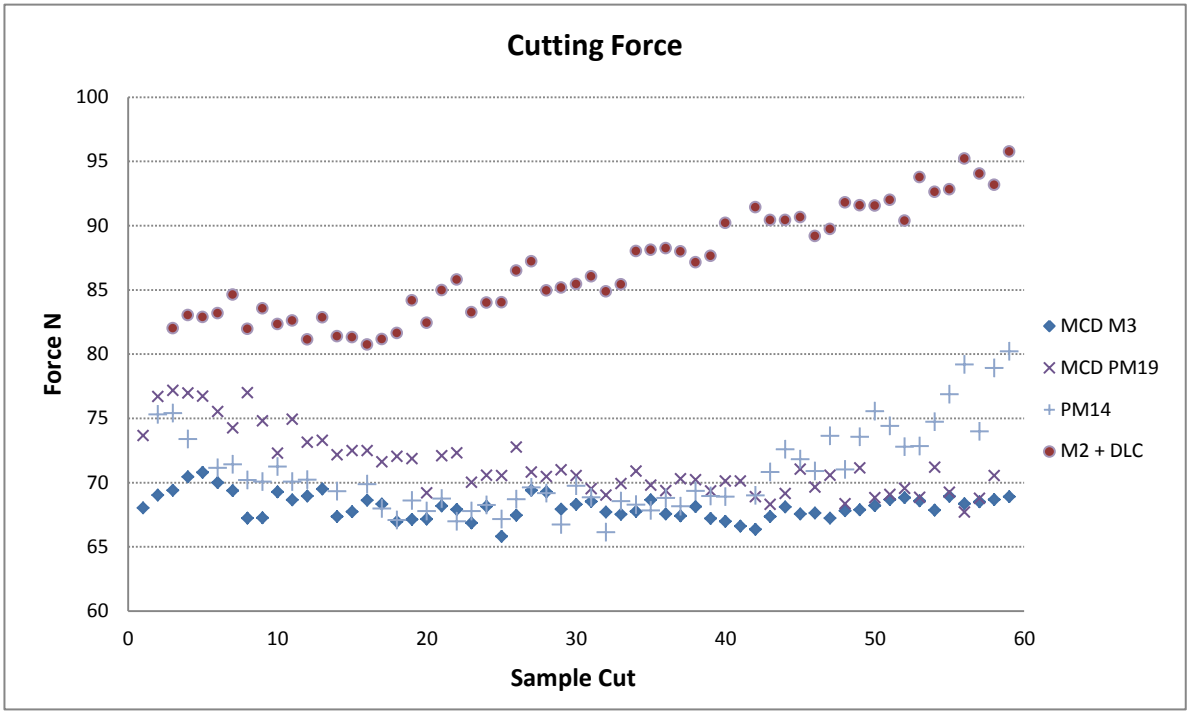

Figure 7.14. Graph of cutting forces of MCD based samples

It is clear from the graph that the variation in the coatings, as well as the addition of the DLC layer, has affected the cutting forces by a significant amount (Fig 7.14). Sample M3 had the lowest initial cutting force of 67N. Samples PM14 and PM19 had comparatively increased forces at the start of the trial, just over 5N greater than M3. The addition of the DLC layer has clearly produced a further increase in forces, up to 82N. It therefore confirms that the roughest surface is in fact producing a decrease in cutting forces in this instance. Sample M3 continued to consistently maintain low cutting forces whilst all other samples varied throughout the trial. Samples PM14 and PM19 and the DLC

coated sample all showed a reduction in cutting force during the first 15 to 20 cuts. For the PM samples, this meant that, by the 30th cut, the MCD samples were all showing similar cutting forces. Sample PM14 maintained a similar cutting force to sample M3 throughout the duration of the trial, whilst PM19 began to have increasing cutting forces after cut 40. The DLC coated sample switched from a gradual decrease to a consistent increase in force at the 15th cut. This suggests that a significant failure may have occurred at that point to create such an abrupt transition.

Analysis of the workpiece finish showed huge discrepancy between the MCD samples. The graph shows that the work piece roughness decreased throughout the trial with all samples, including with the additional DLC layer. Sample PM14 showed the least change of the MCD samples with the average roughness reducing by just 0.03µm from start to finish. The M3 sample showed the greatest variation throughout the trial, as well as creating the roughest work piece finish of all samples tested. Starting at 0.85µm the roughness gradually reduced to 0.65µm (Fig 7.15).

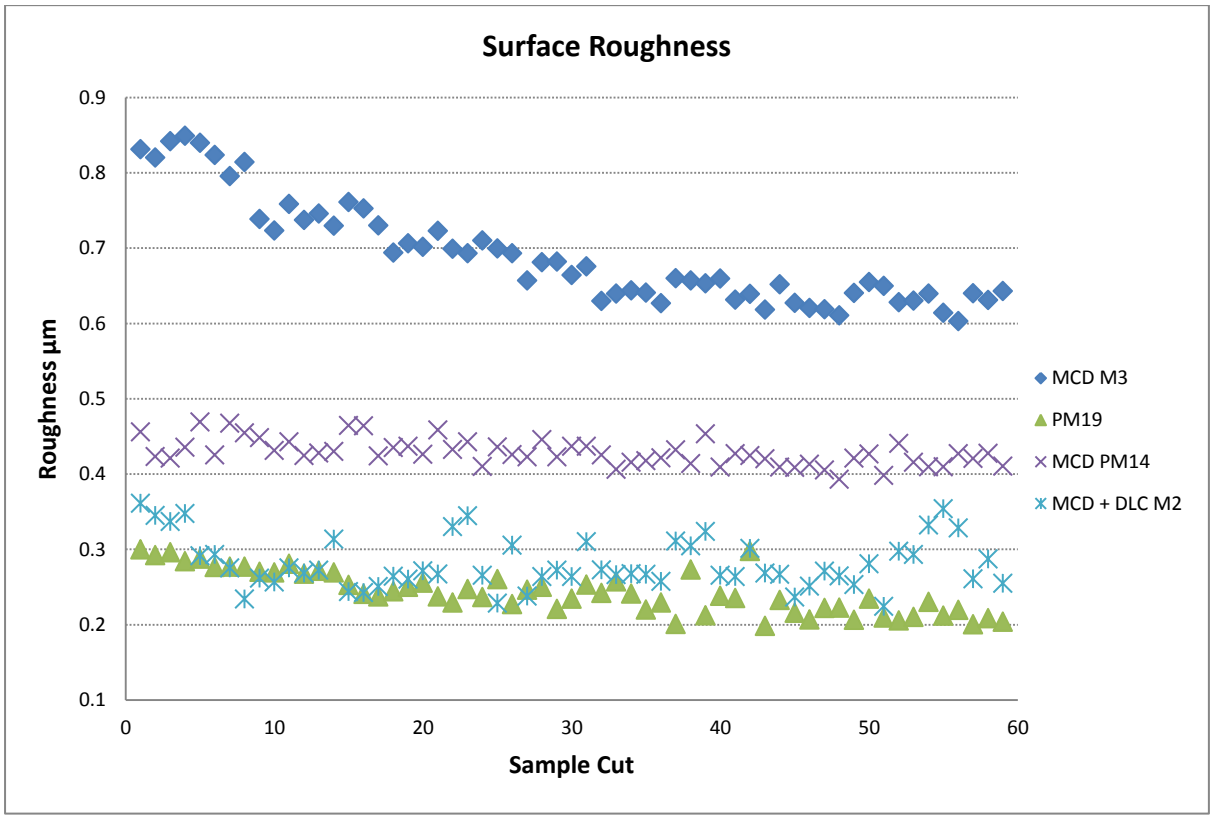

Figure 7.15. Graph of WP roughness produced by MCD based samples

Sample PM19 created the lowest work piece roughness, particularly at the end of the trial as the roughness was just 0.2µm after starting at 0.3µm. The DLC coated insert followed a similar pattern although there were increased fluctuations in the quality of the work piece finish compared to the single MCD coatings. This large variation further highlights the need to individually assess the coatings to determine the cause of the disparity.

Sample M3

The MCD coatings had the lowest amount of aluminium adhesion of all sample types, with sample M3 having the least amount of all. SEM analysis revealed that the aluminium adhesion that had occurred was concentrated at the chip-breaker, as opposed to the major flank edge (Fig 7.16 a).

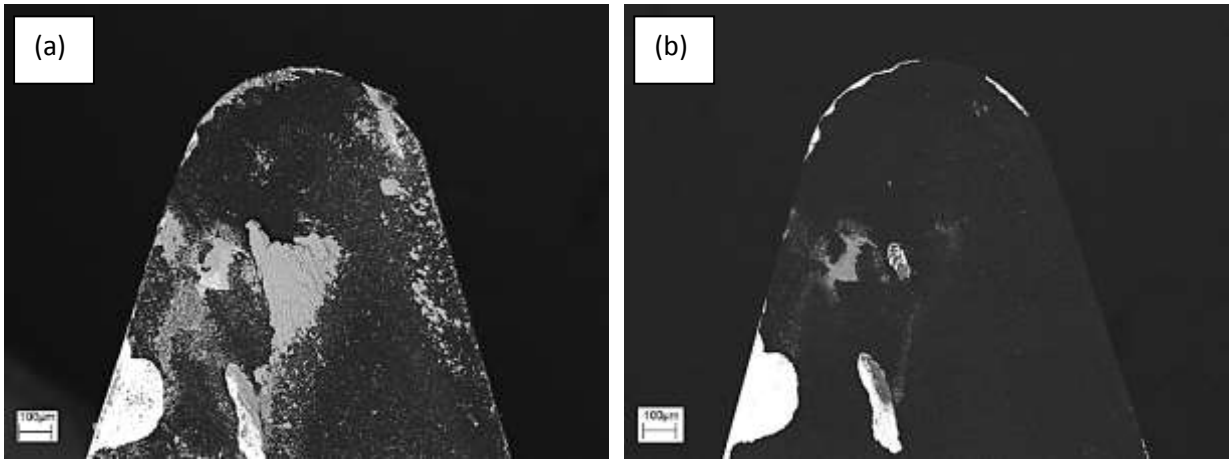

Figure 7.16. SEM micrographs of MCD sample M3 (a) after trial (b) after Al removal

Analysis of the cutting tip after the Al was removed (Fig 7.16 b) has highlighted the areas of coating failure. BSE analysis showed that the aluminium had adhered at cutting edge at specific points due to delamination of the coating. The main body of Al adhesion is also deposited over a small area of delamination at the chip-breaker. It is likely that the coating failure would have led to an increase in the amount of BUE deposited. Small amounts of aluminium can be seen to have deposited in the usual areas at the major and minor flank edges of the rake face. A small amount of Al adhesion has developed at the minor flank edge of the cutting plane, as with all samples, despite there being no coating delamination at that point.

High magnification imagery reveals further unique performance features of the MCD coating compared to the other samples. Firstly it can be seen that the peaks of the crystals have been worn down in the crater wear patch (Fig 7.17 a). Despite having a similar, albeit reduced wear pattern, however, the insert does not have the same transition and does not produce the increased aluminium adhesion that is present in the baseline and DLC coated samples (Fig 7.17 b).

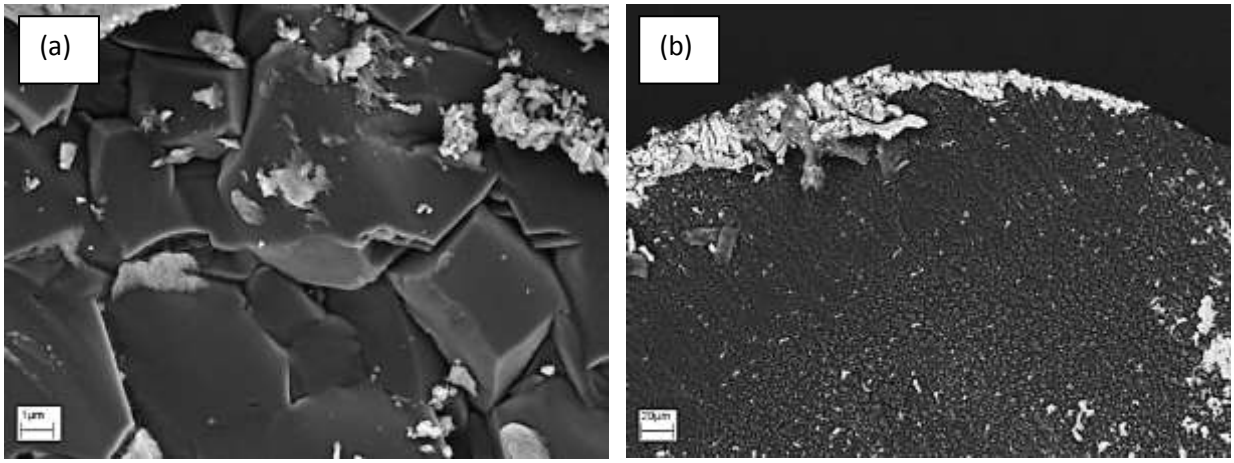

Figure 7.17. SEM micrographs of MCD sample M3 (a) crater wear patch (b) cutting tip

It can be seen that smaller aluminium particles have adhered to the sharp edges and stuck between the crevices of the MCD crystals. It appears, however, that the BUE only begins to develop around the chip breaker areas were the forces are greater, driving the aluminium into the gaps. The aluminium does not readily adhere to the planes of the MCD crystals, although build up can begin when the aluminium catches on the edges and peaks.

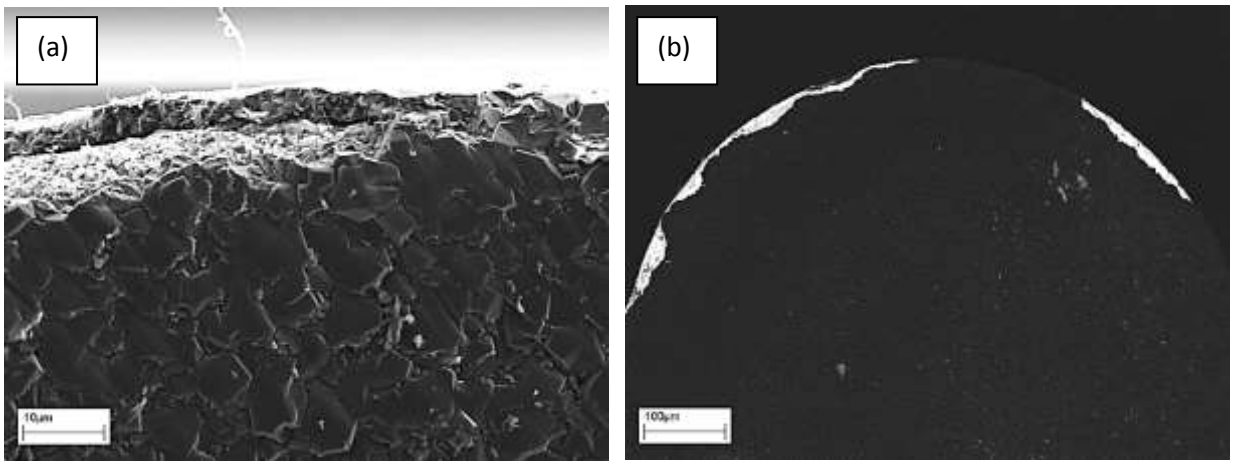

Figure 7.18. SEM micrographs of MCD sample M3 after Al removal (a) X5k (b) X1k magnification

Performance during the cutting trial can be correlated to the post trial analysis of the insert cutting tip. The cutting forces appear to be closely related to aluminium build up as the samples with the least amount of BUE also showed the lowest machining forces, particularly towards the end of the trial. A reduction in cutting force could therefore be attributed to the flattening of the MCD peaks which in turn aided in the swarf flow and led to an improvement in machining efficiency.

It appears that the workpiece roughness produced by sample M3 may have been affected by the delamination of the coating. Although the delamination does not appear to have produced large protruding peaks at the cutting edge (Fig 7.18 a and b), it may still have adversely affected the WP finish. The gradual reduction in surface roughness would therefore be attributed to gradual wearing and flattening of the MCD crystals at the end cutting edge. Protruding crystals may have been broken off as well as being abraded away, however, a gradual reduction in roughness and lack of any abrupt changes would suggest that the wearing down of the crystal peaks can also be directly correlated to the reduction in work piece roughness.

Sample coating PM19

Post-trial SEM analysis indicated the reasons behind the performance variation between the different batches of MCD samples. Aluminium build up was once again centred closer to the chip-breaker and not the outer cutting edge. The sample does, however, have a small BUE at the active cutting edge which corresponds to an area of coating delamination (Fig 7.19 a). This increase in delamination at the cutting edge and addition BUE can be correlated to a reduction in machining efficiency. It is not possible to confirm if the coating is more prone to aluminium adhesion than the M3 sample, as the delamination is clearly exacerbating the occurrence of aluminium BUE. It appears, when considering the crater wear track area, that the sample has performed similar to M3 in its ability to reduce BUE. Due to the coating failure along the minor flank side of the cutting edge it is difficult to know what the workpiece finish would have been if the coating had remained in tacked.

Judging by the workpiece roughness results and excessive wear of the underlying substrate (Fig 7.19 b), it would appear that the coating failed almost instantly.

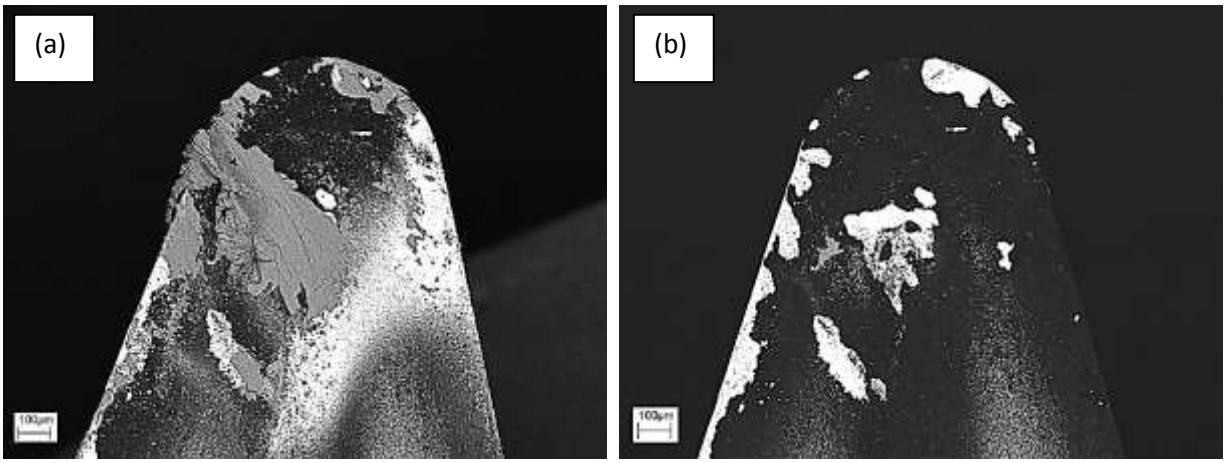

Figure 7.19. SEM micrographs of MCD sample PM19 (a) after trial (b) after Al removal

The roughness was therefore comparable to the uncoated sample with a surface finish of 0.2µm at the end of the trial, dropping 0.1µm after starting from just 0.3µm. Despite the significant increase in delamination, compared to M3, the remaining coating still effectively prevented excessive BUE forming. This resulted in the sample being able to maintain a much improved machining efficiency.

Sample coating PM14

The main difference between this sample and the other MCD samples is that aluminium had also adhered to the major flank of the tool tip (Fig 7.20 a). Although the visible area of build-up of aluminium on the flank is clearly below the active cutting zone, it does indicate that the interaction at the flank is adversely affecting performance. These aluminium deposits suggest that the WP material has begun to more readily stick to the major flank, potentially increasing the cutting forces in the process. Unlike the other MCD samples the cutting forces began to increase towards the end of the trial, possibly due to a specific point of failure of the coating between cut 30 and 40. PM14 did suffer more delamination than the other single coated MCD samples, particularly along the major flank and chip-breaker (Fig 7.20 b), however, this does not fully explain the increase in cutting force which occurred at the end of the cutting trial.

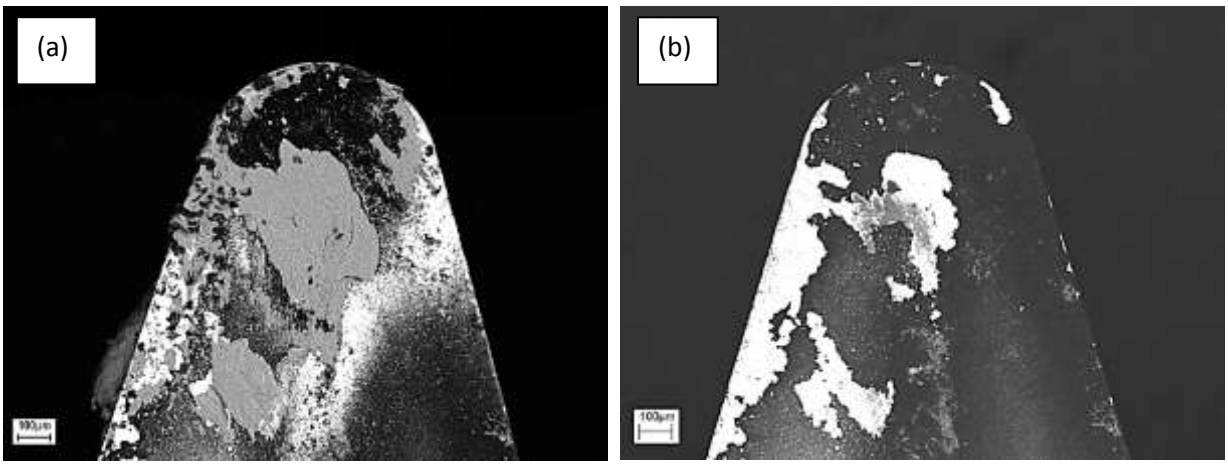

Figure 7.20. SEM micrographs of MCD sample PM14 (a) after trial (b) after Al removal

Micrographs of the end cutting edge show that the coating had remained relatively intact in that area and hence, the WP finish was the most consistent of all samples. It is clear, however, that the roughness did gradually reduce, further suggesting that the WP finish improves as the MCD surface is worn down to a smoother surface.

Sample coating DLC on MCD M2

The DLC coating led to a increase in BUE (Fig 7.21 a), however, it was also clear from the BSE analysis that the sample suffered from significant amounts of delamination with half of the coating being removed during the trial (Fig 7.21 c). Due to coating failure it is not possible to fully evaluate how the additional DLC layer affected the machining performance, however, post-trial analysis suggests that the additional layer has not improved the performance, particularly in terms of aluminium adhesion. BSE analysis of the cutting tip shows that aluminium has adhered to the coating surface more readily than to the MCD coating (Fig 7.21 b). The cutting force measurements indicate that the additional DLC layer increased the friction between the WP and the insert, although the efficiency still improved as the coating was worn down. The failure in the coating appears to have initiated at cut 15 as this is the point at which the cutting force begins to increase.

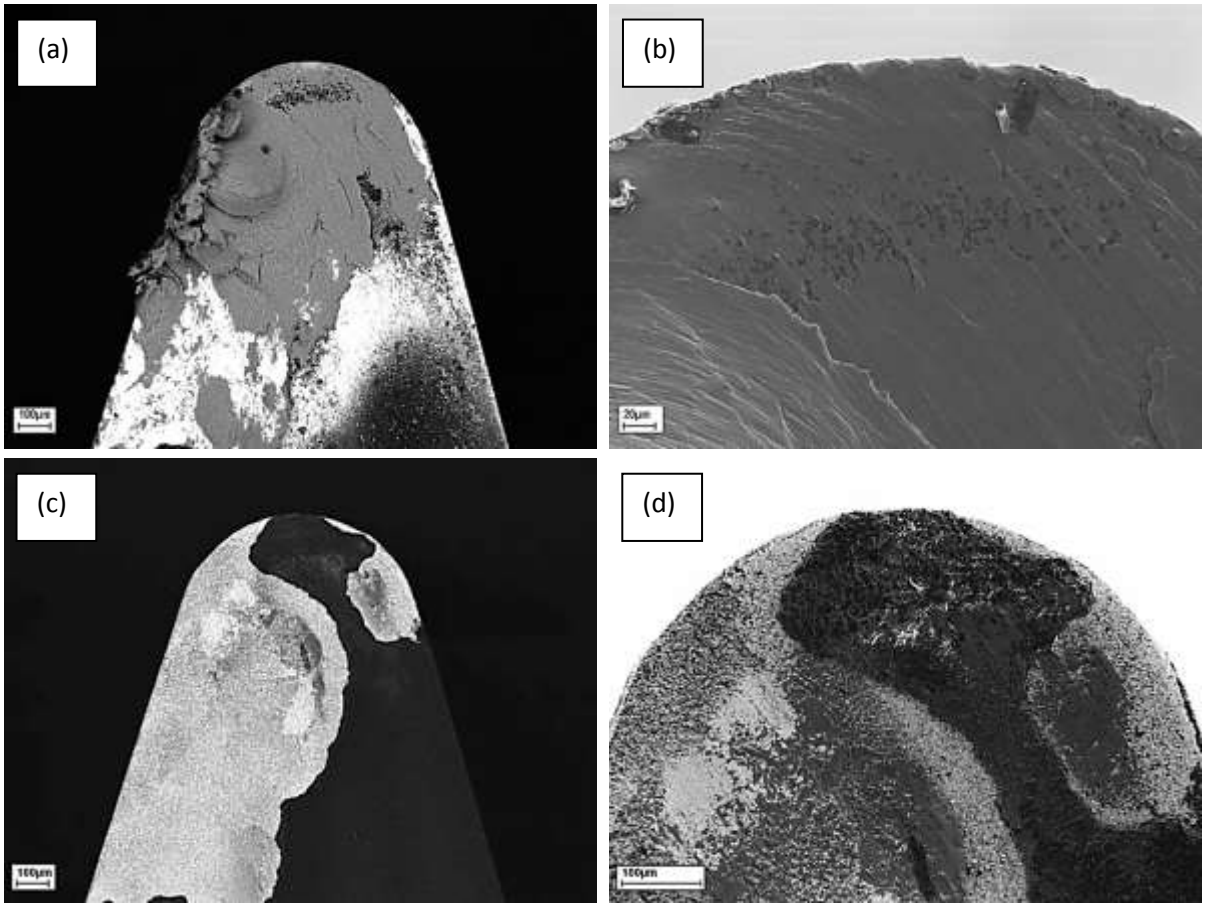

Figure 7.21. SEM micrographs of DLC on MCD sample after trial (a) X150 magnification (b) X1k magnification, and after Al removal (a) X150 magnification (d) X500 magnification

Despite a gradual improvement in surface roughness, fluctuations in the WP finish indicate that the coating along the cutting edge is likely to have broken away in sections. This would have created spikes in roughness as protruding edges are created and subsequently worn away. The DLC deposition process should not have compromised the MCD coating as the temperatures in the PECVD process are not high enough to affect the integrity of the diamond. The fact that the coating failed to a greater degree than all MCD coatings may simply be due to the poor reliability of the diamond adhesion to the substrate. It may however, be attributable to increased friction and adhesion of the DLC layer. The increase in cutting forces due to the DLC layer may have caused the increased delamination of the coating, particularly as the aluminium adhered in areas which would otherwise have remained clear. The enlarged BUE will have further increased the forces acting to pull the coating from the substrate, as opposed to the cutting forces which are predominantly pushing down on the surface.

7.3.4. NCD based samples

Cutting force measurements show that the NCD coatings generally had a slight increase in cutting forces compared to the MCD samples, as well as having a greater variation between samples. All samples had initial cutting forces, between 75N and 80N, including the sample with the additional DLC layer (Fig 7.22). The samples all show a reduction in cutting force over the first 15 cuts, with the NCD samples exhibiting a reduction of almost 10N. The DLC sample on the other hand shows the least change of just 5N, however, it does also undergo an initial increase in force during the second cut, causing a jump of 10N, before gradually decreasing until cut 18. The force, similar to that of the sample R4, then begins to rise throughout the remainder of the trial.

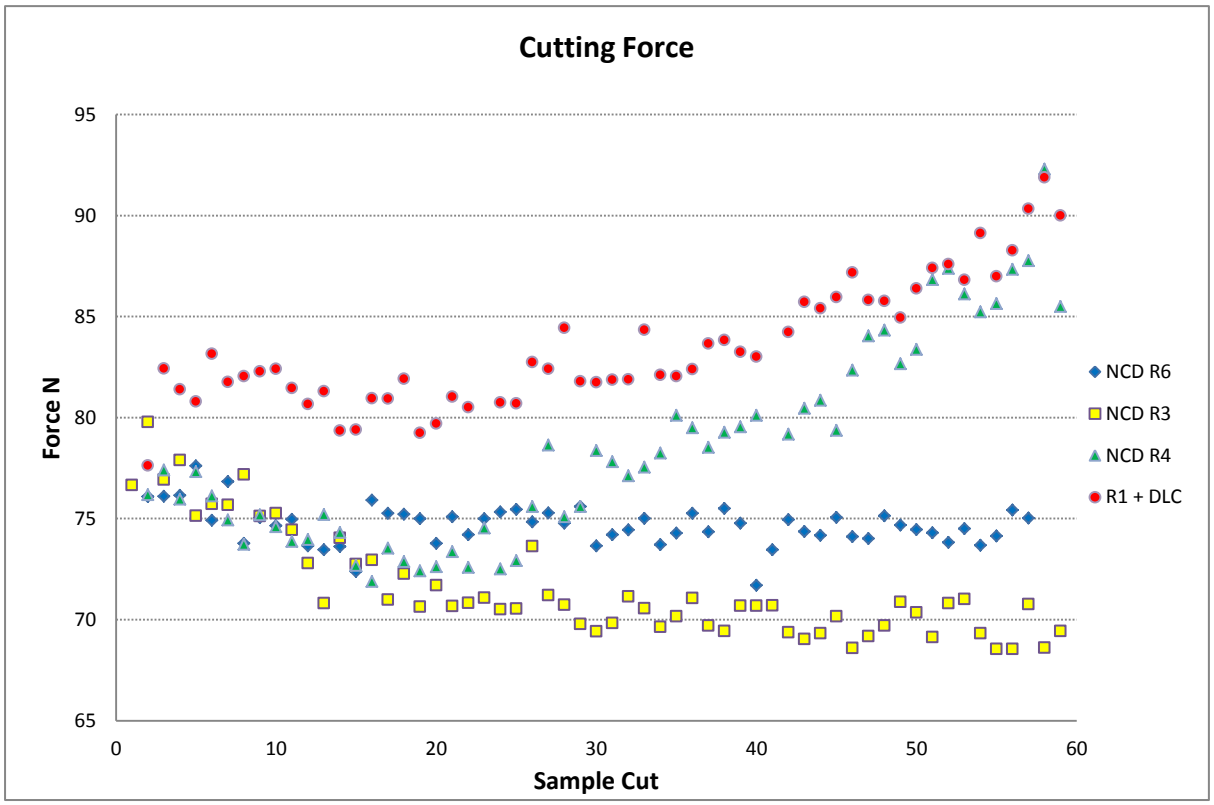

Figure 7.22. Graph of the cutting forces of NCD based samples

Sample R4 showed a similar, albeit greater reduction in force for a similar time before a large shift causes the force to rise significantly by 20N in the last 40 cuts. This shift indicated a large failure is likely to have occurred around cut 20.

Samples R6 and R3 maintained a relatively steady performance throughout the trial. Sample R3 showed the best performance by having a constant gradual reduction in force, with the final cutting force being less than 70N. Sample R6 followed a similar pattern as sample R3, yet the reduction in cutting force was less pronounced and generally remained 5N above sample R3.

The surface roughness has similarly shown significant variation between samples (Fig 7.23). The results also show, to a lesser extent, the transition point around cut 15 at which point the roughness levelled and became more consistent.

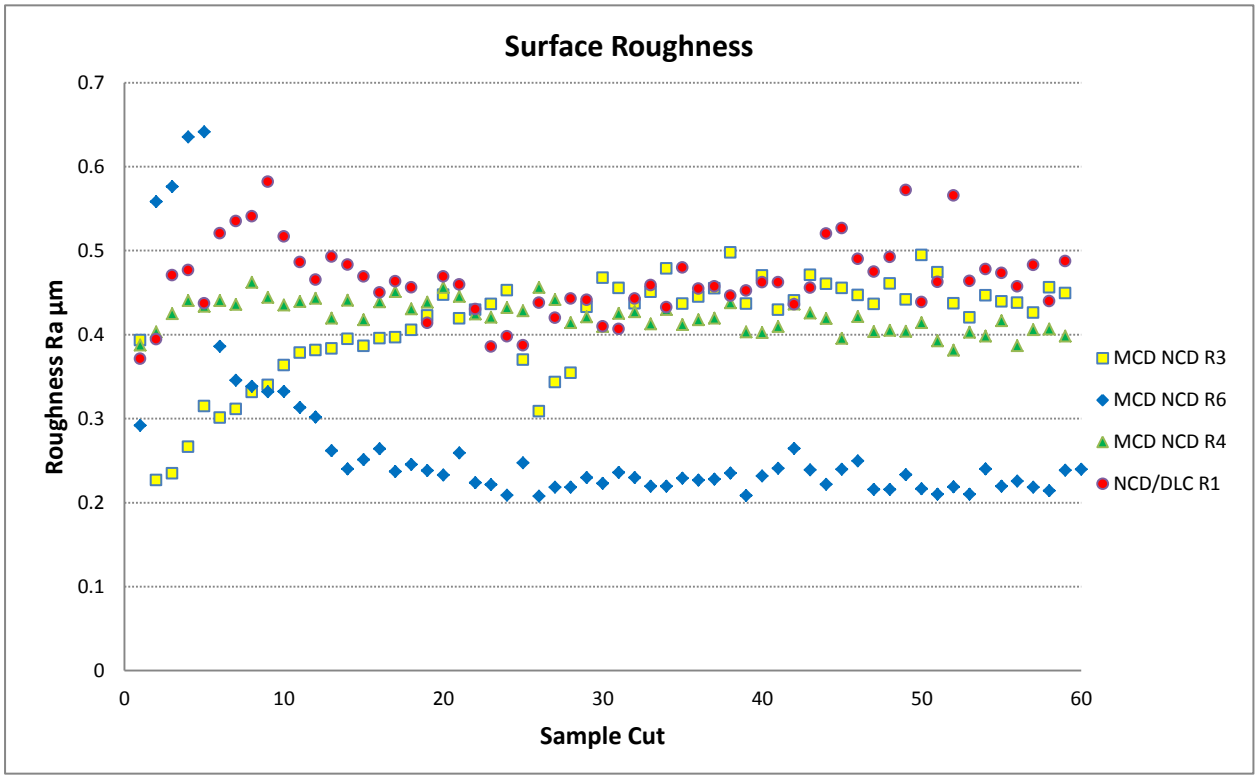

Figure 7.23. Graph of WP roughness of NCD based samples

The fluctuations in WP roughness suggest that coating degradation at the end cutting edge occurred throughout the duration of the cutting trials. Sample R4 was the only insert to maintain a relatively constant roughness after a slight increase in the first 3 cuts. Sample R3 started at the same roughness of 0.39µm but after the first cut dropped down to 2.3µm before rising quickly back to 4.5µm. Despite maintaining this average roughness for the rest of the test, the deviations were far greater than with the R4 sample.

Sample R6 produced a notable difference performance in term of WP finish. The first cut showed a roughness of just 0.29µm, however, for the next 4 cuts the WP roughness increased up to 0.65µm. The WP roughness then gradually reduced over the next 20 cuts to around 2.4µm which it maintained for the duration of the trial. WP roughness produced by the DLC coated sample, despite starting at 0.36µm, increased sharply in the first 9 cuts to 5.8µm before gradually reducing to 0.45µm similar to sample R3.

Sample coating R6

BSE analysis of the insert after the trial highlights the various failures of the coating and verifies the force and roughness measurements. The total amounts of coating delamination and aluminium adhesion is comparable with the MCD samples, however, the structure of the aluminium BUE is noticeably different (Fig 7.24 a).

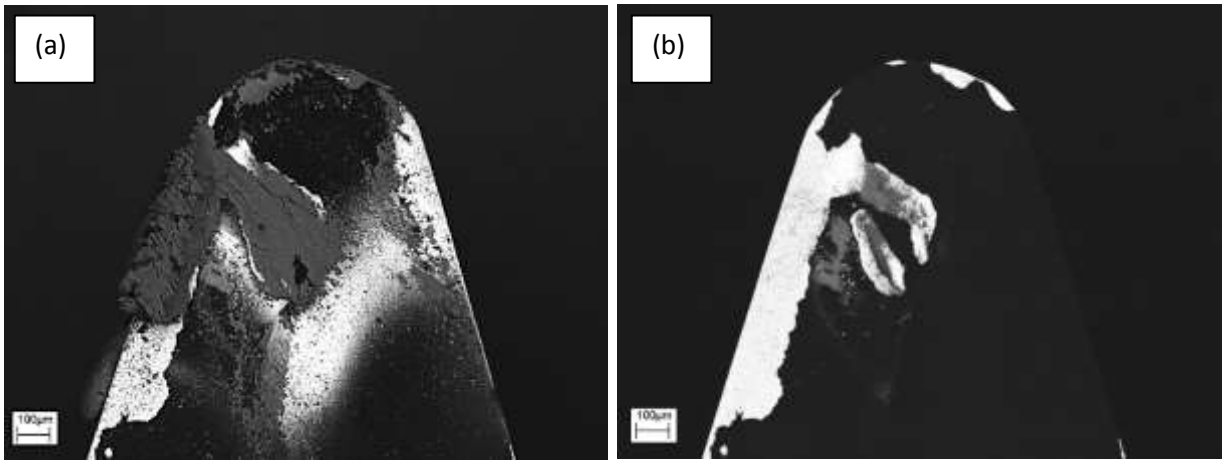

Figure 7.24. SEM micrographs of NCD sample R6 (a) after trial (b) after Al removal

Aluminium has built up more predominantly along the cutting edge and appears to be in the form of serrated chip BUE. Once again the majority of BUE is over areas of delamination, this further highlights the coatings ability to significantly reduce aluminium adhesion. The coating most likely began delaminating at the end cutting edge after the first cut leading to the increase in WP roughness. It appears that any protruding edges of the coating were broken away and then worn down to the substrate causing the final roughness measurements to correspond to those of the uncoated insert (Fig 7.24 b).

Aluminium has adhered to a greater extent to the NCD coating surface than to the MCD surface. BSE analysis highlights the areas in which the aluminium has adhered to the coated surface. The crater wear patch has some aluminium adhesion, as well as a slight transition line, as was seen in the uncoated samples (Fig 7.25 a). In this instance, the aluminium appears to more readily stick to the smoother nodular surface of the NCD, than to the sharp crystal peaks that constitute the MCD coating surface morphology.

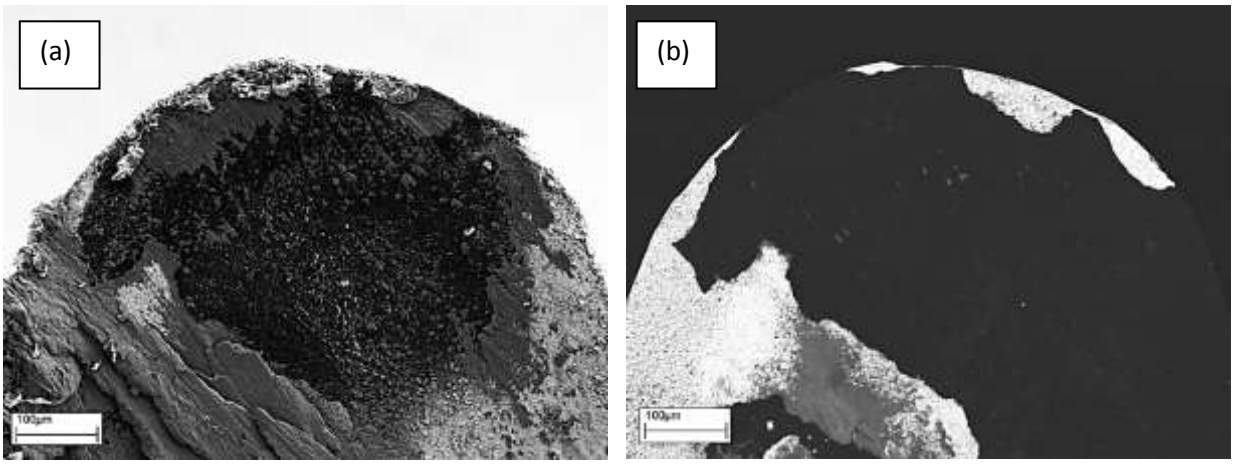

Figure 7.25. SEM micrographs of NCD sample R6 tool tip (a) after trial (b) after Al removal

The SEM micrographs also highlight that flank wear has led to a displacement of the cutting edge at the very tip of the insert (Fig 7.25 b). It has occurred however, just before the end cutting edge and therefore has not affected WP roughness. The type of irregular tool wear is likely to be a result of failure of the diamond coating at the cutting edge. This then exposes areas of the softer WC-Co substrate, which in turn wears at a much faster rate than the diamond.

Sample coating R3

Analysis of sample R3 revealed it to have a very similar performance to the R6 sample. Subtle differences, however, have meant that despite reduced performance in BUE, coating delamination and WP finish, the efficiency has in fact improved. BUE has formed predominantly along the major flank cutting edge and chip breaker (Fig 7.26 a), predominantly in areas of coating delamination.

It can be seen that the end cutting edge has worn erratically which is the reason for the poor WP finish, this is due to the coated and uncoated sections wearing at different rates. Also BSE imaging shows that, at the trailing edge of the cutting tip, further delamination has occurred after the trial (Fig 7.26 b).

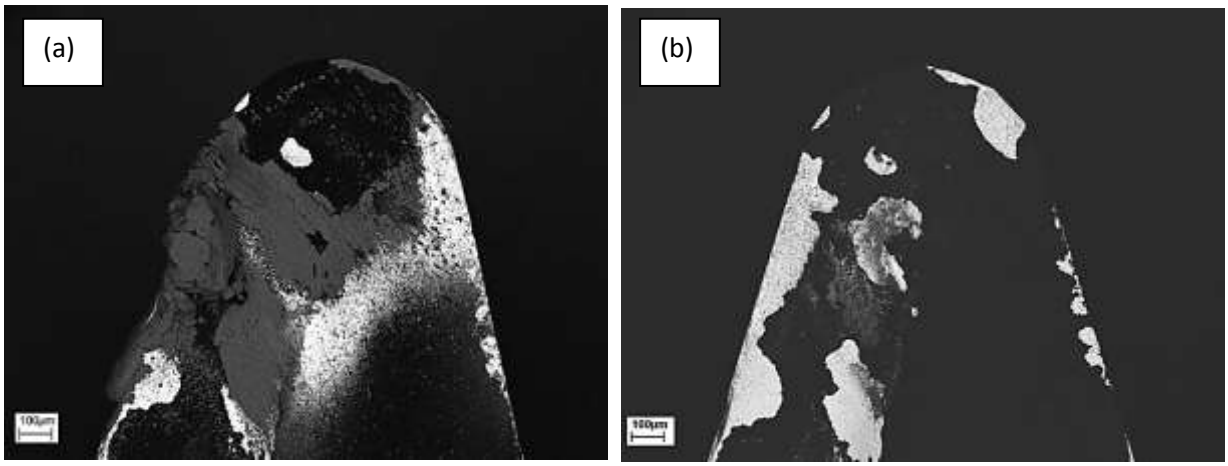

Figure 7.26. SEM micrographs of NCD sample R3 (a) after trial (b) after Al removal

Micrographs of the crater patch show how the aluminium adheres to the broad peaks of the NCD coating. Although this adhesion is predominantly either side of the crater wear patch, it has occurred in the centre of the wear patch as well. As the aluminium builds up it gets forced deeper into the crevices between the peaks, particularly in areas under high pressure. High resolution micrographs show how the NCD surface has been worn away throughout the trial to create small flat sections separated by fissures (Fig 7.27).

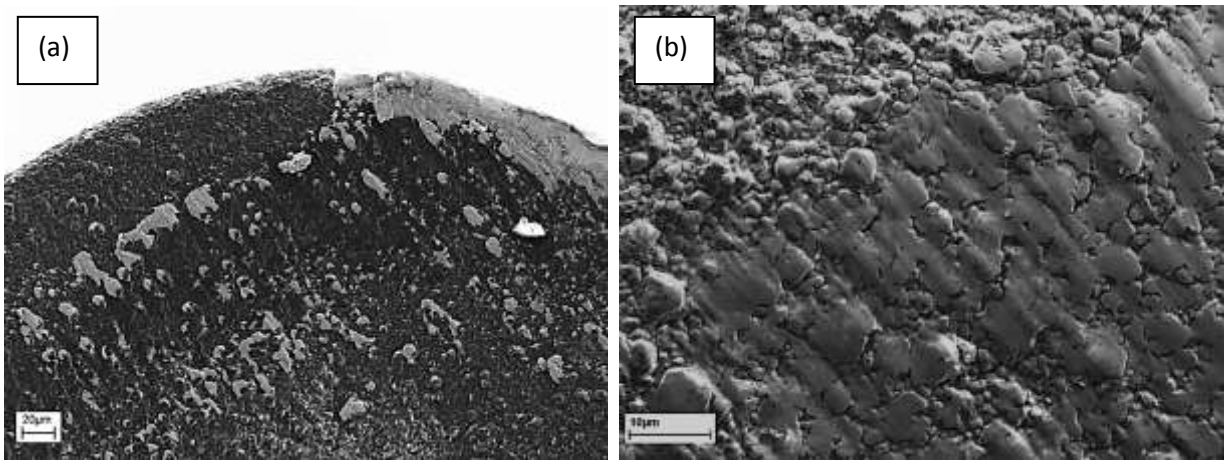

Figure 7.27. SEM micrographs of NCD sample R3 crater wear patch (a) after trial (b) after Al removal

Sample coating R4

BSE analysis revealed large areas of delamination at the cutting tip of sample R4 and showing a large failure had occurred with the coating (Fig 7.28 b). This failure has led to a significant increase in the amount of aluminium adhesion to the tool tip (Fig 7.28 a). Although the micrographs show that the build up at the cutting edge is somewhat less than the other NCD samples.

The cutting force measurements indicated that the coating failure initiated at cut 20, as the forces abruptly switched from a pattern of gradual reduction to a relatively steep increase. This suggests that it requires a threshold amount of delamination of the coating, with both the MCD and NCD samples, before the aluminium begins to build up in such a way that the cutting forces are negatively affected. This is evident as the other samples, despite suffering delamination of the coating, continued to maintain a relatively low or reducing cutting force.

Measurements of the WP roughness revealed this sample produced the most consistent results of the NCD based samples. SEM analysis highlights that this is due to the end cutting edge maintaining its integrity throughout the course of the trial. The pattern of delamination also further highlights inconsistency in coating adhesion. This is due to the fact that the lower patch of delamination is surrounded by a small area of coating, which has managed to remain adhered to the substrate.

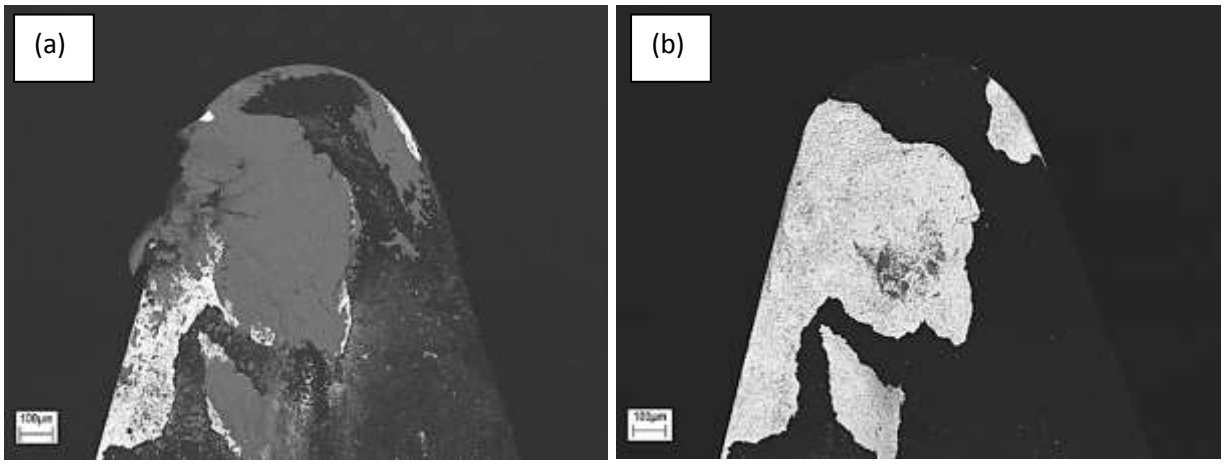

Figure 7.28. SEM micrographs of NCD sample R4 (a) after trial (b) after Al removal

Sample coating DLC on NCD/MCD R1

The DLC coated NCD sample showed a similar performance to sample R4 and suffered large amounts of delamination of the coating. Analogous to the previous samples, the delamination also emanates primarily from the major cutting edge and the chip breaker (Fig. 7.29 b). This can be seen to have contributed to a significant increase in Al adhesion at the cutting edge and the chip-breaker, as well as the area between (Fig 7.29 a). Despite the aluminium predominantly adhering to the areas of delamination, it has also clearly adhered more readily to the DLC layer than to the NCD surface. This is evident as the aluminium has adhered heavily to the coating surface at the cutting edge, as well as in the area below the crater wear patch.

Higher resolution micrographs of the surface revealed that the DLC layer had remained on the NCD in the low force areas, such as at the cutting edge, however, the DLC coating appeared to be compromised in other areas. DLC has worn away at the crater wear land as expected, along with a certain amount of the NCD coating. It can be seen, however, that it has led to delamination of the DLC coating from the NCD coating in the area just below the wear land. Analysis of the cutting forces indicates that the coating also failed at the 20^{th} cut as the cutting forces began to increase steadily from that point. The micrographs of the cutting tip show that the coating has delaminated at the end cutting edge. The WP roughness measurements suggest that the coating failures were continuous through the trial leading to the fluctuations in machining performance.

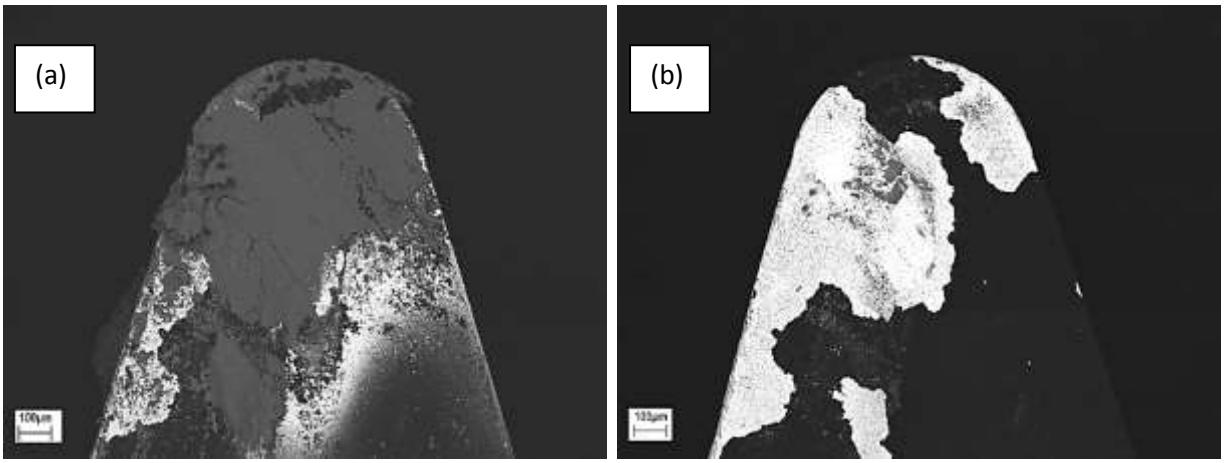

Figure 7.29. SEM micrographs of DLC on NCD (a) after trail (b) after Al removal

7.4. Discussion

The extended cutting trials have revealed a number of findings in regards to the performance of combined diamond and DLC coatings for dry turning aluminium alloy Al 6082. They have also further confirmed the finding of the short trials used in the coating development process by highlighting the performance of the coatings in terms of friction, wear and adhesive properties.

The extended trials revealed the relatively poor performance of the uncoated WC-Co and TiN coated inserts when dry turning aluminium. The aluminium built up very quickly before reaching a saturation point in which the cutting forces stopped increasing. This finding was expected as previous research had shown aluminium to adhere strongly to both uncoated and TiN coated machine tools (Gómez-Parra *et al.*, 2013; Gangopadhyay, 2008). The reasons for this are to do with both surface roughness and chemical affinity of the insert material to the aluminium. As the temperature increases past a critical value, the cobalt begins to chemically react and bond with the aluminium, this will in turn lead to an increase in Al adhesion. Once aluminium has begun to adhere to the tool surface it quickly builds up and masks and blunts the cutting edge. Similarly TiN coatings are known to offer little advantage when machining aluminium as they also induce chemical bonding with the Al. It is well known, however, that the cutting temperatures play a significant role in the wear of cutting tools, particularly when BUE is a cause of failure (Kouam, 2012; Chattopadhyay *et al.*, 2009; Nouari *et al.*, 2003). The possibility of BUE affecting WP finish did not appear to be an issue in this instance as the end cutting edge never showed any significant amounts of aluminium build up. The WP finish therefore remained relatively unaffected. In addition to the excessive adhesion of the WP material to the tool tip, it was also clear that the tool wear suffered by the inserts would potentially have a detrimental effect on WP tolerances on a micro level. It was seen that the active cutting edge had been worn down over the course of the test, mostly at the outer cutting edge, but also at the end cutting edge. The wearing of the outer cutting edge would clearly not impact the WP roughness as the subsequent cut removes the material it has just cut.

A change in geometry of the end cutting edge will, however, understandably have an effect on the quality of finish of the workpiece. The roughness results did show that the overall WP finish was not significantly impacted due to the gradual wear of the cutting edge and did not suffer and fractures or other failures that would have significantly altered the WP quality.

The diamond and DLC coatings all showed an improvement in machining efficiency over the baseline samples, despite suffering failures in the coatings. They did on the other hand, highlight a significant increase in WP roughness in comparison. It was discovered that the aluminium adhesion was lowest with the MCD coating, despite it having the roughest surface. The NCD surface was shown to have increased adhesion, whilst the addition of the DLC layer increased aluminium adhesion even more when compared to the diamond coatings. These finding have gone against previous research which suggested that a smoother surface produced by a DLC top layer will help further reduce adhesion when machining aluminium (Hanyu *et al.*, 2005). This is in part due to the differences in the type of machining, dry turning compared to semi-dry drilling, although this doesn't fully explain the large variation in performance. The results of this trial were more in line with a group who found the combined coating to also show reduced tribological performance in which it was concluded that wear and delamination of the softer DLC layer led to reduced performance (Amaral *et al.*, 2012).

Although failure of the coating interfaces, both diamond to WC-Co substrate and DLC to diamond, contributed to a significant reduction in performance. It was discovered, from the initial shorter development trials and extended final trials, that for this particular machining scenario, the DLC layer suffered significant amounts of aluminium adhesion compared to the MCD and NCD coatings.

It is known that smoother surfaces can increase adhesive properties due to the increased contact area between the sliding surfaces (Chen *et al.*, 1990; Rigney *et al.*, 1984). In this case the surfaces include the evacuating chip from the WP and the cutting tip of the insert. The adhesive properties between the two surfaces will depend on many factors such as the pressure, temperature and swarf flow rate (Sedlaček *et al.*, 2008), as well as the contact surface morphologies (Chern *et al.*, 2011).

This is also tied in with the scale of the surface features and texture (Myshkin *et al.*, 2003). It has been shown that the combination of these factors in this instance has led to a reduction in performance.

The real time measurements of machining force, coupled with the post-trial analysis of the work piece and cutting insert revealed a number of other common performance features regarding this particular cutting tip geometry. Some features, such as the positioning and formation of crater and chip-breaker wear patches, were prevalent on all types of coating, whist particular coating types also produced more unique results. Other common areas of wear and delamination are evident on only the diamond based samples (Fig 7.30). The delamination patterns observed on the samples is often related to the initial wear, however, other factors have also affected how certain areas of the coating have performed.

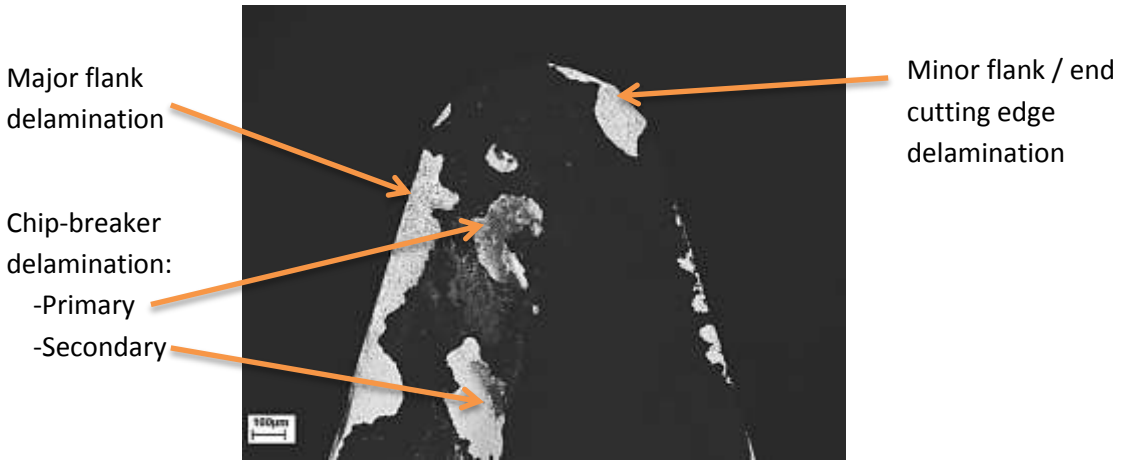

Figure 7.30. Wear and delamination patterns of diamond based coatings

Common areas of delamination were not always based around the points on the cutting tip which endured the majority of cutting force. Diamond coatings regularly delaminated along the major flank up to 0.5mm away from where the cutting processes were happening. In some cases delamination seemed to occur in inactive areas of the cutting edge when active areas remained undamaged. Delamination at the minor flank, near the end cutting edge, also occurred at points which were not actively cutting the workpiece. In some cases, as seen in the above picture, further delamination

occurred at the minor flank, somewhat removed from the high impact areas of the cutting zone. The reasons for these failures at the cutting edge can be attributed to a number of factors. The literature has discussed the potential for increased stresses in the coatings due to geometrical variations such as sharp edges (Sheikh-Ahmad *et al.*, 2015; Renaud *et al.*, 2009). In addition to this, forces acting on the coating at these points will also be more inclined to be pushing the coating away from the substrate, unlike the crater wear area in which the cutting force generally push down on the surface. The pattern in which the aluminium deposited on the rake face further highlighted the direction of swarf flow. It became clear that the failure of coating in the end cutting edge area was initiated in most cases below that point. As the swarf travelled across the cutting tip, as it reached the protruding edge of the minor flank, it then contacted with enough force to generate an additional patch of adhesion (Fig 7.31). This indicated that the swarf would have been exerting a relatively high pressure on the minor flank edge causing the coating to break away. Once the initial delamination had occurred the coating became compromised and the failure began to spread towards the end cutting edge, which then affected the WP finish.

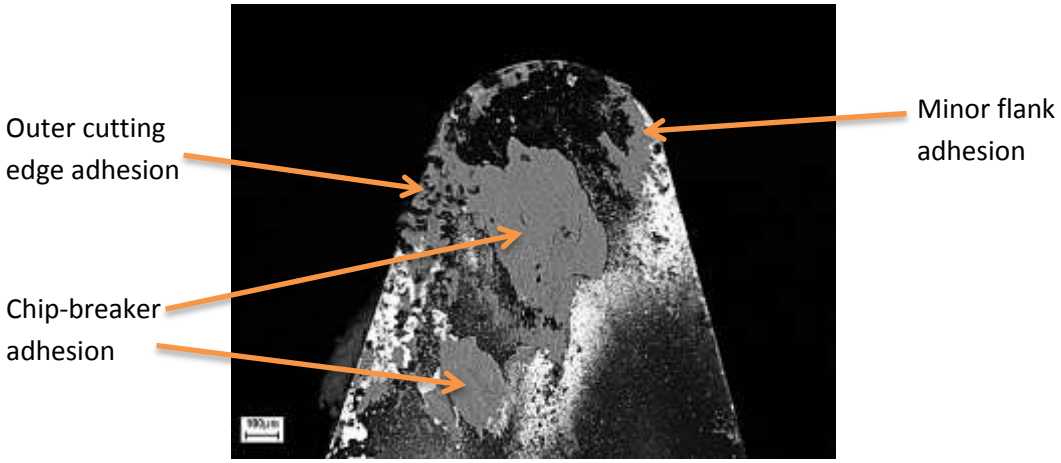

Figure 7.31. Common areas of aluminium adhesion for all coatings

The failures of the coatings further down the flanks may be as a result of reduced cohesive strength within the diamond. Due to the nature of the fabrication process it was known that the coatings would be optimised for maximum thickness at the cutting tip edge. The coatings would then reduce

in thickness the further from the cutting edge it went. It is therefore understandable that the coating in these areas will be considerably thinner than at the very cutting tip and hence lacked the cohesive strength required to prevent delamination. The relief angle of the insert would have meant that the forces acting on the active cutting edge would have also been pushing the coating away from the substrate, increasing the occurrence of delamination.

As well as the typical areas of adhesion at the cutting edge, chip-breaker and minor flank, it was also observed that the different coatings seemed to alter the way in which aluminium was adhering to the rake face. This was in most instances as a result of the varying sliding interaction between the different surface morphologies. Although in some cases it appeared to be as a result of progressive coating failures. The baseline inserts, even with additional DLC coatings, all showed a large amount of aluminium adhering to the cutting edge, which was centred on the outer cutting edge of the cutting zone. The MCD coatings seemed to have the effect of shifting this main area of adhesion to the chip-breaker as they all had a much reduced BUE. The NCD coatings showed an increase again, of the adhesion at the outer cutting edge, however, unlike the baseline samples, the BUE was in the form of a more segmented build up going down the major flank. Due to the coating failures along the major flank, it is not possible to determine how much of this formation is as a result of the coating delamination. The failure of the combined coatings in the extended trials also made it not possible to properly judge the full impact on the aluminium adhesion formation. It is worth noting, however, that delamination of the diamond based coatings did not reveal a substrate identical to the uncoated sample, as the surface had been acid etched prior to deposition. This variation caused by the acid etching will undoubtedly influence the interaction with the aluminium. Previous research has shown how the etching of the WC-Co surface can alter the wettability characteristics with molten aluminium (Chattopadhyay *et al.*, 2009). This further highlights how delamination of the coating can expose a surface with much poorer tribological properties than the uncoated surface provided.

Performance of the single layer coatings were similar to that reported in the literature. The diamond coatings suffered little in term of wear, yet failed due to delamination (Zhang *et al.*, 2010; Roy *et al.*, 2009; Dai *et al.*, 2000). The DLC, on the other hand, adhered much more readily to the various substrates coated, however, they were not hard enough to withstand the forces at the cutting tip and wore away very quickly (Bhowmick *et al.*, 2015; dos Santos *et al.*, 2007a; Fukui *et al.*, 2004; Vandevelde *et al.*, 1999). This is largely due to the lower temperature threshold of the DLC compared to the diamond coatings. It was known that the DLC coating would begin to degrade above 300°C, whilst the dry machining temperature in the area of the crater wear would have potentially reached 600°C or above. This high temperature and pressure leads to graphitisation of the coating causing it to fail prematurely (Liu *et al.*, 1997; Liu *et al.*, 1996). The diamond, however can reach temperatures up to 800°C without beginning to show signs of material degradation (Evans *et al.*, 1964; Howes, 1962). Although the DLC coating was expected to wear at the cutting edge, the geometry of the cutting tip meant that the DLC degraded in the crater wear area. This degradation then led to further delamination throughout the entire contact patch between the cutting tip and chip, which ultimately removed any positive effect of the coating (Liu *et al.*, 1996).

In order to judge the potential for an improved WP roughness it was necessary to apply a filter to the measurements. The filter was based on the actual roughness created by the cutting tip geometry and the feed rate. Unfortunately, due to regular delamination at the end cutting edge, it became difficult to judge the influence the coatings had on the WP finish. The results did suggest, however, that the WP roughness produced by the various coatings, after the filter was applied, produced a WP roughness that was slightly rougher than the measured coating roughness. This is likely due to the fact that the coating roughness measurements had to be conducted in an area slightly off the cutting edge. This area, judging by the SEM micrographs, was slightly smoother due to marginally smaller MCD crystal sizes. The WP roughness may therefore be directly comparable to the coating roughness, although it was not possible to confirm.

7.5. Conclusion

Extended cutting trials have been conducted in order to simulate the average life cycle of a cutting insert in an industrial setting. The results highlighted a number of key benefits offered from each coating, as well as uncovering the disadvantages associated with diamond and DLC tool coatings for this particular application.

The MCD coating clearly suffered the least amount of aluminium adhesion, followed by the NCD coatings. The DLC coatings, despite being smoother, in fact increased the rate of aluminium adhesion when applied to the diamond. The baseline WC-Co and TiN samples showed a much increased rate of adhesion which translated into significantly increased cutting forces. The addition of DLC appeared to slow the progression of the BUE, judging by the cutting force measurements, however, by the end of the trial the amount of adhered aluminium was comparable.

It was clear that the diamond was failing due to delamination of the coating whilst the DLC was wearing away, most likely as a result of graphitisation due to the combine pressure and temperature at the cutting tip. The failure modes and fault progressions associated with the diamond coatings on this particular tool geometry were also discovered. The development of the built up edge in conjunction with the coating delamination also highlighted how slight variations in coating performance at the early stages of cutting can significantly alter the structure of the built up edge. This in turn can affect the cutting performance of the tool throughout the remainder of its use. Due to the unreliability of the coatings, mainly in regards to the film adhesion to the substrate, there were still significant variations between samples. Despite this issue, a detailed analysis of the sample inserts still allowed for a good understanding of benefits and drawbacks of the individual and combined coating combinations. It was discovered nonetheless, that even with up to 20% of the diamond coating having delaminated at the cutting tip, significant improvement in efficiency were still observed. This was evident due to the cutting forces remaining comparatively lower than the baseline samples.

8. Conclusions and recommendations for future work

8.1. Final summary and discussion

The purpose of the project was to investigate the efficacy of a combination of diamond and DLC coatings for improving machining performance of cutting tools when dry turning aluminium alloys. The importance of the investigation was highlighted in terms of the need to reduce or remove the requirement for coolants, which can be harmful to both operator and environment. The need to reduce the dependency on such cooling regimes is also reflected in the increasing costs associated with their use (Kouam, 2012). The reason coolants are required for the machining of aluminium, and other ductile metals, is that the cutting temperatures cause the workpiece to adhere to the cutting tip in the form of BUL and BUE. This phenomenon effectively blunts the cutting edge, resulting in reduced efficiency and premature tool failure (List *et al.*, 2005; Carrilero *et al.*, 2002; Gangopadhyay, 2008).

Diamond and DLC coatings are already a prominent feature of the machine tool industry and have been shown to offer significant improvements in machining performance for a number of specific applications, particularly machining aluminium alloys. As well as providing some of the hardest wearing material known to man, diamond is also unreactive to non-ferrous materials. This means that as well as demonstrating extremely low wear rates, they can also greatly reduce material transfer and hence inhibit build-up of the workpiece on the cutting tip (Zhang *et al.*, 2010; dos Santos *et al.*, 2007b; Polini, 2006; Rech, 2006; Fukui *et al.*, 2004).

Diamond like carbon, although not as hard and wear resistant as diamond, has been shown to offer similar properties in terms of wear resistance and chemical stability, as well as benefitting from reduced friction due to their ultra-smooth surfaces (Markwitz *et al.*, 2014; Moseler *et al.*, 2005; Bull, 1995). Despite the significant improvements in machining performance offered by these coatings, there are still a number of problems to overcome, poor adhesion of diamond coatings to common tool materials, and relatively poor thermal stability of DLC, coupled with a significant increase in

production costs, has prevented the wider use of such materials being exploited in industry (Bhowmick *et al.*, 2015; Dumpala *et al.*, 2014; Barletta *et al.*, 2011; Roy *et al.*, 2009; Bhowmick *et al.*, 2008; Li *et al.*, 2006; Polini, 2006; Helen Xu *et al.*, 2005; Okpalugo *et al.*, 2004; Zhang *et al.*, 2004). For this reason, dry cutting of aluminium alloys is still not viable for the majority of industrial machining application.

This study investigates the potential for combining diamond and DLC coatings in order to benefit from both the extreme wear resistance of diamond, as well as the low friction that is associated with DLC coatings. The aim was to utilise diamond as a base layer, to provide a wear resistant cutting edge, with the addition of a smooth lubricious surface layer of DLC to enhance swarf flow and reduce its adhesion of the workpiece to the cutting tip. One study had indicated that combined diamond and DLC had the ability to greatly improve cutting performance, compared to single layer diamond coatings of varying surface morphologies, when drilling aluminium alloys, (Hanyu *et al.*, 2005). There were, however, no investigations concerning other machining applications such as turning or milling, which arguably have very different dynamic processes taking place at the tool – workpiece interface.

Diamond coatings deposited using a HFCVD method, at Bristol School of Chemistry, were combined with DLC coatings produced, via PECVD techniques, at Renishaw Advanced Materials Ltd. Brunel University. The emphasis of this study was focused on the development of the DLC layer, as well as the characterisation and testing of the combined coatings. This was to aid in the development of the coatings, before conducting extended cutting trials, and to verify the potential for combination coatings to produce the performance increase required to make dry machining of aluminium alloys an economically viable option for industry.

An experimental method was devised in which the coatings being produced could be characterised in terms of surface structure, topography and material chemistry. Controlled machining trials then made it possible to examine the connection between coating characteristics and cutting

performance for this type of machining application. SEM provided the main analysis tool, as it allowed for visual verification of substrate and coating surface quality. Coupled with BSE and EDS analysis it was possible to quantifiably evaluate coating composition and performance. AFM was used to quantify coating surface morphology and topographical features, whilst Raman spectroscopy was employed to assess the chemistry of the diamond and DLC coatings. Raman analysis helped ensure continuity between deposited coatings, as well as highlight any variations in bonding configurations produced by altering deposition parameters. SEM analysis was also used to highlight discrepancies in the surface layer of the WC-Co substrate, as well as common failures and defects in commercially available coated inserts.

The diamond and DLC coating were developed over the course of the project by adjusting sample preparation techniques and deposition parameters to better suit this application. Analysis of the initial diamond coatings showed the films to be thin and inhomogeneous, indicating that deposition rates were much lower than predicted. SEM analysis using BSE techniques, coupled with image analysis methods, allowed for a novel analysis regime to be applied in which coating coverage and uniformity could be quantified. BSE analysis highlighted weaknesses in the coatings such as: poor deposition in the flutes of the cutting tool tip and an inadequate distribution between the rake face and flanks of the insert. This meant that sample positioning and deposition time could be adjusted in order to optimise the coating at the cutting tip and ensure quality coatings were being produced. Further to the BSE analysis, SE2 micrographs highlighted failures in adhesion between the diamond and WC-Co substrate. Higher resolution imaging and EDX measurements confirmed the causes of the failures to be linked to etching process used to prepare the WC-Co substrates for the deposition on the diamond layer. Examination of the surface morphology of the deposited diamond coatings aided in the development of the deposition parameters, particularly in terms of the methane to hydrogen ratios of the precursor gases. It was discovered that, for the HFCVD deposition process used for the deposition of the coatings, along with the sample positioning within the reactor, the methane percentage required to produce MCD and NCD structure had to be as low as 1% and 3%

respectively. Raman spectroscopy was used to confirm that the structures being created were diamond in nature, whilst also highlighting an increase in none diamond formation in the form of graphitic and disordered bonding structures. AFM analysis was used to quantify topographical aspects of the coatings and show how the roughness, along with other topographical features, depended on the methane concentrate in the precursor gases. By examining different points on the surface, it was also shown that small variations in the distance between substrate surface and reactor filament produced significant changes in the coating structure.

DLC coatings were developed on the uncoated WC-Co insert prior to being applied to the diamond substrate. The investigation was based on a previously developed coating, which had been shown to greatly improve the efficiency and tool life of HSS drills when machining aluminium (Zolgharni *et al.*, 2008). Initial SEM analysis of the deposited coatings showed that the DLC was able to produce a relatively uniform, well adherent coating across the entire surface of the WC-Co insert. Higher resolution SE2 imaging of the coating surface further revealed variation in coating morphology as a result of WC rich and cobalt rich areas on the substrate surface. These variations were linked to previous findings regarding substrate effects on the deposition mechanisms associated with the deposition of a-C:H coatings (Salvadori *et al.*, 2006; Cheng *et al.*, 2000). The DLC coating was seen to mimic the cobalt surface topography, whilst the coating over the WC crystals transformed the sharp crystalline peaks into a rounded nodular structure. Tribological performance of the tool coatings were tested through the use of controlled cuttings trials using aluminium alloy Al 6082 as the workpiece material. SEM examination of the tool cutting tips after the trial showed that the hardness and wear resistance of the standard DLC coating was insufficient as a crater wear patch had developed after less than 5 minutes of cutting.

Investigations were then conducted in order to examine the influence of deposition parameters on the coating characteristics, tribological performance, and hence machining performance of the DLC coated turning inserts. The effects of bias voltage, deposition time and precursor gas pressure were

investigated in order to explore the potential for further improvements in the coating performance for this application. An experiment was devised in which the bias voltage during the deposition stages in the coating process was varied. 6 sample sets were produced with voltage increments of 100V between 100V and 600V. The literature had shown that at low voltages, the impinging ion energy is too low to create the diamond like sp^3 bonding, and a soft polymeric coating is formed instead. As the energy was increased, the proportion of C-C diamond bonding increases, creating a harder, more wear resistant coating. This in turn increases the residual stresses within the coating, thus limiting the voltage and thickness, as the coatings are expected to reach a threshold point at which the forces will overcome the adhesive force between the coating and substrate, causing the film to delaminate (Ouchabane *et al.*, 2010; Kim *et al.*, 2005; Zhang *et al.*, 2002).

The samples coatings produced were characterised and trialled. SEM analysis of the samples initially revealed that the coatings deposited below 200V produced an altered surface with very different morphology when compared to the coatings above 300V. The coating deposited at 600V not only showed large amounts of delamination, it could also be seen that some areas of the coating had begun to delaminate during the deposition process. AFM and Raman spectroscopy was used to further characterise the coatings between 200V and 500V. Raman spectra of the disordered and graphitic peaks were used to compare bonding structures, these provided an estimate of the sp^3 concentrations based on a peak deconvolution method described in the literature (Ferrari *et al.*, 2004; Ferrari, 2002; Ferrari *et al.*, 2001). It was shown that as the voltage, and hence deposition energy, was increased, the amount of sp^3 bonding in the coating reduced. This finding correlated with reports in the literature, which concluded that the measurements were as a result of the hydrogen concentrations in the coatings. Despite the sp^3 structures being associated with the diamond bonding in the coating, where hydrogenated coatings are concerned, a certain amount of the measured sp^3 content can be attributed to C-H bonds, as well as the strong C-C diamond bonding. As the deposition energies increase, the hydrogen content of the coatings, much of which is bonded in the sp^3 formation, will be reduced. This means that the decrease in diamond like bonds,

as measured by Raman spectroscopy, in turn corresponded to an increase in coating hardness. AFM analysis of the coatings on a sample Si wafer showed that there was little difference in topography between 300V and 500V. The 200V coating, however, had a higher abundance of peaks despite the average roughness remaining similar.

SEM analysis of the coatings after cutting trials confirmed that higher voltages were producing harder wearing coatings with reduced wear rates. The 500V coating was shown to have the best abrasion resistance whilst maintaining a low enough residual stress that delamination wasn't an issue. The decrease in coating wear could also be seen to help reduce the amount of aluminium that adhered to the cutting tip. This was evident as all sample coatings deposited at 400V and below suffered from a wear land which had exposed the underlying WC substrate. The transition line between the substrate and coating was seen to greatly increase the occurrence of aluminium adhesion in the area. For the 500V sample, a clear transition between the wear land and unworn section of coating was visible despite the WC substrate having not been exposed. There was however, little or no increase in the deposited aluminium as a result. This finding confirmed that the wear land transition between coated and uncoated surfaces was a major contributing factor to the rate of aluminium build-up on the cutting tool.

An investigation of deposition time was conducted to test the effects of the coating thickness. The literature had highlighted the link between coating thickness and internal stresses, with the build up of internal stresses being one of the limiting factors when wanting to deposit thicker coatings. Coatings were produced using deposition times of 15, 24 and 33 minutes, in comparison to the 45 minutes used in the standard coating. The purpose of the experiment was to test if the reduced stresses expected from thinner coatings would improve tribological performance for this application. Characterisation of the samples showed that the structure of the coatings remained similar, with just a slight variation in roughness of the thinnest coating due to the increased effects of the underlying substrate topography. Cutting trials of the samples, however, showed a reduction in performance.

This was attributed to the reduced DLC material mass wearing through to the substrate at a faster rate. Deposition gas pressure was also altered by reducing the flow of precursor gases into the chamber during coating. Three sample coatings were produced at flow rates of 1/3, 1/2 and 2/3 of the standard coating. It was discovered that the deposition rates fell as a result of the reduced gas density. Raman analysis of the coatings showed that the bonding structure remained the same, whilst AFM measurements revealed that the coating deposited at the lowest gas pressure produced a much smoother surface compared to all other coatings. This may, however, have been due to the underlying substrate effects of the Si wafer. SEM analysis of the coated inserts after the machining trials showed no improvements in cutting performance.

It was seen from the SEM analysis of the coatings produced, that the surface structure at the cutting edge of the inserts often contained large nodular cluster formations compared to the coating structure on the rake face of the inserts. An experiment was therefore devised in order to quantify the potential variation that may occur as a result of the geometrical features of the substrate. The experiment involved depositing the standard DLC coating onto Si wafer samples positioned horizontally and vertically on the cathode plate. This meant that the vertical samples would have an exposed protruding edge whilst the horizontal samples were flat on the cathode plate. Variations in the coatings produced were measured in the form of: coating topography, thickness and bonding configuration. The samples were also subject to scratch tests in order to determine how any altered characteristics affected the tribological performance. The results highlighted large variations in the coatings as a result of sample position. It was discovered that the coating structure had been significantly altered at the top 1mm of the protruding edge, when compared to the coating produced on the flat surface. Coating thickness was shown to vary by 50% whilst average roughness was increased by over 30 times. Measurements of skewness and kurtosis further highlighted discrepancies in the way the coating was forming. It could be seen that as the distance to the protruding edge of the vertical sample is reduced, valley formations became a more prominent feature of the morphology. Raman analysis also highlighted an increase in sp^2 bonding in the coating.

As a result, friction was seen to increase by 50%, and critical load values were halved on the vertical sample compared to the horizontal one. The causes of the variations were discussed in terms of the deposition mechanisms associated with hydrogenated DLC coatings. Variations in the effective ion impingement energies, due to the plasma sheath formation around sharp edges, were presented as the reason behind the large differences in the coating morphology and chemistry. The results showed that despite substrate geometry effects often being considered negligible, DLC coatings deposited using the PECVD method were shown to be greatly affected by substrate geometry, particularly when sharp edges were coated (Nelson *et al.*, 2014).

Developed DLC coatings were deposited onto MCD and NCD diamond coatings. This was to ensure that there were no adverse effects to the DLC coating as a result of the differences in substrate surface material chemistry and morphology. SEM analysis of the combined coatings showed that the DLC had deposited uniformly and adhered well to all substrates. It was discovered, however, that the silicon interlayer would still be necessary to ensure good adhesion to the diamond substrates. This was determined as SEM micrographs showed areas of delamination between the DLC and diamond coatings when no interlayer was applied, whilst the coatings with interlayers showed no delamination. AFM analysis it was shown that the addition of the DLC layer acted to reduce roughness on all surfaces, with the greatest reduction in roughness being seen when the DLC was applied to the MCD coating. Raman analysis showed that there was no discernible variation in the bonding structure of the coatings on the various substrates. SEM analysis also indicated that the variation in coating morphology at the insert cutting edges was reduced due to the diamond layer. This was likely due to the fact that the diamond layer acted to round off the cutting edge on the micro level, resulting in a less prominent edge effect in the overlaying DLC coating. Short cutting trials also revealed that the DLC layer was contributing to an increase in BUE when applied to the MCD and NCD coatings. This finding contradicted previous research and showed that for this application, the smoother DLC surface does not reduce aluminium adhesion to the cutting tip.

Extended cutting trials, aimed at simulating the expected life cycle of the cutting inserts, were conducted on the developed single layer and combined diamond and DLC coatings. The aim was to test the efficacy of the combined coatings and determine their potential for offering the performance improvement required for efficient dry turning of aluminium. The cutting regime used the same cutting parameters as the development trials, although the test was extended so that 60 cutting passes were made, with a total material volume of 1147cm^3 being removed over the course of 46 minutes. Cutting forces were monitored throughout the trial and a measure of WP roughness was taken at the end of each cut. The results showed that, as expected, the rougher coating surfaces produced the roughest workpiece finishes. Due to failures of the coatings it was not possible to fully determine how effective the additional DLC layer was at improving the workpiece finish produced by the diamond coatings. It became clear, however, that the rougher MCD coating showed the least amount of aluminium adhesion of all samples, whilst the NCD coatings showed similar performance. The diamond coatings could be seen to have effectively reduced the amount of aluminium adhesion by up to 50% when compared to the uncoated and TiN coated samples. Measurements of the machining forces also revealed how the reduced BUE corresponded to a 30% reduction in cutting force by the end of the trial. SEM analysis of the samples post-trial, in conjunction with the cutting force measurements during the trial, showed that machining efficiency was still greatly improved even when the coatings had suffered up to 20% delamination at the cutting tip. This was an interesting result as it was expected that failures of the diamond coatings would create raised edges that would hinder swarf flow and lead to reduced efficiency. To the contrary, it was discovered that the ability of the diamond coatings to inhibit aluminium adhesion, meant that a significant amount of the coating had to delaminate before the cutting forces were adversely affected.

Addition of the DLC to the diamond layer was shown to increase the rate of aluminium adhesion build up at the cutting tip. It could be seen from the extended trials that this was in part, due to the wearing of the DLC layer. This result supported findings reported in the literature in which combined coatings were found to reduce long term tribological performance (Amaral *et al.*, 2012). In addition

to this result, however, analysis of the inserts after short trials (section 6.3.3) showed that adhesion was increased in areas of the cutting tip, even when there was no sign of coating damage. The reasons for this are likely due to the complex nature of the tribological interactions between chip and tool tip. It is already understood that smoother surface will not necessarily lead to reduced friction and adhesion (Heinrichs *et al.*, 2012; Chen *et al.*, 1990; Chen *et al.*, 1985). Material transfer effects during sliding, in this case swarf sliding over the tool tip, are dependent on several factors such as; the materials properties, environmental factors and most importantly, the dynamics of the interaction. Contact pressures, sliding speed and microstructures of the asperity surfaces will all affect the potential adhesive properties between the material surfaces. The analysis of the tool tips after cuttings trials suggested that the forces acting on the insert were sufficient to force the aluminium alloy into the crevices between the nodular asperities of the DLC coating. The nano-scale roughness of the DLC produced a more adherent surface for the workpiece material to attach to. This allowed the BUE to develop and coalesce at a faster rate, whilst the MCD surface, despite its much higher micro-scale roughness, only suffered from adhesion initiating at the very tips of the crystal peaks. This meant that more aluminium had to adhere to a smaller surface area before it could coalesce into a larger BUE. This significantly reduced the deposition of BUE, meaning that the MCD coating showed similar performance through the entire cutting trial, as shown in section 7.3.1.

8.2. Contributions to Knowledge

The main purpose of the study was to investigate the potential of using a combined diamond and DLC layered coatings for effective dry turning of aluminium alloys. The aim was to further improve upon the performance gains that had been reported for the individual, single layer coatings. Previous research had shown that combined coatings could greatly improve machining performance when drilling aluminium, however, there had been no investigations into the potential for improving performance in turning and milling applications. Due to the very different contact dynamics of machining inserts, compared to drills, it was therefore necessary to investigate whether similar performance improvements could be generated. The results of the investigation showed that the application of DLC to diamond coatings will not necessarily lead to reduced friction and adhesion. In fact, under the right circumstances, in terms of the dynamics of the sliding contact interface between the tool tip and the workpiece, the smoother DLC coating can produce an increase in aluminium adhesion. For this particular cutting regime it was discovered that the roughest diamond coating suffered the least amount of BUE, which was in stark contrast to the general expectations of the surface interactions.

The additional investigation into the effects of substrate geometry revealed that the common assumption that coating quality should not be effected was not correct. It was shown that sharp edges can alter the plasma sheath in such a way, as to cause concentrations of impinging ions with lower effective energies. These variations in the surrounding plasma field have been shown to significantly alter the topography, morphology and chemistry of the DLC coating. In addition, it was seen that the application of a diamond layer to a cutting tool can effectively round off the cutting edge with a subsequent increase to cutting radius. This effectively reduced the edge effects on the DLC layer and ensured a more homogeneous coating was achieved.

8.3. Recommendations for future perspectives

The investigations conducted in this work have given rise to a number of potential further studies which could allow for an improved understanding of PECVD deposition of DLC coatings. Further investigation of the properties and tribology of the combined diamond and DLC coatings would also be of great interest. The investigation of the effects of substrate geometry has opened up a number of further questions relating to how substrate material characteristics, particularly its electrical conductivity, may influence the reported effects on coating quality. In addition to this, the influence of geometry will also be affected by the deposition parameters. With this in mind, further studies designed to investigate whether negative effects may be reduced by altering deposition parameters would also be of interest. This could also be tied in with an investigation designed to determine what limits may be imposed on substrate geometries in order to guarantee a coating of sufficient quality.

It would also be of interest, with the application of the combined coating to a flat surface, to conduct further tribological tests. This would help to quantify the variations in friction and adhesion properties of different materials under different loads. It may therefore be possible to determine how the contact pressures interact with the micro-asperities of the coating surface. This will help to gain an improved understanding of which cutting applications may stand to benefit from a combined coating structure.

Although the investigation discussed here found that the additional DLC layer did not have the desired effect of further reducing aluminium adhesion to the cutting tip, it does not mean that the same effect will occur in similar turning or milling applications. Due to the extensive variety of cutting tools available, and the fact that DLC coatings have been reported to offer performance improvements in similar machining applications, a further study involving different tool geometries and cutting parameters would be necessary to determine the full potential of combined coatings.

Bibliography

A A Ogwu, e.a. (1999) *The effect of the substrate bias on the Raman spectra and thermal stability of diamond-like carbon (DLC) and silicon-modified DLC films prepared by plasma-enhanced chemical vapour deposition (PECVD)*.

Aisenberg, S. and Chabot, R. (1971) 'Ion-beam deposition of thin films of diamondlike carbon', *Journal of Applied Physics,* 42(7), pp. 2953-2958.

Ali, M. and Ürgen, M. (2012) 'Growth of in situ multilayer diamond films by varying substrate–filament distance in hot-filament chemical vapor deposition', *Journal of Materials Research,* 27(24), pp. 3123-3129.

Almeida, F., Sacramento, J., Oliveira, F. and Silva, R. (2008) 'Micro-and nano-crystalline CVD diamond coated tools in the turning of EDM graphite', *Surface and Coatings Technology,* 203(3), pp. 271-276.

Amaral, M., Carreira, D., Fernandes, A., Abreu, C., Oliveira, F., Gomes, J. and Silva, R. (2012) 'A DLC/diamond bilayer approach for reducing the initial friction towards a high bearing capacity', *Wear,* 290, pp. 18-24.

Andersson, J., Erck, R.A. and Erdemir, A. (2003) 'Friction of diamond-like carbon films in different atmospheres', *Wear,* 254(11), pp. 1070-1075.

Angus, J.C., Will, H.A. and Stanko, W.S. (1968) 'Growth of diamond seed crystals by vapor deposition', *Journal of Applied Physics,* 39(6), pp. 2915-2922.

Astakhov, V.P. (2004) 'The assessment of cutting tool wear', *International Journal of Machine Tools & Manufacture,* 44(6), pp. 637-647.

Astakhov, V.P. (2011) 'Turning', in Davim, J.P. (ed.) *Modern Machining Technology.* Woodhead Publishing, pp. 1-78.

Bachmann, P.K. and Vanenckevort, W. (1992) 'Diamond Deposition Technologies', *Diamond and Related Materials,* 1(10-11), pp. 1021-1034.

Balachova, O.V., Alves, M.A.R., Swart, J.W., Braga, E.S. and Cescato, L. (1999) 'Influence of the substrate thickness and radio frequency on the deposition rate of amorphous hydrogenated carbon a-C : H films', *Journal of Applied Physics,* 85(6), pp. 3345-3347.

Banerjee, D., Mukherjee, S. and Chattopadhyay, K.K. (2010) 'Controlling the surface topology and hence the hydrophobicity of amorphous carbon thin films', *Carbon,* 48(4), pp. 1025-1031.

Bao, T., Morrison Jr, P.W. and Woyczynski, W.A. (2005) 'Parametric optimization of microhardness of diamond-like carbon films prepared by plasma enhanced chemical vapor deposition', *Thin Solid Films,* 485(1–2), pp. 27-41.

Barletta, M., Rubino, G. and Gisario, A. (2011) 'Adhesion and wear resistance of CVD diamond coatings on laser treated WC–Co substrates', *Wear,* 271(9–10), pp. 2016-2024.

Batory, D., Jedrzejczak, A., Kaczorowski, W., Szymanski, W., Kolodziejczyk, L., Clapa, M. and Niedzielski, P. (2015) 'Influence of the process parameters on the characteristics of silicon-incorporated a-C:H:SiOx coatings', *Surface and Coatings Technology,* 271, pp. 112-118.

Beffort, O., Vaucher, S. and Khalid, F. (2004) 'On the thermal and chemical stability of diamond during processing of Al/diamond composites by liquid metal infiltration (squeeze casting)', *Diamond and related materials,* 13(10), pp. 1834-1843.

Benzhour, K., Szatkowski, J., Rozploch, F. and Stec, K. (2010) 'The Influence of Argon on the Deposition and Structure of Polycrystalline Diamond Films', *Acta Physica Polonica a,* 118(3), pp. 447-449.

Bhowmick, S. and Alpas, A.T. (2008) 'The performance of hydrogenated and non-hydrogenated diamond-like carbon tool coatings during the dry drilling of 319 Al', *International Journal of Machine Tools & Manufacture,* 48(7-8), pp. 802-814.

Bhowmick, S., Banerji, A., Khan, M.Z.U., Lukitsch, M.J. and Alpas, A.T. (2015) 'High temperature tribological behavior of tetrahedral amorphous carbon (ta-C) and fluorinated ta-C coatings against aluminum alloys', *Surface and Coatings Technology,* 284, pp. 14-25.

Bobzin, K., Bagcivan, N., Goebbels, N. and Yilmaz, K. (2009) 'Effect of the Substrate Geometry on Plasma Synthesis of DLC Coatings', *Plasma Processes and Polymers,* 6, pp. S425-S428.

Bogus, A., Gebeshuber, I.C., Pauschitz, A., Roy, M. and Haubner, R. (2008) 'Micro- and nanomechanical properties of diamond film with various surface morphologies', *Diamond and Related Materials,* 17(12), pp. 1998-2004.

Boothroyd, G. and Knight, W. 'Fundamentals of machining and machine tools, 1989', *Reproduced with permission of the copyright owner.Further reproduction prohibited without permission,* .

Bruno, P., Cicala, G., Losacco, A.M. and Decuzzi, P. (2004) 'Mechanical properties of PECVD hydrogenated amorphous carbon coatings via nanoindentation and nanoscratching techniques', *Surface & Coatings Technology,* 180, pp. 259-264.

Bull, S.J. (1995) 'Tribology of Carbon Coatings - Dlc, Diamond and Beyond', *Diamond and Related Materials,* 4(5-6), pp. 827-836.

Buršíková, V., Navrátil, V., Zajíčková, L. and Janča, J. (2002) 'Temperature dependence of mechanical properties of DLC/Si protective coatings prepared by PECVD', *Materials Science and Engineering: A,* 324(1–2), pp. 251-254.

Byrne, G., Dornfeld, D. and Denkena, B. (2003) 'Advancing cutting technology', *Cirp Annals-Manufacturing Technology,* 52(2), pp. 483-507.

Capote, G., Bonetti, L.F., Santos, L.V., Trava-Airoldi, V.J. and Corat, E.J. (2006) 'Adherent diamond-like carbon coatings on metals via PECVD and IBAD', *Brazilian Journal of Physics,* 36(3B), pp. 986-989.

Carrilero, M.S., Bienvenido, R., Sanchez, J.M., Alvarez, M., Gonzalez, A. and Marcos, M. (2002) 'A SEM and EDS insight into the BUL and BUE differences in the turning processes of AA2024 Al-Cu alloy', *International Journal of Machine Tools & Manufacture,* 42(2), pp. 215-220.

Caschera, D., Cossari, P., Federici, F., Kaciulis, S., Mezzi, A., Padeletti, G. and Trucchi, D.M. (2011) 'Influence of PECVD parameters on the properties of diamond-like carbon films', *Thin Solid Films,* 519(12) pp. 4087-4091.

Casiraghi, C., Ferrari, A.C. and Robertson, J. (2005) 'Raman spectroscopy of hydrogenated amorphous carbons', *Physical Review B,* 72(8).

Chabert, P. (2007) 'Electromagnetic effects in high-frequency capacitive discharges used for plasma processing', *Journal of Physics D-Applied Physics,* 40(3), pp. R63-R73.

Chattopadhyay, A., Sarangi, S.K. and Chattopadhyay, A.K. (2008) 'Effect of negative dc substrate bias on morphology and adhesion of diamond coating synthesised on carbide turning tools by modified HFCVD method', *Applied Surface Science,* 255(5), pp. 1661-1671.

Chattopadhyay, A.K., Roy, P., Ghosh, A. and Sarangi, S.K. (2009) 'Wettability and machinability study of pure aluminium towards uncoated and coated carbide cutting tool inserts', *Surface & Coatings Technology,* 203(8), pp. 941-951.

Chen, J., Huang, H. and Xu, X. (2009) 'An experimental study on the grinding of alumina with a monolayer brazed diamond wheel', *The International Journal of Advanced Manufacturing Technology,* 41(1-2), pp. 16-23.

Chen, L.H. and Rigney, D.A. (1990) 'Adhesion theories of transfer and wear during sliding of metals', *Wear,* 136(2), pp. 223-235.

Chen, L.H. and Rigney, D.A. (1985) 'Transfer during unlubricated sliding wear of selected metal systems', *Wear,* 105(1), pp. 47-61.

Cheng, Y.H., Wu, Y.P., Chen, J.G., Qiao, X.L., Xie, C.S., Tay, B.K., Lau, S.P. and Shi, X. (2000) 'On the deposition mechanism of a-C:H films by plasma enhanced chemical vapor deposition', *Surface and Coatings Technology,* 135(1), pp. 27-33.

Chern, S., Horng, J. and Chen, S. (2011) 'Study of temperature distribution of sliding block with asperity surface', *Surface and Interface Analysis,* , pp. 1509-1513.

Cho, C., Hong, B. and Lee, Y. (2005) 'Wear life evaluation of diamond-like carbon films deposited by microwave plasma-enhanced CVD and RF plasma-enhanced CVD method', *Wear,* 259(1–6), pp. 789-794.

Choi, W.S., Chung, I., Lee, Y. and Hong, B. (2004) 'Characterization of diamond-like carbon thin films prepared by a microwave plasma enhanced chemical vapor deposition method', *Surface and Coatings Technology,* 180–181, pp. 254-258.

Choi, W.S., Heo, J., Chung, I. and Hong, B. (2005) 'The effect of RF power on tribological properties of the diamond-like carbon films', *Thin Solid Films,* 475(1-2), pp. 287-290.

Chou, Y.K., Thompson, R.G. and Kumar, A. (2010) 'CVD-diamond technologies for dry drilling applications', *Thin Solid Films,* 518(24), pp. 7487-7491.

Clay, K.J., Speakman, S.P., Morrison, N.A., Tomozeiu, N., Milne, W.I. and Kapoor, A. (1998) 'Material properties and tribological performance of rf-PECVD deposited DLC coatings', *Diamond and Related Materials,* 7(8), pp. 1100-1107.

Csorbai, H.K., Kovach, G., Peto, G., Csikvari, P., Karacs, A., Solyom, A., Hars, G. and Kalman, E. (2007) 'Diamond-DLC double layer used in corrosive protective coating', *Applied Surface Science,* 253(11), pp. 5070-5075.

Dai, M., Zhou, K., Yuan, Z., Ding, Q. and Fu, Z. (2000) 'The cutting performance of diamond and DLC-coated cutting tools', *Diamond and Related Materials,* 9(9–10), pp. 1753-1757.

Damasceno, J.C., Camargo, S.S., Freire, F.L. and Carius, R. (2000) 'Deposition of Si-DLC films with high hardness, low stress and high deposition rates', *Surface & Coatings Technology,* 133, pp. 247-252.

Daudt, N.d.F., Pereira Barbosa, J.C., Braz, D.C., Pereira, M.B. and Alves Junior, C. (2012) 'TiN thin film deposition by cathodic cage discharge: effect of cage configuration and active species', *12th High-Tech Plasma Processes Conference (Htpp-12),* 406(1), pp. 2021.

Davim, J.P. and Mata, F. (2007) 'New machinability study of glass fibre reinforced plastics using polycrystalline diamond and cemented carbide (K15) tools', *Materials & Design,* 28(3), pp. 1050-1054.

Dimla Snr., D.E. (2000) 'Sensor signals for tool-wear monitoring in metal cutting operations—a review of methods', *International Journal of Machine Tools and Manufacture,* 40(8), pp. 1073-1098.

Ding, X., Zeng, X.T. and Hu, Z.Q. (2004) 'Substrate geometry effect on the uniformity of amorphous carbon films deposited by unbalanced magnetron sputtering', *Thin Solid Films,* 461(2), pp. 282-287.

Donnet, C., Fontaine, J., Grill, A. and Le Mogne, T. (2000) 'The role of hydrogen on the friction mechanism of diamond-like carbon films', *Tribology Letters,* 9(3-4), pp. 137-142.

dos Santos, G.R., da Costa, D.D., Amorim, F.L. and Torres, R.D. (2007a) 'Characterization of DLC thin film and evaluation of machining forces using coated inserts in turning of Al-Si alloys', *Surface & Coatings Technology,* 202(4-7), pp. 1029-1033.

dos Santos, G.R., da Costa, D.D., Amorim, F.L. and Torres, R.D. (2007b) 'Characterization of DLC thin film and evaluation of machining forces using coated inserts in turning of Al–Si alloys', *Surface and Coatings Technology,* 202(4–7), pp. 1029-1033.

Dumpala, R., Kumar, N., Kumaran, C.R., Dash, S., Ramamoorthy, B. and Ramachandra Rao, M.S. (2014) 'Adhesion characteristics of nano- and micro-crystalline diamond coatings: Raman stress mapping of the scratch tracks', *Diamond and Related Materials,* 44, pp. 71-77.

Endler, I., Leonhardt, A., Scheibe, H.J. and Born, R. (1996) 'Interlayers for diamond deposition on tool materials', *Diamond and Related Materials,* 5(3-5), pp. 299-303.

Erasmus, R.M., Comins, J.D., Mofokeng, V. and Martin, Z. (2011) 'Application of Raman spectroscopy to determine stress in polycrystalline diamond tools as a function of tool geometry and temperature', *Diamond and Related Materials,* 20(7), pp. 907-911.

Erdemir, A. (2002) 'Friction and wear of diamond and diamond-like carbon films', *Proceedings of the Institution of Mechanical Engineers Part J-Journal of Engineering Tribology,* 216(J6), pp. 387-400.

Erdemir, A. and Donnet, C. (2006) 'Tribology of diamond-like carbon films: recent progress and future prospects', *Journal of Physics D-Applied Physics,* 39(18), pp. R311-R327.

Erdemir, A., Eryilmaz, O.L., Nilufer, I.B. and Fenske, G.R. (2000) 'Effect of source gas chemistry on tribological performance of diamond-like carbon films', *Diamond and Related Materials,* 9(3-6), pp. 632-637.

Erdemir, A., Nilufer, I.B., Eryilmaz, O.L., Beschliesser, M. and Fenske, G.R. (1999) 'Friction and wear performance of diamond-like carbon films grown in various source gas plasmas', *Surface and Coatings Technology,* 120-121, pp. 589-593.

Evans, T. and James, P. (1964) 'A study of the transformation of diamond to graphite', *Proceedings of the Royal Society of London A: Mathematical, Physical and Engineering Sciences.* The Royal Society, 260-269.

Fang, N. and Dewhurst, P. (2005) 'Slip-line modeling of built-up edge formation in machining', *International Journal of Mechanical Sciences,* 47(7), pp. 1079-1098.

Ferrari, A.C. (2002) 'Determination of bonding in diamond-like carbon by Raman spectroscopy', *Diamond and Related Materials,* 11(3), pp. 1053-1061.

Ferrari, A.C. and Robertson, J. (2004) 'Raman spectroscopy of amorphous, nanostructured, diamond-like carbon, and nanodiamond', *Philosophical transactions.Series A, Mathematical, physical, and engineering sciences,* 362(1824), pp. 2477-2512.

Ferrari, A.C. and Robertson, J. (2000) 'Interpretation of Raman spectra of disordered and amorphous carbon', *Physical Review B,* 61(20), pp. 14095-14107.

Ferrari, A. and Robertson, J. (2001) 'Resonant Raman spectroscopy of disordered, amorphous, and diamondlike carbon', *Physical Review B,* 64(7), pp. 075414.

Filik, J., May, P.W., Pearce, S.R.J., Wild, R.K. and Hallam, K.R. (2003) 'XPS and laser Raman analysis of hydrogenated amorphous carbon films', *Diamond and Related Materials,* 12(3-7), pp. 974-978.

Fitzer, E. and Rozploch, F. (1988) 'Laser Raman spectroscopy for determination of the C-C bonding length in carbon', *Carbon,* 26(4), pp. 594-595.

Fukui, H., Okida, J., Omori, N., Moriguchi, H. and Tsuda, K. (2004) 'Cutting performance of DLC coated tools in dry machining aluminum alloys', *Surface and Coatings Technology,* 187(1), pp. 70-76.

Gangopadhyay, S. (2008) 'EFFECT OF CUTTING SPEED AND SURFACE CHEMISTRY OF CUTTING TOOLS ON THE FORMATION OF BUL OR BUE AND SURFACE QUALITY OF THE GENERATED SURFACE IN DRY TURNING OF AA6005 ALUMINIUM ALLOY', *Machining Science and Technology,* 14(2), pp. 208-223.

Gómez-Parra, A., Álvarez-Alcón, M., Salguero, J., Batista, M. and Marcos, M. (2013) 'Analysis of the evolution of the Built-Up Edge and Built-Up Layer formation mechanisms in the dry turning of aeronautical aluminium alloys', *Wear,* 302(1–2), pp. 1209-1218.

Gracio, J.J., Fan, Q.H. and Madaleno, J.C. (2010) 'Diamond growth by chemical vapour deposition', *Journal of Physics D-Applied Physics,* 43(37) pp. 374017.

Grill, A. (1999) 'Diamond-like carbon: state of the art', *Diamond and Related Materials,* 8(2-5), pp. 428-434.

Grzesik, W., (1999). 'Experimental investigation of the cutting temperature when turning with coated indexable inserts', *International journal of machine tools and manufacture*, *39*(3), pp. 355-369.

Hainsworth, S.V. and Uhure, N.J. (2007) 'Diamond like carbon coatings for tribology: production techniques, characterisation methods and applications', *International Materials Reviews,* 52(3), pp. 153-174.

Hanyu, H., Kamiya, S., Murakami, Y. and Kondoh, Y. (2005) 'The improvement of cutting performance in semi-dry condition by the combination of DLC coating and CVD smooth surface diamond coating', *Surface and Coatings Technology,* 200(1-4), pp. 1137-1141.

Hanyu, H., Kamiya, S., Murakami, Y. and Saka, M. (2003a) 'Dry and semi-dry machining using finely crystallized diamond coating cutting tools', *Surface and Coatings Technology,* 174-175, pp. 992-995.

Hanyu, H., Murakami, Y., Kamiya, S. and Saka, M. (2003b) 'New diamond coating with finely crystallized smooth surface for the tools to achieve fine surface finish of non-ferrous metals', *Surface and Coatings Technology,* 169-170, pp. 258-261.

Heinrichs, J., Olsson, M. and Jacobson, S. (2012) 'Mechanisms of material transfer studied in situ in the SEM:: Explanations to the success of DLC coated tools in aluminium forming', *Wear,* 292–293, pp. 49-60.

Helen Xu, G., Liang, H., Woodford, J.B. and Johnson, J.A. (2005) 'Temperature Dependence of Diamondlike Carbon Film Tribological Characteristics', *Journal of the American Ceramic Society,* 88(11), pp. 3110-3115.

Howes, V. (1962) 'The graphitization of diamond', *Proceedings of the Physical Society,* 80(3), pp. 648-662.

Hsu, J., Tzeng, S. and Wu, Y. (2008) 'Influence of hydrogen on the mechanical properties and microstructure of DLC films synthesized by r.f.-PECVD', *Vacuum,* 83(3), pp. 622-624.

Hu, J., Chou, Y.K., Thompson, R.G., Burgess, J. and Street, S. (2007) 'Characterizations of nano-crystalline diamond coating cutting tools', *Surface & Coatings Technology,* 202(4-7), pp. 1113-1117.

Huang, Z.Q., He, Y.H., Cai, H.T., Wu, C.H., Xiao, Y.F. and Huang, B.Y. (2008) 'Thermal residual stress analysis of diamond coating on graded cemented carbides', *Journal of Central South University of Technology,* 15(2), pp. 165-169.

Ikenaga, N., Sakudo, N., Awazu, K., Yasui, H. and Hasegawa, Y. (2006) 'Study on hybrid nano-diamond films formed by plasma chemical vapor deposition (CVD)', *Vacuum,* 80(7), pp. 810-813.

Inkin, V.N., Kirpilenko, G.G., Dementjev, A.A. and Maslakov, K.I. (2000) 'A superhard diamond-like carbon film', *Diamond and Related Materials,* 9(3-6), pp. 715-721.

Kouam, J. (2012) 'Dry, Semi-Dry and Wet Machining of 6061-T6', *Aluminium Alloy*InTech .

Jia, K. and Fischer, T. (1997) 'Sliding wear of conventional and nanostructured cemented carbides', *Wear,* 203, pp. 310-318.

Jiang, J. and Arnell, R.D. (2000) 'The effect of substrate surface roughness on the wear of DLC coatings', *Wear,* 239(1), pp. 1-9.

Jindal, P., Santhanam, A., Schleinkofer, U. and Shuster, A. (1999) 'Performance of PVD TiN, TiCN, and TiAlN coated cemented carbide tools in turning', *International Journal of Refractory Metals and Hard Materials,* 17(1), pp. 163-170.

Jones, B.J., Anguilano, L. and Ojeda, J.J. (2011) 'Argon plasma treatment techniques on steel and effects on diamond-like carbon structure and delamination', *Diamond and Related Materials,* 20(7), pp. 1030-1035.

Jones, B.J., Mahendran, A., Anson, A.W., Reynolds, A.J., Bulpett, R. and Franks, J. (2010) 'Diamond-like carbon coating of alternative metal alloys for medical and surgical applications', *Diamond and Related Materials,* 19(7–9), pp. 685-689.

Jones, B.J., Wright, S., Barklie, R.C., Tyas, J., Franks, J. and Reynolds, A.J. (2008) 'Nanostructure and paramagnetic centres in diamond-like carbon: Effect of Ar dilution in PECVD process', *Diamond and Related Materials,* 17(7-10), pp. 1629-1632.

Joy, D.C. (1991) 'An introduction to Monte Carlo simulations', *Scanning microscopy,* 5(2), pp. 329-337.

Kalin, M., Vizintin, J., Vercammen, K., Barriga, J. and Arnsek, A. (2006) 'The lubrication of DLC coatings with mineral and biodegradable oils having different polar and saturation characteristics', *Surface & Coatings Technology,* 200(14-15), pp. 4515-4522.

Kamiya, S., Takahashi, H., D'Antonio, P., Polini, R. and Traversa, E. (2002) 'Quantitative comparison of adhesive toughness for various diamond films on Co-cemented tungsten carbide', *Diamond and Related Materials,* 11(3-6), pp. 716-720.

Kilic, D.S. and Raman, S. (2007) 'Observations of the tool–chip boundary conditions in turning of aluminum alloys', *Wear,* 262(7–8), pp. 889-904.

Kim, H., Jung, D.H., Park, B., Yoo, K.C., Lee, J.J. and Joo, J.H. (2005) 'The effect of the substrate bias voltage and the deposition pressure on the properties of diamond-like carbon produced by inductively coupled plasma assisted chemical vapor deposition', *Surface and Coatings Technology,* 193(1–3), pp. 255-258.

Kim, M.G., Lee, K.R. and Eun, K.Y. (1999) 'Tribological behavior of silicon-incorporated diamond-like carbon films', *Surface & Coatings Technology,* 112(1-3), pp. 204-209.

Kim, Y.T., Cho, S.M., Choi, W.S., Hong, B. and Yoon, D.H. (2003) 'Dependence of the bonding structure of DLC thin films on the deposition conditions of PECVD method', *Surface & Coatings Technology,* 169, pp. 291-294.

Kohary, K. and Kugler, S. (2001) 'Growth of amorphous carbon: Low-energy molecular dynamics simulation of atomic bombardment', *Physical Review B,* 63(19), pp. 193404.

Konca, E., Cheng, Y.T., Weiner, A.M., Dasch, J.M. and Alpas, A. (2006) 'Elevated temperature tribological behavior of non-hydrogenated diamond-like carbon coatings against 319 aluminum alloy', *Surface & Coatings Technology,* 200(12-13), pp. 3996-4005.

Konca, E., Cheng, Y.T., Weiner, A.M., Dasch, J.M. and Alpas, A.T. (2005) 'Effect of test atmosphere on the tribological behaviour of the non-hydrogenated diamond-like carbon coatings against 319 aluminum alloy and tungsten carbide', *Surface & Coatings Technology,* 200(5-6), pp. 1783-1791.

Kwon, Y. and Fischer, G.W. (2003) 'A novel approach to quantifying tool wear and tool life measurements for optimal tool management', *International Journal of Machine Tools & Manufacture,* 43(4), pp. 359-368.

Lai, W.C., Wu, Y., Chang, H. and Lee, Y. (2011) 'Enhancing the adhesion of diamond films on cobalt-cemented tungsten carbide substrate using tungsten particles via MPCVD system', *Journal of Alloys and Compounds,* 509(12), pp. 4433-4438.

Li, H.X., Xu, T., Chen, J.M., Zhou, H.D. and Liu, H.W. (2004) 'The effect of applied dc bias voltage on the properties of a-C:H films prepared in a dual dc–rf plasma system', *Applied Surface Science,* 227(1–4), pp. 364-372.

Li, H., Xu, T., Wang, C., Chen, J., Zhou, H. and Liu, H. (2006) 'Annealing effect on the structure, mechanical and tribological properties of hydrogenated diamond-like carbon films', *Thin Solid Films,* 515(4), pp. 2153-2160.

Li, Y.S., Tang, Y., Yang, Q., Shimada, S., Wei, R., Lee, K.Y. and Hirose, A. (2008) 'Al-enhanced nucleation and adhesion of diamond films on WC-Co substrates', *International Journal of Refractory Metals & Hard Materials,* 26(5), pp. 465-471.

Lifshitz, Y. (1999) 'Diamond-like carbon — present status', *Diamond and Related Materials,* 8(8-9), pp. 1659-1676.

Lin, T., Yu, G.Y., Wee, A.T.S., Shen, Z.X. and Loh, K.P. (2000) 'Compositional mapping of the argon-methane-hydrogen system for polycrystalline to nanocrystalline diamond film growth in a hot-filament chemical vapor deposition system', *Applied Physics Letters,* 77(17), pp. 2692-2694.

Lin, Z., Lv, S., Yu, Z., Li, M., Lin, T., Ba, D., Choi, C. and Lee, I. (2008) 'Effect of bias voltage on Diamond-like carbon film deposited on PMMA substrate', *Surface and Coatings Technology,* 202(22–23), pp. 5386-5389.

List, G., Nouari, M., Gehin, D., Gomez, S., Manaud, J.P., Le Petitcorps, Y. and Girot, F. (2005) 'Wear behaviour of cemented carbide tools in dry machining of aluminium alloy', *Wear,* 259, pp. 1177-1189.

Liu, Y., Erdemir, A. and Meletis, E. (1996) 'A study of the wear mechanism of diamond-like carbon films', *Surface and Coatings Technology,* 82(1), pp. 48-56.

Liu, Y. and Meletis, E. (1997) 'Evidence of graphitization of diamond-like carbon films during sliding wear', *Journal of Materials Science,* 32(13), pp. 3491-3495.

Ma, T., Hu, Y., Wang, H. and Li, X. (2007a) 'Effect of impact angle and substrate roughness on growth of diamondlike carbon films', *Journal of Applied Physics,* 101(1), pp. 014901-014908.

Ma, Y.P., Sun, F.H., Xue, H.G., Zhang, Z.M. and Chen, M. (2007b) 'Deposition and characterization of nanocrystalline diamond films on Co-cemented tungsten carbide inserts', *Diamond and Related Materials,* 16(3), pp. 481-485.

Maheswaran, R., Ramaswamy, S., Thiruvadigal, D.J. and Gopalakrishnan, C. (2011) 'Systematic study of various stages during the growth process of diamond-like carbon film by atomic force microscopy', *Journal of Non-Crystalline Solids,* 357(7), pp. 1710-1715.

Maître, N., Camelio, S., Barranco, A., Girardeau, T. and Breelle, E. (2005) 'Physical and chemical properties of amorphous hydrogenated carbon films deposited by PECVD in a low self-bias range', *Journal of Non-Crystalline Solids,* 351(10–11), pp. 877-884.

Markwitz, A., Mohr, B., Carpeño, D.F. and Hübner, R. (2014) 'Ultra-smooth diamond-like carbon coatings with high elasticity deposited at low temperature by direct ion beam deposition', *Surface and Coatings Technology,* 258, pp. 956-962.

Martinho, R., Silva, F. and Baptista, A. (2007) 'Wear behaviour of uncoated and diamond coated Si 3 N 4 tools under severe turning conditions', *Wear,* 263(7), pp. 1417-1422.

McNamara, D., Alveen, P., Damm, S., Carolan, D., Rice, J.H., Murphy, N. and Ivanković, A. (2015) 'A Raman spectroscopy investigation into the influence of thermal treatments on the residual stress of polycrystalline diamond', *International Journal of Refractory Metals and Hard Materials,* 52, pp. 114-122.

Meneve, J., Dekempeneer, E., Wegener, W. and Smeets, J. (1996) 'Low friction and wear resistant a-C:H/a-Si1−xCx:H multilayer coatings', *Surface and Coatings Technology,* 86-87(Part 2), pp. 617-621.

Miyoshi, K., Wu, R.L.C. and Lanter, W.C. (1997) 'Friction and wear of diamond like carbon on fine-grain diamond', *Tribology Letters,* 3(2), pp. 141-145.

Moseler, M., Gumbsch, P., Casiraghi, C., Ferrari, A.C. and Robertson, J. (2005) 'The ultrasmoothness of diamond-like carbon surfaces', *Science (New York, N.Y.),* 309(5740), pp. 1545-1548.

Mousinho, A.P., Mansano, R.D. and Salvadori, M.C. (2009) 'Influence of substrate surface topography in the deposition of nanostructured diamond-like carbon films by high density plasma chemical vapor deposition', *Surface and Coatings Technology,* 203(9), pp. 1193-1198.

Mustafa, A. and Tanju, K. (2011) 'Investigation of the machinability of the Al 7075 alloy using DLC coated cutting tools', *Scientific Research and Essays,* 6(1), pp. 44-51.

Myshkin, N.K., Grigoriev, A.Y., Chizhik, S.A., Choi, K.Y. and Petrokovets, M.I. (2003) 'Surface roughness and texture analysis in microscale', *Wear,* 254(10), pp. 1001-1009.

Nelson, N., Rakowski, R.T., Franks, J., Woolliams, P., Weaver, P. and Jones, B.J. (2014) 'The effect of substrate geometry and surface orientation on the film structure of DLC deposited using PECVD', *Surface and Coatings Technology,* 254, pp. 73-78.

Nemanich, R., Glass, J., Lucovsky, G. and Shroder, R. (1988) 'Raman scattering characterization of carbon bonding in diamond and diamondlike thin films', *Journal of Vacuum Science & Technology A,* 6(3), pp. 1783-1787.

Neto, M.A., Fernandes, A.J.S., Silva, R.F. and Costa, F.M. (2008) 'Nucleation of nanocrystalline diamond on masked/unmasked Si3N4 ceramics with different mechanical pretreatments', *Diamond and Related Materials,* 17(4-5), pp. 440-445.

Ni, W.Y., Cheng, Y.T., Weiner, A.M. and Perry, T.A. (2006) 'Tribological behavior of diamond-like-carbon (DLC) coatings against aluminum alloys at elevated temperatures', *Surface & Coatings Technology,* 201(6), pp. 3229-3234.

Nouari, M., List, G., Girot, F. and Coupard, D. (2003) 'Experimental analysis and optimisation of tool wear in dry machining of aluminium alloys', *Wear,* 255, pp. 1359-1368.

Okpalugo, T.I.T., Maguire, P.D., Ogwu, A.A. and McLaughlin, J.A.D. (2004) 'The effect of silicon doping and thermal annealing on the electrical and structural properties of hydrogenated amorphous carbon thin films', *Diamond and Related Materials,* 13(4-8), pp. 1549-1552.

O'sullivan, D. and Cotterell, M., (2001) 'Temperature measurement in single point turning', *Journal of Materials Processing Technology*, *118*(1), pp. 301-308.

Ouchabane, M., Salah, H., Herrmann, M., Tabet, N., Henda, K., Touchrift, B. and Kechouane, M. (2010) 'Influence of bias voltage on the structure and deposition mechanism of diamond-like carbon films produced by RF (13.56?MHz) CH4 plasma', *physica status solidi (a),* 207(10), pp. 2311-2318.

Pastewka, L., Moser, S. and Moseler, M. (2010) 'Atomistic insights into the running-in, lubrication, and failure of hydrogenated diamond-like carbon coatings', *Tribology Letters,* 39(1), pp. 49-61.

Peng, X.L., Barber, Z.H. and Clyne, T.W. (2001) 'Surface roughness of diamond-like carbon films prepared using various techniques', *Surface and Coatings Technology,* 138(1), pp. 23-32.

Pessoa, R.S., Fraga, M.A., Santos, L.V., Galvão, N.K.A.M., Maciel, H.S. and Massi, M. (2015) '18 - Plasma-assisted techniques for growing hard nanostructured coatings: An overview', in Aliofkhazraei, M. (ed.) *Anti-Abrasive Nanocoatings.* Woodhead Publishing, pp. 455-479.

Polini, R. (2006) 'Chemically vapour deposited diamond coatings on cemented tungsten carbides: Substrate pretreatments, adhesion and cutting performance', *Thin Solid Films,* 515(1), pp. 4-13.

Polini, R., Bravi, F., Mattei, G., Marcheselli, G. and Traversa, E. (2002) 'Effect of WC grain growth inhibitors on the adhesion of chemical vapor deposition diamond films on WC-Co cemented carbide', *Diamond and Related Materials,* 11(2), pp. 242-248.

Polini, R., Casadei, F., D'Antonio, P. and Traversa, E. (2003) 'Dry turning of alumina/aluminum composites with CVD diamond coated Co-cemented tungsten carbide tools', *Surface & Coatings Technology,* 166(2-3), pp. 127-134.

Qi, Y., Konca, E. and Alpas, A.T. (2006) 'Atmospheric effects on the adhesion and friction between non-hydrogenated diamond-like carbon (DLC) coating and aluminum - A first principles investigation', *Surface Science,* 600(15), pp. 2955-2965.

Ravi, N., Bukhovets, V.L., Varshavskaya, I.G. and Sundararajan, G. (2007) 'Deposition of diamond-like carbon films on aluminium substrates by RF-PECVD technique: Influence of process parameters', *Diamond and Related Materials,* 16(1), pp. 90-97.

Rech, J. (2006) 'Influence of cutting tool coatings on the tribological phenomena at the tool–chip interface in orthogonal dry turning', *Surface and Coatings Technology,* 200(16–17), pp. 5132-5139.

Ren, X.J., Yang, Q.X., James, R.D. and Wang, L., (2004). 'Cutting temperatures in hard turning chromium hardfacings with PCBN tooling', *Journal of Materials Processing Technology*, *147*(1), pp. 38-44.

Renaud, A., Hu, J., Qin, F. and Chou, Y.K. (2009) 'Numerical simulations of 3D tool geometry effects on deposition residual stresses in diamond coated cutting tools', *International Journal of Mechatronics and Manufacturing Systems,* 2(4), pp. 490-502.

Rigney, D.A., Chen, L.H., Naylor, M.G.S. and Rosenfield, A.R. (1984) 'Wear processes in sliding systems', *Wear,* 100(1), pp. 195-219.

Robertson, J. (2008) 'Comparison of diamond-like carbon to diamond for applications', *Physica Status Solidi A-Applications and Materials Science,* 205(9), pp. 2233-2244.

Robertson, J. (2002) 'Diamond-like amorphous carbon', *Materials Science & Engineering R-Reports,* 37(4-6), pp. 129-281.

Ronkainen, H., Varjus, S., Koskinen, J. and Holmberg, K. (2001) 'Differentiating the tribological performance of hydrogenated and hydrogen-free DLC coatings', *Wear,* 249(3-4), pp. 260-266.

Roy, P., Sarangi, S.K., Ghosh, A. and Chattopadhyay, A.K. (2009) 'Machinability study of pure aluminium and Al-12% Si alloys against uncoated and coated carbide inserts', *International Journal of Refractory Metals & Hard Materials,* 27(3), pp. 535-544.

Sakudo, N., Ikenaga, N., Yasui, H. and Awazu, K. (2008) 'Amorphous carbon coating mixed with nano-diamonds', *Thin Solid Films,* 516(14), pp. 4483-4486.

Salvadori, M.C., Martins, D.R. and Cattani, M. (2006) 'DLC coating roughness as a function of film thickness', *Surface and Coatings Technology,* 200(16–17), pp. 5119-5122.

Sánchez, J.M., Rubio, E., Álvarez, M., Sebastián, M.A. and Marcos, M. (2005) 'Microstructural characterisation of material adhered over cutting tool in the dry machining of aerospace aluminium alloys', *Journal of Materials Processing Technology,* 164–165, pp. 911-918.

Sarangi, S.K., Chattopadhyay, A. and Chattopadhyay, A.K. (2008a) 'Effect of pretreatment methods and chamber pressure on morphology, quality and adhesion of HFCVD diamond coating on cemented carbide inserts', *Applied Surface Science,* 254(13), pp. 3721-3733.

Sarangi, S.K., Chattopadhyay, A. and Chattopadhyay, A.K. (2008b) 'Effect of pretreatment, seeding and interlayer on nucleation and growth of HFCVD diamond films on cemented carbide tools', *International Journal of Refractory Metals & Hard Materials,* 26(3), pp. 220-231.

Schwan, J., Ulrich, S., Batori, V., Ehrhardt, H. and Silva, S. (1996) 'Raman spectroscopy on amorphous carbon films', *Journal of Applied Physics,* 80(1), pp. 440-447.

Schwarz, C., Heeg, J., Rosenberg, M. and Wienecke, M. (2008) 'Investigation on wear and adhesion of graded Si/SiC/DLC coatings deposited by plasma-enhanced-CVD', *Diamond and Related Materials,* 17(7–10), pp. 1685-1688.

Sedlaček, M., Podgornik, B. and Vižintin, J. (2008) 'Tribological properties of DLC coatings and comparison with test results: Development of a database', *Materials Characterization,* 59(2), pp. 151-161.

Sein, H., Ahmed, W., Jackson, M., Polini, R., Hassan, I., Amar, M. and Rego, C. (2004) 'Enhancing nucleation density and adhesion of polycrystalline diamond films deposited by HFCVD using surface treaments on Co cemented tungsten carbide', *Diamond and Related Materials,* 13(4-8), pp. 610-615.

Sheeja, D., Tay, B.K., Leong, K.W. and Lee, C.H. (2002) 'Effect of film thickness on the stress and adhesion of diamond-like carbon coatings', *Diamond and Related Materials,* 11(9), pp. 1643-1647.

Sheikh-Ahmad, J. and Chipalkati, P. (2015) 'Effect of Cutting Edge Geometry on Thermal Stresses and Failure of Diamond Coated Tools', *Procedia Manufacturing,* 1, pp. 663-674.

Silva, W.M., Jesus, L.M., Carneiro, J.R., Souza, P.S., Martins, P.S. and Trava-Airoldi, V.J. (2015) 'Performance of carbide tools coated with DLC in the drilling of SAE 323 aluminum alloy', *Surface and Coatings Technology,* 284, pp. 404-409.

Singh, R.K., Xie, Z.H., Bendavid, A., Martin, P.J., Munroe, P. and Hoffman, M. (2008) 'Effect of substrate roughness on the contact damage of DLC coatings', *Diamond and Related Materials,* 17(6), pp. 975-979.

Singha, A., Ghosh, A., Roy, A. and Ray, N.R. (2006) 'Quantitative analysis of hydrogenated diamondlike carbon films by visible Raman spectroscopy', *Journal of Applied Physics,* 100(4), pp. 4910-4918.

Sun, F.H., Zhang, Z.M., Chen, M. and Shen, H.S. (2003) 'Improvement of adhesive strength and surface roughness of diamond films on Co-cemented tungsten carbide tools', *Diamond and Related Materials,* 12(3-7), pp. 711-718.

Sun, Z. (2000) 'Morphological features of diamond-like carbon films deposited by plasma-enhanced CVD', *Journal of Non-Crystalline Solids,* 261(1–3), pp. 211-217.

Theye, M.-., Paret, V. and Sadki, A. (2001) 'Relations between the deposition conditions, the microstructure and the defects in PECVD hydrogenated amorphous carbon films; influence on the electronic density of states', *Diamond and Related Materials,* 10(2), pp. 182-190.

Tiejun, L., Qihong, L., Jingxing, D., Yunrong, W., Jun, Z., Jingru, L., Zhiming, Z. and Fanghong, S. (2002) 'Improved adhesion of diamond coating on cobalt-cemented tungsten carbide hardmetal by using pulsed-UV-laser substrate surface pretreatment', *Applied Surface Science,* 193(1), pp. 102-119.

Tzeng, S., Fang, Y., Chih, Y., Hu, Y., Hsu, J., Wu, C. and Wu, G. (2011)'Surface characterization and nanomechanical properties of diamond-like carbon films synthesized by RF plasma enhanced chemical vapor deposition', *Thin Solid Films,* 519(15), pp. 4870-4873.

Valentini, L., Kenny, J.M., Mariotto, G. and Tosi, P. (2001) 'Deposition of hydrogenated amorphous carbon films from CH4/Ar plasmas: Ar dilution effects', *Journal of Materials Science,* 36(21), pp. 5295-5300.

Vandevelde, T.C.S., Vandierendonck, K., Van Stappen, M., Mong, W.D. and Perremans, P. (1999) 'Cutting applications of DLC, hard carbon and diamond films', *Surface & Coatings Technology,* 113(1-2), pp. 80-85.

Varnin, V.P., Laptev, V.A. and Ralchenko, V.G. (2006) 'The state of the art in the growth of diamond crystals and films', *Inorganic Materials,* 42, pp. S1-S18.

Vladimirov, A.B., Trakhtenberg, I.S., Rubshtein, A.P., Plotnikov, S.A., Bakunin, O.M., Korshunov, L.G. and Kuzmina, E.V. (2000) 'The effect of substrate and DLC morphology on the tribological properties coating', *Diamond and Related Materials,* 9(3–6), pp. 838-842.

Wada, A., Ogaki, T., Niibe, M., Tagawa, M., Saitoh, H., Kanda, K. and Ito, H. (2011) 'Local structural analysis of a-SiCx:H films formed by decomposition of tetramethylsilane in microwave discharge flow of Ar', *Diamond and Related Materials,* 20(3), pp. 364-367.

Waddell, E., Gibson, D., Lin, L. and Xiuhua, F. (2011) 'Modelling and optimization of film thickness variation for plasma enhanced chemical vapour deposition processes', *Advances in Optical Thin Films Iv,* 8168, pp. 81681I.

Wang, P., Wang, X., Xu, T., Liu, W.M. and Zhang, J.Y. (2007) 'Comparing internal stress in diamond-like carbon films with different structure', *Thin Solid Films,* 515(17), pp. 6899-6903.

Wei, C. and Yen, J. (2007) 'Effect of film thickness and interlayer on the adhesion strength of diamond like carbon films on different substrates', *Diamond and Related Materials,* 16(4–7), pp. 1325-1330.

Wei, Q., Ashfold, M.N.R., Mankelevich, Y.A., Yu, Z.M., Liu, P.Z. and Ma, L. (2011) 'Diamond growth on WC-Co substrates by hot filament chemical vapor deposition: Effect of filament–substrate separation', *Diamond and Related Materials,* 20(5-6), pp. 641-650.

Wei, Q., Yu, Z.M., Ashfold, M.N.R., Ye, J. and Ma, L. (2010) 'Synthesis of micro- or nano-crystalline diamond films on WC-Co substrates with various pretreatments by hot filament chemical vapor deposition', *Applied Surface Science,* 256(13), pp. 4357-4364.

Whitfield, M.D., Savage, J.A. and Jackman, R.B. (2000) 'Nucleation and growth of diamond films on single crystal and polycrystalline tungsten substrates', *Diamond and Related Materials,* 9(3-6), pp. 262-268.

Wu, W.J. and Hon, M.H. (1999) 'Thermal stability of diamond-like carbon films with added silicon', *Surface & Coatings Technology,* 111(2-3), pp. 134-140.

Wu, W.J., Pai, T.M. and Hon, M.H. (1998) 'Wear behavior of silicon-containing diamond-like carbon coatings', *Diamond and Related Materials,* 7(10), pp. 1478-1484.

Xu, X., Li, Y. and Malkin, S. (2001) 'Forces and energy in circular sawing and grinding of granite', *Journal of Manufacturing Science and Engineering,* 123(1), pp. 13-22.

Xu, N., Yin, D., Liu, Z. and Zheng, X. (1997) 'The effects of applied bias voltage on structure and hydrogen content of a-C:H films', *Journal of Physics D-Applied Physics,* 30(5), pp. 763-768.

Yanming, Q. and Zehua, Z. (2000) 'Tool wear and its mechanism for cutting SiC particle-reinforced aluminium matrix composites', *Journal of Materials Processing Technology,* 100(1–3), pp. 194-199.

Yoshimura, H., Toda, Y., Moriwaki, T., Shibasaka, T. and Okida, J. (2006) 'Study on near dry cutting of aluminum alloys', *Machining Science and Technology,* 10(3), pp. 289-299.

Zhang, D., Shen, B. and Sun, F. (2010) 'Study on tribological behavior and cutting performance of CVD diamond and DLC films on Co-cemented tungsten carbide substrates', *Applied Surface Science,* 256(8), pp. 2479-2489.

Zhang, W., Tanaka, A., Wazumi, K. and Koga, Y. (2002) 'Structural, mechanical and tribological properties of diamond-like carbon films prepared under different substrate bias voltage', *Diamond and Related Materials,* 11(11), pp. 1837-1844.

Zhang, W., Tanaka, A., Wazumi, K., Koga, Y. and Xu, B.S. (2004) 'The effect of annealing on mechanical and tribological properties of diamond-like carbon multilayer films', *Diamond and Related Materials,* 13(11-12), pp. 2166-2169.

Zhang, W., Tanaka, A., Xu, B.S. and Koga, Y. (2005) 'Study on the diamond-like carbon multilayer films for tribological application', *Diamond and Related Materials,* 14(8), pp. 1361-1367.

Zhang, X.C., Xu, B.S., Wang, H.D. and Wu, Y.X. (2006) 'Analyses of interfacial stresses and normal stresses within an elongated film strip/substrate system', *Thin Solid Films,* 515(4), pp. 2251-2256.

Zhang, Y.F., Zhang, F., Gao, Q.J., Peng, X.F. and Lin, Z.D. (2001) 'The roles of argon addition in the hot filament chemical vapor deposition system', *Diamond and Related Materials,* 10(8), pp. 1523-1527.

Zhao, J., Lemoine, P., Liu, Z., Quinn, J., Maguire, P. and McLaughlin, J. (2001) 'A study of microstructure and nanomechanical properties of silicon incorporated DLC films deposited on silicon substrates', *Diamond and Related Materials,* 10(3-7), pp. 1070-1075.

Zhong, M., Zhang, C. and Luo, J. (2008) 'Effect of substrate morphology on the roughness evolution of ultra thin DLC films', *Applied Surface Science,* 254(21), pp. 6742-6748.

Zhong, Z.R., Wang, X.W. and Feng, X.H. (2007) 'Effects of pressure and temperature on sp(3) fraction in diamondlike carbon materials', *Journal of Materials Research,* 22, pp. 2770-2775.

Zhou, S., Zhihao, Z., Ning, X. and Xiaofeng, Z. (1994) 'Study of the growth rate of diamond film by hot-filament CVD', *Materials Science and Engineering: B,* 25(1), pp. 47-52.

Zolgharni, M., Jones, B.J., Bulpett, R., Anson, A.W. and Franks, J. (2008) 'Energy efficiency improvements in dry drilling with optimised diamond-like carbon coatings', *Diamond and Related Materials,* 17(7-10), pp. 1733-1737.

Appendix

A1. Extended cutting trial details

Cut	WP Dia mm	Revolutions	Cut Distance m	Time min	Volume cm^3	Total Distance m	Total Volume cm^3
1	100	2000.00	628.00	1.90	46.8645	628.00	46.87
2	99	1966.67	611.36	1.85	45.620275	1239.36	92.49
3	98	1933.33	594.93	1.80	44.39175	1834.28	136.88
4	97	1900.00	578.70	1.75	43.178925	2412.99	180.06
5	96	1866.67	562.69	1.71	41.9818	2975.67	222.04
6	95	1833.33	546.88	1.66	40.800375	3522.56	262.84
7	94	1800.00	531.29	1.61	39.63465	4053.84	302.47
8	93	1766.67	515.90	1.56	38.484625	4569.75	340.96
9	92	1733.33	500.73	1.52	37.3503	5070.47	378.31
10	91	1700.00	485.76	1.47	36.231675	5556.23	414.54
11	90	1666.67	471.00	1.43	35.12875	6027.23	449.67
12	89	1633.33	456.45	1.38	34.041525	6483.68	483.71
13	88	1600.00	442.11	1.34	32.97	6925.79	516.68
14	87	1566.67	427.98	1.30	31.914175	7353.78	548.59
15	86	1533.33	414.06	1.25	30.87405	7767.84	579.47
16	85	1500.00	400.35	1.21	29.849625	8168.19	609.32
17	84	1466.67	386.85	1.17	28.8409	8555.03	638.16
18	83	1433.33	373.56	1.13	27.847875	8928.59	666.01
19	82	1400.00	360.47	1.09	26.87055	9289.06	692.88
20	81	1366.67	347.60	1.05	25.908925	9636.66	718.79
21	80	1333.33	334.93	1.01	24.963	9971.59	743.75
22	79	1300.00	322.48	0.98	24.032775	10294.07	767.78
23	78	1266.67	310.23	0.94	23.11825	10604.30	790.90
24	77	1233.33	298.20	0.90	22.219425	10902.50	813.12
25	76	1200.00	286.37	0.87	21.3363	11188.87	834.46
26	75	1166.67	274.75	0.83	20.468875	11463.62	854.92
27	74	1133.33	263.34	0.80	19.61715	11726.96	874.54
28	73	1100.00	252.14	0.76	18.781125	11979.10	893.32
29	72	1066.67	241.15	0.73	17.9608	12220.25	911.28
30	71	1033.33	230.37	0.70	17.156175	12450.62	928.44
31	70	1000.00	219.80	0.67	16.36725	12670.42	944.81
32	69	966.67	209.44	0.63	15.594025	12879.86	960.40
33	68	933.33	199.29	0.60	14.8365	13079.15	975.24
34	67	900.00	189.34	0.57	14.094675	13268.49	989.33
35	66	866.67	179.61	0.54	13.36855	13448.10	1002.70
36	65	833.33	170.08	0.52	12.658125	13618.18	1015.36
37	64	800.00	160.77	0.49	11.9634	13778.95	1027.32
38	63	766.67	151.66	0.46	11.284375	13930.61	1038.61
39	62	733.33	142.77	0.43	10.62105	14073.38	1049.23
40	61	700.00	134.08	0.41	9.973425	14207.45	1059.20

41	60	666.67	125.60	0.38	9.3415	14333.05	1068.54
42	59	633.33	117.33	0.36	8.725275	14450.38	1077.27
43	58	600.00	109.27	0.33	8.12475	14559.66	1085.39
44	57	566.67	101.42	0.31	7.539925	14661.08	1092.93
45	56	533.33	93.78	0.28	6.9708	14754.86	1099.90
46	55	500.00	86.35	0.26	6.417375	14841.21	1106.32
47	54	466.67	79.13	0.24	5.87965	14920.34	1112.20
48	53	433.33	72.12	0.22	5.357625	14992.45	1117.56
49	52	400.00	65.31	0.20	4.8513	15057.77	1122.41
50	51	366.67	58.72	0.18	4.360675	15116.48	1126.77
51	50	333.33	52.33	0.16	3.88575	15168.82	1130.66
52	49	300.00	46.16	0.14	3.426525	15214.97	1134.08
53	48	266.67	40.19	0.12	2.983	15255.17	1137.07
54	47	233.33	34.44	0.10	2.555175	15289.60	1139.62
55	46	200.00	28.89	0.09	2.14305	15318.49	1141.76
56	45	166.67	23.55	0.07	1.746625	15342.04	1143.51
57	44	133.33	18.42	0.06	1.3659	15360.46	1144.88
58	43	100.00	13.50	0.04	1.000875	15373.96	1145.88
59	42	66.67	8.79	0.03	0.65155	15382.76	1146.53
60	41	33.33	4.29	0.01	0.317925	15387.05	1146.85

A2. Publications arising from this research

First Author

N Nelson, RT Rakowski, J Franks, P Wooliams, P Weaver, BJ Jones
The Effect of Substrate Geometry and Surface Orientation on the Film Structure of DLC Deposited using PECVD
Journal of Surface and Coatings Technology, 254 (2014) 73-78

N Nelson, R Rakowski, J Franks, P Woolliams, BJ Jones
Microstructural variation and inhomogeneity in rf PECVD diamond like carbon films caused by sample geometry
International Conference on Diamond and Carbon Materials, Italy, September 2013
Elsevier (Supporting Journal; Diamond and Related Materials)
0925-9635

Named Author

C Wang, K Cheng, N Nelson, W Sawangsri, R Rakowski
Cutting Force based analysis and correlative observation on the tool wear in diamond turning of single-crystal silicon
Journal of Engineering Manufacture
Submitted: 8th April 2014 Accepted: 20th June 2014

International Conferences

European Conference on Applications of Surface and Interface Analysis (Cardiff 2011)

Presented poster titled: Geometrical effects on diamond-like carbon thin films deposited by plasma enhanced CVD